



Departamento de Física de Partículas

HOLOGRAPHY AND HOLOMORPHY IN QUANTUM FIELD THEORIES AND GRAVITY

Eduardo Conde Pena
Santiago de Compostela, abril de 2012.

UNIVERSIDADE DE SANTIAGO DE COMPOSTELA

Departamento de Física de Partículas

HOLOGRAPHY AND HOLOMORPHY IN QUANTUM FIELD THEORIES AND GRAVITY

Eduardo Conde Pena

Santiago de Compostela, abril de 2012.

UNIVERSIDADE DE SANTIAGO DE COMPOSTELA

Departamento de Física de Partículas

HOLOGRAPHY AND HOLOMORPHY IN QUANTUM FIELD THEORIES AND GRAVITY

Tese presentada para optar ao grao
de Doutor en Física por:

Eduardo Conde Pena

Abril, 2012

UNIVERSIDADE DE SANTIAGO DE COMPOSTELA

Departamento de Física de Partículas

Alfonso Vázquez Ramallo, Catedrático de Física Teórica da Universidade de Santiago de Compostela,

CERTIFICO: que a memoria titulada “*Holography and holomorphy in quantum field theories and gravity*” foi realizada, baixo a miña dirección, por Eduardo Conde Pena, no departamento de Física de Partículas desta Universidade e constitúe o traballo de Tese que presenta para optar ao grao de Doutor en Física.

Asinado:

Alfonso Vázquez Ramallo.

Santiago de Compostela, abril de 2012.

A mis padres

*What I cannot create,
I cannot understand.*

Became famous when found
in Feynman's last chalkboard.

Agradecimientos

En primer lugar me gustaría agradecer a Alfonso Ramallo la oportunidad de hacer el doctorado bajo su tutela. Es alguien de quien un estudiante de doctorado tiene mucho que aprender: por ejemplo su metodología de trabajo, su dedicación y su continua ilusión son excelentes valores para “un joven aprendiz”. Le tengo que agradecer las muchas veces que nos hemos sentado a hacer cuentas codo con codo, algo nada común y que alivia sobremanera la tortuosa iniciación al mundo de la investigación. Espero no haber agotado su paciencia con mi ignorancia y algunas de mis manías: aunque sigo aprovechando demasiado la celulosa, ¡logré acabar el paquete de los 500 folios en blanco! La atmósfera agradable en nuestro grupo, con el “Big Three” que forma junto a Javier Mas y Jose Edelstein, ha sido un muy agradable caldo de cultivo para mi formación.

Junto a Alfonso, las personas que mas me han influido en mi formación como físico, y a quien también debo unas enormes “gracias” son (curiosamente hispano-hablantes las dos) Carlos Núñez y Freddy Cachazo. Carlos ha sido poco menos que mi co-advisor durante prácticamente todo mi doctorado y, aunque haya sido por ósmosis, algo me ha conseguido pasar de su inagotable saber de Field Theory. Carlos, tu entusiasmo perpetuo es altamente contagioso ¡Te debo mucho en la Física y también en lo personal! A Freddy lo he conocido hace poco, y por un breve tiempo durante mi estancia en Canadá; pero le ha sobrado para marcarme también con su visión preclara de la Física. Gracias también por dedicarme una buena parte de tu tiempo a trabajar juntos en Canadá.

Of course, my physics personality (and my personal character as well!) cannot be understood without all the people (students, post-docs, colleagues, etc...) that I have met along the way. If this were an advertisement, I should make a disclaimer: I may contain traces of all these people. In the first place, I would like to thank all the physicists, and also friends, with whom I have shared appreciable time (and some enjoyable collaborations!) in Santiago, like Daniel Areán, Javier Tarrío, John Shock, Dimitrios Zoakos, Xián Camanho, Paolo Benincasa (who explained a lot of new things to me), etc. From all of them I have learnt Physics, and spent great times both in Santiago and in meetings abroad. During my different stays abroad, all of them very amusing, I have met many more people that I would also like to recall here: of course Jérôme Gaillard, from Swansea, who also spent a very fructiferous year in Santiago, and with whom it is a pleasure to collaborate; in Swansea there were actually many nice people: Johannes Schmude, Agostino Patella, Joyce Myers, Prem Kumar, Maurizio Piai, Biaggio Lucini, Adi Armoni, ... all constituted a group whose nicety, as Carlos would say, is difficult to match. Dalla mia permanenza a Trieste, voglio ringraziare un' altra volta a Daniel, che fece che le due mesi e mezzo che fu lá furono molto belli (e con molta epica sportiva!). Discussing some Physics with Chethan Krishnan was very stimulating, e mi porto un sacco di ricordi della gente italiana: Alessandro Lovato e Andrea Prudenziati, i due guerrieri sulla bici, Luca Lepori (la sua storia della chiave e il Taurus é la piú divertente che mai ho sentito in inglese), e tantissima altra gente con chi ho viaggiato a Croazia, fatto diverse “meeting at 6pm, 6 floor, left wing”, bagnato nell Adriatico dopo la notte, etc. And I cannot forget either all the people I met in Perimeter Institute during my more recent stay: the many lunch discussions about anything with João Caetano and John

Toledo, the collaboration with Sayeh Rajabi, y toda la comunidad hispana que allí conocí, como Pedro Liendo (aunque él sólo estuviera de paso) y Coco (Jorge Escobedo). Finalmente, en esta sección de Física, me gustaría agradecer en último lugar a quien empezó un poco todo y me introdujo, o alimentó, el gusanillo por la Física: mi profesor de bachillerato Fernando Botana; gracias por unas irreverentes y muy especiales clases de Física.

E por suposto, de fóra da Física (aínda que moitos dos implicados sexan físicos) lévome os meus recordos máis doces destes cinco anos de doutorado. Moitos dos meus compañeiros dunha moi agradábel nosa promoción, e doutras promocións e carreiras, ficaron por Compostela e con eles seguí a compartir tempo nas pedras da zona vella: Xián (outra vez), Álex, Lu, Jesús, Ana, Celes, Gonza, Vane, os diversos Migueles matemáticos, Algúns logo marcharon, pero as conexións ficaron: Delia, Xe (a túa casa en Madrid podería dicirse que é a miña segunda residencia oficial ;)), a Xouba; moitas grazas polas numerosas reunións que temos feito estes anos. Da facultade tamén me levo o recordo de moita outra xente, como de Luíño, que ao igual que Carlos tamén posee un contaxioso entusiasmo, e particularmente de Dani, Brais e Breixo. Dani e Breixo aprendéronme a esquiar tirándome dende o curuto da pista máis alta de Andorra, e as nosas peregrinaxes anuais á neve están cheas de engrazadas anécdotas. Brais contribuíu á miña introdución no mundo da bici, e con el e Breixo demos renda solta durante todos estes anos á nosa paixón polo balón e compartimos alegrías e desilusións nos “Autos Liouville”, que ficará como o equipo do meu corazón. Por suposto teño que voltar a contar a Daniel outra vez aquí; agardo que todas as boas tradicións que creamos estes anos sigan por moitos vindeiros! Outra xente que coñecín fóra de Santiago e que me gustaría mencionar aquí tamén son Jacek e Alberto, proba de que as amizades “a distancia” son posíbeis. Tampouco me quero esquecer de todo o grupo do CLM de italiano, con quen compartín unha viaxe máxica ao sur de Italia. Moi especialmente, grazas a Ceres e ao Mapache/Orsetto, dúas das persoas máis entretidas que coñecín na miña vida, que non reparan en loucuras, e con quen compartín momentos moi singulares durante as miñas estadias fóra. Some special thanks go to “amazing Grace”, whose magical personality made my first stay abroad in Swansea unforgettable, and with whom I shared some more good times afterwards, and hopefully I will share more in times to come; 57 forever! E finalmente, as grazas máis especiais van para o Koala, que me leva apoiando dende tempos inmemoriais e que sempre estivo aí durante todos estes anos en Compostela. Es a constante universal ;). Esta parte de agradecementos tería que ter sido escrita en Fontes. . . mais cando menos algo do que alí escribín ficou aquí plasmado!

Y para finalizar, en este caso es cierto que “los últimos serán los primeros” (un dicho que nunca entendí muy bien, la verdad; pero este puede ser un buen ejemplo), me gustaría agradecer a toda mi familia, productores de un entorno hogareño maravilloso, que me ha servido de “campo base” para llegar hasta donde me encuentro ahora. Obviamente, muy especialmente las gracias van para mi familia “más cercana”, Marta, mis padres y Lambda incluida, donde siempre he recibido un apoyo fundamental para mí; y en particular a mis padres, a quienes esta tesis va dedicada y que han generado de la nada mi (importantísima) inercia en la vida. Y lo han hecho sin necesidad ninguna de saber de Física.

“Caminante, no hay camino, se hace camino al andar.”

Contents

1	Introduction	5
1.1	Motivation	5
1.2	Context of this thesis	6
1.3	Content of this thesis	10
1.4	Fix the notation	11
2	Scattering amplitudes on the complex plane	15
2.1	A briefing into scattering amplitudes	15
2.1.1	The spinor-helicity formalism	18
2.1.2	Three-point amplitudes	20
2.2	On-shell recursion relations	21
2.2.1	The BCFW construction	21
2.2.2	Generalizing BCFW	25
2.2.3	Comments on zeroes	27
2.3	The complex-UV behavior	28
2.3.1	Factorization in the P_{ij} channel	29
2.3.2	The exponent ν	33
2.3.3	Four-particle amplitudes	35
2.4	Building theories	36
2.4.1	A general classification	37
2.4.2	Minimal-coupling interactions	38
2.4.3	Higher-derivative interactions	45
2.4.4	A summary	49
3	Non-perturbative physics with String Theory	51
3.1	The gauge/gravity correspondence	51
3.2	Some words on supersymmetry	53
3.2.1	Reducing the supersymmetry of $\mathcal{N} = 4$ SYM	55
3.2.2	The Maldacena-Núñez solution	57
3.2.3	The Klebanov-Strassler solution	60
3.3	Flavor in the gauge/gravity correspondence	64
3.3.1	The smearing technique	66

4	Flavor Physics in 3d Chern-Simons-matter theories	75
4.1	The AdS_4/CFT_3 correspondence	75
4.1.1	The ABJM solution	78
4.1.2	ABJM geometry	80
4.1.3	The Ooguri-Park solution	83
4.2	Deforming the ABJM background	84
4.2.1	Supersymmetry analysis	86
4.2.2	Anti-de-Sitter solutions	87
4.2.3	Running solutions	89
4.3	Adding flavors	92
4.3.1	Supersymmetric embeddings of flavor D6-branes	92
4.3.2	Backreacted massless flavor	94
4.3.3	Flavored Anti-de-Sitter solutions	97
4.3.4	Backreaction with massive flavors	102
4.4	Some flavor effects in the dual field theory	104
4.4.1	Free energy on the sphere	104
4.4.2	Wilson loops and quark-antiquark potentials	106
4.4.3	Dimensions of scalar meson operators	108
4.4.4	Dimensions of high spin operators	110
4.4.5	Particle-like branes	110
4.A	The method of supersymmetry variations	112
4.A.1	Supersymmetry for the Anti-de Sitter solutions	114
4.A.2	Supersymmetry for the unflavored ABJM solution	116
5	Flavor Physics in $\mathcal{N} = 1$ theories	117
5.1	The CNP solution	117
5.1.1	The type IIB background	118
5.1.2	Some complex geometry	121
5.1.3	Physics of CNP	124
5.1.4	Physics of a solution without flavors	131
5.2	De-singularizing CNP	134
5.2.1	The macroscopic approach	135
5.2.2	The microscopic approach	139
5.2.3	Analysis of singularities	143
5.3	Physics of SQCD with massive flavors	148
5.3.1	Solutions of the master equation	148
5.3.2	Seiberg duality	154
5.3.3	Wilson loops	155
5.3.4	k-string tensions	157
5.4	Physics of cascading theories	161
5.4.1	The rotation	162
5.4.2	Solving the master equation again	166
5.4.3	Field theory comments	171
5.4.4	Towards applications	174

5.A	A glance at the microscopic approach	179
5.A.1	Holomorphic structure in the Abelian limit	179
5.A.2	Abelian limit of the simple class of embeddings	180
5.A.3	An example of a non-compatible embedding	183
6	Miscellanea of more flavor physics	185
6.1	A Kutasov-like duality	185
6.1.1	The $\mathbb{H}_2 \times \widetilde{SL}_2$ ansatz	186
6.1.2	Supersymmetry analysis	188
6.1.3	Brane setup	190
6.1.4	A geometrical remark	191
6.1.5	Master equation solutions	192
6.1.6	The Field Theory interpretation	196
6.2	SQCD in low dimensions	200
6.2.1	A macroscopic point of view	202
6.2.2	A microscopic interpretation for the flavor branes	209
7	A final summary	215
8	Conclusions	219
9	Resumo	223
9.1	O réxime perturbativo: amplitudes de <i>scattering</i>	226
9.2	O réxime non perturbativo	229
9.2.1	Sabor en teorías de Chern-Simons	230
9.2.2	Sabor en teorías con supersimetría $\mathcal{N} = 1$	231
9.2.3	Outras teorías con sabor	233
10	Conclusiones	235

Chapter 1

Introduction

1.1 Motivation

Curiosity about the Universe we live in is an old habit of humans, who (most of the time) have marveled at how the world surrounding us works. If we go beyond a simple description, and attempt to understand why things happen, or more precisely, attempt to predict how things will happen; then this is really what Physics is all about. Propose a theory that explains what you see (preferably explaining several things you see, and ideally predicting what you do not see yet as well!), and test it “in the lab”. This is what Galileo said.

Now, we have come a long way since Galileo’s times. We have seen that the classical intuition we grow used to reason with does not apply anymore in the “microscopic world” of atoms and subatomic particles, where the intuitive Classical Mechanics must be substituted by the more abstruse Quantum Mechanics. Our conception of “macroscopic” everyday notions like time has also departed from the classical vision, giving rise to a relativistic one where space and time merge into a new entity, the space-time, which is dynamical as well. Both Quantum Mechanics and Relativity have proven to be of great experimental success, and they are the two pillars any physical theory must encompass nowadays. The theories that meet this requirement are the so-called Quantum Field Theories (QFTs), and they are the most accurate tool we have today to describe Nature. More precisely, these theories aim to describe the “building blocks” of Nature, *i.e.* the known fundamental interactions: gravity, electromagnetism, strong force, and weak interaction. Of these four, the last three are described by gauge theories, the most popular among all field theories. But gravity has withstood so far all attempts to be combined with Quantum Mechanics, and the successful attempts at building a quantum gravity, like String Theory, still seem nowadays far from being useful to describe our Universe.

So on the one hand gravity does not fit well in the quantum picture, and on the other hand QFTs, while yielding some spectacular predictions, are still far from being completely figured out (in general we are only able to extract a partial amount of the information they contain). There is still much to be understood. It is the aim of this Ph.D. thesis to explore some of the recent tools, related with holography and holomorphy, that help us to improve this understanding, and hopefully will ultimately improve our comprehension of our Universe.

1.2 Context of this thesis

Quantum field theories (see [1, 2] for some introductory textbooks) are extremely powerful tools. However, we do not understand them as well as we would ideally like. First of all, they still lack a fully rigorous mathematical foundation, and second, we do not know how to extract, in general, all the dynamics they encode. Notice that for instance solving these two issues for the Yang-Mills theory is one of the Millennium Prize problems [3], and would explain why the strong force is short-ranged or why we never see individual quarks, as we observe experimentally in the laboratory.

A useful QFT contains interactions. The strengths of these interactions are characterized by couplings. Say we only have one coupling $g \in \mathbb{R}$. One typically distinguishes two regimes in a QFT: a perturbative one, and a non-perturbative one. In the perturbative one, we usually assume that g is small (although this is not necessary), and compute quantities in a power series in g . When g is small, this series can be truncated to the first terms, and we obtain a sensible approximation for the quantity we are computing. This method gives some information about the dynamics that is local in the space of the couplings. But many dynamical features like confinement, symmetry breaking or dualities require understanding the QFT at all values of the coupling, *i.e.* it requires non-perturbative information.

A fruitful way of thinking about the difference between perturbative and non-perturbative regimes is by recalling the properties of holomorphic functions¹. Make g complex (this actually comes naturally for many QFTs), and think of the observables derived from the QFT as complex functions of g . Imagine an observable given by

$$\mathfrak{D} = \int_{-\infty}^{\infty} dx e^{-x^2 - gx^4} = \frac{e^{\frac{1}{8g}}}{2\sqrt{g}} K_{\frac{1}{4}}((8g)^{-1}) , \quad (1.2.1)$$

where $K_{\frac{1}{4}}$ is a Bessel function of the second kind. Notice that this integral resembles the path integral of a theory with a quartic interaction, but done in one instead of infinite dimensions. The integral (1.2.1) can be computed exactly for all values of g , but in practice this is not the case. One generically expands in g :

$$\mathfrak{D} = \int_{-\infty}^{\infty} dx e^{-x^2} \sum_{n=0}^{\infty} \frac{(-gx)^{4n}}{n!} \stackrel{!!!}{=} \sum_{n=0}^{\infty} \frac{(-g)^n}{n!} \int_{-\infty}^{\infty} dx x^{4n} e^{-x^2} = \sum_{n=0}^{\infty} (-g)^n \frac{\sqrt{\pi} (4n)!}{2^{4n} (2n)! n!} =: \mathfrak{D}_{\text{pert}} . \quad (1.2.2)$$

We have obtained a perturbative expansion $\mathfrak{D}_{\text{pert}}$ for the observable \mathfrak{D} , in powers of g , but the middle step, where we changed the order of the infinite sum and the integral, is not correct. The resulting series in the right-hand-side of (1.2.2) has a zero-radius of convergence (despite the observable being perfectly well-defined for any value of the coupling)! It is what one calls an asymptotics series. This is what one usually has in QFT (see for instance the easy example Dyson discusses in [5]). However, summing “some of the first” terms one obtains an excellent approximation of the exact result if g “is small”. It is when we sum “a lot of them” that the perturbative expansion (1.2.2) starts to diverge from the non-perturbative result (1.2.1). How is this possible?

¹I take the example from [4], where an interesting, although not fully rigorous, account of these topics can be found.

The puzzle is solved by performing a saddle-point approximation in the integral. Then one has to find the minima of the integrand, and there are three of them:

- One is $g = 0$, and the saddle point approximation corresponds to the expansion $\mathfrak{D}_{\text{pert}}$ around $g = 0$. This is the perturbative contribution.
- But there are other two minima when $g = -\frac{1}{2x^2}$ (although the physical region might be only $g > 0$, one must take into account all $g \in \mathbb{C}$). The contribution to the observable around these minima, $\mathfrak{D}_{\text{non-pert}}$, is proportional to $e^{-\frac{1}{4g}}$. These are the non-perturbative contributions! They are usually called instantonic contributions as well.

Notice that for fixed g , the second minima happen at complex values for $x = \pm \frac{i}{\sqrt{2g}}$, which *a priori* are not in the region of integration of (1.2.1). The story is delicate, but it turns out that it is only when we take into account the contribution around these second minima as well:

$$\mathfrak{D} = \mathfrak{D}_{\text{pert}} + \mathfrak{D}_{\text{non-pert}} , \quad (1.2.3)$$

that we recover the exact result, *i.e.* the sum of the three contributions in (1.2.3) does coincide with the exact result (1.2.1). This toy example makes clear the difference between perturbative and non-perturbative information. The perturbative contribution is, as we said, local in the couplings: all the derivatives of $e^{-\frac{1}{4g}}$ vanish at $g = 0$, so the instantonic contributions are invisible to perturbation theory. Notice that g can be as big as desired in the expansions in (1.2.2); strong coupling is an independent notion from non-perturbative. The reason why they are usually associated has to do with the regime of validity of the perturbative approximation. The sum of the first n terms of the perturbative approximation $\mathfrak{D}_{\text{pert}}$ in (1.2.2) is a good approximation to the exact \mathfrak{D} as long as $e^{-\frac{1}{4g}} \ll g^n$, which happens roughly for $n \ll g^{-1}$: *i.e.* , the smallest the coupling g , the better perturbation theory approximates the exact result.

While the perturbative regime of QFTs is reasonably under control, the traditional techniques (Feynman diagrams) can certainly be improved. About the non-perturbative regime much less is known, but recent years have seen an increasing activity in this regard, much of it carried out by the String Theory community. This thesis will deal with both some new methods that apply in the perturbative regime, and some other methods that are useful to study non-perturbative dynamics. A few words about the historic origin of these techniques, that can be found within String Theory, follows.

On the perturbative side, for a long period after its development in the 50's, the way the perturbation theory of a QFT was understood was through Feynman diagrams. They are a very intuitive representation as everything is pictured in terms of local processes. However, as soon as the demands increased, for instance in the computation of scattering amplitudes (needed by experimentalists at the big accelerators), it became clear that Feynman diagrams were not the most efficient computational tool. After the 80's, a slow but constant progress was taking place; and a big boom happened when twistor techniques, inspired on String Theory, were introduced in [6]. A lot of activity has been going on in the field thereafter. The more general tools that have appeared are the on-shell recursion relations. The landmark

example is the BFW formula [7], that allows to compute scattering amplitudes at tree level recursively, by continuing them to the space of complex momenta and using *holomorphy* properties of functions on the complex plane. This formula, as well as the many other developments (that also apply to loop computations), have brought new fresh insights into the world of perturbation theory, that are useful for both theorists and experimentalists, and that are changing the way we think about it.

On the non-perturbative side, the contributions coming from String Theory have been more numerous and have already left a significant imprint. The cornerstone of all these contributions is the *AdS/CFT* correspondence [8] (*AdS* stands for the anti-de-Sitter space, and CFT for conformal field theory), a beautiful realization within String Theory of the earlier ideas of the large- N expansion of gauge theories [9] and holography [10]. Maldacena's extraordinary idea that $\mathcal{N} = 4$ Super-Yang-Mills could be described via type IIB String Theory living in $AdS_5 \times S^5$ and vice versa, in a duality that interchanges strong and weak coupling regimes, has revolutionized not only the community of string theorists, but it is bound to make a very broad impact in Theoretical Physics (if it has not already). Maldacena's idea has been generalized in several directions, and the picture that seems to be emerging is that of a certain type of *holography*: a strongly coupled QFT is best described by a theory in one more dimension, where this extra dimension is related to the energy scale of the QFT, and the renormalization group equations are encoded in the Einstein equations of the higher-dimensional theory, which turns out to contain gravity. If one incorporates supersymmetry in the mix, a fascinating interplay between holomorphy, Quantum Field Theories, holography and gravity emerges, conforming a new canvas in Theoretical Physics that will likely stay for years to come. As a final remark, it is mandatory to mention that other impressive non-perturbative methods have also flourished under the AdS/CFT correspondence during the last years, and that will not be touched in this thesis, such as integrability [11] or localization techniques ([12, 13]).

What is String Theory?

It is impossible to ignore the impact of String Theory (some standard references in chronological order are [14, 15, 16]) on the community of Theoretical Physics over the last couple of decades. It was born in the 70's as a theory of the strong force, but has evolved so much that it is difficult today to believe that that was the original germ.

String Theory is, in short, the quantum theory of an oscillating relativistic string. If we add supersymmetry, then we talk about Superstring Theory. This string describes a two-dimensional surface, called world-sheet, as it propagates in some D -dimensional space-time. The tension of the string is $T = (2\pi\alpha')^{-1}$, where α' is a positive parameter called the Regge slope. The size of this string is $l_s \sim \sqrt{\alpha'}$. The action of the string is essentially proportional to the area of the world-sheet. When one quantizes this action (notice that space-time coordinates become quantum fields), one obtains a prediction for the dimension D ($D = 10$ for the superstring), and a set of possible vibration modes for the oscillating string. Each of these modes represents a particle/field. Since there is an infinite number of different oscillating modes, String Theory is not a Quantum Field Theory in the ordinary

sense. It is “something more”². It is yet unclear what this exactly is, and whether it will be useful to describe Nature (most likely, it will not be in the original sense of “Theory Of Everything” people used to think about).

More is known about the low-energy limit of String Theory, where we explore energies much smaller than the inverse size of the string l_s . In this limit one can restrict to the massless sector of the Superstring Theory. In this sector, we find the so-called Neveu-Schwarz-Neveu-Schwarz (NSNS) ten-dimensional fields: a metric $g_{\mu\nu}$, a two-form field B_2 (called B-field or Kalb-Ramond field), and a dilaton Φ ; the so-called Ramond-Ramond fields: a series of p -forms C_p ; and all their fermionic superpartners. Requiring that the theory on the world-sheet is conformal, one obtains a set of equations of motion for these fields. At first order in α' , these equations are the equations of supergravity. So *supergravity is the low-energy regime of String Theory* (the only regime we will be concerned about in this thesis). Actually, there are several possibilities for the consistent quantization of the string that lead to different String theories: type IIA/B, type I and two heterotic. The general belief is that all of these theories, related through a web of dualities, are limits of a unique eleven-dimensional theory called M-theory, about which little is known apart from the fact that its low-energy limit is eleven-dimensional supergravity.

Apart from α' , String Theory has another parameter, g_s , that characterizes how strings scatter. It is related to the dilaton, when this is constant, as $g_s = e^\Phi$. And apart from strings, String Theory was found to have another kind of higher-dimensional objects, the so-called branes. These objects could have been presumably discovered had one quantized open strings instead of closed ones (the equivalence of these two descriptions goes under the name of open/closed string duality), since branes are the objects where open strings can end. In the case of type IIA/B String Theory, these objects are called D p -branes [18, 19], and they carry the charge of RR potentials C_{p+1} (p is even in type IIA and odd in type IIB). The discovery of branes revolutionized the field, since the theories living on their world-volume have similarities with the QFTs we are used to. Of course, this lies at the heart of the *AdS/CFT* correspondence.

Although String Theory was a little over-hyped in the 90's, announced as the theory unifying all known interactions; what is clear is that String Theory has inspired a ridiculously big number of novel methods and ideas that are applied in a ridiculously wide range of fields: from pure-mathematics areas (where several Fields Medals have been awarded as a result), to Conformal Field Theories, supersymmetric theories, scattering amplitudes or Condensed Matter, just to name a few. Hopefully more surprises will be disclosed in the coming years, as we slowly keep figuring out String Theory, leading to new insights and ideas that will remain, even if String Theory fades away in the distant future.

²As one of the modes of oscillation is a graviton, String Theory is certainly a quantum theory of gravity. Although some other ideas for quantum gravity float around ($\mathcal{N} = 8$ Supergravity, Loop Quantum Gravity, Causal Sets, etc. . .), String Theory is hitherto the firmest consistent framework where one can, for instance, explain in glorious details the microscopic origin of the Bekenstein-Hawking entropy [17].

1.3 Content of this thesis

This thesis can be split into two disconnected parts, that can be read independently. The first one comprises chapter 2, where the attention is focused on the perturbative techniques. An original account of the new recursion relations put forward in the works [20, 21] is presented there. The second part, that encompasses chapters 3-6, is based on the papers [22, 23, 24, 25, 26, 27, 28] and deals with the non-perturbative methods derived from holography. Several examples where the gauge/gravity correspondence is used to explore non-perturbative features of different gauge theories are worked out.

Let us be a bit more detailed. We start in chapter 2 with the simplest part of the thesis, both technically and conceptually; but the most general and powerful one as well. We study from an S-matrix perspective, the scattering amplitudes of any QFT of massless particles at tree level. This is possible thanks to a generalization of the BCFW recursion relation found in [20]. One can then require a certain consistency condition on four-particle amplitudes, proposed originally in [29] and applied without limitations in [21], which has far-reaching implications for the possible theories one can build. Most of the known QFTs are recovered (as expected, although we do it from point of view quite different from the traditional one), but the main result has to do with what QFTs cannot be built consistently.

After this study of the perturbative regime of QFTs, which sheds some new light on why they are what they are, we move to the study of their non-perturbative regime for chapters 3-6. In chapter 3, we write a brief introduction to the holographic techniques we are going to use, that go under the name of gauge/gravity correspondence. We assume the reader is familiar with the generalities of the correspondence, and focus on the particular topic that is central to the second part of this thesis, that is the “addition of flavor” into the “supersymmetric sector” of this duality, *i.e.* the correspondence between supersymmetric gauge theories and supergravity theories.:

To describe realistic gauge theories via holography, an important ingredient not present in the original Maldacena’s example is fundamental matter, commonly called flavor. It has been known for a while how to incorporate flavor in the correspondence, namely by introducing extra “flavor” D-branes. In order to have phenomenologically interesting flavor³, one has to work in the Veneziano limit, that amounts on the gravity side to introducing a large number of flavor branes, that will therefore modify the original “unflavored” theory. Computing the backreaction of the flavor branes on the geometry is a highly non-trivial task. We study this backreaction and its observable consequences in the dual QFT in different setups, hopefully illustrating how this idea could be implemented for any setup.

In particular, we study flavor in three different setups, namely Chern-Simons-matter theories, $\mathcal{N} = 1$ theories and SQCD-like theories in less than four dimensions. We have arranged them according “how clean the duality is”:

- First we start with Chern-Simons-matter theories in chapter 4. The field theory with flavor is conformal, and correspondingly the supergravity solution has an AdS factor. This setup is ideal for the applicability of gauge/gravity techniques.
- Then, in chapter 5, we study a particular class of $\mathcal{N} = 1$ theories with known gravity

³Richer phase transitions, Seiberg-like dualities, screening effects, different central charges in a CFT, etc.

duals. These theories are not conformal and display a non-trivial RG flow encoded in a non-trivial non- AdS geometry. They have been very well studied, and consequently one has a reasonable handle on how the duality works. They are the most interesting for phenomenological purposes.

- We examine in chapter 6 several other examples of gauge/gravity dualities, showing how they can be used to study features like non-perturbative dualities in $\mathcal{N} = 1$ theories, and to build duals to SQCD theories in less than four dimensions. Since the duality is not so clear in these cases, we focus on the supergravity constructions, leaving aside most of the field theory discussions made in the original references.

Finally, we draw some conclusions of all the work in chapter 8, and compose an extra-brief summary in chapter 7.

1.4 Fix the notation

Just before we get started with business, we stop to comment on the notation and conventions we are going to use. It is standard notation, but it is better to gather it here instead of scattering it around different places in the thesis.

We start with supergravity actions, frame conventions and equations of motion. We are sketchy since we will not use the actions directly in this thesis (details can be found in the articles the thesis is based on). The equations of motion of the low energy limit of any of the type II String Theories can be derived from an action of the form:

$$S_{II} = \frac{1}{2\kappa_{10}^2} \int_{\mathcal{M}_{10}} e^{-2\Phi} (R + 4 (\partial_\mu \Phi) (\partial^\mu \Phi)) \omega_{\text{Vol}(\mathcal{M}_{10})} + \int_{\mathcal{M}_{10}} (\text{fluxes}) , \quad (1.4.1)$$

where⁴ $\omega_{\text{Vol}(\mathcal{M}_{10})} = d^{10}x \sqrt{-\det[g]}$ is the volume form of the manifold \mathcal{M}_{10} , with $(g)_{\mu\nu}$ being the matrix associated with the ten-dimensional metric. The constant $2\kappa_{10}^2 = (2\pi)^7 g_s^2 \alpha'^4 = 8\pi G_N^{10}$ measures the ten-dimensional Newton constant G_N^{10} . The R term is not the canonical one for a gravitational action. This is why we say that the action (1.4.1) is in the string frame (it is the action the string sees!). We can go to the more canonical action if we perform the following redefinition of the metric:

$$(g_{\mu\nu})_{\text{Einstein frame}} = e^{-\frac{\Phi}{2}} (g_{\mu\nu})_{\text{string frame}} . \quad (1.4.2)$$

We call this moving from the string to the Einstein frame. The other fields, RR fluxes B-field and dilaton Φ , are not affected, but the action changes. The new action reads

$$S_{II} = \frac{1}{2\kappa_{10}^2} \int_{\mathcal{M}_{10}} \left(R - \frac{1}{2} (\partial_\mu \Phi) (\partial^\mu \Phi) \right) \omega_{\text{Vol}(\mathcal{M}_{10})} + \int_{\mathcal{M}_{10}} (\text{fluxes}) , \quad (1.4.3)$$

Which frame to choose is a matter of convenience. For instance the equations of motion for $g_{\mu\nu}$ (*i.e.* the Einstein equations) and the dilaton are nicer for the Einstein frame action

⁴We always use $\omega_{\text{Vol}(X)}$ to denote the Riemannian volume form of the manifold X , while $\text{Vol}(Y)$ always denotes the volume of the manifold Y . We hope this does not cause confusion.

(1.4.3). On the contrary, the equations of motion for the RR fluxes are somewhat more appealing if we use the action (1.4.1) in string frame. The Dirac-Born-Infeld (DBI) action of the Dp -branes also depends on the frame we use.

$$(S_{\text{DBI}})_{\text{string frame}} = -T_{Dp} \int_{Dp} e^{-\Phi} \sqrt{-\det [\iota^* (g + \mathcal{F} - B_2)]}, \quad (1.4.4)$$

$$(S_{\text{DBI}})_{\text{Einstein frame}} = -T_{Dp} \int_{Dp} e^{\frac{p-3}{4}\Phi} \sqrt{-\det [\iota^* (g + e^{-\Phi/2} (\mathcal{F} - B_2))]}, \quad (1.4.5)$$

where ι is the embedding of the world-volume of the Dp -brane in the ten-dimensional geometry, and ι^* its pullback. Sometimes we will also use hats to denote pullbacks, *e.g.* $\hat{g} := \iota^*(g)$. The Wess-Zumino (WZ) action is the same in both frames:

$$\begin{aligned} S_{\text{WZ}} &= T_{Dp} \int_{Dp} \iota^* (e^{\mathcal{F}-B_2} \wedge C_{\text{all } p}) := \\ &:= \int \iota^* \left(C_{p+1} + (\mathcal{F} - B_2) \wedge C_{p-1} + \frac{1}{2} (\mathcal{F} - B_2) \wedge (\mathcal{F} - B_2) \wedge C_{p-3} + \dots \right), \end{aligned} \quad (1.4.6)$$

In the actions above, \mathcal{F} denotes the field-strength of the world-volume gauge field \mathcal{A} , and T_{Dp} the tensions of the branes, which are:

$$T_{Dp} = \frac{1}{(2\pi)^p g_s (\alpha')^{\frac{p+1}{2}}}. \quad (1.4.7)$$

We will make extensive use of Cartan's formalism (see for instance [30]) for the geometry of General Relativity, to which we will refer many times in the text simply as Gravity. In a D -dimensional space-time with signature $(-1, 1, \dots, 1)$, we introduce a set of D one-forms e^a , called the *vielbein*, which is “the square root of the metric”:

$$e^a = e^a_\mu dx^\mu, \quad g_{\mu\nu} = \eta_{ab} e^a_\mu e^b_\nu, \quad (1.4.8)$$

where η_{ab} is the D -dimensional Minkowski metric. The latin indices $\{a, b, \dots\}$ are called *flat indices*, while the Greek ones $\{\mu, \nu, \dots\}$ are called *curved indices*. The notion of affine connection is substituted by the *spin connection*: another set of $D(D-1)/2$ one-forms ω^a_b . In the absence of torsion the spin connection is not independent from the metric and coincides with the Levi-Civita connection:

$$\omega^a_b = \omega^a_{b\mu} dx^\mu, \quad 0 = de^a + \omega^a_b \wedge e^b. \quad (1.4.9)$$

Generically, working in flat indices is much easier than doing it in curved ones. An excellent implementation of Cartan's formalism for *Mathematica*, developed by Prof. Bonanos, can be found at <http://www.inp.demokritos.gr/~sbonano/RGTC/RiemannTensorCalculus.html>. Our convention for the Hodge operation $*$ is:

$$* (e^{a_1 \dots a_n}) = \epsilon^{a_1 \dots a_n}_{b_1 \dots b_{D-n}} e^{b_1 \dots b_{D-n}}, \quad \epsilon^{012 \dots 9} = 1. \quad (1.4.10)$$

has a sign difference with respect to Bonanos' implementation. We are denoting $e^{a_1 \dots a_n} = e^{a_1} \wedge \dots \wedge e^{a_n}$. Moreover, $\epsilon^{a_1 \dots}$ will always denote the Levi-Civita fully antisymmetric tensor. The way its indices are raised and lowered depends on the type of indices involved. For the indices in the Levi-Civita tensor of (1.4.10), this is done with the flat Minkowski ten-dimensional metric.

Finally, let us mention that we will have spinors ϵ in our geometries (notice that the ten-dimensional manifolds must be then spin manifolds). The spinors of type II supergravities are two component spinors, on which the Pauli matrices τ_i can act:

$$\epsilon = \begin{pmatrix} \epsilon_+ \\ \epsilon_- \end{pmatrix}, \quad \tau_1 = \begin{pmatrix} 0 & 1 \\ 1 & 0 \end{pmatrix}, \quad \tau_2 = \begin{pmatrix} 0 & -i \\ i & 0 \end{pmatrix}, \quad \tau_3 = \begin{pmatrix} 1 & 0 \\ 0 & -1 \end{pmatrix}. \quad (1.4.11)$$

The Dirac matrices of the D -dimensional Clifford algebra will be denoted by Γ_a ($\{\Gamma_a, \Gamma_b\} = 2\eta_{ab}$), with the indices a are flat indices referring to the corresponding vielbein, and $\Gamma_{a_1 \dots a_n}$ will denote the antisymmetrized product:

$$\Gamma_{a_1 \dots a_n} = \Gamma_{[a_1, \dots, a_n]} = \begin{cases} \Gamma_{a_1} \cdots \Gamma_{a_n} & \text{if all the indices are different} \\ 0 & \text{in other case} \end{cases} \quad (1.4.12)$$

Chapter 2

Scattering amplitudes on the complex plane

Contextualizing this chapter

Traditionally understood through Feynman diagrams, the perturbation theory of Quantum Field Theories is benefiting from a lot of recent activity in the field. This activity has brought a lot of new insights to the theoretical understanding of perturbation theory (especially at the tree level), but it has brought joy to the experimental community as well, since the new methods are much more efficient at computing the scattering amplitudes needed in the lab. In this chapter we want to discuss an S-matrix approach to the tree level of theories of interacting massless particles. The idea is to use the results in [20, 21] to provide a self-contained presentation of an useful way of thinking about the perturbation theory of a very general class of theories (containing all the known “fundamental” theories). This new way of thinking is in some sense a revival of the S-matrix program of the 60’s, trying to provide an axiomatic approach to theory-building.

2.1 A briefing into scattering amplitudes

The main experimental access we have to high energy physics is through the experiments done at the big colliders. What one does is to accelerate two beams of particles until they have a high kinetic energy, and then let them collide. Then we observe the leftovers of this collision, and infer the physics going on. This might seem like an intricate way of doing experiments, but the nature of Quantum Mechanics, where trajectories of particles do not exist anymore, does not leave room for many other options.

Then, the most relevant piece of information of a theory is how particles scatter, *i.e.* the probabilities of obtaining certain final configuration of particles given an initial one, or more precisely, the cross section of the process. This cross section is, up to kinematical factors, the modulus squared of the scattering amplitude of the process. Let us start by recalling the definition of the scattering amplitudes from the S-matrix of a QFT:

$$S = \mathbb{1} + i \mathbb{T} , \tag{2.1.1}$$

where $\mathbb{1}$ is the identity matrix. A theory is *unitary* when its S-matrix satisfies:

$$S^\dagger S = \mathbb{1}. \quad (2.1.2)$$

Unitarity is, in short, the requirement that all probabilities are positive and their adding up to one. This is something we definitely desire for any physical theory, and it is a built-in requirement in an S-matrix approach. The way to compute scattering amplitudes from the S-matrix is to strip the identity (that accounts for the particles not interacting) from (2.1.1), and sandwich with the asymptotic states in the Hilbert space that define the set of incoming and outgoing particles, $|\{p_{\text{in}}\}\rangle, |\{p_{\text{out}}\}\rangle$. The amplitude M for the scattering of the ingoing particles into the outgoing ones is then

$$M(\{p_{\text{in}}\}, \{p_{\text{out}}\}) \delta^{(4)}\left(\sum p_{\text{in}} + \sum p_{\text{out}}\right) = \langle \{p_{\text{in}}\} | i\mathbb{T} | \{p_{\text{out}}\} \rangle. \quad (2.1.3)$$

Along all the chapter, we use for convenience the convention that all the particles are outgoing. This is easily achieved by exchanging ingoing particles by outgoing anti-particles with opposite momentum (this operation is sometimes referred to as crossing symmetry¹). Then we want to study the object

$$M_n(p_1, \dots, p_n), \quad \sum_{i=1}^n p_i = 0. \quad (2.1.4)$$

Notice that here we are characterizing the particles just by their momenta. In the case of particles with spin $s \neq 0$, we need also polarization tensors to fully characterize the particles scattering. Moreover, the particles can have quantum numbers though, like the color in YM. In these cases, one strips the algebraic factors out and talks about color-ordered amplitudes. It should be understood that the amplitude (2.1.4) includes all these subtleties. For most of the things we are going to say in this chapter, these subtleties are not very important.

We distinguish several perturbative contributions to (2.1.4):

$$M_n = M_n^{\text{tree}} + \sum_{L=1}^{\infty} M_n^L, \quad (2.1.5)$$

where each of the contributions comes with a different power of the coupling constants. The term with the smallest power is the tree-level contribution, and the rest are the loop contributions. *We focus only on the tree level*, which is arguably the most important one, as it is needed in the computation of all loop amplitudes. Moreover, when the coupling constants are “small”, the tree level can be a good approximation of the full amplitude.

So how does one compute the object in (2.1.4)? If we have a Lagrangian dictating how the scattering particles interact, it is possible to use the Feynman representation of the amplitude M_n . This representation is constituted by a sum of (in general) various different diagrams, each of them representing “a way the scattering can happen in terms of local processes that can be read from the Lagrangian”. There is also a set of rules that follow

¹The crossing symmetry of the S-matrix is a general result of QFT, see for instance [2].

from the Lagrangian explaining how each of these diagrams should be computed. The tree level comprises the diagrams that can be drawn with no free momentum in them.

This sounds certainly nice, as we are used to see Lagrangians all the time, and the way from there to compute an amplitude is completely systematic and standardized nowadays (it took a while to understand well how to deal with non-Abelian gauge symmetries, the Fadeev-Popov method being the preferred tool today). So, why would we want then an alternative to Feynman diagrams?

- The main reason is simplicity. Feynman diagrams are not simple, or better, they are not a smart path to get simple results, when possible. It happens some times that one has to sum over a humongous number of Feynman diagrams to finally get zero. This happens because the Feynman representation does not generically make the symmetries of the theory explicit. Locality is preserved individually by the diagrams, but not other important properties like gauge invariance, which is only recovered after summing over all of them.

Moreover, in general, as the number of particles n increases, the number of Feynman diagrams to sum over increases exponentially with n , rendering the method highly impractical for say $n \sim 7, 8$ already.

- We can also say that the need of a Lagrangian might actually not be such a good thing. First of all, a Lagrangian is not always available, as it is the case for instance for some rational CFT's (for which correlators are perfectly well-defined), or some more exotic theories like the six-dimensional $(2, 0)$ theory. But more importantly (and more conjecturally as well), it might turn out that Lagrangians are not the most convenient way to do Physics after all.

Lagrangians contain a lot of off-shell structure, that is useless when computing scattering amplitudes. If we think about the path integral, this off-shell structure encodes all the information needed to compute the action of a particle traveling any path away from the one dictated by the equations of motion. Then one averages over all these paths to get the final answer. This is an intuitive picture, but a very impractical one, since at the end we only care about on-shell (observable) quantities. Let us illustrate this with an example: the Lagrangian for YM has two interaction vertices, a three-point vertex, and a four-point one. It turns out that the three-point one contains enough information to compute any n -point amplitude. The four-point vertex contains no physical information, its only mission being to guarantee gauge invariance off-shell²!

In summary, the Feynman representation of scattering amplitudes is intuitive because it pictures them in terms of local processes, but the price to pay is the inclusion of a lot of off-shell structure that obscures their computation. Moreover, it would be useful to find a representation which does not rely so heavily on locality, because although all the theories we use to describe Nature nowadays are local, there are hints that non-local descriptions

²The situation is even more spectacular for Gravity (which is a fine theory at tree level), because the Lagrangian contains an infinite number of interaction vertices, but only the three-point one is relevant for the computation of scattering amplitudes!

could be more useful. After all, String Theory is a non-local theory (strings are extended objects in space-time).

We would like this representation to mimic the ideas of the S-matrix program [31, 32, 33], whose aim was to have an axiomatic procedure to build scattering amplitudes starting from a set of four basic assumptions:

1. **Poincaré invariance.** As we are trying to describe theories in four-dimensional flat Minkowski space-time. Actually we just need the space to be asymptotically flat.
2. **Existence of asymptotic one-particle states.** They describe the particles we scatter. They are in correspondence with the irreducible representations of the Poincaré group.
3. **Analyticity.** We require that the S-matrix is analytic in the external momenta, as we continue them to complex values³.
4. **Locality.** This amounts to require that all the singularities of the S-matrix come from propagators. We will see towards the end of the chapter if this condition can be dropped.

One of the reasons⁴ for the failure of the original S-matrix program is that people were focusing on very complicated field theories: the ones with scalar massive particles (it turns out that non-Abelian gauge theories are much simpler; the simplest theories are not those with the simplest Lagrangian [34]). With hindsight, *we decide to focus only on theories with massless particles (recall moreover that we only work at tree level)*.

So for this chapter, everything is massless and tree-level. Then, a perfect tool for building the representation we want for this kind of theories seems to be the BCFW construction [7], that we review in the next section. This construction violates locality at intermediate steps while preserving gauge invariance, opposite to the Feynman representation, that preserves locality but loses gauge invariance at intermediate steps.

2.1.1 The spinor-helicity formalism

In this subsection, we briefly introduce the spinor-helicity representation of the scattering amplitudes, which is an extremely convenient way of writing them, especially in the case of massless particles. Instead of the traditional representation of amplitudes via momenta and polarization tensors, in the spinor-helicity formalism everything is expressed in terms of pairs of spinors $\lambda^{(i)}, \tilde{\lambda}^{(i)}$ and the helicities $\{h_i\}$ of the particles. In four dimensions, this is possible because of the isomorphism $SO(3, 1) \cong SL(2, \mathbb{C})$, which is implemented by the Pauli matrices $\tau_{a\dot{a}}^\mu = (\mathbb{1}_{a\dot{a}}, \vec{\tau}_{a\dot{a}})$:

$$p_\mu \longrightarrow p_{a\dot{a}} = \tau_{a\dot{a}}^\mu p_\mu = \lambda_a \tilde{\lambda}_{\dot{a}}, \quad (2.1.6)$$

³The analyticity requirement has been connected to causality, but the issue is not settled.

⁴The biggest obstruction to the S-matrix program was really to focus on a theory with asymptotic hadrons, for which no clear perturbative expansion existed.

where the last step is possible because p_μ is light-like, and therefore $\det(p_{a\dot{a}}) = m^2 = 0$. The spinors λ_a and $\tilde{\lambda}_{\dot{a}}$ transform respectively in the $(\mathbf{1}/2, 0)$ and $(0, \mathbf{1}/2)$ representation of $SL(2, \mathbb{C})$. In the real momentum space, these two spinors are related by complex conjugation: $\tilde{\lambda}_{\dot{a}} = \bar{\lambda}_a$. But in the complexified Minkowski space, the isometry group is $SO(3, 1, \mathbb{C}) \cong SL(2, \mathbb{C}) \times SL(2, \mathbb{C})$ and each of the two spinors λ_a and $\tilde{\lambda}_{\dot{a}}$ can be taken to belong to a different copy of $SL(2, \mathbb{C})$, so that they are not related by complex conjugation and, therefore, are independent of each other.

It is possible to define two inner product for spinors, one for each representation of $SL(2, \mathbb{C})$ under which they can transform:

$$\langle \lambda, \lambda' \rangle \equiv \epsilon^{ab} \lambda_a \lambda'_b, \quad [\tilde{\lambda}, \tilde{\lambda}'] \equiv \epsilon^{\dot{a}\dot{b}} \tilde{\lambda}_{\dot{a}} \tilde{\lambda}'_{\dot{b}}, \quad (2.1.7)$$

with $\epsilon_{12} = 1 = \epsilon_{\dot{1}\dot{2}}$, $\epsilon^{12} = -1 = \epsilon^{\dot{1}\dot{2}}$, and $\epsilon^{ac}\epsilon_{cb} = \delta^a_b$. Notice that the inner products (2.1.7) are Lorentz invariant. In particular, the momentum squared of a pair of massless particles $p_i = \lambda^{(i)} \tilde{\lambda}^{(i)}$ and $p_j = \lambda^{(j)} \tilde{\lambda}^{(j)}$ takes the form:

$$(p_i + p_j)^2 = 2p_i \cdot p_j = \langle \lambda^{(i)}, \lambda^{(j)} \rangle [\tilde{\lambda}^{(i)}, \tilde{\lambda}^{(j)}] =: \langle i, j \rangle [i, j]. \quad (2.1.8)$$

Recall that in a Poincaré invariant theory, irreducible massless representations are classified by their helicity which can be $h = \pm s$ with s any integer or half-integer known as the spin of the particle. Assuming the existence of one-particle states and that the Poincaré group acts on scattering amplitudes as it acts on individual states, the helicity operator acts on the amplitudes as follows:

$$\left(\lambda_a^{(i)} \frac{\partial}{\partial \lambda_a^{(i)}} - \tilde{\lambda}_{\dot{a}}^{(i)} \frac{\partial}{\partial \tilde{\lambda}_{\dot{a}}^{(i)}} \right) M_n(1^{h_1}, \dots, n^{h_n}) = -2h_i M_n(1^{h_1}, \dots, n^{h_n}). \quad (2.1.9)$$

The final ingredient we need to complete the spinor-helicity formalism are the polarization tensors. As shown in [29], polarization tensors of massless particles of integer spin s can be expressed in terms of polarization vectors of spin 1 particles as follows:

$$\epsilon_{a_1 \dot{a}_1, \dots, a_s \dot{a}_s}^+ = \prod_{i=1}^s \epsilon_{a_i \dot{a}_i}^+, \quad \epsilon_{a_1 \dot{a}_1, \dots, a_s \dot{a}_s}^- = \prod_{i=1}^s \epsilon_{a_i \dot{a}_i}^-, \quad (2.1.10)$$

while for half-integer spin $s + 1/2$ they are

$$\epsilon_{a_1 \dot{a}_1, \dots, a_s \dot{a}_s, b}^+ = \tilde{\lambda}_b \prod_{i=1}^s \epsilon_{a_i \dot{a}_i}^+, \quad \epsilon_{a_1 \dot{a}_1, \dots, a_s \dot{a}_s, b}^- = \lambda_b \prod_{i=1}^s \epsilon_{a_i \dot{a}_i}^-, \quad (2.1.11)$$

and where polarization vectors of spin 1 particles are given by

$$\epsilon_{a\dot{a}}^+ = \frac{\mu_a \tilde{\lambda}_{\dot{a}}}{\langle \mu, \lambda \rangle}, \quad \epsilon_{a\dot{a}}^- = \frac{\lambda_a \tilde{\mu}_{\dot{a}}}{[\tilde{\lambda}, \tilde{\mu}]}, \quad (2.1.12)$$

with μ_a and $\tilde{\mu}_{\dot{a}}$ arbitrary reference spinors.

We have explained how all the physical data of a massless particle can be recovered from $\lambda, \tilde{\lambda}$ and h . The presence of arbitrary reference spinors in (2.1.12) should not be a surprise, as

polarization tensors cannot be uniquely fixed once $\{\lambda, \tilde{\lambda}, h\}$ is given. If a different reference spinor is chosen, say, μ' for $\epsilon_{a\dot{a}}^+$ then

$$\epsilon_{a\dot{a}}^+(\mu') = \epsilon_{a\dot{a}}^+(\mu) + \frac{\langle \mu', \mu \rangle}{\langle \mu', \lambda \rangle \langle \lambda, \mu \rangle} \lambda_a \tilde{\lambda}_{\dot{a}}, \quad (2.1.13)$$

If the particle has helicity $h = 1$ then it is easy to recognize (2.1.13) as a gauge transformation and the amplitude must be invariant. One does not need to worry about the apparent freedom of (2.1.13), as Weinberg showed in [35] that for any spin s , the only way to guarantee the correct Poincaré transformations of the S-matrix of massless particles is by imposing invariance under (2.1.13). In other words, Poincaré symmetry requires that M_n gives the same answer independently of the choice of reference spinor μ .

As mentioned earlier, the spinor-helicity formalism as discussed here is strictly four-dimensional. Generalisations have been proposed in [36, 37, 38] for higher dimensions and in [39] for three-dimensions. Our main results heavily rely on the four-dimensional spinor-helicity formalism. However, as showed in [40], the BCFW-structure of the tree-level amplitude is a general feature of a theory and is not related to the dimensionality of the space-time. Therefore, in order to generalize them to dimensions different than four, a little bit of more work needs to be done.

2.1.2 Three-point amplitudes

Three-particle amplitudes are zero for real momenta. This happens because it is kinematically prohibited to have two massless particles scattering into a single massless particle. However, when the momenta are complex, three-particle amplitudes have no problem in existing. Let us write here the expression for the three-particle amplitudes, first found in [29]. They follow just from Poincaré invariance, and correct helicity scalings as determined by equation (2.1.9):

$$M_3(1^{h_1}, 2^{h_2}, 3^{h_3}) = \kappa_{1+h}^H \langle 1, 2 \rangle^{d_3} \langle 2, 3 \rangle^{d_1} \langle 3, 1 \rangle^{d_2} + \kappa_{1-h}^A [1, 2]^{-d_3} [2, 3]^{-d_1} [3, 1]^{-d_2}, \quad (2.1.14)$$

where $d_1 := h_1 - h_2 - h_3$, $d_2 := h_2 - h_3 - h_1$, $d_3 := h_3 - h_1 - h_2$. The subscripts in the coupling constants indicate their dimension, while the superscript H/A indicates the holomorphic/anti-holomorphic part of the amplitude.

Notice that the amplitude (2.1.14) has to go to zero as $\langle i, j \rangle$ and $[i, j]$ are both sent to zero, *i.e.* on the real sheet. This implies that if $d_1 + d_2 + d_3 = -h_1 - h_2 - h_3 < 0$, then the coupling constant κ^H needs to be set to zero in order to avoid infinities. Similarly, if $d_1 + d_2 + d_3 = -h_1 - h_2 - h_3 > 0$ then κ^A needs to be set to zero. For $d_1 + d_2 + d_3 = 0$, both of the terms in (2.1.14) are allowed.

It should also be noticed that $\delta = |d_1 + d_2 + d_3| = |h_1 + h_2 + h_3|$ provides the number of the derivatives for the interaction (this can be understood through a simple dimensionality argument⁵). As pointed out in [29], the expression (2.1.14) for the three-particle amplitude

⁵The argument goes as follows: In the Feynman representation, an amplitude for an interaction with δ derivatives would read $M_3 \sim (\text{coupling constant}) (\text{polarization tensors}) (p^\delta)$. Polarization tensors are dimensionless. Comparing this amplitude with $M_3 = (\text{coupling constant}) \langle 1, 2 \rangle^{d_3} \langle 2, 3 \rangle^{d_1} \langle 3, 1 \rangle^{d_2}$ if $h_1 + h_2 + h_3 < 0$ or with $M_3 = (\text{coupling constant}) [1, 2]^{-d_3} [2, 3]^{-d_1} [3, 1]^{-d_2}$ if $h_1 + h_2 + h_3 > 0$, it is clear that it results $\delta = |h_1 + h_2 + h_3|$.

is fully non-perturbative, so it could be used for more general purposes than the ones we have here.

2.2 On-shell recursion relations

An n -point amplitude encompasses lower-point amplitudes. More precisely, this happens in certain particular kinematic limits. For instance, we have the collinear/multiparticle limits, where the sum of the momenta of a subset of particles $\mathcal{K} \subset \{p_1, \dots, p_n\}$ becomes on-shell, *i.e.*

$$P_{\mathcal{K}}^2 = \left(\sum_{\mathcal{K}} p_k\right)^2 \rightarrow 0 \quad \implies \quad M_n(p_1, \dots, p_n) \rightarrow M_{k+1}(\mathcal{K}, -P_{\mathcal{K}}) \frac{1}{P_{\mathcal{K}}^2} M_{n+1-k}(P_{\mathcal{K}}, \bar{\mathcal{K}}) , \quad (2.2.1)$$

where we denoted $\bar{\mathcal{K}} = \{p_1, \dots, p_n\} \setminus \mathcal{K}$. Equation (2.2.1) holds because in this limit, the scattering process is completely dominated by the production of an on-shell particle with momentum $P_{\mathcal{K}}$. Notice that $\frac{1}{P_{\mathcal{K}}^2}$ accounts for the propagator of this on-shell particle (which is massless, as we are assuming our theories only contain massless particles). Another interesting set of kinematical limits are the soft limits. In these, there is one particle “going soft”:

$$p_k \rightarrow 0 \quad \implies \quad M_n(p_1, \dots, p_n) \rightarrow (\text{soft factor}) M_{n-1}(p_1, \dots, \hat{p}_k, \dots, p_n) , \quad (2.2.2)$$

where the last amplitude does not contain p_k , and the soft factor⁶ is a kinematical factor that is singular in the soft limits.

An honest question to ask is whether it is possible to reconstruct higher point amplitudes from lower-point ones. This is what one would call a recursion relation. Recursion relations have existed for a while [41, 42, 43, 44, 45, 46], but it has only been after 2005 that they have become a powerful tool that can be applied to a great variety of theories. In that year, Britto, Cachazo, Feng and Witten (BCFW) published a landmark paper [7] where they explained with great simplicity the origin of some recursion relations valid for gluons found the previous year by the first three authors [47]. This origin turns out to be just some simple complex analysis. Let us explain it here.

2.2.1 The BCFW construction

Pick up two of the scattering particles, i and j , and deform their momenta as:

$$p_i \rightarrow p_i(z) = p_i - z q , \quad p_j \rightarrow p_j(z) = p_j + z q , \quad (2.2.3)$$

where $z \in \mathbb{C}$, and q is a four-momentum that we fix by requiring that the new deformed momenta are still on-shell:

$$(p_i(z))^2 = 0 , \quad (p_j(z))^2 = 0 \quad \implies \quad q^2 = 0 , \quad p_i \cdot q = 0 , \quad p_j \cdot q = 0 . \quad (2.2.4)$$

⁶Soft factors are not known in general for a given theory. Notable examples are YM and Gravity.

Using the spinor-helicity formalism of section 2.1.1, it is very easy to find a solution to these constraints for q . This solution is not unique, and one possibility is to take $q = \lambda^{(i)}\tilde{\lambda}^{(j)}$. Then the deformation (2.2.3) reads on the spinors of $p_i = \lambda^{(i)}\tilde{\lambda}^{(i)}$ and $p_j = \lambda^{(j)}\tilde{\lambda}^{(j)}$ as:

$$\tilde{\lambda}^{(i)} \rightarrow \tilde{\lambda}^{(i)}(z) = \tilde{\lambda}^{(i)} - z \tilde{\lambda}^{(j)}, \quad \lambda^{(j)} \rightarrow \lambda^{(j)}(z) = \lambda^{(j)} + z \lambda^{(i)}. \quad (2.2.5)$$

This is the shift introduced by BCFW. It is clear that after this complex deformation, we still have a set of n external particles with their momenta on-shell, and satisfying total momentum conservation. This means that we can consider the scattering amplitude for these particles:

$$M_n(p_1, \dots, p_n) \rightarrow M_n^{(i,j)}(z) = M_n(p_1, \dots, p_i(z), \dots, p_j(z), \dots, p_n). \quad (2.2.6)$$

Actually, this is a one-parameter family of amplitudes, the parameter being z . This family depends on the particles chosen for the deformation (i, j) . Since one of our assumptions was analyticity, it turns out that we can think of $M_n^{(i,j)}(z)$ as an analytic function of the complex variable z . We declare that *working at tree level is equivalent to requiring that $M_n^{(i,j)}(z)$ is a rational function of z* . This actually comes from thinking how M_n^{tree} looks like in the Feynman representation, where each diagram will contribute a rational function under the deformation (2.2.3). Moreover, from the Feynman representation it is also clear that the only singularities of $M_n^{(i,j)}(z)$ can come from the propagators P_K that acquire z -dependence with the deformation. The latter will be those for which $p_i \in K$ or $p_j \in K$ (if both or neither p_i, p_j is in K , P_K does not get a z -dependence). In these cases:

$$(P_K(z))^2 = (P_K \pm z q)^2 = P_K^2 \pm 2z P_K \cdot q = P_K^2 \left(1 - \frac{z}{z_K}\right), \quad (2.2.7)$$

so $M_n^{(i,j)}(z)$ will clearly have simple poles at the points $z = z_K$, and these are its only singularities. The whole BCFW idea is to reconstruct $M_n^{(i,j)}(z)$ from the residues at the poles. Is this always possible? Let us look at the following integral:

$$M_n^{(i,j)}(\infty) = \frac{1}{2\pi i} \oint_{\mathcal{C}} dz \frac{M_n^{(i,j)}(z)}{z} = M_n(0) + \sum_K \text{Res} \left[\frac{M_n^{(i,j)}(z)}{z}; z_K \right], \quad (2.2.8)$$

where we take the region of integration \mathcal{C} to be a very large circle on the complex plane, or equivalently a very small circle around $z = \infty$ in the Riemann sphere. As we will see below, the residues of $\frac{M_n^{(i,j)}(z)}{z}$ are given by products of lower-point amplitudes. That means they are known. $M_n(0)$ is precisely the physical amplitude, which of course is independent of the particles we chose to shift. So in the case $M_n^{(i,j)}(\infty) = 0$, we can write

$$M_n = - \sum_K \text{Res} \left[\frac{M_n^{(i,j)}(z)}{z}; z_K \right], \quad (2.2.9)$$

and this will give us the recursion relation. The question to ask is when does $M_n^{(i,j)}(\infty) = 0$ hold. Before coming back to this below, we can notice that, since $M_n^{(i,j)}$ is a rational function, its behavior at infinity is

$$M_n^{(i,j)}(z) \underset{z \rightarrow \infty}{\sim} z^\nu, \quad \text{for some } \nu \in \mathbb{Z}. \quad (2.2.10)$$

When $\nu < 0$, the amplitude vanishes at infinity, and we can write (2.2.9), where identifying properly the residues we obtain the BCFW formula:

$$M_n = \sum_{\mathcal{K}} M_L^{(i,j)}(z_{\mathcal{K}}) \frac{1}{P_{\mathcal{K}}^2} M_R^{(i,j)}(z_{\mathcal{K}}), \quad (2.2.11)$$

where the sum is over the channels \mathcal{K} for which $P_{\mathcal{K}}$ acquires a z -dependence (which, as we discussed above, happens whenever $p_i \in \mathcal{K}$ or $p_j \in \mathcal{K}$, but not both). $M_L^{(i,j)}(z_{\mathcal{K}})$ and $M_R^{(i,j)}(z_{\mathcal{K}})$ are the scattering amplitudes of the deformed particles on the “left and right side of the channel” respectively, evaluated at the deformation value $z = z_{\mathcal{K}}$:

$$M_L^{(i,j)}(z_{\mathcal{K}}) = M_{1+k}((\mathcal{K} \setminus \{p_i\}) \cup \{p_i(z_{\mathcal{K}}), -P_{\mathcal{K}}(z_{\mathcal{K}})\}), \quad (2.2.12)$$

$$M_R^{(i,j)}(z_{\mathcal{K}}) = M_{1+n-k}((\bar{\mathcal{K}} \setminus \{p_j\}) \cup \{p_j(z_{\mathcal{K}}), P_{\mathcal{K}}(z_{\mathcal{K}})\}), \quad (2.2.13)$$

where we assumed $p_i \in \mathcal{K}$. Notice that both of these amplitudes have all the particles on-shell and satisfying momentum conservation, so they are on-shell scattering amplitudes, their only peculiarity being that some of the intervening momenta are complex. This is why the BCFW formula is called an *on-shell* recursion relation. Let us give a proof of (2.2.11).

Proof

Assume you have a complex deformation that is linear in the internal momenta of the trees: $(P_{\mathcal{K}}(z))^2 = P_{\mathcal{K}}^2 \left(1 - \frac{z}{z_{\mathcal{K}}}\right)$. This is the case for the BCFW deformation (2.2.7), but it also holds for other deformations, for which this proof is valid as well.

Then, as we argued above, $M_n^{(i,j)}(z)$ is a rational function of z , whose only singularities are simple poles⁷. If this function vanishes at infinity, then it is always possible to write a partial-fractions expansion for it:

$$M_n^{(i,j)}(z) = \sum_{\mathcal{K}} \frac{c_{\mathcal{K}}}{1 - \frac{z}{z_{\mathcal{K}}}}. \quad (2.2.14)$$

To determine the value of the constants $c_{\mathcal{K}}$, we use the physical input provided by equation (2.2.1). As we go close to the point $z = z_{\mathcal{K}}$, *i.e.* $z = z_{\mathcal{K}} + \varepsilon$ with $\varepsilon \rightarrow 0$, the behavior of the amplitude (2.2.14) to leading order in ε is

$$M_n^{(i,j)}(z_{\mathcal{K}} + \varepsilon) \sim c_{\mathcal{K}} \frac{z_{\mathcal{K}}}{\varepsilon}. \quad (2.2.15)$$

On the other hand, by going close to the point $z = z_{\mathcal{K}}$ we are making the momentum $P_{\mathcal{K}}$ on-shell, where we expect the amplitude to factorize into the product of two subamplitudes,

$$\begin{aligned} M_n^{(i,j)}(z_{\mathcal{K}} + \varepsilon) &\sim \frac{M_{k+1}(\mathcal{K}(z_{\mathcal{K}} + \varepsilon), -P_{\mathcal{K}}(z_{\mathcal{K}} + \varepsilon)) M_{n+1-k}(P_{\mathcal{K}}((z_{\mathcal{K}} + \varepsilon)), \bar{\mathcal{K}}(z_{\mathcal{K}} + \varepsilon))}{(P_{\mathcal{K}}(z_{\mathcal{K}} + \varepsilon))^2} \sim \\ &\sim M_L^{(i,j)}(z_{\mathcal{K}}) \frac{1}{P_{\mathcal{K}}^2} M_R^{(i,j)}(z_{\mathcal{K}}) \frac{z_{\mathcal{K}}}{\varepsilon}. \end{aligned} \quad (2.2.16)$$

⁷Notice that if the kinematical input were such that $z_{\mathcal{K}} = z_{\mathcal{K}'}$, we could always go to an arbitrarily close set of momenta for which this does not happen.

Comparing equations (2.2.15) and (2.2.16), we easily get that

$$c_K = M_L^{(i,j)}(z_K) \frac{1}{P_K^2} M_R^{(i,j)}(z_K), \quad (2.2.17)$$

and this proves the BCFW formula (2.2.11). ■

Let us now give some well-deserved praise to the BCFW recursion relation. The most obvious fact is that it answers the question posed at the beginning of the section, and provides a way to compute higher-point amplitudes from lower-point ones, using just on-shell information. This proves that all the off-shell information contained in the Feynman representation is not really needed for computing scattering amplitudes. Moreover, it makes the computation of tree amplitudes with BCFW much faster and more efficient than doing it via Feynman diagrams. The main two features of BCFW that allow for that are:

- **Need to sum only over a subset of channels.** In the Feynman representation, one has to sum over all the possible trees to get the amplitude. The number of possible trees grows very rapidly with n , and this is what makes very impractical the use of Feynman diagrams to compute higher-point amplitudes. In the BCFW representation, instead, we only have to sum over the trees that contain propagators that acquire a z -dependence through the BCFW shift (2.2.5). For instance, for the computation of a Maximally-Helicity-Violating (MHV) amplitudes in YM, *i.e.* with two negative-helicity gluons and the rest positive-helicity gluons, it turns out that for a wisely chosen deformation there is only one BCFW diagram to be summed over, for any n ! This explains the simplicity of the Parke-Taylor formula [48]:

$$M_n(1^+, \dots, i^-, \dots, j^-, \dots, n^+) = \frac{\langle i, j \rangle^4}{\prod_{k=1}^n \langle k, k+1 \rangle}, \quad n+1 \equiv 1. \quad (2.2.18)$$

There are other possible shifts similar to the BCFW one, where one deforms more than two particles. However, the BCFW is the one capturing less channels as only two particles are shifted. Notice that after summing over all the BCFW diagrams, all the channels present in the Feynman representation have to show up. This indeed happens because the individual BCFW diagrams show poles that do not correspond to propagating particles (this is why we say that BCFW breaks locality at intermediate steps), that in the final answer conspire to generate the missed channels.

- **Recursive structure.** Knowing all the k -point amplitudes with $k \leq n-1$, it is possible to build the n -point one. This is very powerful when implemented in a computer, which can very quickly perform some recursive steps to compute an amplitude. On the theoretical side, one can iterate down the BCFW recursion relations. This will stop when we reach an amplitude that cannot be decomposed further. For theories with three-point amplitudes, the process stops at the three-point level. Reversing the logic, it turns out that the minimal info we need to build amplitudes are three-point amplitudes, that can be exactly determined for any theory as we showed in section 2.1.2. This will actually hold for theories for which amplitudes are BCFW-constructible (*i.e.* , for which condition (2.2.9) holds), which is just a subset of all possible theories. These theories were dubbed as “constructible” in the very nice paper [29].

By now the reader should be convinced that having BCFW recursion relations for the amplitudes of a theory is a great thing to have, both for theoretical and practical purposes. So far we have not said anything about what theories satisfy the condition $\nu < 0$, needed for BCFW to apply. It happens that for the simplest theories, like YM, Gravity or other supersymmetric theories like $\mathcal{N} = 1$ Supergravity or $\mathcal{N} = 4$ SYM, for any amplitude there always exist a choice of a BCFW shift that produces a good complex-UV behavior for the deformed amplitude, *i.e.* $M_n^{(i,j)}(\infty) = 0$. Nevertheless, in more phenomenological theories like Einstein-Maxwell or generically theories with fermions, like QED or QCD, there are amplitudes for which there is no BCFW shift yielding $\nu < 0$. In any case, it would be desirable to understand more about the boundary contribution $M_n^{(i,j)}(\infty) = 0$, and the conditions under which is present.

In the next subsection, we assume that we have a theory with $\nu \geq 0$, and we show how to generalize the BCFW recursion relation to this case. Later on we will come back to the determination of the exponent ν for a given theory.

2.2.2 Generalizing BCFW

Let us come back to the integral that defined the BCFW recursion relation (2.2.8). If we think about $M_n^{(i,j)}(z)$ as a function on the Riemann sphere, by the argument principle it easily follows that this meromorphic function must have as many zeroes as poles (all counted with their respective multiplicity) in the whole Riemann sphere. Since BCFW is valid when $M_n^{(i,j)}(\infty) = 0$, we can think that the BCFW integral (2.2.8) is really just an integral around one of the zeroes of the function. In the case $\nu \geq 0$, the point at infinity will not be a zero anymore, but there will be zeroes $z_0^{(l)}$ somewhere else in the Riemann sphere. We can then think of studying the object

$$0 = \frac{1}{2\pi i} \oint_{\mathcal{C}} dz \frac{M_n^{(i,j)}(z)}{z - z_0^{(l)}}, \quad (2.2.19)$$

where \mathcal{C} is now a contour around the point $z = z_0^{(l)}$. It turns out that by studying such integrals, one arrives [20] at the following generalization of the BCFW formula, valid for any theory of massless particles:

$$M_n = \sum_{\kappa} M_L^{(i,j)}(z_{\kappa}) \frac{f_{\kappa}^{(i,j)}}{P_{\kappa}^2} M_R^{(i,j)}(z_{\kappa}), \quad f_{\kappa}^{(i,j)} = \begin{cases} 1, & \text{if } \nu < 0, \\ \prod_{l=1}^{\nu+1} \left(1 - \frac{P_{\kappa}^2}{P_{\kappa}^2(z_0^{(l)})}\right), & \text{if } \nu \geq 0, \end{cases} \quad (2.2.20)$$

where $\{z_0^{(l)}\}_{l=1}^{\nu+1}$ is a set of $\nu + 1$ zeroes of the deformed amplitude $M_n^{(i,j)}(z)$. Let us prove (2.2.20).

Proof

Since $M_n^{(i,j)}(z)$ does not vanish at infinity, it is not possible to write an expansion like that in (2.2.14). But it is not complicated to write an alternative expansion, where the poles

we discussed at the end of section 2.2.1, namely the need to sum over just a subset of the possible channels, and the recursive structure. The last point implies, in particular, that *our new formula extends the notion of constructibility to all theories of massless particles*.

In practice, to compute an amplitude with the recursion relation (2.2.20), there are two new pieces of information we need: one is the knowledge of the value of integer ν , and the other one is the location of $\nu + 1$ zeroes of the amplitude (actually we just need the value of the channel momenta at those zeroes). We discuss extensively the first issue later in section 2.3. In what follows, let us give some ideas on how to fix the zeroes, assuming ν is known.

2.2.3 Comments on zeroes

We have just discussed how the knowledge of a subset of zeroes can fix the large- z behavior of the amplitude under a certain BCFW-deformation, and the boundary term through their location. The result is the recursion relation (2.2.20), which shows the same number of terms as the standard BCFW formula. The question we need to answer now concerns the physical meaning of the location of the zeroes of the amplitudes, or, probably more fruitfully, the physical meaning of the internal propagators when they are evaluated at the location of the zeroes.

Beyond the obvious statement that the location of the zeroes are points in the complexified momentum space where the S-matrix becomes trivial, not much is known about their physical significance. The issue of the zeroes of the complete amplitudes was studied in relation to the analysis of the dispersion relations for the logarithm of the scattering amplitudes [49, 50, 51, 52, 53, 54]. But this does not give us any useful information.

So although they seem to be special points of the S-matrix, zeroes are not on the same footing with poles, since the latter are always known *a priori* for a given amplitude. In some cases, like for instance in $\mathcal{N} = 8$ Supergravity, it is known that in amplitudes with scalars, the soft limits of the scalars produce zeroes. But this is just a particularity of this theory, and moreover a BCFW deformation like (2.2.5) does not give access to these zeroes (one needs to deform three particles at least). The zeroes depend on the deformation, and it is not clear “how physical they are”. So we will take an alternative route to fix them, which is the use of unitarity.

It was noted in [55] that when $\nu > 0$, the BCFW-constructed amplitude failed to account for the proper factorizations along some channels, most notably the one that contained the two deformed particles, $P_{ij}^2 \rightarrow 0$. This means that we can gain some information on the zeroes if we look at the factorization properties along all possible channels. All the collinear/multi-particle channels can be grouped in the following four classes:

$$\begin{aligned}
\lim_{P_{i\mathcal{I}_k}^2 \rightarrow 0} P_{i\mathcal{I}_k}^2 M_n &= M(i, \mathcal{I}_k, -P_{i\mathcal{I}_k}) M(P_{i\mathcal{I}_k}, \mathcal{J}_k, j), \\
\lim_{P_{\mathcal{K}}^2 \rightarrow 0} P_{\mathcal{K}}^2 M_n &= M_{s+1}(\mathcal{K}, -P_{\mathcal{K}}) M_{n-s+1}(P_{\mathcal{K}}, \mathcal{Q}, i, j), \\
\lim_{P_{k_1 k_2}^2 \rightarrow 0} P_{k_1 k_2}^2 M_n &= M_3(k_1, k_2, -P_{k_1 k_2}) M_{n-1}(P_{k_1 k_2}, \mathcal{K}, i, j), \\
\lim_{P_{ij}^2 \rightarrow 0} P_{ij}^2 M_n &= M_3(i, j, -P_{ij}) M_{n-1}(P_{ij}, \mathcal{K}),
\end{aligned} \tag{2.2.26}$$

where it is understood here that the subsets $\mathcal{I}_k, \mathcal{J}_k, \mathcal{K}, \mathcal{Q}$ never contain the deformed particles i and j . A careful analysis of how these channels are correctly captured by our recursion formula (2.2.20) was carried out in [20]. There it was shown that indeed the proper factorization along these channels impose some constraints on the zeroes: the first type of channels in (2.2.26) is already explicit in the generalized BCFW formula, so they bring nothing new; the second and third type yield the constraint than in those limits, the zeroes (as well as the weights) should reduce to the ones of the corresponding lower-point amplitude, therefore connecting zeroes with those of smaller amplitudes. This is a hint that it may be possible to reconstruct the weights from those of lower-point amplitudes, maybe in a recursive manner as well; however, even if this is possible in some cases (see some examples in section 6 of [20]) we have not managed to find a systematic procedure for this. Finally, the last channel is the one yielding more information, and actually allows to completely characterize the zeroes of four-point amplitudes. We discuss it in detail in section 2.3.1.

2.3 The complex-UV behavior

Among all the techniques that are appearing in recent years in the study of scattering amplitudes, like the MHV-vertex expansion of YM [56, 57], the BCJ relations between color and kinematics that allow to build Gravity amplitudes from gluon amplitudes in a very simple manner [58] or the formulation of $\mathcal{N} = 4$ SYM in the Grassmanian [59, 60, 61, 62, 63], to cite some, the BCFW recursion relation is the most general one. This is so because (2.2.11) can be applied to almost any theory of massless particles. The “almost” encodes a very important piece of information, which is the complex-UV behavior. When the deformed amplitude $M_n^{(i,j)}(z)$ vanishes at infinity, we say that it has a “good” complex-UV behavior, or alternatively, that we made a “good” BCFW shift. In the case where this property does not hold, the shift is called “bad” and one needs to take into account the boundary contribution $M_n^{(i,j)}(\infty)$.

Notice that once we chose the particles we want to deform, i and j as in (2.2.5), we still have freedom as the expression (2.2.5) actually defines a set of four deformations, which are determined by the sign of the helicities (h_i, h_j) of the deformed particles:

$$(h_i, h_j) = \{(-, +), (-, -), (+, +), (+, -)\}. \quad (2.3.1)$$

Depending on the helicity configuration (2.3.1) chosen for the two-particle deformation (2.2.5), the induced one-parameter family of amplitudes is a different function of z and, therefore, the boundary term $M_n^{(i,j)}(\infty)$ differs as well.

The question of when a shift is “good” or “bad” naturally arises. To answer it, what has been done in the literature is to look for help in the alternative Feynman representation of scattering amplitudes. One performs the shift at the level of Feynman diagrams, and analyzes how they behave individually with z . This naive analysis gives the right answer for YM [7], where the amplitude vanishes as z^{-1} if we choose in (2.2.5) the configurations $(-, +), (-, -), (+, +)$ (as discussed above in (2.3.1)).

However, this naive analysis gives a completely wrong answer for Gravity amplitudes. Here the individual Feynman diagrams behave as z^{n-5} , but it happens that there are many

cancellations among them. This is the typical problem with the Feynman representation. In [64], a smart alternative representation was found (using several complex shifts) for Gravity amplitudes, where the diagram-by-diagram analysis gave the right answer that Gravity amplitudes vanish as z^{-2} for the configurations $(-, +), (-, -), (+, +)$.

A very general answer to the question of the complex UV-behavior was provided in the nice paper [40]. They noticed that in the limit $z \rightarrow \infty$, the configuration of the deformed momenta is equivalent to that of a hard particle (with momentum $\sim zq$) traveling through a soft background (made by the non-deformed momenta). This configuration can be analyzed with background-field methods, where one essentially computes the effective Lagrangian the hard particles sees, and the coefficient ν can be extracted with relative ease. This method was further extended in [65], and the final conclusion is that whenever the theory contains a particle with maximal spin 1 or 2, if we want to compute an amplitude that involves a particle of this maximal spin, there is always a “good” BCFW shift available.

This is quite nice and at the end, as we said before, there are many relevant theories (like YM, Gravity, and in general supersymmetric theories) whose amplitudes are BCFW-constructible. Nonetheless, there are (also relevant) theories that escape BCFW-constructibility, and more importantly, we need an alternative representation of scattering amplitudes to determine when BCFW is applicable. In other words, the BCFW representation is not self-contained. This clearly prevents us from developing an alternative S-matrix approach to building scattering amplitudes, as one needs to make use of a Lagrangian to determine when the BCFW construction is valid.

In what follows, we present a determination of ν within the generalized BCFW construction we built in the previous section. In this way, the S-matrix program based on the four assumptions named at the beginning of the chapter can be carried on.

2.3.1 Factorization in the P_{ij} channel

A great deal of information is provided by the (i, j) -channel (last line in (2.2.26)), which does not appear explicitly in (2.2.20). As discussed in [55] for the scattering of gluons and gravitons, in the standard BCFW representation this singularity appears as a soft singularity, when the deformed momenta of either particle i or particle j vanishes. We show how requiring the correct factorization in this channel fixes the complex-UV behavior as well as it provides conditions on the zeroes.

The $P_{ij}^2 = \langle i, j \rangle [i, j] \rightarrow 0$ limit can be taken in two different ways. Then, we analyze the limits $[i, j] \rightarrow 0$ and $\langle i, j \rangle \rightarrow 0$ separately. Let us start with $[i, j] \rightarrow 0$. In this limit, the amplitude should factorize as follows

$$\lim_{[i, j] \rightarrow 0} P_{ij}^2 M_n = M_3(i, j, -P_{ij}^{h_{ij}}) M_{n-1}(P_{ij}^{-h_{ij}}, \mathcal{K}), \quad (2.3.2)$$

with⁸ $h_{ij} = -h_i - h_j - \delta$. For future reference, it is convenient to write down here the explicit

⁸ δ is the number of derivatives, and as we argued in section 2.1.2, it should be $-\delta = h_i + h_j + h_{ij}$, as $M_3(i, j, -P_{ij}^{h_{ij}})$ has to be made of the holomorphic spinors.

expression for the three-particle amplitude in (2.3.2):

$$M_3(i, j, -P_{ij}^{h_{ij}}) = \kappa_{1-\delta} (-1)^{2(h_i+h_j)} \langle i, j \rangle^\delta \left(\frac{[i, \mu]}{[j, \mu]} \right)^{2h_i+\delta}, \quad (2.3.3)$$

where we used the fact that, in this limit, the on-shell momentum P_{ij} can be written as

$$P_{ij} = \left(\frac{[i, \mu]}{[j, \mu]} \lambda^{(i)} + \lambda^{(j)} \right) \tilde{\lambda}^{(j)}, \quad (2.3.4)$$

with the identifications

$$\tilde{\lambda}^{(i)} := \frac{[i, \mu]}{[j, \mu]} \tilde{\lambda}^{(j)}, \quad \lambda^{(ij)} := \frac{[i, \mu]}{[j, \mu]} \lambda^{(i)} + \lambda^{(j)}, \quad \tilde{\lambda}^{(ij)} := \tilde{\lambda}^{(j)}, \quad (2.3.5)$$

and $\tilde{\lambda}^{(\mu)}$ being some reference spinor. The expression for the three-particle amplitude (2.3.3) is valid for any $\delta \geq 0$.

Now we take the limit on the left-hand side of (2.3.2) and use the representation (2.2.20) for M_n . It is easy to see that the only terms of the recursion relation which can contribute are the ones which contain a three-particle amplitude on the left blob (we represented this in figure 2.2):

$$\lim_{[i, j] \rightarrow 0} P_{ij}^2 M_n = \lim_{[i, j] \rightarrow 0} P_{ij}^2 \sum_k M_3(\hat{i}, k, -\hat{P}_{ik}^{h_{ik}}) \frac{f_{ik}^{(i, j)}}{P_{ik}^2} M_{n-1}(\hat{P}_{ik}^{-h_{ik}}, \mathcal{J}_k, \hat{j}), \quad (2.3.6)$$

where $h_{ik} = -h_i - h_k - \delta$, the poles are $z_{ik} = [i, k]/[j, k]$ and we are using hats to denote the z -dependent momenta that have to be evaluated at the location of the pole $z = z_{jk}$. The relevant quantities computed at these pole locations are

$$\hat{\lambda}^{(i)} = \frac{[j, i]}{[j, k]} \tilde{\lambda}^{(k)}, \quad \hat{\lambda}^{(j)} = \lambda^{(j)} + \frac{[i, k]}{[j, k]} \lambda^{(i)}, \quad \hat{P}_{ik} = p^{(k)} + \frac{[j, i]}{[j, k]} \lambda^{(i)} \tilde{\lambda}^{(k)}. \quad (2.3.7)$$

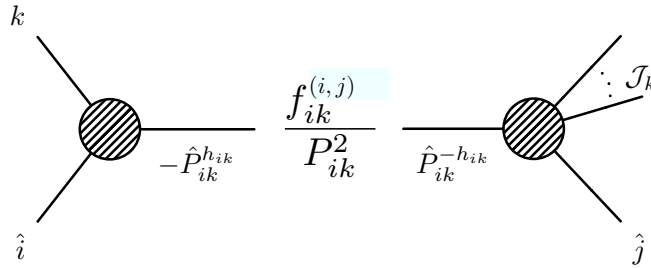


Figure 2.2: Collinear limit $[i, j] \rightarrow 0$. There is just one class of terms contributing to this limit, which is characterized by a three-particle amplitude of type $M_3(\hat{i}, k, -\hat{P}_{ij})$.

From (2.3.7), one can notice that the limit $[i, j] \rightarrow 0$ implies that $\hat{\lambda}^{(i)}$ vanishes, and consequently $\hat{p}^{(i)} \rightarrow 0$, as well as $\hat{p}^{(j)} \rightarrow P_{ij}$ and $\hat{P}_{ik} \rightarrow p^{(k)}$. A further consequence is that

all the $(n-1)$ -particle amplitudes in the sum (2.3.6) are mapped into $M_{n-1} \left(P_{ij}^{h_j}, p_k^{-h_{ik}}, \mathcal{J}_k \right)$, which is almost the one appearing on the right-hand side of (2.3.2). There is an important subtlety though. This $(n-1)$ -particle amplitude has exactly the same momenta for the external states as the one in (2.3.2), but with the fundamental difference that, generically, the helicities carried by the states with momenta P_{ij} and p_k are not the same as the states with same momenta in (2.3.2). However, it is always possible to relate these amplitudes by a dimensionless factor:

$$M_{n-1} \left(P_{ij}^{h_j}, p_k^{-h_{ik}}, \mathcal{J}_k \right) = \mathcal{H}_{n-1}^{(k)} M_{n-1} (P_{ij}^{-h_{ij}}, \mathcal{K}), \quad (2.3.8)$$

with $\mathcal{H}_{n-1}^{(k)} = 1$ if $h_{ij} = -h_j$ and $h_{ik} = -h_k$. Beyond being dimensionless, this factor can depend in an helicity-blind way on the spinors of the particles in \mathcal{J}_k and it has to show the proper helicity scaling with the spinors of P_{ij} and p_k . Using the relation (2.3.8), the $(n-1)$ -particle amplitude can be factored out from the sum (2.3.6), leaving inside the factor $\mathcal{H}_{n-1}^{(k)}$, which can be computed explicitly for a given theory. Let us now focus on the three-particle amplitudes $M_3(\hat{i}, k, -\hat{P}_{ik}^{h_{ik}})$, which can be explicitly written as

$$M_3(\hat{i}, k, -\hat{P}_{ik}^{h_{ik}}) = \kappa_{1-\delta} (-1)^{2(h_i+h_k)} \langle i, k \rangle^\delta \left(\frac{[j, i]}{[j, k]} \right)^{2h_i+\delta}. \quad (2.3.9)$$

From (2.3.3), (2.3.8) and (2.3.9), equation (2.3.6) becomes

$$\begin{aligned} \lim_{[i,j] \rightarrow 0} P_{ij}^2 M_n &= \left[\lim_{[i,j] \rightarrow 0} \sum_k (-1)^{2(h_j+h_k)} \left(\frac{\langle i, k \rangle}{\langle i, j \rangle} \right)^{\delta-1} \left(\frac{[j, i]}{[j, k]} \frac{[j, \mu]}{[i, \mu]} \right)^{2h_i+\delta} \frac{[i, j]}{[i, k]} f_{ik}^{(i,j)} \mathcal{H}_{n-1}^{(k)} \right] \times \\ &\times M_3(i, j, -P_{ij}) M_{n-1}(P_{ij}, \mathcal{K}). \end{aligned} \quad (2.3.10)$$

The above expression reproduces the correct factorization property (2.3.2) if and only if the term in square brackets is one. Let us now analyze it in some detail. First of all, one notices the presence of the factor $[i, j]^{2h_i+\delta+1}$. There are two cases to be studied:

If $2h_i + \delta \geq 0$, the requirement that $f_{ik}^{(i,j)}$ be proportional to some negative power of $[i, j]$ needs to hold in order to reproduce the correct factorization properties.

Let us now look at the explicit expression for $f_{ik}^{(i,j)}$ when $\nu \geq 0$. Unitarity, through the requirement for the amplitude to factorize properly, implies that

$$P_{ik}^2(z_0^{(l)}) \equiv \langle i, k \rangle ([i, k] - z_0^{(l)} [j, k]) = \langle i, k \rangle \alpha_{ik}^{(l)} [i, j], \quad (2.3.11)$$

where $\alpha_{ik}^{(l)}$ is some dimensionless quantity that carries helicity information of particles k and j . Consequently, $f_{ik}^{(i,j)}$ with $\nu \geq 0$ becomes

$$\begin{aligned} f_{ik}^{(i,j)} &\equiv \prod_{l=1}^{\nu+1} \left(1 - \frac{P_{ik}^2}{P_{ik}^2(z_0^{(l)})} \right) \equiv (-1)^{\nu+1} \left(\prod_{l=1}^{\nu+1} \frac{P_{ik}^2}{P_{ik}^2(z_0^{(l)})} \right) \prod_{l=1}^{\nu+1} \left(1 - \frac{P_{ik}^2(z_0^{(l)})}{P_{ik}^2} \right) = \\ &= (-1)^{\nu+1} \left(\frac{[i, k]}{[i, j]} \right)^{\nu+1} \left(\prod_{l=1}^{\nu+1} \alpha_{ik}^{(l)} \right)^{-1} \prod_{l=1}^{\nu+1} \left(1 - \alpha_{ik}^{(l)} \frac{[i, j]}{[i, k]} \right). \end{aligned} \quad (2.3.12)$$

From (2.3.12), the collinear limit (2.3.10) can be conveniently written as

$$\lim_{[i,j] \rightarrow 0} P_{ij}^2 M_n = \left[\lim_{[i,j] \rightarrow 0} \sum_k (-1)^\xi \left(\frac{\langle i, k \rangle}{\langle i, j \rangle} \right)^{\delta-1} \left(\frac{[i, k] [j, \mu]}{[j, k] [i, \mu]} \right)^{2h_i+\delta} \left(\frac{[i, j]}{[i, k]} \right)^{2h_i+\delta-\nu} \frac{\mathcal{H}_{n-1}^{(k)}}{\prod_{l=1}^{\nu+1} \alpha_{ik}^{(l)}} \right] \times \\ \times M_3(i, j, -P_{ij}) M_{n-1}(P_{ij}, \mathcal{K}), \quad (2.3.13)$$

where $\xi = 2(h_i + h_j + h_k) + \delta + \nu + 1$. Notice that, in this limit, the term in the second round-brackets in (2.3.13) is actually one. Thus, the correct factorization requirement in the (i, j) -channel can be finally written as

$$\lim_{[i,j] \rightarrow 0} \sum_k (-1)^{2(h_i+h_j+h_k)+\delta+\nu+1} \left[\left(\frac{\langle i, k \rangle}{\langle i, j \rangle} \right)^{\delta-1} \left(\frac{[i, j]}{[i, k]} \right)^{2h_i+\delta-\nu} \frac{\mathcal{H}_{n-1}^{(k)}}{\prod_{l=1}^{\nu+1} \alpha_{ik}^{(l)}} \right] = 1. \quad (2.3.14)$$

By construction, all the factors of $[i, j]$ in (2.3.14) are explicit, so the only possibility to satisfy this equation is to have the power of $[i, j]$ to vanish. Then, the condition (2.3.14) univocally fixes ν , and therefore the large- z behavior of the amplitudes, for a given theory:

$$\nu = 2h_i + \delta. \quad (2.3.15)$$

And this is the equation we were looking for. We see that the large- z behavior ν depends just on the helicities of the particles whose momenta have been deformed as well as on the number of derivatives of the three-particle interactions (we are assuming this number is unique within the theory). Furthermore, this number does not depend on the total number of external particles, in agreement with the general predictions of [40].

In the case $2h_i + \delta < 0$, the term in square brackets in (2.3.10) is finite and different from zero for $f_{ik}^{(i,j)} = 1$, i.e. the standard BCFW recursion relation holds. Thus the helicity of particle i (whose anti-holomorphic spinor has been deformed) needs to be negative in any case. Notice that, in fact, the momenta deformation (2.2.5) with helicities $(h_i, h_j) = (-, +)$ is what in the literature has been referred to as “good shift” (while the case $(h_i, h_j) = (+, -)$ is usually called “wrong shift”).

Using the same type of reasoning, one can discuss the holomorphic limit $\langle i, j \rangle \rightarrow 0$. There, again, there is just one class of terms contributing to this limit, which is characterized by a three-particle amplitude of type $M_3(\hat{P}_{ij}, k, \hat{j})$. We obtain the conditions

$$P_{jk}^2(z_0^{(l)}) = \langle i, j \rangle \alpha_{jk}^{(l)} [j, k], \\ \lim_{\langle i, j \rangle \rightarrow 0} \sum_k (-1)^{2(h_i+h_k)+\delta+\nu+1} \left[\left(\frac{[j, k]}{[i, j]} \right)^{\delta-1} \left(\frac{\langle i, j \rangle}{\langle j, k \rangle} \right)^{\delta-2h_j-\nu} \frac{\tilde{\mathcal{H}}_{n-1}^{(k)}}{\prod_{l=1}^{\nu+1} \alpha_{jk}^{(l)}} \right] = 1, \quad (2.3.16)$$

and the factor $\tilde{\mathcal{H}}_{n-1}^{(k)}$ is defined analogously to $\mathcal{H}_{n-1}^{(k)}$ in (2.3.8):

$$M_{n-1}(p_k^{-h_{jk}}, P_{ij}^{h_i}, \mathcal{I}_k) = \tilde{\mathcal{H}}_{n-1}^{(k)} M_{n-1}(P_{ij}^{-h_{ij}}, \mathcal{K}). \quad (2.3.17)$$

Notice that the two conditions (2.3.14) and (2.3.16) do not need to hold simultaneously since a given theory may factorize just under one of the two limits.

2.3.2 The exponent ν

Let us briefly summarize the results of the previous subsection. When we perform a BCFW deformation (2.2.5) on two particles i and j (that gives a valid ⁹ representation (2.2.20)), we have found if the following two assumptions hold *The amplitude we are studying factorizes under the P_{ij}^2 channel (it can be through $\langle i, j \rangle$, $[i, j]$, or both), and all the interactions of the theory have δ derivatives (this is equivalent to requiring that all the coupling constants of the theory have the same dimensions)*; then

$$M_n^{(i,j)}(\infty) \neq 0 \quad \Leftrightarrow \quad \begin{cases} \delta + 2h_i \geq 0 & \text{(if the amplitude factorizes when } [i, j] \rightarrow 0), \\ \delta - 2h_j \geq 0 & \text{(if the amplitude factorizes when } \langle i, j \rangle \rightarrow 0). \end{cases} \quad (2.3.18)$$

When the amplitude factorizes under the two limits, it must happen that $\delta + 2h_i = \delta - 2h_j$. Notice that under these assumptions the large- z behavior is independent of the number of external states and it depends only on the characteristics of the interactions and on the helicities of the deformed particles. This recovers the lessons learned using background-field methods in [40].

Since we know that $M_n^{(i,j)}(\infty) \neq 0 \Leftrightarrow \nu \geq 0$, it seems very tempting to identify

$$\nu = \begin{cases} \delta + 2h_i & \text{(if the amplitude factorizes when } [i, j] \rightarrow 0), \\ \delta - 2h_j & \text{(if the amplitude factorizes when } \langle i, j \rangle \rightarrow 0). \end{cases} \quad (2.3.19)$$

However, this identification has been only proven in the case $\nu \geq 0$. A naive survey provides some evidence for (2.3.19) though. For the “good” shift of YM, $(h_i, h_j) = (-, +)$, we have $\delta = 1$, and then $\nu = 1 + 2(-1) = -1$, and this is indeed the right answer. The same happens for Gravity, where the “good” shift is $(h_i, h_j) = (--, ++)$ and the number of derivatives is two, so the prediction for the complex-UV exponent is $\nu = 2 + 2(-2) = -2$. Again the right result!

In this subsection we argue that the degree of the pole/zero produced by a soft singularity in a three-particle amplitude coincides with the complex-UV exponent ν of the amplitude in the large- z limit. We first analyze generically the soft limits in a three-particle amplitude, and afterwards we make contact with the expressions appearing in the collinear limit analysis of the previous subsection and with the known large- z behaviors.

First, let us recall here the expression for the three-particle amplitudes that we already wrote in section 2.1.2:

$$M_3(1^{h_1}, 2^{h_2}, 3^{h_3}) = \kappa_{1+h}^H \langle 1, 2 \rangle^{d_3} \langle 2, 3 \rangle^{d_1} \langle 3, 1 \rangle^{d_2} + \kappa_{1-h}^A [1, 2]^{-d_3} [2, 3]^{-d_1} [3, 1]^{-d_2}. \quad (2.3.20)$$

For interactions with $\delta = -h_1 - h_2 - h_3 > 0$, the three-particle amplitude is given just by the holomorphic term. It is convenient to solve the relation connecting the helicities of the particles and the number of derivatives δ for one of the helicities (say h_3) and substitute it into the expression for the three-particle amplitude in such a way that the number of

⁹If an amplitude factorizes under a single two-particle channel, and we choose to deform the two particles of the channel, the representation (2.2.20) (the same as the BCFW representation) would be vanishing.

derivatives of the interaction becomes an explicit parameter:

$$M_3(1^{h_1}, 2^{h_2}, 3^{h_3}) = \kappa \frac{\langle 2, 3 \rangle^{\delta+2h_1} \langle 3, 1 \rangle^{\delta+2h_2}}{\langle 1, 2 \rangle^{\delta+2h_1+2h_2}}. \quad (2.3.21)$$

Let us analyze the amplitude (2.3.21) when particle 1 becomes soft: $p^{(1)} \rightarrow 0$. Thinking that the momentum of a massless particle in the complexified momentum space is the direct product of two independent spinors, the soft limit can be taken in two different ways, *i.e.* by sending either $\lambda^{(1)}$ or $\tilde{\lambda}^{(1)}$ to zero.

For the limit $\lambda^{(1)} \rightarrow 0$, let us choose $\lambda^{(1)} = \varepsilon \eta$, so that the limit of interest is performed by taking the parameter ε to zero. Moreover, recalling that for an amplitude such as (2.3.21) momentum conservation implies that the anti-holomorphic spinors of the three particles are all proportional to each other, we can set all of them to be equal. As a consequence, from momentum conservation, the holomorphic spinors are related to each other through the relation $\lambda^{(3)} = -\varepsilon \eta - \lambda^{(2)}$. Using these relations into (2.3.21) we get

$$M_3(\varepsilon) = \kappa (-1)^{2h_1+2h_2} \langle \eta, 2 \rangle^\delta \varepsilon^\delta, \quad (2.3.22)$$

which vanishes as $\varepsilon \rightarrow 0$.

Let us now consider the anti-holomorphic limit $\tilde{\lambda}^{(1)} \rightarrow 0$. Again, the anti-holomorphic spinors are proportional to each other. We choose them to be $\tilde{\lambda}^{(2)} = \tilde{\eta} = \tilde{\lambda}^{(3)}$ and $\tilde{\lambda}^{(1)} = \varepsilon \tilde{\eta}$, so that the soft limit is realized by taking ε to zero. Through momentum conservation, the holomorphic spinors are related to each other as $\lambda^{(3)} = -\varepsilon \lambda^{(1)} - \lambda^{(2)}$. From these relations among the spinors, the dependence of the amplitude on ε is

$$M_3(\varepsilon) = \kappa (-1)^{2h_1+2h_2} \langle 1, 2 \rangle^\delta \varepsilon^{\delta+2h_1}, \quad (2.3.23)$$

whose behavior in the limit $\varepsilon \rightarrow 0$ depends on the sign of the exponent $\delta + 2h_1$.

Similarly, the analysis of the anti-holomorphic three-particle amplitude, which needs to be considered whenever $h_1 + h_2 + h_3 > 0$ with $\delta = h_1 + h_2 + h_3$, leads to the following behaviors in the soft limits

$$\begin{aligned} M_3(\varepsilon) &= \kappa (-1)^{2h_1+2h_2} [1, 2]^\delta \varepsilon^{\delta-2h_1}, & \lambda^{(1)} &= \varepsilon \eta, \\ M_3(\varepsilon) &= \kappa (-1)^{2h_1+2h_2} [\tilde{\eta}, 2]^\delta \varepsilon^\delta, & \tilde{\lambda}^{(1)} &= \varepsilon \tilde{\eta}, \end{aligned} \quad (2.3.24)$$

from which it is easy to infer that the amplitude vanishes as $\tilde{\lambda}^{(1)} \rightarrow 0$, while the behavior of the amplitude in the limit $\lambda^{(1)} \rightarrow 0$ depends on the sign of the exponent $\delta - 2h_1$.

Let us now make contact with the analysis of the collinear limit containing both deformed momenta done in section 2.3.1. For this purpose, let us suppose that the deformed momenta belong to the particles labelled by 1 and j , for which the anti-holomorphic and the holomorphic spinors have respectively been shifted. When we analyze the collinear limit taken as $[1, j] \rightarrow 0$, the only terms which might contain a singularity in this channel are the ones containing a three-particle amplitude involving particle 1. For this amplitude, all the anti-holomorphic spinors are proportional to each other and therefore it is expressed by the holomorphic term in (2.3.20). Furthermore, the anti-holomorphic spinor of particle 1 turns out to be directly proportional to $[1, j]$ and hence it vanishes in the limit $[1, j] \rightarrow 0$. This case thus reduces to the one in (2.3.23) with $\varepsilon \sim [1, j]$.

Similarly, the only terms which might contain a singularity as $\langle 1, j \rangle \rightarrow 0$ are the ones containing a three-particle amplitude involving particle j . This amplitude is expressed in terms of the anti-holomorphic spinors and the holomorphic spinor of particle j turns out to be directly proportional to $\langle 1, j \rangle$ so that it vanishes in this limit. Hence, this case reduces to the one in the first line of (2.3.24) with $\varepsilon \sim \langle 1, j \rangle$.

Therefore, the relevant soft-limit scalings are $\delta + 2h_1$, in case the momentum $p^{(1)}$ becomes soft through its anti-holomorphic spinor, and $\delta - 2h_j$ in case the soft limit is taken by sending the holomorphic spinor to zero.

As we mentioned in the previous subsection, the standard BCFW representation holds if the collinear singularity in the $(1, j)$ -channel appears as a soft singularity. If the amplitude admits just one factorization limit: either $[1, j] \rightarrow 0$ or $\langle 1, j \rangle \rightarrow 0$, this requirement will be satisfied if and only if $\delta + 2h_1 < 0$ or $\delta - 2h_j < 0$ respectively. If both factorization limits are allowed, the inequalities just written down need to be satisfied simultaneously and their left-hand-sides need to coincide, relating the helicities of the particles whose momenta have been deformed.

In the cases $\delta + 2h_1 \geq 0$ and/or $\delta - 2h_j \geq 0$, the deformed particles still become soft in the relevant limit, but by themselves they are not enough to provide with the correct pole. The introduction of the “weights”, which depend on a subset of zeroes of the amplitude, enhances the soft limit to produce the correct pole. As we have previously seen, these “weights” contain explicitly the large- z parameter ν , which the factorization requirement fixes to be exactly the soft-limit exponent(s).

At a conceptual level, it appears clear the connection between the soft exponents and the large- z parameter ν , both for $\nu \geq 0$ and for $\nu < 0$. While the exact equivalence has been proven to be $\nu = \delta + 2h_1$ and/or $\nu = \delta - 2h_j$ for $\nu \geq 0$, so far we provided heuristic arguments for which this equivalence should hold also in the case $\nu < 0$. Together with the “experimental evidence”, *i.e.* the fact that formula (2.3.19) yields the correct value of ν for all known theories satisfying the two assumptions¹⁰ listed just before (2.3.18), *we take formula (2.3.19) to be our definition of the exponent ν in our S-matrix approach.* Notice that this formula makes no reference whatsoever to a Lagrangian formulation, and it is just based on the four assumptions listed at the beginning of the chapter.

2.3.3 Four-particle amplitudes

In the case of four-particle amplitudes, the analysis in 2.3.1 is enough to fix the value of the channel momenta at the location of the zeroes, when these are needed, *i.e.* when $\nu \geq 0$. Let us show how.

We label the four scattering particles by i, j, k, m . In order to solve equations (2.3.14) and (2.3.16), we first notice that by momentum conservation, the condition (2.3.11) becomes

$$P_{ik}^2(z_0^{(l)}) = \alpha^{(l)} P_{ij}^2, \quad P_{im}^2(z_0^{(l)}) = -(1 + \alpha^{(l)}) P_{ij}^2, \quad (2.3.25)$$

¹⁰Notice that there are some cases where these assumptions do not hold, like for instance a YM MHV amplitude where i and j are not consecutive does not display the P_{ij} channel, and (2.3.19) is not applicable. Indeed, applying that formula would give the wrong result as this amplitude vanishes as z^{-2} . However, it is always possible to pick up two particles i and j to deform so that the amplitude does display the P_{ij} channel.

where $\alpha^{(l)}$ is some complex number. There are at most two helicity factors $\mathcal{H}_{n-1}^{(k)}$ entering in equations (2.3.14) and (2.3.16). They are easily computable, since they are just quotients of three-particle amplitudes. They are given by

$$\begin{aligned}\mathcal{H}_3^{(k)} &= \left(\frac{[k, m]}{[m, j]} \right)^{2(\delta+h_i)}, & \mathcal{H}_3^{(m)} &= (-1)^\delta \left(\frac{[k, m]}{[j, k]} \right)^{2(\delta+h_i)}, \\ \tilde{\mathcal{H}}_3^{(m)} &= \left(\frac{\langle k, m \rangle}{\langle i, k \rangle} \right)^{2(\delta-h_j)}, & \tilde{\mathcal{H}}_3^{(k)} &= (-1)^\delta \left(\frac{\langle k, m \rangle}{\langle m, i \rangle} \right)^{2(\delta-h_j)}.\end{aligned}\tag{2.3.26}$$

Fixing the parameter ν to $\delta + 2h_i$ in (2.3.14), and to $\delta - 2h_j$ in (2.3.16), and using (2.3.26), these equations get heavily simplified:

$$\begin{aligned}1 &= (-1)^{2h_i+2h_k+1} \left(\prod_{l=1}^{\nu+1} \alpha^{(l)} \right)^{-1} + (-1)^{2h_k} \left(\prod_{l=1}^{\nu+1} (1 + \alpha^{(l)}) \right)^{-1}, \\ 1 &= (-1)^{2h_k+1} \left(\prod_{l=1}^{\nu+1} \alpha^{(l)} \right)^{-1} + (-1)^{2h_i+2h_k} \left(\prod_{l=1}^{\nu+1} (1 + \alpha^{(l)}) \right)^{-1}.\end{aligned}\tag{2.3.27}$$

Notice that we assumed that both the P_{ik}^2 and P_{im}^2 channels are present in the BCFW decomposition. If only one of them is appearing, one has to drop the corresponding terms in (2.3.27). These conditions can be solved to give a very simple relation for the channel momenta evaluated at the location of the zeroes:

$$\prod_{\text{BCFW channels}} P_{\mathcal{K}}^2(z_0^{(l)}) = (-P_{ij}^2)^{\#\text{BCFW channels}},\tag{2.3.28}$$

where we assume that the shifted particles are i and j . Supplemented with momentum conservation (alternatively using the parameterization (2.3.25)), this relation fixes the value of the channel momenta at the location of the zeroes (actually, the dependence of the four-point amplitudes on these momenta is always through the product appearing in (2.3.28), so there is no need even to solve for the momenta separately).

We then finally have all the ingredients to pursue our alternative construction of the tree level of theories of massless particles.

2.4 Building theories

In this final section, we want to describe how it is possible to construct theories at tree level within the axiomatic approach we described at the beginning of the chapter, where we wrote down the four main assumptions upon which we wanted to build our theories. Up to now, we have built up all the necessary ingredients to embrace this alternative approach, closer in spirit to the S-matrix program of the 60's. Let us spell out in what follows, the procedure to build theories with the tools we have developed.

First of all, it is important to characterize the class of theories we are going to study. These are *theories of only massless particles, whose coupling constants have all the same*

dimensions, and possessing a three-particle vertex. This is a very general class that includes all fundamental theories, but there are some theories that are left out, like for instance $\lambda\phi^4$, which does not have a three-point vertex, or YM plus higher-order operators, like F^3 , since there would be coupling constants of different dimensions within the theory. Moreover, *we only consider theories with just two different types of particles*, which leaves out most of the supersymmetric theories as well. Of course, these are not limitations of our formalism, but rather limitations on the length of the analysis we want to carry out. A real limitation of the formalism happens for instance when we try to analyze theories that do not have a propagator $1/P^2$, which do not admit a BCFW decomposition for its amplitudes, and therefore cannot be treated with our methods. Apart from conformal gravity, I am not aware of more examples of this phenomenon. It is important too to keep in mind that all the time we work only at tree level. The steps to follow are:

1. Define a theory by its possible three-particle interactions. Say for instance that we want a theory where particles of spin $s = 2$ can self-interact via a two-derivative interaction. This means that we should have two three-point vertices $M_3(g_1^{-2}, g_2^{+2}, g_3^{\pm 2})$, where g_i are gravitons. These vertices are known exactly, in virtue of the results presented in section 2.1.2.
2. Then we start to construct the scattering amplitudes of the theory. The first non-trivial ones are the four-point amplitudes. To construct them, we use the generalized BCFW formula (2.2.20) (implying that we work only at tree level) so that no constraint is put on the type of theory that can come out, *i.e.* it can have a “bad” complex-UV behavior. To use (2.2.20) we need to know what are the zeroes, but we have already showed in section 2.3.3 how to fix them for four-particle amplitudes.
3. To build four-point amplitudes through (2.2.20), one has to choose what particles to shift. Different choices, say (i, j) and (i', j') will lead to, in principle, different amplitudes. The four-point amplitude should not depend on this choice though. Therefore, we must impose the consistency condition:

$$M_4^{(i,j)}(0) = M_4^{(i',j')}(0). \quad (2.4.1)$$

This consistency condition has been already explored in [29] (where it was dubbed the *four-particle test*), returning known spectacular results (like the need of gauge invariance in order to define a theory of self-interacting gluons, or the need of supersymmetry to couple a gravitino to Gravity) in a very simple fashion. Here it arises in a very natural way, and it will impose constraints as well on the possible theories one can define.

2.4.1 A general classification

We are ready to tackle the three steps we described above. Our goal is to scan all possible theories that can be built with this procedure.

The first step above amounts to classify the theories through the dimensionality of the three-particle coupling constant, *i.e.* in a Lagrangian language, through the number of derivatives of the three-particle interaction:

1. $[\kappa] = 1 - s$ (s -derivative interactions: $\delta = s$). This class contains two sub-classes of theories: a self-interacting particle of spin s with three-particle amplitudes having, as possible helicity configurations, $(\mp s, \mp s, \pm s)$; and spin- s /spin- s' interactions, whose three-particle amplitudes may have, as possible helicity configurations, $(-s', +s', \mp s)$;
2. $[\kappa] = 1 - 3s$ ($3s$ -derivative interactions: $\delta = 3s$). In this class we find the theories of a self-interacting particle of spin s , whose three-particle amplitudes admit the helicity configuration $(\mp s, \mp s, \mp s)$;
3. $[\kappa] = 1 - (2s' + s)$ ($(2s' + s)$ -derivative interactions: $\delta = 2s' + s$). Here we find three-particle amplitudes whose helicity structure may be $(\mp s', \mp s', \mp s)$;
4. $[\kappa] = 1 - |2s' - s|$ ($|2s' - s|$ -derivative interactions: $\delta = |2s' - s|$). Finally we have the class characterized by three-particle amplitudes whose helicity configuration may be $(\mp s', \mp s', \pm s)$. Depending on whether s' is less or greater than $2s$, the three-particle amplitude with a given helicity configuration (between the two allowed) can be represented by the holomorphic term in (2.1.14) in one case or the anti-holomorphic one in the other case. For $s = 2s'$, the theories have 0-derivative interactions, and both the holomorphic and the anti-holomorphic pieces are present in the three-particle amplitude.

All the classes above exhaust all the possibilities for three-particle interactions, except that in which three particles of different species meet in a three-point vertex. Since this does not correspond to some particle emitting another particle, which is the usual way we conceive an interaction, we consider this possibility too exotic and we do not analyze it, although it could be interesting to see if there would be any constraint on this type of theory.

In the next subsections we carry out the other two steps: we build four-particle amplitudes for the theories above, and impose the condition (2.4.1). As we will see, this imposes severe constraints on the theories above to exist, leaving only a few consistent possibilities, which amazingly happen to correspond to the theories we already know!

2.4.2 Minimal-coupling interactions

We start our analysis by exploring the scattering of particles of spin s whose coupling has dimension $[\kappa] = 1 - s$. This is usually called the minimal coupling, and it corresponds to s -derivative interactions. From (2.1.14), it turns out that such theories are characterized by two possible helicity configurations for the three-particle amplitudes if $s \neq 0$:

$$\begin{aligned} M_3(1^{-s}, 2^{-s}, 3^{+s}) &= \kappa \varepsilon_{a_1 a_2 a_3} \left(\frac{\langle 1, 2 \rangle^3}{\langle 2, 3 \rangle \langle 3, 1 \rangle} \right)^s, \\ M_3(1^{+s}, 2^{+s}, 3^{-s}) &= \kappa \varepsilon_{a_1 a_2 a_3} \left(\frac{[1, 2]^3}{[2, 3][3, 1]} \right)^s, \end{aligned} \tag{2.4.2}$$

where $\varepsilon_{a_1 a_2 a_3}$ are structure constants related to possible internal quantum numbers. In the case that the theory does not show any internal symmetry, these structure constants can be set to one. Imposing invariance of the amplitude under permutations of the scattering

$h_i \backslash h_j$	$-s$	$+s$
$-s$	$-s$	X
$+s$	X	$-s$

Table 2.1: Complex-UV behavior ν for self-interacting particles of spin s . In this table, the complex-UV behavior ν is shown as a function of the helicities h_i and h_j of the particles whose momenta have been deformed. The cells containing a single value for ν correspond to the cases where the amplitude factorizes both in the $\langle i, j \rangle \rightarrow 0$ and $[i, j] \rightarrow 0$ limits. In the other cells, the value in the lower (upper) triangle corresponds to the case in which the amplitude factorizes in the $[i, j] \rightarrow 0$ ($\langle i, j \rangle \rightarrow 0$) limit, while the “X” indicates that the amplitude does not have such a factorization limit.

particles, it is easy to see that the structure constants need to be completely symmetric in their indices for even spin s , while completely anti-symmetric for odd spin s .

If $s = 0$, the three-particle amplitude is given by a coupling constant, which is given by the sum of the holomorphic and anti-holomorphic coupling constants in (2.1.14).

The three-point helicity configurations admitted in this class of theories allow to have just one class of non-trivial four-point amplitudes which is characterized by having two particles with negative helicity and two with positive helicity. So the four-point amplitude we have to build is:

$$M_4(1^{-s}, 2^{-s}, 3^{+s}, 4^{+s}). \quad (2.4.3)$$

To do that, we use the following BCFW deformation:

$$\tilde{\lambda}^{(i)}(z) = \tilde{\lambda}^{(i)} - z \tilde{\lambda}^{(j)}, \quad \lambda^{(j)}(z) = \lambda^{(j)} + z \lambda^{(i)}, \quad (2.4.4)$$

where for the moment the particles are kept with arbitrary helicities. First of all, let us discuss the complex-UV limit. A complete analysis of the behavior of the amplitude at infinity as a function of the helicities of the particles is displayed in table 2.1. Let us comment on it more extensively.

The first feature to notice is that the choices $(h_i, h_j) = (-s, +s)$ and $(h_i, h_j) = (+s, -s)$ lead respectively to the behaviors z^{-s} and z^{3s} . This is in agreement with the known results for Yang-Mills and Gravity under the standard BCFW-deformation ($\sim z^{-s}|_{s=1,2}$) and the “wrong” one ($\sim z^{3s}|_{s=1,2}$). The other two choices for the helicities of the deformed particles seem to show two possible values for the parameter ν if we use (2.3.19), depending on how the collinear limit is taken. This puzzle is quickly resolved by noticing that the amplitude factorizes under just one of the two ways in which the limit $P_{ij}^2 \rightarrow 0$ can be realized. It is easy to understand also which limit is allowed by just looking at the helicity configuration of the three-particle amplitudes of the eventual factorization. To give an example let us consider for instance $(h_1, h_2) = (-s, -s)$. Under the limit $P_{12}^2 \rightarrow 0$, the amplitude $M_4(1^{-s}, 2^{-s}, 3^{+s}, 4^{+s})$ would factorize into

$$\lim_{P_{12}^2 \rightarrow 0} P_{12}^2 M_4 = M_3(1^{-s}, 2^{-s}, -P_{12}^{h_{12}}) M_3(P_{12}^{-h_{12}}, 3^{+s}, 4^{+s}). \quad (2.4.5)$$

The class of theories we are discussing admits just the three-particle amplitudes (2.4.2) and therefore the helicity h_{12} is fixed to be $h_{12} = +s$. It is clear from (2.4.2) that in the limit $\langle 1, 2 \rangle \rightarrow 0$, the sub-amplitude $M_3(1^{-s}, 2^{-s}, -P_{12}^{h_{12}})$ vanishes. So the amplitude does not factorize in this complex limit. However, in the limit $[1, 2] \rightarrow 0$ none of the two three-particle amplitudes vanishes and the amplitude does factorize.

Notice also that in the case of a scalar theory, all the factorization limits are allowed and the amplitude behaves as a constant as z is taken to infinity.

Having established generically the complex-UV limit, we now focus on the computation of the four-point amplitude, that will allow us to run the four-particle test. As a first helicity choice for the particles whose momenta we deform as in (2.4.4) we pick $(h_1, h_4) = (-s, +s)$. With such a choice, the fall-off of the amplitude as z is taken to infinity is z^{-s} , and therefore for $s \neq 0$ the amplitude admits the standard BCFW representation. The very same happens for a second choice $(h_1, h_2) = (-s, -s)$. Therefore, this four-amplitude was already studied in [29], where the only consistent theories were found to be given by $s = 1$ with internal quantum numbers and $s = 2$. In the case of spin 1, the equality was holding if and only if the structure constants were satisfying the Jacobi identity, while for the spin-2 particles the algebra is reducible and leads to several self-interacting spin-2 particles which do not interact with each other.

For completeness, let us analyze the only missed case, the scalar case. Picking the deformation (2.4.4) and using the fact that the three-particle amplitude is just the coupling constant $\hat{\kappa} = \kappa_H + \kappa_A$, the on-shell representation for the four-particle amplitude turns out to be

$$M_4^{(1,2)}(0) = \hat{\kappa}^2 \frac{f_{13}^{(1,2)}}{P_{13}^2} + \hat{\kappa}^2 \frac{f_{14}^{(1,2)}}{P_{14}^2}, \quad (2.4.6)$$

where the notation on the left-hand-side is meant to stress the fact that this expression has been obtained by deforming the momenta of the particles labelled by 1 and 2. The amplitude behaves as a constant at infinity, which implies that we need the knowledge of just one zero in order to fix the “weights” $f_{1k}^{(1,2)}$ in (2.4.6). Using the conditions (2.3.25) on the zeroes, it can be written as follows

$$M_4^{(1,2)}(0) = \hat{\kappa}^2 \left(\frac{1}{P_{13}^2} + \frac{1}{P_{14}^2} - \frac{1}{\alpha(1+\alpha)P_{12}^2} \right). \quad (2.4.7)$$

The condition (2.3.28) further implies that the coefficient α needs to satisfy the equation $\alpha(1+\alpha) = -1$, where the left-hand-side is exactly the form in which α enters in (2.4.7). Therefore, the final answer from the $(1, 2)$ -deformation is

$$M_4^{(1,2)}(0) = -\hat{\kappa}^2 \frac{\mathbf{s}\mathbf{t} + \mathbf{t}\mathbf{u} + \mathbf{u}\mathbf{s}}{\mathbf{s}\mathbf{t}\mathbf{u}}, \quad (2.4.8)$$

where the Mandelstam variables $\mathbf{s} := P_{12}^2$, $\mathbf{t} := P_{14}^2$ and $\mathbf{u} := P_{13}^2$ have been introduced. It is easy to notice that the contribution from the singularity at infinity, provided by the last term in (2.4.7), contains the pole in the \mathbf{s} -channel which could not be reproduced by the residues of the poles at finite positions.

One can try to perform again this computation by deforming the momenta of the particles 1 and 4. Notice that the result of this can be just obtained from (2.4.7) and (2.4.8) by the

label exchange $2 \leftrightarrow 4$. However, it is easy to see that the expression in (2.4.8) is invariant under such a label exchange and, therefore, the $(1, 4)$ -deformation returns the same result. Therefore, the scalar theory passes the tree-level consistency check, as it should, and equation (2.4.8) is the known result from the $\lambda\phi^3$ -theory.

Furthermore, one can think of considering several species of scalars by introducing internal quantum numbers as in (2.4.2). For this case, as for all the cases of even spin, the structure constants are completely symmetric. Imposing the four-particle test, the consistency requirement implies an algebra structure similar to the one found for several species of spin-2 particles in [29], which is reducible. As a consequence, this theory would reduce to a set of self-interacting scalars which do not interact among them.

Thus, the generalised on-shell representation (2.2.20) allows to obtain all the known self-interacting theories and discard the existence of higher-spin self-interactions within this class of theories (characterized by s -derivative interactions).

Interactions with s -derivatives: spin s /spin s'

Now we let a different particle, with spin s' , into the theory. We consider interactions whose couplings have the same dimension $[\kappa] = 1 - s$. These interactions are defined through the three-particle amplitudes written in 2.4.2, which describe the self-interaction of the particle of spin s , and two further three-particle amplitudes describing the spin- s /spin- s' interaction:

$$\begin{aligned} M_3(1^{-s'}, 2^{+s'}, 3^{-s}) &= \kappa' \varepsilon_{b_1 b_2 a_3} \frac{\langle 3, 1 \rangle^{s+2s'}}{\langle 1, 2 \rangle^s \langle 2, 3 \rangle^{2s'-s}}, \\ M_3(1^{-s'}, 2^{+s'}, 3^{+s}) &= \kappa' \varepsilon_{b_1 b_2 a_3} \frac{[2, 3]^{s+2s'}}{[3, 1]^{2s'-s} [1, 2]^s}, \end{aligned} \quad (2.4.9)$$

where $\varepsilon_{b_1 b_2 a_3}$ is an eventual structure constant whose indices b are referred to the particles of spin s' , while the index a refers to the particle of spin s . Moreover we keep the spin- s /spin- s' coupling constant to be different from the spin- s self-interaction one and an eventual relation, if any, should emerge from consistency requirements. Notice that the spin- s' self-interaction is not allowed because we are focusing on interactions with the same coupling constant dimensions (*i.e.* with a fixed number of derivatives in the interactions) and this would fix s' to be equal to s .

The four-particle analysis involves two types of amplitudes:

$$M_4(1^{-s}, 2^{+s}, 3^{-s'}, 4^{s'}), \quad M_4(1^{-s'}, 2^{+s'}, 3^{-s'}, 4^{+s'}), \quad (2.4.10)$$

which are characterized respectively by three and two factorization channels (in the second amplitude the u -channel is not permitted); and under a two-particle deformation they show two and one pole in z respectively.

As a first step, let us analyze in detail the complex-UV behavior of the amplitudes in (2.4.10) under the (i, j) -deformation (2.4.4). The complex-UV exponents of the amplitudes under all the possible two-particle deformations are listed in table 2.2.

The behavior of the amplitudes when the helicities of particle i and particle j are chosen to be $(h_i, h_j) = (\mp s, \pm s)$ is the same as in the self-interacting case of the previous

$\begin{array}{c} h_j \\ \hline h_i \end{array}$	$-s$	$+s$	$-s'$	$+s'$
$-s$	$\begin{array}{c} \text{X} \\ \hline -s \end{array}$	$-s$	$\begin{array}{c} \text{X} \\ \hline -s \end{array}$	$\begin{array}{c} \text{X} \\ \hline -s \end{array}$
$+s$	$3s$	$\begin{array}{c} \text{X} \\ \hline -s \end{array}$	$\begin{array}{c} \text{X} \\ \hline s + 2s' \end{array}$	$\begin{array}{c} \text{X} \\ \hline s - 2s' \end{array}$
$-s'$	$\begin{array}{c} \text{X} \\ \hline s - 2s' \end{array}$	$\begin{array}{c} \text{X} \\ \hline -s \end{array}$	$\begin{array}{c} \text{X} \\ \hline \text{X} \end{array}$	$\begin{array}{c} \text{X} \\ \hline s - 2s' \end{array}$
$+s'$	$\begin{array}{c} \text{X} \\ \hline s + 2s' \end{array}$	$\begin{array}{c} \text{X} \\ \hline -s \end{array}$	$s + 2s'$	$\begin{array}{c} \text{X} \\ \hline \text{X} \end{array}$

Table 2.2: Complex-UV behavior ν for spin- s /spin- s' interactions. The notation is as in table 2.1. The cells where both triangles show “X” indicate that the amplitude does not factorize in the $P_{ij}^2 \rightarrow 0$ limit, and therefore our analysis does not return a value for ν .

section for both of the two amplitudes under analysis. As before, when h_i and h_j are the same or they correspond to particles of different spin, just one between the holomorphic and anti-holomorphic factorization in the (i, j) -channel is allowed. Following the arguments of the previous section, it is easy to see which one occurs and therefore which one of them fixes the complex-UV behavior. The different numbers in table 2.2 represent the exponent ν of complex-UV behavior under a given assignment for the helicities of the particles whose momenta have been deformed. Under some particular choices, namely $(h_i, h_j) = \{(-s', -s'), (+s', +s')\}$, neither the holomorphic nor the anti-holomorphic factorization in the (i, j) -channel are allowed and therefore, in principle, the analysis of the factorization properties of the amplitudes to fix the large- z parameter ν and the Mandelstam variables when the S-matrix becomes trivial, seems to break down. But, as it is manifest from table 2.2, it is always possible to choose an assignment for the helicities (h_i, h_j) such that at least one of the factorization limits in the (i, j) -channel holds and, as a consequence, the conditions (2.3.25) and (2.3.28) are rigorously valid.

Notice that for the four-point amplitude $M_4(1^{-s}, 2^{+s}, 3^{-s'}, 4^{+s'})$, with $s \neq 0$, it is always possible to choose a deformation, namely the one defined by equation (2.4.4) with $i = 1, j = 2$, for which the amplitude vanishes as $\sim z^{-s}$. As far as the amplitude $M_4(1^{-s'}, 2^{+s'}, 3^{-s'}, 4^{+s'})$ is concerned, the deformation (2.4.4) with $i = 1, j = 2$ induces the large- z behavior $M_4^{(1,2)}(z) \sim z^{s-2s'}$ and, therefore, the standard BCFW recursive relation is valid if and only if $s < 2s'$, while for $s \geq 2s'$ the amplitude shows a recursive structure through the generalised on-shell formula (2.2.20).

Let us start the detailed analysis of the possible constraints on the four-particle amplitudes by looking at the amplitude $M_4(1^{-s'}, 2^{+s'}, 3^{-s'}, 4^{+s'})$. Under the $(1, 2)$ -deformation, the amplitude is given by

$$M_4^{(1,2)}(1^{-s'}, 2^{+s'}, 3^{-s'}, 4^{+s'}) = (\kappa')^2 (-1)^s \frac{f_{14}^{(1,2)}}{t} \frac{\langle 1, 3 \rangle^{2s'} [4, 2]^{2s'}}{s^{2s'-s}}. \quad (2.4.11)$$

Similarly, under the $(1, 4)$ -deformation

$$\tilde{\lambda}^{(1)}(z) = \tilde{\lambda}^{(1)} - z \tilde{\lambda}^{(4)}, \quad \lambda^{(4)} = \lambda^{(4)} + z \lambda^{(1)}, \quad (2.4.12)$$

we get

$$M_4^{(1,4)}(1^{-s'}, 2^{+s'}, 3^{-s'}, 4^{+s'}) = (\kappa')^2 (-1)^s \frac{f_{12}^{(1,4)}}{\mathbf{s}} \frac{\langle 1, 3 \rangle^{2s'} [4, 2]^{2s'}}{\mathbf{t}^{2s'-s}}. \quad (2.4.13)$$

Imposing the four-particle test we get

$$\frac{M_4^{(1,4)}}{M_4^{(1,2)}} = 1 = \frac{f_{12}^{(1,4)}}{f_{14}^{(1,2)}} \left(\frac{\mathbf{s}}{\mathbf{t}} \right)^{2s'-s-1}. \quad (2.4.14)$$

As we mentioned earlier, for $s < 2s'$ the one-parameter families of amplitudes generated by (2.4.4) and (2.4.12) vanish as z is taken to infinity, and the “weights” appearing in the generalised on-shell representation are 1. As a consequence, the consistency relation (2.4.14) is satisfied if and only if $s = 2s' - 1$.

In the case $s \geq 2s'$, the “weights” $f_{14}^{(1,2)}$ and $f_{12}^{(1,4)}$ are fixed through the condition (2.3.28):

$$\begin{aligned} P_{14}^2(z_0^{(i)}) = -P_{12}^2 &\Rightarrow f_{14}^{(1,2)} = (-1)^{s-2s'+1} \left(\frac{\mathbf{u}}{\mathbf{s}} \right)^{s-2s'+1}; \\ P_{12}^2(z_0^{(i)}) = -P_{14}^2 &\Rightarrow f_{12}^{(1,4)} = (-1)^{s-2s'+1} \left(\frac{\mathbf{u}}{\mathbf{t}} \right)^{s-2s'+1}, \end{aligned} \quad (2.4.15)$$

and the consistency condition (2.4.14) turns out to be identically satisfied.

Let us now focus on the amplitude $M_4(1^{-s}, 2^{+s}, 3^{-s'}, 4^{+s'})$ and compute it through the deformations (1, 2) and (1, 4). First of all, from table 2.2 both one-parameter families of amplitudes generated by such deformations behave as $\sim z^{-s}$ as z is taken to infinity.

$$\begin{aligned} M_4^{(1,2)} &= (\kappa')^2 \frac{\langle 1, 3 \rangle^s \langle 1, 4 \rangle^s [4, 2]^{2s'+s}}{[3, 2]^{2s'-s} \mathbf{s}^s} \left(\frac{f_{13}^{(1,2)}}{\mathbf{u}} + \frac{f_{14}^{(1,2)}}{\mathbf{t}} \right), \\ M_4^{(1,4)} &= \kappa' \frac{\langle 1, 3 \rangle^s [4, 2]^{2s'+s}}{[1, 4]^s [3, 2]^{2s'-s}} \left(\kappa \frac{f_{12}^{(1,4)}}{\mathbf{s}} + \kappa' \frac{f_{13}^{(1,4)}}{\mathbf{u}} \right). \end{aligned} \quad (2.4.16)$$

As long as $s \neq 0$, the “weights” are 1 and the consistency condition reads

$$\frac{M_4^{(1,4)}}{M_4^{(1,2)}} = 1 = (-1)^s \left(\frac{\mathbf{s}}{\mathbf{t}} \right)^{s-2} \left[1 - \frac{\mathbf{u}}{\mathbf{t}} \left(\frac{\kappa}{\kappa'} - 1 \right) \right], \quad (2.4.17)$$

which is satisfied if and only if $s = 2$ and $\kappa' = \kappa$, or $s = 1$ and $\kappa = 0$.

For $s = 0$, the “weights” are no longer 1 and the consistency condition becomes

$$\frac{M_4^{(1,4)}}{M_4^{(1,2)}} = 1 = \frac{\kappa}{\kappa'} - \left(\frac{\kappa}{\kappa'} - 1 \right) \frac{\mathbf{st} + \alpha \mathbf{us}}{\mathbf{st} + \mathbf{tu} + \mathbf{us}}, \quad (2.4.18)$$

where α is the parameter characterizing the zeroes in (2.3.25). The four-particle test turns out to be satisfied if and only if $\kappa' = \kappa$.

Summarizing, the four-particle test on the amplitude with two external states of spin s and two with spin s' either sets the coupling constant $\kappa = 0$ and the interaction mediator to have spin 1, or forces the coupling constants κ and κ' to be identical and the interaction mediator to have spin 0 or spin 2. When the test is instead applied to the amplitude with

four external states of spin s' , we either obtain an exact relation between spin s and spin s' , *i.e.* $s = 2s' - 1$, if $s < 2s'$, or no constraint at all for $s \geq 2s'$. Altogether, these relations strongly constrain the types of theories we can have in this class. Specifically, if $s = 2$, we can only have $s' = 3/2$ for $s < 2s'$ when the standard BCFW relations hold, as it was already seen in [29], and $s' \leq 1$ for $s \geq 2s'$.

For $s = 1$, the condition for $s < 2s'$ required by the consistency of the amplitude with all the external states of spin s is never fulfilled. For $s \geq 2s'$, instead, we rediscover the interactions between spin 1 and fermions/scalars. Notice that the self-interaction coupling κ for $s = 1$ needs to be zero, which implies that the spin 1 mediator is actually a photon. Therefore, we have rediscovered Quantum ElectroDynamics (QED) and scalar QED.

Finally, if instead $s = 0$, the only theory admitted has $s' = 1/2$, which corresponds to a Yukawa interaction.

Hence, the generalised on-shell recursion relations (2.2.20) allow us to rediscover not only $\mathcal{N} = 1$ Supergravity, but also Einstein-Maxwell, Fermion-Gravity, Scalar-Gravity, QED, Yukawa theories and all the known theories within the class we are scanning.

In the previous calculations we set the structure constants $\varepsilon_{b_1 b_2 a_3}$ to 1. If instead we allow the theory to have an internal symmetry, it is easy to see what follows. From the analysis of the amplitude with four external states of spin s' , the consistency condition (2.4.14) becomes

$$\sum_{a_P} \varepsilon_{b_1 b_4 a_P} \varepsilon_{a_P b_3 b_2} = \sum_{a_P} \varepsilon_{b_1 b_2 a_P} \varepsilon_{a_P b_3 b_4} \frac{f_{12}}{f_{14}} \left(\frac{s}{t} \right)^{2s'-s-1}, \quad (2.4.19)$$

where the index a in the structure constants is related to the spin- s particles, while the index b is related to the spin- s' ones. The conditions on the spins do not change with respect to the case where the theory was not endowed with an internal symmetry: the theories which satisfy the standard BCFW representation are characterized by $s = 2s' - 1$, while the others must have $s \geq 2s'$. In both cases, the structure constants need to satisfy the algebra

$$\sum_{a_P} \varepsilon_{b_1 b_4 a_P} \varepsilon_{a_P b_3 b_2} = \sum_{a_P} \varepsilon_{b_1 b_2 a_P} \varepsilon_{a_P b_3 b_4}. \quad (2.4.20)$$

From the amplitude with two external states of spin s and two of spin s' , the consistency condition becomes

$$\begin{aligned} & \left[1 - (-1)^s \left(\frac{s}{t} \right)^s \right] \sum_{b_P} \varepsilon_{a_1 b_3 b_P} \varepsilon_{b_P b_4 a_2} + \frac{u}{t} \sum_{b_P} \varepsilon_{a_1 b_4 b_P} \varepsilon_{b_P b_3 a_2} = \\ & = \left(\frac{s}{t} \right)^{s-1} \frac{u}{t} \sum_{a_P} \varepsilon_{a_1 a_2 a_P} \varepsilon_{a_P b_3 b_4} + \left(\frac{s}{t} \right)^{s-1} \frac{u}{t} \left(\frac{\kappa}{\kappa'} - 1 \right) \sum_{a_P} \varepsilon_{a_1 a_2 a_P} \varepsilon_{a_P b_3 b_4}, \end{aligned} \quad (2.4.21)$$

which is satisfied only for $s = 1$ and $\kappa' = \kappa$, with the algebra

$$\sum_{b_P} \varepsilon_{a_1 b_4 b_P} \varepsilon_{b_P b_3 a_2} - \sum_{b_P} \varepsilon_{a_1 b_3 b_P} \varepsilon_{b_P b_4 a_2} = \sum_{a_P} \varepsilon_{a_1 a_2 a_P} \varepsilon_{a_P b_3 b_4}. \quad (2.4.22)$$

This algebra corresponds to the coupling of gluons with matter $s' \leq 1/2$, *i.e.* to flavor in a YM theory.

s	Conditions	Interactions
$s = 0$	$s' = \frac{1}{2}, \kappa = \kappa'$	Yukawa
	$s' = 0, \kappa = \kappa'$	$\lambda\phi^3$
$s = 1$	$s' = 0, \kappa = 0$	scalar QED and YM+scalars
	$s' = \frac{1}{2}, \kappa = 0$	QED and YM+fermions
	$s' = 1, \kappa = \kappa'$	YM
$s = 2$	$s' = 0, \kappa = \kappa'$	scalar GR
	$s' = \frac{1}{2}, \kappa = \kappa'$	Fermion Gravity
	$s' = 1, \kappa = \kappa'$	Einstein-Maxwell
	$s' = \frac{3}{2}, \kappa = \kappa'$	$\mathcal{N} = 1$ supergravity
	$s' = 2, \kappa = \kappa'$	GR

Table 2.3: Summary of the theories characterized by couplings with s -derivative interactions. The fact that $\kappa = \kappa'$ for $s = 2$ is the *quantum version of the equivalence principle*.

Finally, we do not see any signature of a possible existence of higher-spin couplings with and without the introduction of internal quantum numbers. At the beginning of this subsection we have seen that, with our hypothesis, the self-interaction of particles with spin higher than two is trivial. This means that in equation (2.4.21) the coupling constant κ needs to be set to zero. It is easy to see that for $s > 2$ it is not possible to get a pure identity on the structure constants, without any function of the kinematic variables.

For the sake of clarity, we summarize the consistent theories characterized by couplings with s -derivative interactions in table 2.3.

2.4.3 Higher-derivative interactions

In the previous subsection we rediscovered all the fundamental theories that are known in Nature. All of them are characterized by minimal couplings, corresponding to s -derivatives interactions. Minimal couplings are very convenient for a Lagrangian formulation, as this exists for all the theories we found. Much less is known about non-minimal couplings, corresponding to higher-derivative interactions, where a consistent Lagrangian treatment is not known yet. It is then a good opportunity to use the tools developed in this chapter to explore this possibility.

We start by discussing a second class of possible self-interacting theories. This class is characterized by the following three-particle amplitudes

$$\begin{aligned}
M_3(1^{-s}, 2^{-s}, 3^{-s}) &= \kappa'' \varepsilon_{a_1 a_2 a_3} (\langle 1, 2 \rangle \langle 2, 3 \rangle \langle 3, 1 \rangle)^s, \\
M_3(1^{+s}, 2^{+s}, 3^{+s}) &= \kappa'' \varepsilon_{a_1 a_2 a_3} ([1, 2][2, 3][3, 1])^s.
\end{aligned}
\tag{2.4.23}$$

A simple dimensional analysis shows that such interactions would correspond, in the Lagrangian language, to three-point vertices with $3s$ -derivative interactions. This type of coupling typically emerges as an effective interaction at low-energies (*e.g.* F^3 , R^3). In the case of spin 2, a term of the type R^3 is the leading counterterm at two-loops [66], while in [67] it has been proposed an apparently classically consistent theory which shows a 6-derivative interaction, but which does not have general covariance.

From the helicity structure of the three-particle amplitudes (2.4.23), it is straightforward to conclude that there is only one type of non-trivial four-particle amplitude: $M_4(1^{-s}, 2^{+s}, 3^{-s}, 4^{+s})$. We can also infer that such an amplitude can have just one factorization channel, the u -channel.

This implies that a momentum-deformation involving the spinors of particle 1 and particle 3 generates a one-parameter family of amplitudes which does not have any pole at finite location in the parameter z and, as a consequence, the whole amplitude coincides with the contribution $M_4^{(1,3)}(\infty)$ from the singularity at infinity. Our formula (2.2.20) is not applicable then. Nevertheless, a momentum-deformation such as (1, 2) induces the presence of a pole at finite location, making the generalised on-shell recursion relation a meaningful mathematical representation again. However, the amplitude does not have any factorization channel other than the u -channel, which invalidates our analysis of the collinear limit used to fix the complex-UV parameter ν and the conditions on the zeroes. We have to take a leap of faith here.

If one thinks about the limits in which the S-matrix becomes trivial as a generic property of the scattering amplitudes themselves, it is reasonable to assume that the condition (2.3.28) on the zeroes can still hold

$$P_{13}^2(z_0^{(j)}) = -P_{1j}^2, \quad (2.4.24)$$

where j can be either 2 or 4, depending on whether the (1, 2) or (1, 4)-deformation is used. Applying these two deformations plus the condition (2.4.24), we get

$$\begin{aligned} M_4^{(1,2)} &= (\kappa'')^2 (-1)^{\nu+1} \left(\frac{t}{s}\right)^{\nu+1} \frac{\langle 1, 3 \rangle^{2s} [4, 2]^{2s}}{u} s^s, \\ M_4^{(1,4)} &= (\kappa'')^2 (-1)^{\nu+1} \left(\frac{s}{t}\right)^{\nu+1} \frac{\langle 1, 3 \rangle^{2s} [4, 2]^{2s}}{u} t^s, \end{aligned} \quad (2.4.25)$$

where ν is, as usual, the complex-UV behavior parameter, which is left generic here¹¹. The four-particle test

$$\frac{M_4^{(1,4)}}{M_4^{(1,2)}} = 1 = \left(\frac{s}{t}\right)^{2\nu+2-s}, \quad (2.4.26)$$

is satisfied if and only if $\nu = (s-2)/2$, with $s \geq 2$. The four-particle amplitude can therefore be written as

$$M_4(1^{-s}, 2^{+s}, 3^{-s}, 4^{+s}) = (\kappa'')^2 (-1)^{s/2} \frac{\langle 1, 3 \rangle^{2s} [4, 2]^{2s}}{u} (st)^{s/2}. \quad (2.4.27)$$

¹¹If we assumed $\nu < 0$ (and, as a consequence, the “weights” equal to one), it turns out that the four-particle test would imply $s = 0$, for which s derivatives and $3s$ derivatives are the same, and then this case has been analyzed already in section 2.4.2.

A comment is now in order. The expression (2.4.27) for the four-point amplitude satisfies the only collinear limit allowed ($u \rightarrow 0$), as it is manifest from the on-shell construction, as well as it trivially satisfies the soft limits, in which the amplitude vanishes. The form (2.4.27) seems to be consistent, at least for particles with even spin. For particles with odd spin, the expression (2.4.27) shows branch points which in principle are not expected.

For the amplitudes of the previous subsection, the contribution at infinity was taking care of the channels missed by the BCFW terms. This is not the case here, as the contribution from the singularity at infinity is a polynomial of degree $s/2 - 1$ in the Mandelstam variables s and t

$$\begin{aligned} M_4^{(1,2)} &= (\kappa'')^2 \langle 1, 3 \rangle^{2s} [4, 2]^{2s} s^{s/2} P_{(s/2-1)}^{(1,2)}(s, t), \\ M_4^{(1,4)} &= (\kappa'')^2 \langle 1, 3 \rangle^{2s} [4, 2]^{2s} t^{s/2} P_{(s/2-1)}^{(1,4)}(s, t), \end{aligned} \quad (2.4.28)$$

where the polynomials related to two deformations $(1, 2)$ and $(1, 4)$ are mapped into each other by the label exchange $2 \leftrightarrow 4$. The interpretation cannot be the standard one. If we interpret this contribution as coming from the interchange of a massive particle (with a large mass so that its propagator is m^{-2}), by simple dimensional analysis one can conclude that this massive particle should have a large spin $\tilde{s} > 3s$. If this type of behavior holds for higher n -point amplitudes, this would point out to the presence of a tower of infinite massive higher-spin states, resembling the structure of string theory. This could point out to a non-locality of the theory. We reserve further comments for section 2.4.4.

The conclusions above are really just speculations, and a more formal treatment of the issue is needed, that would justify the use of condition (2.4.24) for these cases with only one BCFW channel, and that would allow to go higher than $n = 4$ in the number n of external particles. Therefore, in what follows we summarize the analysis of [21], where the details can be found, of the possibilities of higher-derivative interactions between particles of different spin¹²; an analysis that suffers from the same shortcomings of the one above.

Spin- s /spin- s' interactions with $(2s' + s)$ -derivatives

The idea is to consider three-particle couplings with dimension $[\bar{\kappa}] = 1 - (2s' + s)$, which are characterized by three-particle amplitudes:

$$\begin{aligned} M_3(1^{-s'}, 2^{-s'}, 3^{-s}) &= \bar{\kappa} \varepsilon_{b_1 b_2 a_3} \langle 1, 2 \rangle^{2s'-s} \langle 2, 3 \rangle^s \langle 3, 1 \rangle^s, \\ M_3(1^{+s'}, 2^{+s'}, 3^{+s}) &= \bar{\kappa} \varepsilon_{b_1 b_2 a_3} [1, 2]^{2s'-s} [2, 3]^s [3, 1]^s. \end{aligned} \quad (2.4.29)$$

Without worrying about a possible self-interaction of the particle with spin s , in such a theory it is possible to define just two non-trivial four-particle amplitudes: $M_4(1^{-s'}, 2^{+s'}, 3^{-s'}, 4^{+s'})$ and $M_4(1^{-s}, 2^{+s}, 3^{-s}, 4^{+s'})$. As it happened in the self-interacting case with $3s$ -derivatives,

¹²We always set to one the structure constants for these cases. Strictly speaking, one can keep them and try to see if they are somehow constrained. However, it is important to notice that, under all the useful momentum deformations we can define, the same factorization channel appears and, as a consequence, the four-particle amplitudes computed through the two different deformations would show the same factor involving the structure constants. Therefore, the four-particle test does not impose any constraint on the structure constants.

it is easy to infer from the helicity configurations (2.4.29) that these amplitudes show just one factorization channel (with the label assignment chosen, it turns out to be again the u -channel). Proceeding as for the previous cases, and extrapolating again of the validity of (2.4.24), one finds that the four-particle test allows the following interactions with three-point amplitudes given in (2.4.29):

- An interaction between particles of spin $s' \geq 1$ mediated by a particle with spin $s = 2s'$.
- An interaction between particles of spin $s' \geq 2$ mediated by a particle with spin $s \in [2, 2s' - 2]$.
- More interestingly, in the case where $s = 0$, the amplitude $M_4(1^{-s'}, 2^{+s'}, 3^0, 4^0)$ is expected to factorize both in the u and t channels. As a consequence, it is possible to define generalised on-shell representations for which the analysis of the collinear limits holds, and fixes the conditions on the zeroes faithfully. With the helicity assignments chosen above, such representations are generated by the $(1, 3)$ and $(1, 4)$ -deformations, where for particle 1 the anti-holomorphic spinor gets deformed while for particles 3 and 4 the deformed spinor is the holomorphic one:

$$\begin{aligned} M_4^{(1,3)} &= \kappa^2 f_{14}^{(1,3)} \frac{\langle 1, 4 \rangle^{2s'} [4, 2]^{2s'}}{t}, & f_{14} &= (-1)^{\nu+1} \left(\frac{s}{u} \right)^{\nu+1}, \\ M_4^{(1,4)} &= \kappa^2 (-1)^{2s'} f_{13}^{(1,4)} \frac{\langle 1, 3 \rangle^{2s'} [3, 2]^{2s'}}{u}, & f_{13} &= (-1)^{\nu+1} \left(\frac{s}{t} \right)^{\nu+1}. \end{aligned} \quad (2.4.30)$$

The complex-UV parameter ν is fixed by the analysis of the collinear limits $[1, 4] \rightarrow 0$ and $[1, 3] \rightarrow 0$ for the representations respectively in the first and second line of equation (2.4.30), and, in both cases, it turns out to be given by $\nu = \delta + 2h_1 = 0$. One can immediately see how the two expressions in (2.4.30) do coincide when $\nu = 0$:

$$M_4(1^{-s'}, 2^{+s'}, 3^0, 4^0) = -\kappa^2 \frac{\langle 1, 4 \rangle^{2s'} [4, 2]^{2s'}}{tu} s. \quad (2.4.31)$$

This analysis seems to reveal that, at least at tree level, it is possible to define non-trivial couplings between arbitrary spin- s' particles and a scalar.

Spin- s /spin- s' interactions with $|2s' - s|$ -derivatives

This class of theories is defined by three-particle amplitudes with the following two helicity configurations

$$M_3(1^{-s'}, 2^{-s'}, 3^{+s}), \quad M_3(1^{+s'}, 2^{+s'}, 3^{-s}). \quad (2.4.32)$$

Again one faces the problems of having just one explicit BCFW channel, needing an extrapolation to apply (2.4.24). Proceeding with the four-particle test all the same, there are three cases to analyze separately, depending on whether $2s' - s$ is positive, negative or zero. It turns out that no new high-derivative interaction is allowed by the test within this class.

2.4.4 A summary

Let us now recapitulate and reflect on the results of the previous two subsections, which contain very strong statements. Given the generality of our approach, all the theories not showing up in our analysis are ruled out of the space of consistent theories (or either do not satisfy any of the assumptions we made for the theories at the very beginning of section 2.4).

Since for the theories with a minimal coupling, all the theories we found were already known, we focus mainly on the possibility of describing theories involving higher-spin particles, for which the consistency conditions on the four-particle amplitudes seem to provide us with some classes of theories where the particles have their spin partially constrained. Let us go through all the cases systematically:

1. Self-interactions with s derivatives: These are theories characterized by three-particle amplitudes with helicity configurations $(\mp s, \mp s, \pm s)$, which is the class in which $\lambda\phi^3$, Yang-Mills and Gravity fall. The consistency requirement (2.4.1) rules out the possibility of having any self-interacting theory (with or without internal quantum numbers) with spin $s > 2$.
2. Spin- s /spin- s' interactions with s derivatives: The three-particle amplitudes characterizing this class of theories have helicity configurations $(\mp s', \pm s', \mp s)$, with the spin- s particle playing the role of mediator. The four-particle test on the generalised on-shell recursion relation allows us to rediscover the couplings of gravitons and photons/gluons with particles with lower spin, with their algebra structure (if any), as well as the Yukawa interactions. Again, with our assumptions, we do not find in this class of theories any signature of the possible existence of scattering processes involving high-spin particles.
3. Self-interactions with $3s$ -derivatives: These are theories defined by three-particle amplitudes with helicity configurations $(\mp s, \mp s, \mp s)$. They have the peculiar feature of allowing just one factorization channel in four-particle amplitudes. The consistency condition seems not to forbid the self-interaction of particles with even spin higher or equal to two.
4. Spin- s /spin- s' interactions with $(2s' + s)$ -derivatives: The three-particle amplitudes defining the theories in this class have helicity configurations $(\mp s', \mp s', \mp s)$. The non-trivial consistent interactions that seem to be allowed are between particles with spin $s' \geq 1$ and particles with spin $s = 2s'$, and more generically spin- s /spin- s' interactions with $s \in [2, 2(s' - 1)]$, $s' \geq 2$. We also find consistent interactions between a scalar ($s = 0$) and particles of spin $s' > 0$.
5. Spin- s /spin- s' interactions with $|2s' - s|$ -derivatives: In this last case, the fundamental building-blocks are three-particle amplitudes with helicity structure $(\mp s', \mp s', \pm s)$. The consistency analysis does not seem to reveal any non-trivial interaction apart from the $s = 0$ case we already saw had (notice that for $s = 0$, $2s' + s = |2s' - s|$).

Let us comment in some detail on the last three classes of theories. All of them have in common the feature of possessing just one factorization channel for four-particle amplitudes.

This implies that a BCFW deformation can induce at most one pole for the complex amplitude, corresponding to the same channel in which the amplitude factorizes in momentum space. Therefore, the zeroes cannot be fixed by the collinear limit analysis of section 2.3.1, and formula (2.3.28) cannot be rigorously derived.

We overcame this issue by generalizing the condition (2.3.28) on the zeroes also to these cases, thinking about the zeroes of an amplitude on the same footing as the poles, *i.e.* as “universal” limits in momentum-space. Obviously, this is a strong assumption which needs to be checked. But let us play along and allow ourselves for some speculation, as the expressions we got using this assumption do not seem to show any obvious inconsistency at the four-point level.

An interesting feature of these classes of theories is the form of the contribution from the singularity at infinity $M_4^{(i,j)}(\infty)$. Let us think of the amplitude as the sum of a standard BCFW-term and $M_4^{(i,j)}(\infty)$, rather than in the form (2.2.20). As it can be seen from the expressions (2.4.28) for the $3s$ -derivative interaction (it can be explicitly checked also for the other cases), such terms do not show any pole in the Mandelstam variables. As a consequence $M_4^{(i,j)}(\infty)$ has the structure of a contact interaction. Dimensional analysis on (2.4.28) reveals that such a contact interaction has $2(3s-1)$ -derivatives. It is very likely that, provided that the theory is tree-level consistent, the n -particle amplitude would show an n -particle contact term in this on-shell representation. Focusing, again just as an example, on the $3s$ -derivative interaction case, the number of derivatives of such a contact interaction turns out to be $L_n = (3s-2)n - 6(s-1)$.

More generally, given a theory with δ -derivative three-particle couplings, the n -particle contact term turns out to be characterized by L_n derivatives, with $L_n = (\delta-2)n - 2(\delta-3)$. In the cases of relevance, namely $\delta > 2$, it is easy to see that L_n increases with n . Therefore, these theories seem to be endowed with higher-derivative interaction terms, whose number of derivatives increases with the number of external states. This can be interpreted as a signature of non-locality for these theories. In the known example of supposedly consistent high-spin interactions in flat space, non-locality, a non-Abelian structure and the existence of a large number of propagating degrees of freedom (*e.g.* [68] and references therein) seem to be key features to be able to define high-spin interactions.

Very likely, the theories involving spin higher than two we have discovered will not be consistent (we took just the simplest possible interactions with very few particles involved). However, the main aim of this discussion was to check if, in some sense, the generalised on-shell representation could be a good arena for consistently looking for high-spin theories¹³. Surprisingly enough, starting from four basic hypothesis (Poincaré invariance, analyticity of the S-Matrix, locality, and existence of 1-particle states) we arrived to the possibility of seeing the breaking down of the locality requirement through the contact terms generated as the contribution from the singularity at infinity.

¹³An attempt to use the BCFW construction for high-spin theories was done in [69].

Chapter 3

Non-perturbative physics with String Theory

Contextualizing this chapter

We go over the basics of the gauge/gravity correspondence very briefly, putting the emphasis in the addition of flavor into the correspondence through the smearing technique, and illustrating the general picture for the concepts that we will use throughout the next three chapters. There are excellent reviews out there about all these topics (except for the final topic we treat, which is novel), and we are just obliged to go over them to fix the notation and set up the framework of ideas we use in the rest of this Ph.D. thesis.

3.1 The gauge/gravity correspondence

The rigorous way to define an interacting field theory follows the Wilsonian perspective [70]. One starts from a CFT, with a given basis of operators, and assumes that this provides a description of the dynamics of a fixed point which approximates the behavior at very short distances (high energies) of the field theory of interest (in the case of asymptotically free field theories, the CFT is actually free). One then adds deformations by turning on either the couplings of relevant operators of the CFT, or vacuum expectation values (VEVs) for operators, which trigger a renormalization group (RG) flow to low energies (longer distances). The flow starts in the far ultraviolet (UV), from the original CFT (which is a fixed point of the RG flow), and in the deep infrared (IR) can either end into another non-trivial fixed point, or (in the case of confinement) into a trivial theory. The RG flow itself, and the equations governing it, encode all the most important dynamical properties of the field theory, and studying it in detail provides a very clear strategy to characterize the field theory of interest. However, these flows are typically difficult to study with standard field-theoretic tools, in particular because at some stage of the RG flow (if not all along the flow) the field theory may be strongly coupled.

The chief idea of holography is that the dynamics of this RG flow can be understood as the dynamics of a gravitational system with one more dimension, and this “extra dimension” represents the renormalization scale of the RG flow.

This idea existed prior to Maldacena's conjecture [8] in 1997, but it was a cloud of qualitative beliefs [10] rather than a precise quantitative statement. Maldacena proposed, for the first time, such a statement, implementing holography within String Theory, and realizing moreover the earlier large N ideas of 't Hooft [9]. Although for the next chapters we work all the time with String Theory, it is important to keep in mind that the idea of holography is something more general, that the community of Theoretical Physics (not only from the high-energy area) is still starting to unravel: the appropriate degrees of freedom to describe a strongly interacting quantum field theory in flat space are string-like objects, whose description is given by a gravitational theory living in a higher-dimensional curved space. After all, a quantum field theory admits many descriptions, and the weakly coupled degrees of freedom need not have anything to do with the strongly coupled ones (like in the Seiberg-Witten theory, for instance).

As we said, holography can be motivated within String Theory. In the case of Maldacena's original duality, the story is very well-known, and needs not be repeated in detail here. The motivational idea is to take a stack of N D3-branes in flat spacetime, and focus on its two-descriptions: the one with the closed strings gravitating around the stack, and another with the open strings living on the worldvolume. These descriptions are typically coupled, but in the so-called *decoupling limit* (also called near-horizon limit), where $\alpha' \rightarrow 0$, they decouple. On the one hand, we have type IIB String Theory living on $AdS_5 \times S^5$, and on the other hand the worldvolume theory is $\mathcal{N} = 4$ SYM. Since the two descriptions should be equivalent, Maldacena conjectured that $\mathcal{N} = 4$ SYM is *dual* to type IIB String Theory on $AdS_5 \times S^5$. The parameters of the theories are related as

$$g_{\text{YM}}^2 = g_s, \quad \lambda = g_{\text{YM}}^2 N = g_s N = \frac{R_{AdS}^4}{4\pi\alpha'^2}, \quad (3.1.1)$$

where λ is the 't Hooft coupling of the YM theory and R_{AdS} the radius of the Anti-de-Sitter space. From (3.1.1), we read the *most important feature of the duality*: when the field theory is weakly coupled (and we know what to do with it), *i.e.* $\lambda \ll 1$, then $R_{AdS} \ll \alpha'^2$ and one must take into account all the massive fields of type IIB String Theory (which we have no idea of what to do with). On the contrary, when the field theory is strongly coupled (and we lose control over the traditional perturbation theory), *i.e.* $\lambda \gg 1$, we have $R_{AdS} \gg \alpha'^2$ so that one can keep only the massless modes of type IIB String Theory, and moreover in the large N limit $g_s \rightarrow 0$ to keep λ finite, so that string loop corrections are absent (this limit is described by type IIB supergravity!).

So this sort of duality exchanges strong and weak coupling regimes. This makes it extremely useful and powerful for computing things, but in turn it also makes it extremely hard to prove, since already little is known about strongly coupled quantum field theories, but way less is known about non-perturbative String Theory. This is the reason why, despite the extensive consistency checks this duality has passed, which vigorously suggest that it is true, *Maldacena's conjecture is still nowadays a conjecture*. There are weaker forms of the conjecture, limiting it to the infinite 't Hooft coupling limit of planar (planar = leading order in the large- N expansion) $\mathcal{N} = 4$ SYM, or to just the planar limit with arbitrary λ . But none of these have been proven either (the evidence is heavier in these cases).

Another consequence of the duality being of the strong/weak type is that it is not obvious how to relate the two sides, *i.e.* (for the AdS/CFT duality) how are operators of the CFT

related to the AdS fields. Shortly after Maldacena's paper, two papers appeared [71, 72], explaining the relation. This has come to be known as the *dictionary*, although by now anything that tells us how to make computations (as for example how to compute Wilson loops [73]) with the duality is understood as part of the dictionary. The dictionary is explained in detail in any review, like the famous MAGOO [74], and our idea here is to exemplify it along the way.

After the Maldacena duality between $\mathcal{N} = 4$ SYM and type IIB String Theory on $AdS_5 \times S^5$, a vast number of new examples followed, also motivated within String Theory. One expects the general concept to be applicable to other setups: one takes a configuration of branes on some geometry (it does not need to be flat space-time). There are two descriptions, one is a gauge theory living on the worldvolume of the branes, and the other is the usual gravitational description. Then we take a near-horizon limit, and we decouple the descriptions. Taking a large N limit so that the resulting geometry is weakly curved, we are left with a duality between a gauge theory and a gravity theory (instead of the full string theory).

Typically, there is no *AdS* space in the geometry (it appears when the dual theory is conformal), and therefore the AdS/CFT dictionary is not directly applicable; and the dualities are not as well understood. However, throughout the years, and with many examples to study, a lot of insight has been obtained into how the duality works, conforming the very fructiferous field of knowledge called the *gauge/gravity correspondence*. We hope to illustrate some aspects of it in the following chapters.

3.2 Some words on supersymmetry

Symmetries play a gigantic role in our understanding of Physics. Theoretical physicists have faith in Nature being simple. If not, how would one dare explaining it! To determine the interactions among elementary particles, one looks for some simple principle that could (ideally) characterize completely how the interactions can look like. Symmetry principles do the job. For instance, the symmetries of the space-time require Lorentz-invariant theories. The internal symmetries of a theory are connected with gauge invariance. Lorentz and gauge invariance are extremely successful principles which, properly combined with some other ideas plus some experimental input, essentially lead to the Standard Model.

The question of whether there is any other “fundamental symmetry” arises. For a while people tried to merge space-time and internal symmetries in a non-trivial way into a larger symmetry group. This line of research was halted by the no-go theorem of Coleman and Mandula, who proved that this was not possible. Incidentally, a way of sidestepping the hypothesis of this no-go theorem led to the discovery of another possible symmetry: supersymmetry. This is a symmetry between the different particles in the theory. The basic idea is that one has generators (called supercharges) Q_α such that, very schematically:

$$Q_\alpha |\text{boson}\rangle = |\text{fermion}\rangle, \quad Q_\alpha |\text{fermion}\rangle = |\text{boson}\rangle. \quad (3.2.1)$$

That is, each particle of integer spin has a superpartner of semi-integer spin. It turns out that supersymmetry puts very strong constraints on how a theory can be. *One can think of*

supersymmetric theories being to non-supersymmetric theories what holomorphic functions in \mathbb{C} are to real functions in \mathbb{R} (the analogy between supersymmetry and holomorphy becomes almost an equivalence in some cases, see the famous [75])). In consequence, many more exact results are known for supersymmetric field theories. So despite supersymmetry not being realized (unbroken) in our world, it is still very useful to study it. We gain an invaluable insight on what a quantum field theory really is (*e.g.* the remarkable Seiberg-Witten theory); phenomenologically some supersymmetric theories are not very different from their non-supersymmetric counterparts and who knows whether it will be discovered the day of tomorrow.

Our interest focuses on how supersymmetry in a field theory translates into gravity through the correspondence. The recipe is simple: *a supersymmetric field theory is dual to a supergravity solution*. This means that the dual geometry of a supersymmetric field theory is a spin manifold with some (as many as supercharges we have) globally defined spinors ϵ , that generate the supersymmetries. These are called *Killing spinors*. In flat spacetime, both type IIA/B and eleven-dimensional supergravity possess thirty-two Killing spinors. When we curve the space and introduce fluxes, in general only a fraction of the initial thirty-two spinors will still generate supersymmetry transformations. To determine them, there are two main approaches:

- One is the so-called supersymmetry variations approach. The idea in this approach is to write down, for a given solution of the equations of motion, the local form of the supersymmetry transformations, and check that they are indeed a symmetry of the solution. In practice, the solutions we are interested in are the “bosonic” ones, where only the bosonic fields, such as the metric and the NSNS and RR fluxes are turned on, while the fermionic fields are set to zero. Since the form of the supersymmetry transformations is, schematically, $\delta(\text{fermionic fields}) = (\text{bosonic fields})\epsilon$, we have to impose $(\text{bosonic fields})\epsilon = 0$. These are called, for obvious reasons, the supersymmetry variations. Requiring their vanishing one obtains, in general, a set of projections the Killing spinors must satisfy.
- The other possibility is to use the mathematical formalism of G-structures, which allows to formulate cleanly supersymmetry on manifolds in geometrical terms. The generic definition of a G-structure is a bit abstract, but getting practical, having a G-structure means having some globally defined tensors on the manifold. Thus, a supersymmetric manifold, with globally defined spinors (the Killing spinors!), must have a G-structure. The globally defined tensors of the G-structure can be characterized in terms of these spinors. Moreover, when a system (manifold plus fluxes) with a G-structure is a solution of the supergravity equations of motion, it is possible to reinterpret the supersymmetry variations conditions in differential form for the globally defined tensors. The characterization of supersymmetric solutions of supergravity is consequently very neat in this language. For a recent review on these topics, see [76], where all the rigorous details and references we have shamefully omitted can be found. We illustrate an example of this approach in 4.A.

One can revert the logic above, and start with some spinors on a spin manifold and assume they are Killing, then use either the supersymmetry variations approach or the language

of G-structures to find what the background must be. What one obtains is a first-order system of differential equations for the metric and fluxes, generically called the BPS system (named after the Bogomol'nyi-Prasad-Sommerfeld bound). This is extremely useful, because *the solution of the BPS system will be a solution of the full equations of motion. Instead of solving second-order equations, supersymmetry allows to solve just first-order ones!* This happens in general, but the explicit proof of this fact for the kind of backgrounds we will discuss in chapters 4-6 was done in [77], where it was shown that the fulfillment of the BPS equations, plus the Bianchi identities and a certain very general type of metric ansatz, were enough to guarantee the fulfillment of the type IIA/B supergravity (plus sources) equations of motion.

We will make use of this result extensively throughout this Ph.D. thesis, as all the solutions in the following chapters are supersymmetric¹. Moreover, we mainly use the G-structure approach. The main reason for us is that this formalism is much more suited than the supersymmetric variations one for the study of the addition of flavor, as first noticed by Gaillard and Schmude in [78] (the use of this mathematical formalism for the construction of supergravity solutions goes back several years, see for instance the review by Gauntlett [79]). As we will comment in section 3.3, the addition of flavor is done by introducing branes in the background. We want these branes to preserve (at least some of) the supersymmetry of the background. This is traditionally done with κ -symmetry, but this method can be adapted into the G-structures language [78]. One can build a $(p+1)$ -form from the Killing spinors ϵ , normalized as $\epsilon^\dagger \epsilon = 1$, of the manifold as

$$\mathcal{K}_{p+1} = \frac{1}{(p+1)!} e^{a_0 \dots a_p} \begin{cases} \epsilon^\dagger (\Gamma^{11})^{\frac{p-2}{2}} \Gamma_{a_0 \dots a_p} \epsilon & \text{(IIA)} , \\ \epsilon^\dagger (\tau_3)^{\frac{p-3}{2}} i \tau_2 \Gamma_{a_0 \dots a_p} \epsilon & \text{(IIB)} . \end{cases} \quad (3.2.2)$$

This $(p+1)$ -form “calibrates” the addition of Dp-branes. This means that a Dp-brane will be κ -symmetric, *i.e.* it will be embedded (with embedding map ι) supersymmetrically if:

$$\iota^* (\mathcal{K}_{p+1}) = \omega_{\text{Vol}(Dp)} , \quad (3.2.3)$$

where $\omega_{\text{Vol}(Dp)}$ is the volume form of the Dp-brane. This earns the name *calibration form* for \mathcal{K}_{p+1} . Properly speaking, calibration forms in differential geometry (*i.e.* in the absence of fluxes) are closed forms, and we should call \mathcal{K}_{p+1} a generalized calibration form. However, this difference will not be very relevant for us, and we will lazily keep the name of calibration form.

3.2.1 Reducing the supersymmetry of $\mathcal{N} = 4$ SYM

The more amount of supersymmetry a field theory has, in general the simplest will be theory. Simplicity of a theory does not necessarily mean having a simple Lagrangian [34], but rather that we are able to compute its observables. Supersymmetry constrains the form

¹In general, one can check that the second-order equations of motion are satisfied by the solutions of the BPS system. For all the systems we treat in this thesis, this has been done, and one can go to the original references for details.

of these observables, and hence a large amount of supersymmetry is desirable. This is one of the reasons why $\mathcal{N} = 4$ SYM is so well-understood, as opposed to QCD, much more useful for the everyday life. An intermediate point is reducing as much as possible the supersymmetry, so that the theories are phenomenologically more interesting, but without breaking it completely, so that some of the nice properties of supersymmetry are retained.

Let us illustrate how supersymmetry can be reduced within the gauge/gravity correspondence. For definiteness, and in the interest of chapter 5, we focus on four dimensions, showing how to descend from the $\mathcal{N} = 4$ theory to $\mathcal{N} = 1$ theories. The generalities of the discussion apply to any other dimension. There are three standard main methods to attain the supersymmetry reduction:

- One is to deform $\mathcal{N} = 4$ theory with marginal/relevant operators, or by giving VEVs. The gravity dual should be a geometry which is $AdS_5 \times S^5$ only asymptotically in the UV, typically at large values of some radial coordinate r . The geometry should be r -dependent, this dependence codifying the non-trivial RG flow of the theory. A conceptually clean realization of these ideas is given by the so-called Polchinski-Strassler solution [80], which encodes the flow from $\mathcal{N} = 4$ SYM to a theory with minimal supersymmetry called $N = 1^*$ Yang-Mills. A related construction is the Pilch-Warner background [81].
- Another non-trivial and successful application of these ideas has been developed by Klebanov and collaborators, and relies instead on placing branes at the tip of the conifold, which is one-fourth supersymmetric with respect to the flat space case (breaking $\mathcal{N} = 4 \rightarrow \mathcal{N} = 1$ as we want). Using D3-branes one obtains the Klebanov-Witten solution [82], based on the geometry $AdS_5 \times T^{1,1}$, and dual to a superconformal theory described by a two-node quiver $SU(N) \times SU(N)$ and with a given number of bi-fundamental matter fields. Introducing M fractional D3-branes amounts to introducing an imbalance $SU(N+M) \times SU(N)$, and the theory displays a very non-trivial RG flow constituted of an infinite cascade of Seiberg dualities. This theory was studied by Klebanov and Tseytlin [83], but it does not have an IR fixed point as the gravity solution is singular there. This was resolved by Klebanov and Strassler [84], whose solution we describe in section 3.2.3.
- The next stage in this descendent scale of “conceptually clean” setups is represented by the so-called *wrapped-brane models* [85] (see [86] for an early review). One takes a $D(3+k)$ -brane and wraps it on a compact k -cycle. To preserve supersymmetry on the worldvolume of such a brane, which is curved, one needs to make a topological twist², and therefore the field theory here is obtained by a twisted KK compactification of

²Supersymmetry on a curved manifold (with a non-trivial spin connection ω_μ) requires having *covariantly constant* Killing spinors, *i.e.* $\delta\psi_\mu = (\partial_\mu + \omega_\mu)\epsilon = 0$. If we also want these spinors to be constant (along some directions), we need to introduce an external gauge field A_μ so that the supersymmetric variations of the gravitino read $\delta\psi_\mu = (\partial_\mu + \omega_\mu - A_\mu)\epsilon$. Identifying $A_\mu = \omega_\mu$, we can find constant spinors. On the field theory side, the coupling with the external gauge field twists the theory, *i.e.* it changes the spins of the particles. On the supergravity side, A_μ becomes a non-trivial fibration in the normal bundle external to the brane world-volume.

a higher-dimensional field theory on a curved manifold. The RG flow of the four-dimensional field theory never reaches a fixed point at high energies, and these models can be thought of as dual to effective theories which require a UV completion often non field-theoretic. The advantage of these models is that they are simpler to construct and to study than the ones presented above. The best-known examples are [87, 88]. We review now the latter.

3.2.2 The Maldacena-Núñez solution

In this subsection we briefly review the supergravity dual to $\mathcal{N} = 1$ SYM found by Maldacena and Núñez in [88] (MN), which is based on the four-dimensional supergravity solution that had been obtained by Chamseddine and Volkov in [89]. This is the best understood example of the wrapped-brane models.

The supergravity solution

This supergravity background is generated by N_c D5-branes that wrap a compact two-cycle inside a Calabi-Yau threefold. At low energies this supergravity solution is dual to a four-dimensional gauge theory, whereas, at sufficiently high energies, the theory becomes six-dimensional. Moreover, due to a twisting procedure in the compactification, the background preserves four supercharges. The corresponding ten-dimensional metric in Einstein frame is given by:

$$ds_{10}^2 = g_s \alpha' N_c e^{\frac{\Phi}{2}} \left[\frac{1}{g_s \alpha' N_c} dx_{1,3}^2 + dr^2 + e^{2h} (d\theta^2 + \sin^2 \theta d\phi^2) + \frac{1}{4} \sum_{i=1}^3 (\omega_i - A_i)^2 \right], \quad (3.2.4)$$

where Φ is the dilaton. The angles $\theta \in [0, \pi]$ and $\phi \in [0, 2\pi)$ parameterize a two-sphere which is fibered by the one-forms A_i ($i = 1, 2, 3$), which can be regarded as the components of an $\mathfrak{su}(2)$ non-Abelian gauge vector field. Their expressions can be written in terms of a function $a(r)$ and the angles (θ, ϕ) as follows:

$$A_1 = -a(r) d\theta, \quad A_2 = a(r) \sin \theta d\phi, \quad A_3 = -\cos \theta d\phi. \quad (3.2.5)$$

The $\omega_{1,2,3}$ are $\mathfrak{su}(2)$ left-invariant one-forms satisfying the Maurer-Cartan relations for a three-sphere:

$$d\omega_i = -\frac{1}{2} \epsilon_{jik} \omega_j \wedge \omega_k, \quad (3.2.6)$$

so that they parameterize an \mathbb{S}^3 and can be represented in terms of three angles $\tilde{\theta}, \tilde{\phi}, \psi$ as:

$$\begin{aligned} \omega_1 &= \cos \psi d\tilde{\theta} + \sin \psi \sin \tilde{\theta} d\tilde{\phi}, \\ \omega_2 &= -\sin \psi d\tilde{\theta} + \cos \psi \sin \tilde{\theta} d\tilde{\phi}, \\ \omega_3 &= d\psi + \cos \tilde{\theta} d\tilde{\phi}. \end{aligned} \quad (3.2.7)$$

The three angles $\tilde{\theta}, \tilde{\phi}$ and ψ take values in the range $0 \leq \tilde{\theta} \leq \pi$, $0 \leq \tilde{\phi} < 2\pi$ and $0 \leq \psi < 4\pi$. For a metric ansatz such as the one written in (3.2.4) one obtains a supersymmetric solution

when the functions $a(r)$, $h(r)$ and the dilaton Φ are:

$$\begin{aligned} a &= \frac{2r}{\sinh(2r)}, \\ e^{2h} &= r \coth(2r) - \frac{r^2}{\sinh^2(2r)} - \frac{1}{4}, \\ e^{-2\Phi} &= e^{-2\Phi_0} \frac{2e^h}{\sinh(2r)}, \end{aligned} \quad (3.2.8)$$

where Φ_0 is the value of the dilaton at $r = 0$. Near the origin $r = 0$ the function e^{2h} in (3.2.8) behaves as $e^{2h} \sim r^2$ and the metric is non-singular. The solution of the type IIB supergravity includes a Ramond-Ramond three-form F_3 given by:

$$F_3 = -\frac{g_s \alpha' N_c}{4} (\omega_1 - A_1) \wedge (\omega_2 - A_2) \wedge (\omega_3 - A_3) + \frac{g_s \alpha' N_c}{4} \sum_{i=1}^3 F_i \wedge (\omega_i - A_i), \quad (3.2.9)$$

where F_i is the field strength of the $\mathfrak{su}(2)$ gauge field A_i , defined as:

$$F_i = dA_i + \frac{1}{2} \epsilon_{ijk} A_j \wedge A_k. \quad (3.2.10)$$

When the A_i 's are given by (3.2.5), the different components of F_i are:

$$F_1 = -a' dr \wedge d\theta, \quad F_2 = a' \sin \theta dr \wedge d\phi, \quad F_3 = (1 - a^2) \sin \theta d\theta \wedge d\phi, \quad (3.2.11)$$

where the prime denotes derivative with respect to r .

One can readily verify that, due to the relation (3.2.10), the three-form F_3 written in (3.2.9) is closed, *i.e.* it satisfies the Bianchi identity $dF_3 = 0$. Moreover, the field strength (3.2.9) satisfies the flux quantization condition corresponding to N_c color D5-branes, namely:

$$-\frac{1}{2\kappa_{10}^2 T_{D5}} \int_{S^3} F_3 = N_c, \quad (3.2.12)$$

where the three-sphere is the one parameterized by the three angles $\tilde{\theta}$, $\tilde{\phi}$ and ψ at a fixed value of all the other coordinates.

The dual field theory

It was argued in [88] that the background written above is dual to $\mathcal{N} = 1$ four-dimensional SYM in the IR. Indeed, the dual theory corresponding to the supergravity construction above is a twisted compactification of $N = (1, 1)$ SYM in six dimensions on a two-sphere. From the four-dimensional point of view, the field content of such a theory is a gauge boson, a gaugino and an infinite tower of Kaluza-Klein (KK) adjoint matter (composed by massive chiral and vector superfields). In the IR, the KK modes can be integrated out, and the field content is that of $\mathcal{N} = 1$ SYM. Notice that the twist is essential not to have scalars in the compactified theory (they become fermions with the twisting procedure). In the

supergravity picture, the reason for the twist was to realize the $\mathcal{N} = 1$ supersymmetry on the curved space. It is also important to notice that YM theories in $d > 4$ need a UV completion. In the particular case of the $\mathcal{N} = (1, 1)$ six-dimensional theory we are dealing with, this is provided by Little String Theory³.

At the perturbative level, the full spectrum of the theory was studied in [90, 91], where it was seen that, in the large N_c limit, it is the same spectrum as the one of the $\mathcal{N} = 1^*$ four-dimensional SYM in a Higgs vacuum⁴. In [91], a further check was made as the actions of these two theories were written down and shown to be equal.

A proposal for a concrete four-dimensional effective Lagrangian of the vector $\mathcal{N} = 1$ multiplet and the different KK modes has been written in [92]. It is better expressed using $\mathcal{N} = 1$ notation, where the massless vector multiplet and its curvature are denoted by (V, \mathcal{W}) , and the massive ones by (V_k, \mathcal{W}_k) , and we also have massive adjoint chiral multiplets Φ_k . The Lagrangian in $\mathcal{N} = 1$ superspace is of the form

$$\begin{aligned} \mathcal{L} &= \int d^4\theta \left(\sum_k \Phi_k^\dagger e^V \Phi_k + \mu_k |V_k|^2 \right) + \int d^2\theta \left(\mathcal{W}\mathcal{W} + \sum_k \mathcal{W}_k \mathcal{W}_k + \tilde{W}(\Phi_k, V_k) \right) + \text{h.c.}, \\ &= \int d^4\theta \sum_k \Phi_k^\dagger e^V \Phi_k + \int d^2\theta \left(\mathcal{W}\mathcal{W} + \sum_k W(\Phi_k) \right) + \text{h.c.}, \end{aligned} \quad (3.2.13)$$

where in the second line we are below the KK scale and have integrated out the massive modes. W is an effective superpotential determining the interactions among the KK modes, which in principle could be derived from the \tilde{W} written in [91]. Schematically, in the usual four-dimensional notation the Lagrangian (3.2.13) has the form

$$\mathcal{L} = \text{Tr} \left[-\frac{1}{4} F_{\mu\nu}^2 - i \bar{\lambda} \gamma^\mu D_\mu \lambda + \tilde{\mathcal{L}}(\Phi_k, V_k, \mathcal{W}_k) \right], \quad (3.2.14)$$

which is indeed the Lagrangian of $\mathcal{N} = 1$ SYM plus some adjoint massive matter.

All these arguments are quite compelling, but the best way to see that the supergravity solution is encoding the IR physics of $\mathcal{N} = 1$ SYM is by obtaining some non-trivial non-perturbative effects from the geometry. A brief but nice compilation can be found in [93]. Let us review some of them.

$\mathcal{N} = 1$ SYM is a confining theory. The quark-antiquark potential comes from a string hanging from the boundary $r = \infty$, where the quarks are located, and probing the geometry. It turns out that the string prefers to sit at $r = 0$, where the dilaton has a minimum. The tension of this string happens to be proportional to e^{Φ_0} , which is different from zero, and the theory therefore confines. Notice however that the KK modes in the four-dimensional

³Notice that the dilaton in (3.2.8) diverges for large values of r , and an S-duality must be performed, that flips the sign of the dilaton and changes D5-branes by NS5-branes, whose worldvolume theory is Little String Theory.

⁴A relevant deformation of $\mathcal{N} = 4$ SYM consists of adding mass to the scalars of the theory. The resulting theory is the so-called $\mathcal{N} = 1^*$, that confines in the IR (see [80] for a supergravity realization). The different vacua are labeled by representations of $SU(2)$, and the Higgs vacua are obtained by expanding the fields around one of these representations.

theory have masses of the order $1/\sqrt{g_s \alpha' N_c}$. Since this mass is of the order of the strong coupling scale, the dynamics of the KK modes cannot be decoupled from the dynamics of confinement. A proposal to determine when a computation of a given observable is affected by the KK dynamics can be found in [94].

Another non-trivial IR property of $\mathcal{N} = 1$ SYM is the formation of a gaugino condensate $\langle \lambda^2 \rangle \neq 0$. It turns out that the function $a(r) \sim \langle \lambda^2 \rangle$. Indeed, $a \sim 0$ in the far UV, but it starts to grow as we go to $r = 0$, where it becomes $a = 1$. The point where it starts to grow can be identified with the dynamically generated scale Λ_{QCD} of the gauge theory. Actually, there is another supersymmetric solution for the functions in the metric (3.2.4) and the one-forms A_i . In this solution, the function $a(r)$ vanishes, $e^{2h} = r$ and $e^{2\Phi-2\Phi_0} = \frac{e^{2r}}{4\sqrt{r}}$. This makes the one-forms A_i an Abelian one-form $\mathfrak{su}(2)$ connection. This is why this solution is usually called Abelian MN. The functions in the Abelian solution are just the UV limit ($r \rightarrow \infty$) of the ones written in (3.2.8). When we go to $r = 0$, it happens that this background has a (bad) singularity. Let us connect this with the phenomenon of R-symmetry breaking that the field theory displays.

The Lagrangian of $\mathcal{N} = 1$ SYM has a $U(1)$ R-symmetry that acts as $\lambda \rightarrow e^{-i\varepsilon} \lambda$. This corresponds with the $\psi \rightarrow \psi + 2\varepsilon$ isometry of the Abelian background, that as we said, is the MN geometry in the UV. This R-symmetry is spontaneously broken down to \mathbb{Z}_2 by the gaugino condensation⁵. In the supergravity solution, the $\psi \rightarrow \psi + 2\varepsilon$ stops being an isometry precisely when $a(r)$ is non-zero.

Other non-trivial IR properties captured by the MN solution are the existence of BPS domain walls that separate the different vacua of the theory (on the supergravity side, these walls are a particular kind of wrapped branes), and the tensions of the k -strings (to which we come back in section 5.3.4).

Finally, we can mention that even some UV properties of $\mathcal{N} = 1$ SYM are correctly reproduced by the supergravity solution. A relation between the radial coordinate r and the energy scale μ can be found by noticing that the gaugino condensate has a protected dimension equal to 3, and then one can make the identification $a \sim \langle \lambda^2 \rangle \sim \left(\frac{\Lambda_{\text{QCD}}}{\mu} \right)^3$. Using a probe brane computation [95, 96], one can extract the β -function of the theory, and it is a bit shocking that the NVSZ β -function of SYM is recovered, since the field theory is weakly coupled in the UV while (accordingly) the supergravity solution becomes strongly coupled (the dilaton grows unbounded) at large values of r .

3.2.3 The Klebanov-Strassler solution

Now it is the turn for the models built by placing D3-branes on Calabi-Yau threefolds. The landmark example is the Klebanov-Strassler (KS) solution [84]. It provides a regular type IIB supergravity solution dual to a four-dimensional field theory with very rich dynamics, such as confinement and chiral symmetry breaking. Despite never being weakly coupled, the

⁵Actually, the $U(1)$ R-symmetry was already anomalous at the quantum level, since by instantonic corrections it is broken down to \mathbb{Z}_{2N_c} ; and this was captured as well by the modification of the RR potential C_2 in the supergravity solution with the metric isometry $\psi \rightarrow \psi + 2\varepsilon$, which acts as a large gauge transformation for C_2 , and it is therefore quantized as $2N_c \varepsilon \in 2\pi\mathbb{Z}$.

field theory is very well-understood, which makes the matchings coming from the gravity side more spectacular.

The supergravity solution

The Klebanov-Strassler background is based on the previous (in time) Klebanov-Tseytlin solution [83], where they studied fractional D3-branes on the conifold. Such a solution has a (bad) singularity in the IR, and the resolution of KS is to consider N_c fractional D3-branes on the deformed conifold. The notation N_c can be a bit misleading since it is not the number of colors of the gauge group, and in the literature one usually calls it M , but this notation will be more convenient for later purposes. The KS theory is also related to the Klebanov-Witten theory [82], but unlike that one, it is not conformal and there is no AdS_5 factor in the metric. Nonetheless, the theory departure from conformality (in the UV) is mild and one usually says that the theory is *nearly conformal*. The metric, in string frame, reads as follows:

$$ds^2 = h^{-\frac{1}{2}} dx_{1,3}^2 + h^{\frac{1}{2}} ds_{\text{deformed conifold}}^2, \quad (3.2.15)$$

$$h = (g_s \alpha')^2 \frac{2^{\frac{5}{3}} N_c^2}{\epsilon^{\frac{8}{3}}} \int_r^\infty dx \frac{2x \coth(2x) - 1}{\sinh^2(2x)} (\sinh(4x) - 4x)^{\frac{1}{3}}, \quad (3.2.16)$$

where ϵ is the deformation parameter of the deformed conifold, and r its radial coordinate when its metric is written as

$$ds^2 = \frac{\epsilon^{4/3}}{2^{1/3}} (\sinh(4r) - 4r)^{\frac{1}{3}} \left[\frac{4 \sinh^2(2r)}{3(\sinh(4r) - 4r)} \left(dr^2 + \frac{1}{4} (\omega_3 + \cos \theta d\phi)^2 \right) + \right. \\ \left. + \frac{\tanh(2r)}{4} (d\theta^2 + \sin^2 \theta d\phi^2) + \coth(2r) ((\omega_1 + \text{sech}(2r) d\theta)^2 + (\omega_2 - \text{sech}(2r) \sin \theta d\phi)^2) \right]. \quad (3.2.17)$$

Notice that with this way of writing the metric of the deformed conifold, the geometry looks similar to the MN one with the fibration function $a(r) = \text{sech}(2r)$. The usual way the metric of the deformed conifold is written (the one for instance KS use in their paper) involves a set of five one-forms g^i . It is straightforward to check that such metric is the same as (3.2.17).

The fractional D3-branes can be thought of as D5-branes wrapping a two-sphere, through which there is a non-trivial flux of the field B_2 , and constrained to live at the tip of the conifold. The solution then has RR fluxes F_3 and F_5 , and NSNS flux B_2 . They read

$$B_2 = \frac{g_s \alpha' N_c}{4} \frac{2r \coth(2r)}{\sinh(2r)} \left[\cosh(2r) (\sin \theta d\theta \wedge d\phi - \sin \tilde{\theta} d\tilde{\theta} \wedge d\tilde{\phi}) - \right. \\ \left. - \sin \theta d\phi \wedge \omega_1 - d\theta \wedge \omega_2 \right], \quad (3.2.18)$$

$$H_3 = dB_2, \quad (3.2.19)$$

$$F_3 = \frac{g_s \alpha' N_c}{2} \left[\frac{2r \coth(2r) - 1}{\sinh(2r)} dr \wedge (d\theta \wedge \omega_1 + \omega_2 \wedge d\phi) - \right. \\ \left. - \frac{r}{\sinh(2r)} (d\theta \wedge \omega_2 \wedge \omega_3 + \sin \theta d\phi \wedge \omega_1 \wedge \omega_3 - \cos \theta d\theta \wedge d\phi \wedge \omega_2) + \right.$$

$$+ \frac{1}{2} (\sin \theta d\theta \wedge d\phi \wedge \omega_3 - \omega_1 \wedge \omega_2 (\omega_3 + \cos \theta d\phi)) \Big] , \quad (3.2.20)$$

$$F_5 = - (1 + *) (\partial_r h^{-1}) dx_0 \wedge dx_1 \wedge dx_2 \wedge dx_3 \wedge dr . \quad (3.2.21)$$

Finally, the dilaton is a constant

$$e^\Phi = g_s . \quad (3.2.22)$$

The KS background is regular, and it can be trusted everywhere as long as $g_s N_c \gg 1$. Notice that for large values of r (which correspond to the UV of the dual theory), and defining $\rho \sim e^{\frac{2}{3}r}$, the metric of the deformed conifold asymptotes that of the singular conifold: $ds_{\text{deformed conifold}}^2 \rightarrow d\rho^2 + \rho^2 ds_{T^{1,1}}^2$. Therefore, in the UV, the KS background is the same as the Klebanov-Tseytlin one. This is in analogy with the situation of the non-Abelian and Abelian MN solutions. The fact that $a(r) = \text{sech}(2r) \neq 0$ is responsible for the deformation of the conifold and the consequent smoothing of the geometry in the IR. As in MN, this is related to the formation of a gaugino condensate.

One would like to have a condition like (3.2.12), counting the ranks of the gauge groups, but the situation is more subtle in the KS background, due to the presence of a non-trivial B-field. This was nicely explained in [97]. There are two ways of counting the different charges present in the background. One way is via an integral like (3.2.12), that defines the *Maxwell charge*. In general:

$$Q_{Dp}^{\text{Maxwell}} = \frac{1}{2\kappa_{10}^2 T_{Dp}} \int F_{8-p} . \quad (3.2.23)$$

This charge is gauge-invariant, but it is not quantized in general (for instance, the Maxwell D3-charge for F_5 in (3.2.21) gives a continuous r -dependent function). Thus, this cannot be matched with the rank of any group. The alternative is to compute the *Page charge*:

$$\begin{aligned} Q_{Dp}^{\text{Page}} &= \frac{1}{2\kappa_{10}^2 T_{Dp}} \int F_{8-p} e^{-B_2 \wedge F_{\text{all } p}} := \\ &:= \frac{1}{2\kappa_{10}^2 T_{Dp}} \int \left(F_{8-p} - B_2 \wedge F_{6-p} + \frac{1}{2} B_2 \wedge B_2 \wedge F_{4-p} + \dots \right) . \end{aligned} \quad (3.2.24)$$

The Page charge is not a gauge-invariant quantity (because B_2 is not), but in turn it gives quantized (topological) results, since the integrand is a closed form.

As we comment below, the dual field theory is a quiver with gauge group $SU(N + N_c) \times SU(N)$, and the number N is precisely the Page D3-charge. This will always be an integer number, but it is r -dependent. This is so because, as we said, B_2 is not gauge-invariant and for the supergravity solution to be a good description one needs⁶ $0 \leq b_0 < 1$, where $b_0 = \frac{1}{4\pi^2 g_s \alpha'} \int B_2$. Since B_2 “is growing” towards the UV, and when it grows too large, one performs a large gauge transformation to B_2 , whose effect is $b_0 \rightarrow b_0 - 1$, and takes $N \rightarrow N + N_c$. This will be interpreted as a Seiberg duality in the dual theory. See [97] (where they generalize the solution to account for the inclusion of fundamental matter into the theory) for more details. Seiberg duality will be later discussed in section 5.1.3, although in a context a little bit different.

⁶One way to see this is by defining the two gauge couplings of the theory in terms of supergravity quantities. For this definition to make sense one needs to have $0 \leq b_0 < 1$.

The dual field theory

The picture we have briefly described above seems to indicate that the KS theory is a quiver theory $SU(N + N_c) \times SU(N_c)$, where the number N changes along the RG flow. This was already clear to KS in [83], although the complete picture for the dual theory was further studied in later works (see [98] for a very pedagogical review), and understood in [99]. The KS field theory is extremely interesting, but very subtle as well, so our main aim here is just to point out a few interesting features of the dual theory that we will use later on. The two previous references are excellent places to learn more about the field theory picture.

The dual theory does not flow to a conformal point in the UV, so one needs a cutoff Λ_{UV} where it can be defined properly. At such a cutoff, the theory is a quiver with gauge group $SU((k+1)N_c) \times SU(kN_c)$. There are four bi-fundamentals: A_1, A_2, B_1, B_2 interacting with a tree-level superpotential

$$W \propto \text{Tr} [A_1 B_1 A_2 B_2 - A_1 B_2 A_2 B_1] \quad (3.2.25)$$

and the theory has an $SU(2) \times SU(2) \times U(1)_B$ symmetry. The two $SU(2)$ groups rotate the A_i and B_i fields respectively, and the so-called baryonic $U(1)_B$ acts as $A_i \rightarrow e^{i\alpha} A_i$, $B_i \rightarrow e^{-i\alpha} B_i$. When the fields A_i, B_i acquire a VEV, the theory is said to be on the *baryonic branch*. The KS theory is at a special point on the baryonic branch, where $|A| = |B|$. For other points on the baryonic branch, one has to generalize the background [100].

If we start to follow the theory along the RG flow, the two gauge couplings are such that one (the one corresponding to the first group $SU((k+1)N_c)$) increases, while the other one decreases. We reach a point where the former becomes infinite, and we have to go to a Seiberg-dual description. At this point, the $SU(kN_c)$ is acting like a flavor group with $2kN_c$ flavors, so Seiberg duality takes $(k+1)N_c \rightarrow 2kN_c - (k+1)N_c = (k-1)N_c$. We are left with an $SU((k-1)N_c) \times SU(kN_c)$ theory, where now the increasing gauge coupling is the one corresponding to the second group. As we decrease along the flow, there is a *cascade of Seiberg dualities*. The supergravity counterpart was discussed after equation (3.2.24). The last step of the cascade is a quiver theory $SU(2N_c) \times SU(N_c)$ that is delicate to analyze, but what happens is that the $SU(2N_c)$ degrees of freedom get confined and only the $SU(N_c)$ remains. The $U(1)_B$ is spontaneously broken in this step, generating a Goldstone boson that can be found in the supergravity solution [101]. This final $\mathcal{N} = 1$ $SU(N_c)$ theory is not SYM, although it is in its universality class: the theory confines, it has a sine law for the k-strings, it has N_c equivalent vacua separated by domain walls, and it exhibits dynamical chiral symmetry breaking: a gaugino condensate is formed at a scale determined by the deformation parameter of the conifold $\langle \lambda\lambda \rangle \propto \epsilon^2$, and there is a breaking of the R-symmetry $\mathbb{Z}_{2N_c} \rightarrow \mathbb{Z}_2$.

We have not mentioned what happens if we take $\Lambda_{UV} \rightarrow \infty$. In this direction (*i.e.*, towards the UV), the cascade never stops and the ranks of the groups just get bigger and bigger. Each step is closer to a Klebanov-Witten fixed point (where the gauge group is $SU(N) \times SU(N)$; notice that for $k \gg 1$ this is approximately true), but there is always a small imbalance that makes the cascade continue. The theory is then said to be nearly conformal. For many purposes, this is as good as having a conformal fixed point.

Let us make a final remark that will be relevant for section 5.4. In both of solutions in [83] and [100], the numerology of the quivers of the cascade is of the form $SU((k+1)N_c) \times$

$SU(k N_c)$. This happens because the dual field theories are in the baryonic branch. To go to a cascade with a numerology of the form $SU((k+1)N_c+l) \times SU(k N_c+l)$, where $l < N_c$, one has to consider l extra (free) D3-branes on the conifold. In this case, the theory is said to be in the *mesonic branch*. We come back to it in section 5.4.3.

3.3 Flavor in the gauge/gravity correspondence

All we have seen up to now is how to use String Theory as a tool to study the non-perturbative regime of gauge theories that only contain adjoint matter (gluons if one thinks in YM theories). This is certainly remarkable, but not very useful for phenomenological purposes, as fundamental matter is an essential ingredient of the Standard Model. Can you think of a world without electrons, quarks or neutrinos? Fortunately, fundamental matter has its place in the gauge/gravity correspondence.

The gauge/gravity correspondence can be motivated by thinking of the picture of branes in String Theory, as we did a few pages ago. It is useful to think about this picture for the problem of how to add fundamental matter. *Since in the case of QCD, the fundamental matter is comprised by a set of different quarks (with different flavors), we will abuse of the notation a bit, and generically use the words “addition of flavor” throughout this Ph.D. thesis with the meaning of adding fundamental matter.* A quark is an object that transforms in the fundamental representation of the gauge group of our gauge theory. We say that it carries one fundamental index (whereas a gluon carries two), thinking of the representations of the group $SU(N_c)$. There is an object in String Theory that also carries a fundamental index, and this is one of the free ends of an open string. This fundamental index is the so-called Chan-Paton factor. Then, having fundamental matter in our theory, which is defined in the world-volume of the stack of N_c color branes, is the same as having open strings ending there. But these open strings have another free end, that should end at another brane, different from the color ones (if not, it would have two fundamental indexes and represent a gluon). This other brane is what we call a “*flavor brane*”.

So, the way to incorporate flavor in the correspondence is by adding an open string sector to the String Theory side, *i.e.* adding flavor branes. Then, the states corresponding to the strings that go from the flavor branes to the stack of color branes are dual to the quarks we want to introduce. When the flavor and color branes are intersecting, these strings can stretch to zero size, meaning that the fundamental matter we are adding is massless. If we want to have a massive quark, we have to introduce a separation r_q between the color and flavor branes, and the mass of the quark m_q is equal to the minimal energy a string stretching from the color to the flavor brane can have. In general $m_q \sim r_q$ in string units.

But notice that we also have open strings that start and end on the flavor brane, and they are dual to the gluons of the gauge theory living on the flavor brane itself. That is, the quark comes with its own gluon. We do not want to have the latter state in the spectrum. A way to get rid of it is by having the quotient of the volumes of flavor branes over the volume of color branes to be infinite [102]. This is because the quotient between the gauge couplings of the $SU(N_c)$ theory on the color branes and the gauge coupling of the induced $U(1)$ theory for the quark is related to this quotient of volumes. If this number is infinity, the coupling of the $U(1)$ theory for the quark is zero, therefore it decouples and we do not

need to care about it. The whole argument follows through if instead of one flavor brane, we use a stack of N_f flavor branes. In this case, we are adding N_f different quarks, *i.e.* N_f flavors; and there is an $SU(N_f)$ symmetry since they are all equally good⁷.

Let us now focus on how to add flavor branes on the gravity side. In order for the gravity approximation to be valid, recall that we need the gauge theory to be in the large N_c limit, so $N_c \gg 1$. If we add a number of flavor branes $N_f \ll N_c$, the geometry will not notice them, and it will not change. This is the so-called “probe approximation”. The dynamics of these probe branes is given by their DBI+WZ action evaluated on the background generated by the color branes. *The probe approximation is also called the quenched approximation* because the dual physics is that of a gauge theory that can only have quarks as external vertices in the different processes one wants to study. There cannot be quarks running in the loops of Feynman diagrams, and one says that “they are quenched” (in the terminology of lattice gauge theory). So this quenched approximation, although it allows to have quarks in the theory, is missing a big part of the non-perturbative dynamics due to the flavor. If we are interested in this physics, we need to go to the Veneziano limit [103]. This is a limit in which the gauge theory has both a large number of colors N_c and a large number of flavors N_f , but the ratio $\frac{N_f}{N_c}$ is finite. Apart from the planar diagrams that were already contributing in the ’t Hooft limit, in the Veneziano limit one also includes the contribution of planar diagrams with boundaries. The boundaries come from quarks that (now can) run in the loops. We say that *the flavor is unquenched, or dynamical, in the Veneziano limit*.

So, say that you have a gravity background that is dual to some gauge theory that only has adjoint matter. You want to incorporate fundamental matter into the picture. What are the steps to follow?

- **In the quenched approximation**, once the flavor branes are identified (say they are Dp-branes whose world-volume has to span the radial direction⁸) one only needs to identify a “good place” where they can sit, *i.e.* a good embedding for the flavor brane world-volume into the background geometry. This means that once the flavor brane is put there, it should stay there. In other words, the configuration must be stable. The way to check this is by computing the spectrum of perturbations around the flavor brane embedding, and seeing that it is finite. A generic way to assure stability is supersymmetry: when the brane can be placed in the geometry without breaking its supersymmetries, its DBI and WZ actions are equal, meaning that they balance out, and the brane feels no force, and it is therefore stable.

Once this embedding is identified, all is left to do is to place the brane there, and compute all you want. The main thing that has been done in the literature is to compute meson spectra from here, which is a fundamental observable of the dual field theory and, in the cases where these spectra are known in the dual theory, it provides strong checks on the correspondence. This has been known for a while, and a good account of these topics can be found in the review [104].

⁷The reason why it is $SU(N_f)$ and not $U(N_f)$ is the same why it is $SU(N_c)$ in the Maldacena correspondence.

⁸Apart from making the volume of the flavor branes infinite with respect to the color branes, this condition is also needed by the dictionary: to consider insertion of quark operators in the dual theory, the flavor brane must extend up to the boundary, where the theory is defined.

- **In the case of unquenched flavor**, there is still the need to identify the possible embeddings where the flavor branes can sit. But this is fairly complicated, as the geometry where we have to find these embeddings is not known! The fact that $N_f \sim N_c \gg 1$ means that one cannot neglect the backreaction of the flavor branes on the geometry, that will change once these branes are added. At the level of the action, the one to be studied is

$$S = S_{\text{gravity}} + S_{\text{sources}} , \quad (3.3.1)$$

where the action S_{gravity} determines the original unflavored background, and S_{sources} is the sum of the actions of the N_f flavor branes.

So in order to know where to put the branes we need to know the geometry, and in order to know the geometry we need to know where we put the branes; we have a very non-trivial problem. *One of the main points of this Ph.D. thesis is to show how to solve this systematically.* The only known way out is to write down a general form for the geometry, so general that it can account for the backreaction of the flavor branes, but with enough details so that embeddings for flavor branes can be found.

Our interest for the next four chapters is focused on the addition of unquenched flavor into the correspondence. This is a formidable task. To tackle it, we present in the next subsection a technique that simplifies a bit the problem, and that in the case where there is supersymmetry, it can be coupled with G-structures tools, yielding a very powerful way of finding solutions dual to supersymmetric gauge theories with unquenched flavor. Holography and holomorphy play pals to face this problem.

3.3.1 The smearing technique

We study the problem of introducing N_f flavor branes, with $N_f \sim N_c \gg 1$. We assume that we know where we can place these branes, so what we have to do is to solve the equations of motion derived from the action (3.3.1). We will always study systems of branes in type II String theory, so S_{gravity} will be either S_{IIA} or S_{IIB} .

If the flavor branes are one on top of each other, the action S_{sources} in (3.3.1) is the non-Abelian DBI+WZ action for a stack of N_f flavor Dp-branes:

$$S = S_{\text{IIA,IIB}} + \sum_{N_f} S_{\text{DBI+WZ}} = \int_{\mathcal{M}_{10}} d^{10}x \mathcal{L}_{\text{IIA,IIB}} + N_f \int_{\text{Dp}} d^{p+1}y \mathcal{L}_{\text{DBI+WZ}} . \quad (3.3.2)$$

Notice that the two integrals in (3.3.2) have different dimensionality. Then, the equations of motion that follow from such an action will contain delta-functions. Moreover, the metric functions will acquire a dependence on the coordinates that are transverse to the flavor branes. Thus, the equations of motion will be a system of coupled non-linear partial differential equations (PDEs). Such a system is extremely hard to solve. In addition, the backreaction of such a stack of flavor branes is likely to break some isometries of the unflavored background. Translating with the dictionary, the addition of flavor is breaking some global symmetries. In many cases, we do not want this to happen.

The smearing technique solves both of these problems by exploiting the fact that there are a large number of flavor branes: one smears their distribution over the coordinates transverse

to them, in such a way that the original isometries are restored. Notice that this has the effect of breaking the flavor symmetry $SU(N_f) \rightarrow U(1)^{N_f}$. What is the action for the sources in this smeared configuration? Let us focus on the WZ part, and we assume that the flavor Dp-brane only couples to the RR potential C_{p+1} (the argument holds for the general case as well):

$$S_{\text{sources}} = \lim_{N_f \rightarrow \infty} \sum_{N_f} T_{\text{Dp}} \int_{\text{Dp}} \iota^* (C_{p+1}) = T_{\text{Dp}} \int_{\mathcal{M}_{10}} C_{p+1} \wedge \Xi, \quad (3.3.3)$$

where ι^* denotes the pullback of the embedding ι of the flavor brane into the ten-dimensional geometry, and Ξ accounts for how we distribute the flavor branes. Ξ is called the *smearing form*, and it is a $(9-p)$ -form transverse to the volume form of the flavor branes everywhere. The second equality in (3.3.3) holds because the WZ action is linear in the sources. Notice that this does not apply to the DBI action, which has a square root and is highly non-linear in the sources. Fortunately, in the case the sources preserve some supersymmetry, DBI and WZ actions are equal, and therefore the DBI part will be linear as well. We will be more specific about this below. Then we can write for the action we have to solve:

$$S = \int_{\mathcal{M}_{10}} d^{10}x \mathcal{L}_{\text{IIA, IIB}} + \int_{\mathcal{M}_{10}} d^{10}x \mathcal{L}_{\text{DBI+WZ}}^{\text{smeared}}, \quad (3.3.4)$$

So both integrands are ten-dimensional, and the equations of motion no longer have delta-functions. In addition we are restoring (at least some of) the original isometries, and if the unflavored system was obtained from a set of ordinary differential equations, the addition of smeared flavor equations also yields equations of motion that are ordinary differential equations.

For the action (3.3.4) to be valid, we need some conditions on the parameters of the background to hold.

- First of all, for the DBI action to be valid for a Dp-brane, it is needed that the brane “weighs too much” so that the open strings attached to them can be considered as perturbations, or in other words, for open string processes to be suppressed. The coupling for these processes is g_s . However, when we have N_f coincident branes, the effective coupling for string processes is $g_s N_f$, that should be small. Actually, since the branes are smeared, the effective coupling is not exactly $g_s N_f$, but rather $\sim g_s N_f / \text{Vol}(\mathcal{M}_t)$, where \mathcal{M}_t is the volume (in string units) of the transverse space over which the branes are smeared. So we should require $g_s N_f / \text{Vol}(\mathcal{M}_t) \ll 1$ for the DBI action to be valid in a smeared setup.
- The other point to worry about is that the second equality in (3.3.3). For it to be true (or more correctly, a good approximation⁹), it is not enough with having $N_f \gg 1$. We should have enough flavor branes so that the typical separation D between any

⁹In the smeared action of (3.3.4) (see for instance (3.3.3) for the specific smeared Lagrangian), there are no flavor branes anymore, but rather a sort of “flavor gas”, whose action approximates that of a certain smeared distribution of branes. Notice that in this way, one avoids the problem of the maximal amount (24) of D7-branes we can place on a compact space [105]. Indeed, the smeared setups do not suffer from this problem [106].

two of them is of the order of $l_s \sim \sqrt{\alpha'}$. If we think of the d -dimensional total space transverse to the branes as a hypercube of volume L^d , it must be that $L^d = N_f D^d$. Then, for the continuum approximation of the smearing to be valid, we need to have (in string units) $D \sim L/N_f^{1/d} \ll 1$.

We illustrate these approximations in the very clean smeared setup of section 4.3.3.

Recapitulating, *the smearing technique provides a way to simplify the very difficult problem of adding unquenched fundamental matter into the correspondence. The smearing breaks the flavor symmetry of the localized configuration $SU(N_f) \rightarrow U(1)^{N_f}$, but it restores the isometries that the localized configuration would break.* This technique was first used in [107, 108]. At present, we understand reasonably well how to use this technique for the addition of unquenched flavor in the gauge/gravity correspondence, and this has been recently reviewed in [109]. This review has a look at the evolution of the problem in the literature, and includes some of the results we discuss in this Ph.D. thesis, which hopefully can complement it.

Let us be a little bit more explicit with respect to the action (3.3.4) we have to solve. *We work in Einstein frame.* We were quite explicit with the WZ part of the flavor brane action in (3.3.3). What about the DBI part? In the case the flavor branes sit along supersymmetric embeddings, we saw in section 3.2 that their volume form can be related to the pullback of a calibration $(p+1)$ -form \mathcal{K}_{p+1} as in (3.2.3). Therefore, we can write the DBI action of one of the flavor branes as

$$S_{\text{DBI}} = -T_{\text{D}p} \int_{\text{D}p} d^{p+1}y e^{\frac{p-3}{4}\Phi} \sqrt{-\det[\iota^*(g)]} = -T_{\text{D}p} \int_{\text{D}p} e^{\frac{p-3}{4}\Phi} \mathcal{K}_{p+1}. \quad (3.3.5)$$

This form of the action is linear in the sources, so the action for the smeared set of N_f flavor branes will be:

$$\lim_{N_f \rightarrow \infty} \sum_{N_f} -T_{\text{D}p} \int_{\text{D}p} e^{\frac{p-3}{4}\Phi} \mathcal{K}_{p+1} = -T_{\text{D}p} \int e^{\frac{p-3}{4}\Phi} \mathcal{K}_{p+1} \wedge \Xi, \quad (3.3.6)$$

where Ξ is the smearing form. The whole action of the smeared sources becomes:

$$S_{\text{sources}} = -T_{\text{D}p} \int \left(e^{\frac{p-3}{4}\Phi} \mathcal{K}_{p+1} - C_{p+1} \right) \wedge \Xi. \quad (3.3.7)$$

Recall that we are assuming that the flavor branes only couple to the potential C_{p+1} , but all we are saying is generalizable to more complicated cases (see for instance [110] or appendix E of [23] for the case of the KS background, that has several different fluxes).

If S_{sources} has the form of (3.3.7), we see that both the equation for the dilaton, as well as obviously the Einstein equations will have contributions from the sources. But these equations of motion are second-order, and we will always solve the systems with first-order equations and the help of supersymmetry. So to us, the most relevant contribution of (3.3.7) to the equations of motion comes in the equations of motion for the fluxes, that are first-order. Since the part of the type II supergravity action relevant for these equations goes as

$$S_{\text{IIA, IIB}} \sim -\frac{1}{2\kappa_{10}^2} \int e^{\frac{3-p}{2}\Phi} (F_{p+2})^2, \quad (3.3.8)$$

using $F_{p+2} = dC_{p+1}$ the resulting equation of motion is:

$$d \left((-1)^{9-p} e^{\frac{3-p}{2}\Phi} * F_{p+2} \right) = 2\kappa_{10}^2 T_{Dp} \Xi. \quad (3.3.9)$$

Since $(-1)^{9-p} e^{\frac{3-p}{2}\Phi} * F_{p+2} = F_{10-p}$, we see that *the introduction of smeared Dp sources induces a violation of the Bianchi identity for F_{8-p} :*

$$dF_{8-p} = 2\kappa_{10}^2 T_{Dp} \Xi. \quad (3.3.10)$$

At the computational level, this will be the more important consequence of the smearing for us. Recall that our method to find solutions is to solve first-order BPS equations, that supplemented with the fulfillment of the Bianchi identities, provides a type II supergravity solution. Equation (3.3.10) will guide us when writing a good ansatz for a flavored solution. Notice that, in virtue of (3.3.10), *the smearing form has to be a closed form.*

The smearing form Ξ contains the information about how the fluxes are affected by the backreaction of the flavor branes. It tells us as well how the flavor brane are distributed, so it also gives an idea on what kind of backreaction the branes will produce in the geometry. *The smearing form is the key ingredient that allows us to write an ansatz for a possible supergravity solution of the action (3.3.4).* Then, the basic question raised in the application of the smearing technique is how to compute the smearing form. We present in what follows two methods to deal with this question. Both have been used in the literature, and each of them has their pros and cons. However, a generic connection between them had not been established, and we present it the last. With this connection, both methods can be combined, making the smearing technique a very powerful tool to build supergravity duals to supersymmetric gauge theories with flavor in the fundamental representation. Chapters 4 through 6 will hopefully serve as an illustration of this.

A microscopic approach to computing Ξ

Imagine that for some reason you know a family of embeddings where your flavor branes can be placed supersymmetrically, generating the desired smeared configuration. We say that in this case *we know the microscopic embeddings*. This usually happens in the cases where the embeddings for the flavor branes are either obvious or either known beforehand. In [111] a recipe for building the smearing form out of a family of embeddings was given. We just re-state here:

Imagine we want to smear some Dp-branes in a 10-dimensional space. The first thing we need to know for that is a family of supersymmetric embeddings. A Dp-brane embedding in 10D is characterized by $9 - p$ constraints:

$$f_1(y^i) = 0, \quad \dots, \quad f_{9-p}(y^i) = 0, \quad (3.3.11)$$

where we are taking $\{y^0, \dots, y^p\}$ as world-volume coordinates. If we are to have a family of embeddings, these f_k should vary smoothly with some parameters $\{\mu_1, \dots, \mu_l\}$ which parameterize the family of embeddings. If our family of embeddings is obtained by acting, in the sense of a continuous group action, with some operator on one of the embeddings,

then the coordinates μ_j will just parameterize this Lie group. Thus, we consider the previous functions f_k to depend on the embedding parameters as well.

$$f_1(y^i; \mu_j) = 0, \quad \dots, \quad f_{9-p}(y^i; \mu_j) = 0. \quad (3.3.12)$$

If we now smear our Dp-branes over the family of embeddings characterized by (3.3.12), the resulting macroscopic smearing form, which recall that it has to be transverse to the volume form of the branes, will be given by:

$$\Xi = \int_G d\mu \tau \delta(f_1) \cdots \delta(f_{9-p}) [df_1 \wedge \cdots \wedge df_{9-p}], \quad (3.3.13)$$

where $d\mu$ is a measure for the parameter space G , and τ is the density of branes we want to use, and it must be such that

$$\int_G d\mu \tau = N_f. \quad (3.3.14)$$

Usually, we want a density τ that respects the symmetries of the background, so that the smearing does not single out any particular brane; *i.e.* so that the branes don't clump anywhere, so to speak. Note that in (3.3.13), the exterior derivative will only act on the y^i coordinates of the f_k .

This method seems like a no-brainer, very easy to implement, but the catch is that the integral (3.3.13) is, in general, extremely hard to compute. In fact, except for some very simple cases, it has never been computed directly. In [111], a very non-trivial example of this integral was computed; but this was done, after some hard work nonetheless, assuming a given ansatz for the final form of Ξ .

And we are actually lying about the degree of difficulty of this microscopic approach, as we assumed we knew a family of supersymmetric embeddings. This is actually very hard as well. The usual way to find them is via κ -symmetry. Since κ -symmetry is formulated in terms of coordinates, this is not easy unless one has a coordinate representation where the embeddings turn out to be simple. Much work has been devoted to conifold-like geometries (see [112, 113, 114, 115]), where there is an underlying complex structure, which we unravel in section 5.1.2, that simplifies the task of finding these κ -symmetric embeddings (see section 5.2.2). This type of structure is unknown for other geometries though.

This microscopic approach is illustrated in several places in this Ph.D. thesis: see section 6.2.2 for some simple examples, and section 5.A for a direct computation of the integral (3.3.13) in a very non-trivial background.

Now a macroscopic approach

Since the smearing form contains the information of where the flavor branes are extended, it seems impossible to compute it unless we have the knowledge of the embeddings. In the case we have supersymmetry, it turns out that the supersymmetric embeddings are strongly constrained by supersymmetry, and the latter is actually enough to determine Ξ . Such a connection was first raised in [78]. Since one never knows about the embeddings in this approach, it is called macroscopic. We proceed to describe it.

When the flavor branes sit along κ -symmetric embeddings, it means that in the action (3.3.7) the DBI part is equal to the WZ part, *i.e.* :

$$e^{\frac{p-3}{4}\Phi} \mathcal{K}_{p+1} = C_{p+1} . \quad (3.3.15)$$

If we take derivatives in this relation, and recalling that we have $F_{p+2} = dC_{p+1}$, we get the RR $(p+2)$ -form in terms of the calibration form \mathcal{K}_{p+1} :

$$F_{p+2} = d \left(e^{\frac{p-3}{4}\Phi} \mathcal{K}_{p+1} \right) . \quad (3.3.16)$$

Now go back to (3.3.9). Combining it with (3.3.16), we obtain the following characterization of the smearing form Ξ in supersymmetric backgrounds:

$$\Xi = (2\kappa_{10}^2 T_{Dp})^{-1} (-1)^{9-p} d \left(e^{\frac{3-p}{2}\Phi} * d \left(e^{\frac{p-3}{4}\Phi} \mathcal{K}_{p+1} \right) \right) . \quad (3.3.17)$$

This means that calibration form already knows about the possible places where we can put the branes supersymmetrically. This calibration form can be defined in terms of spinor bilinears (see [78] for the details of this construction), as we will illustrate several times throughout the text. The only thing we need to know to compute \mathcal{K} is the G-structure of the background. In general, one only needs to count supersymmetries (for instance $SU(3)$ -structures are $\frac{1}{4}$ -supersymmetric, G_2 -structures are $\frac{1}{8}$ -supersymmetric, and $Spin(7)$ -structures are $\frac{1}{16}$ -supersymmetric), an ansatz for the metric can be given, and the calibration form can be computed.

Contrary to the microscopic method, this macroscopic approach is really a no-brainer. Once the G-structure of the background has been defined, and an ansatz for the metric has been written, the fluxes and smearing form can be computed from the calibration form according to (3.3.16) and (3.3.17).

Let us now put both the microscopic and macroscopic approaches into perspective, putting the emphasis on their comparison to see what are the advantages of one and the other. Notice that in principle they are independent methods to compute the smearing form. We also show how to link them. The combination of both is probably the best approach when dealing with smeared flavor.

Connection between the macroscopic and microscopic approaches

In the presence of supersymmetry, the macroscopic approach is clearly the simplest to be carried out. The information about how we can distribute a possible set of flavor branes is already encoded in the G-structure carried by the background. From the supergravity perspective, of finding a solution to the equations of motion, this is more than enough. We just need to use the relation between the smearing form and the G-structure, (3.3.17). The generality of this approach is also its main drawback: the G-structure already knows about all the possible deformations we can make to a given background that preserve supersymmetry, but it does not tell us what these deformations are owing to. In other words, the smearing form (3.3.17) is giving information about the location of some Dp branes, but we do not know whether these are “good” flavor branes (that need to satisfy certain characteristics

to be interpreted as such in the correspondence), or they are just some random Dp branes paced supersymmetrically. Without the information about where the branes are placed, the dual field theory interpretation is unclear.

On the other hand, this last problem we described does not exist in the microscopic approach, since we know exactly where the branes are being placed. The dual field theory interpretation is clear. Moreover, (3.3.13) is valid regardless of whether we have supersymmetry or not. As we already stressed two subsections above, the main difficulty of this approach is technical. There are two complicated things to do, one is to find κ -symmetric embeddings in a very generic geometry (it cannot be known exactly because the backreaction has not taken place yet), and the second one is to compute the integral in (3.3.13). These are challenging tasks.

So, essentially, *the macroscopic approach is easy from the supergravity side, but complicated from the field theory side; while it is the opposite for the microscopic approach, whose field theory interpretation is clear, but the supergravity computations are very hard.* Could it be possible to find a method taking the best from both approaches?

This is indeed possible, and we describe it in what follows. The necessary ingredients are formula (3.3.13) to know the smearing form, plus one supersymmetric embedding of the family over which we smear (usually called representative or fiducial embedding). With this, the microscopic interpretation is under control, and the supergravity computation of Ξ is very easy. The method grew up of some unpublished notes from Ángel Paredes, and it was illustrated in [22, 23]. We review these computations in sections 4.3.2, 5.2.2, and 5.A.3. We spell out the idea of the method here.

Imagine we have the situation we start with in the microscopic approach: a family of supersymmetric embeddings is used to smear N_f flavor branes. This family should be generated by some isometry (of the background). We assume we have a radial coordinate r in the geometry, and that the resulting brane distribution is homogeneous in the transverse coordinates (this can be easily extended to similar cases). The idea is then to use this fact that the family of embeddings is spanned by a symmetry, so that one representative embedding should account for the whole family.

On the one hand, a generic representative of the family has an action

$$S_{\text{single}} = \int_{\text{Dp}} d^{p+1}y \mathcal{L}_{\text{single}}. \quad (3.3.18)$$

If this representative embedding is “equivalent” to any of the others within the family, we quantify this by having the action of a brane spread along it not to depend on the symmetry (transverse) coordinates. For the configuration we are assuming, we expect it just to depend on the radial coordinate:

$$\mathcal{L}_{\text{single}} = \mathcal{L}_{\text{single}}(r). \quad (3.3.19)$$

On the other hand, if we integrate the action of the smeared distribution over the transverse coordinates we also obtain an action that only depends on the radial coordinate. This process of integrating over the transverse coordinates should account for the effect of the N_f

branes we are smearing. This translates into the following key equation:

$$\begin{aligned} S_{\text{smeared}} &= N_f S_{\text{single}} \implies \\ \implies \int \left(\begin{smallmatrix} \text{non-radial} \\ \text{coord. of } \mathcal{M}_{10} \end{smallmatrix} \right) \mathcal{L}_{\text{smeared}} &= N_f \int \left(\begin{smallmatrix} \text{non-radial} \\ \text{coord. of } D_p \end{smallmatrix} \right) \mathcal{L}_{\text{single}}, \end{aligned} \quad (3.3.20)$$

where $\mathcal{L}_{\text{smeared}}$ stands for the Lagrangian of the smeared configuration, that can be read from (3.3.7). Notice that the two integrals in the second line of (3.3.20), which can be thought of as effective radial actions, are just functions of the radial coordinate.

Generically, the smearing form should contain some parameter proportional to N_f . And in the case where the flavors we are adding are massive, there is also some unknown function $S(r)$, related to the non-trivial RG flow of a theory with massive quarks. Any unknown in the smearing form (like the two we just mentioned) should be fixed by equation (3.3.20). *The power of this method resides in that both sides of the equation can be computed in different fashions.* For the LHS we only need the macroscopic approach, and for the RHS we need a microscopic piece of information: one representative of the family of embeddings. The macroscopic and microscopic approaches merge into a hybrid approach. Notice that there is no need of knowing the whole family of embeddings (which can be found in any case once a representative is known, and the isometries are known as well), neither a need to perform the microscopic integration (3.3.13) giving rise to the macroscopic smearing form.

There are two ways of implementing equation (3.3.20) in practice:

- One is using in (3.3.20) the DBI part of the brane action.

$$\int \left(\begin{smallmatrix} \text{non-radial} \\ \text{coord. of } \mathcal{M}_{10} \end{smallmatrix} \right) \mathcal{L}_{\text{smeared}}^{\text{DBI}} = N_f \int \left(\begin{smallmatrix} \text{non-radial} \\ \text{coord. of } D_p \end{smallmatrix} \right) \mathcal{L}_{\text{single}}^{\text{DBI}}. \quad (3.3.21)$$

The RHS is very easy to compute once we know the embedding, since it is just the square root of the determinant of the induced metric on the brane. But the LHS poses more trouble, since it is only specially easy to compute when we have supersymmetry:

$$d^{10}x \mathcal{L}_{\text{smeared}}^{\text{DBI}} = -d^{10}x T_{Dp} e^{\frac{p-3}{4}\Phi} \sqrt{-\det[g]} |\Xi| = -T_{Dp} e^{\frac{p-3}{4}\Phi} \mathcal{K}_{p+1} \wedge \Xi, \quad (3.3.22)$$

where g is the ten-dimensional metric, and the modulus of an k -form η is defined as

$$|\eta| = \sqrt{\frac{1}{k!} \eta_{\mu_1, \dots, \mu_k} h^{\mu_1, \dots, \mu_k}}. \quad (3.3.23)$$

Recall that the last step in (3.3.22) is only valid when we are preserving some supersymmetry, and without it the smeared action is not linear in the smearing form, i.e: not linear in the sources. Note that linearity in the sources is essential for (3.3.20) to hold. In the cases without supersymmetry (3.3.21) is not valid and yields a wrong result.

- The other one is using in (3.3.20) the WZ part of the brane action.

$$\int \left(\begin{smallmatrix} \text{non-radial} \\ \text{coord. of } \mathcal{M}_{10} \end{smallmatrix} \right) \mathcal{L}_{\text{smeared}}^{\text{WZ}} = N_f \int \left(\begin{smallmatrix} \text{non-radial} \\ \text{coord. of } D_p \end{smallmatrix} \right) \mathcal{L}_{\text{single}}^{\text{WZ}}. \quad (3.3.24)$$

Since

$$d^{10}x \mathcal{L}_{\text{smeared}}^{\text{WZ}} = T_{\text{D}p} C_{p+1} \wedge \Xi, \quad (3.3.25)$$

this term is always linear in the sources, regardless of whether we have supersymmetry or not.

Obviously, in the case we have supersymmetry, in virtue of (3.3.15), both prescriptions are identical. All of this seems quite simple, but some criticism is due.

In principle the hybrid method can be run for any sort of embedding. However, it is hard to think that any given family of embeddings, even if supersymmetric, generates (when we place flavor branes along the embeddings of the family) a backreaction of the metric that is compatible with the initial ansatz we assumed for this metric (unless this is the most general possible). It seems nonetheless that this hybrid method is able to detect this “compatibility property”, and we present in what follows some arguments in favor of that.

The trick of the hybrid method is to compute the effective radial action of the smeared brane distribution, and to compare it with N_f times the effective radial action of a single brane sitting at one of the embeddings of the family over which we smear. Both actions should be equal. We focus on the WZ part. In the most general case of massive flavors, we said that the smearing form contains a function $S(r)$. The case of massless flavors can be thought as a special case of the former, with $S(r) = 1$, so we assume that the smeared action always contains two terms, one proportional to $S(r)$, and another proportional to $S'(r)$:

$$\mathcal{L}_{WZ}^{\text{smeared}} = F_1(r, g_{\mu\nu}) S(r) + F_2(r, g_{\mu\nu}) S'(r), \quad (3.3.26)$$

where F_1 and F_2 depend on the functions of the ansatz for the metric. We conjecture that the first test to detect if a family of embeddings generates a backreaction compatible with the ansatz is to take any representative embedding of this family and compute its WZ effective radial action, and then check whether or not the result depends functionally on the functions of the ansatz as in (3.3.26). If the representative embedding passes this first test, then the effective WZ radial Lagrangian density for the representative embedding is of the form:

$$\mathcal{L}_{WZ}^{\text{single}} = F_1(r, g_{\mu\nu}) G(r) + F_2(r, g_{\mu\nu}) H(r), \quad (3.3.27)$$

where F_1 and F_2 are the same as in (3.3.26) and $G(r)$ and $H(r)$ are functions of r which do not depend on the functions of the ansatz. The second test to verify that (3.3.27) is of the form (3.3.26). One must have:

$$\frac{dG(r)}{dr} = H(r). \quad (3.3.28)$$

If this were the case, the second test is passed as well, and we conjecture that the backreaction is compatible with the ansatz (and, furthermore, that the profile function $S(r)$ is proportional to $G(r)$).

We will put in practice all the discussion we have made about the different approaches to compute the smearing form in section 5.2 (see also section 5.A). A very non-trivial geometry is discussed, where the smearing form is computable from both macroscopic and microscopic approaches independently, and the compatibility tests provided above can be validated.

Chapter 4

Flavor Physics in 3d Chern-Simons-matter theories

Contextualizing this chapter

In our pursuit to describe flavor physics within the gauge/gravity correspondence, we choose to start with the cleanest example possible, *i.e.* the case where the field theory has conformal invariance, correspondingly the geometry has an AdS factor, and the dictionary is therefore fully operative. The presence of an arbitrary amount of fundamental matter is typically incompatible with having conformal invariance. This is not the case for a certain type of highly supersymmetric Chern-Simons-matter theories. These theories appear on the field theory side of the AdS_4/CFT_3 duality [116], living on the worldvolume of M2-branes.

Rapidly after the birth of AdS_4/CFT_3 correspondence, people noticed this interesting fact about flavors and worked on it both from the field theory side and the gravity side. Great progress was made on the former, but from the latter the geometries turned out to be quite complicated. Some checks of the flavored duality could be performed though. In [22] a very simple solution was found using the smearing technique for incorporating the flavors. This solution captures very well the flavor dynamics coming from the field theory side, and its simplicity allows for the computation of a great deal of non-perturbative observables. We describe it in what follows, as well as some of its possible applications.

4.1 The AdS_4/CFT_3 correspondence

In the paper where everything started [8], Maldacena observed that taking the decoupling limit in the supergravity solutions corresponding to different branes in flat space, one obtained an AdS solution in three cases. One was the case of D3-branes that gave rise to the celebrated duality between type IIB supergravity in $AdS_5 \times S^5$ and $\mathcal{N} = 4$ SYM. The other two were the cases of M2-branes and M5-branes in eleven-dimensional supergravity, which is to M-theory what type IIA/B supergravity is to type IIA/B String Theory. These two AdS solutions should be dual to conformal field theories, and the main reason why these dualities are not so famous as the $AdS_5 \times S^5$ example is because the dual field theories were not known at the time. While one knows the low-energy theory living on a stack of Dp-branes,

the same cannot be said for M-branes.

A lot of effort has been dedicated to elucidating what is the theory living on the world-volume of a stack of M2-branes. This should be the conformal point to which $\mathcal{N} = 8$ three-dimensional SYM flows in the IR¹. Such a fixed point must be a maximally supersymmetric theory with (super)conformal invariance. A first step towards this goal was done in [117], where three-dimensional superconformal theories were constructed. These theories turned out to be Chern-Simons theories, but had only $\mathcal{N} = 1$ and $\mathcal{N} = 2$ supersymmetry. The crucial breakthrough took place with the results of Bagger and Lambert [118, 119, 120] and Gustavsson [121], who constructed superconformal Chern-Simons-matter theories with extended supersymmetry $\mathcal{N} \geq 6$, and proposed that they described the low energy dynamics of coincident M2-branes.

However, the key work [116] appeared in 2008, when inspired by these results, Aharony, Bergman, Jafferis and Maldacena (ABJM) constructed an $\mathcal{N} = 6$ supersymmetric Chern-Simons-matter theory which is believed to describe the dynamics of multiple M2-branes at a $\mathbb{C}^4/\mathbb{Z}_k$ singularity. The theory is now known as the ABJM theory. An early review can be found in [122], and since then numerous checks of the duality between M-theory on $AdS_4 \times \mathbb{S}^7/\mathbb{Z}_k$ and the ABJM theory have been made, and it is of course, and by far, the best understood example of the AdS_4/CFT_3 correspondence. The same that happened for its big brother, the $AdS_5 \times \mathbb{S}^5$ correspondence, these new findings have inspired a lot of work on the field theory side, where some non-perturbative aspects have been unraveled in splendid works [123]. Let us now give a very brief overview of the ABJM realization of the AdS_4/CFT_3 correspondence.

With hindsight, one starts with a three-dimensional Chern-Simons-matter theory with two gauge fields transforming in the adjoint of $U(N) \times U(N)$, and four complex fields C_I , ($I = 1, \dots, 4$) transforming in the bifundamental representation $(\mathbf{N}, \bar{\mathbf{N}})$ (and also the conjugate C_I^\dagger transforming in the $(\bar{\mathbf{N}}, \mathbf{N})$). The action is the standard one for levels $(k, -k)$. The complex fields should play the role of the scalars in the $AdS_5 \times \mathbb{S}^5$ example, so the isometry group of $\mathbb{S}^7/\mathbb{Z}_k$, which is $SU(4) \times U(1)$, should be a global symmetry in the theory. Therefore, one has to find a supersymmetric extension of the Chern-Simons-matter theory with an $SU(4)$ R-symmetry. If we require that this extension has no dimensionful parameters (so that we have chances of having conformal invariance), there is only one such extension: the ABJM theory, whose Lagrangian was first written in [116].

Notice that the field content of the ABJM theory is the same as that of the Klebanov-Witten theory, obviously with the difference of being in a different dimension. The analogy goes deeper, as the action of the ABJM theory has a superpotential for the chiral fields C_I that is the same as the Klebanov-Witten one if we call $\{C_1, C_2, C_3, C_4\} = \{A_1, A_2, B_1^\dagger, B_2^\dagger\}$, namely:

$$W = \frac{2\pi}{k} \epsilon^{ij} \epsilon^{kl} \text{Tr} [A_i B_k A_j B_l] . \quad (4.1.1)$$

Although this superpotential only has a manifest $U(1) \times SU(2) \times SU(2)$ symmetry, the full Lagrangian has an enhanced $SU(4) = SO(6)$ R-symmetry, which corresponds to $\mathcal{N} = 6$ in

¹This can be seen from a supergravity perspective. In three dimensions, $\mathcal{N} = 8$ SYM is the theory on a stack of D2-branes. The type IIA supergravity solution has a non-trivial dilaton that grows in the IR, where one has to uplift to 11d supergravity, getting the M2-branes.

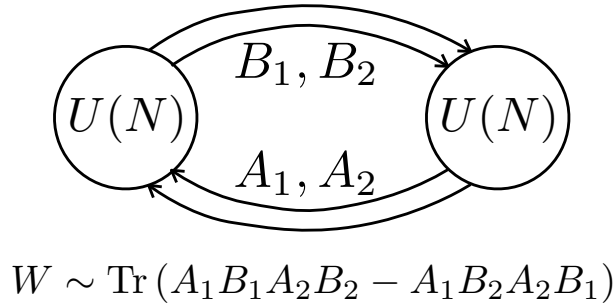


Figure 4.1: Quiver of the ABJM theory.

three dimensions. Additionally, we have another $U(1)$ R-symmetry acting as $A_i \rightarrow e^{i\alpha} A_i$, $B_i \rightarrow e^{-i\alpha} B_i$. The ABJM theory has therefore twenty-four supercharges². Moreover, the Lagrangian has a conformal invariance at the classical level. This carries through to the quantum level. A possible way to see it is by noticing that there are no relevant or marginal operators that can be added to the Lagrangian preserving $\mathcal{N} = 6$ supersymmetry.

All these facts and symmetries are matched by the supergravity solution $AdS_4 \times \mathbb{S}^7/\mathbb{Z}_k$. The presence of the AdS factor is of course signaling conformal invariance. The solution preserves twenty-four out of the thirty-two Killing spinors of eleven-dimensional supergravity. And as we already said, the isometry group of the $\mathbb{S}^7/\mathbb{Z}_k$ factor of the metric is $SU(4) \times U(1)$. Moreover, as checked by ABJM, if one considers the brane construction of the type of Chern-Simons-matter gauge theory we are considering, it is possible to see that it corresponds to M2-branes probing a $\mathbb{C}^4/\mathbb{Z}_k$ singularity.

Regarding the couplings, in the large N limit one works with the 't Hooft coupling, which is, for the ABJM theory, $\lambda = \frac{N}{k}$. Therefore, the theory is strongly coupled for $N \gg k$. In this regime, the theory admits a supergravity description in a weakly-coupled M-theory in terms of the $AdS_4 \times \mathbb{S}^7/\mathbb{Z}_k$ geometry. If we represent \mathbb{S}^7 as a $U(1)$ Hopf bundle over \mathbb{CP}^3 , the \mathbb{Z}_k orbifold acts by quotienting the \mathbb{S}^1 fiber. When the Chern-Simons level k is large ($k^5 \gg N$), the size of the fiber is small and the system is better described in terms of type IIA supergravity by performing a dimensional reduction to ten dimensions along the Hopf fiber of $\mathbb{S}^7/\mathbb{Z}_k$. In this ten-dimensional description the geometry is of the form $AdS_4 \times \mathbb{CP}^3$ with fluxes.

Of course, with the precise knowledge of the field theory dual to a system of multiple M2-branes on $\mathbb{C}^4/\mathbb{Z}_k$, one can run all the AdS/CFT machinery, and test some of the non-trivial predictions of the AdS/CFT correspondence. In particular, in [123] it was checked by means of a purely field theoretic calculation, using matrix model techniques and localization, that the number of low energy degrees of freedom of N coincident M2-branes scales as $N^{\frac{3}{2}}$ for large N , as predicted by the gravity dual (see also [124]). Moreover, the ABJM model has been generalized in several directions. By adding fractional M2-branes, the gravity dual of $U(M) \times U(N)$ Chern-Simons-matter theories with $M \neq N$ was constructed in [125].

²In the cases $k = 1, 2$, the supersymmetry is enhanced to $\mathcal{N} = 8$, which is not visible in the action written by ABJM, but it is explicit in the actions of [118, 119, 120, 121].

If the sum of Chern-Simons levels for the two gauge groups is non-zero, the corresponding gravity dual can be found in massive type IIA supergravity by considering solutions in which the Romans mass parameter is non-vanishing [126, 127] (see also [128]). The ABJM construction has been extended to include different quivers and gauge groups with several amount of supersymmetry in refs. [129, 130, 131, 132, 133, 134, 135].

In this chapter we study the generalization of the ABJM model which is obtained by adding flavors, *i.e.* fields transforming in the fundamental representations $(\mathbf{N}, \mathbf{1})$ and $(\mathbf{1}, \mathbf{N})$ of the $U(N) \times U(N)$ gauge group. The holographic dual of such a system was proposed in refs. [136, 137]. In the type IIA description the addition of massless flavor is achieved by considering D6-branes that fill the AdS_4 space and wrap an \mathbb{RP}^3 submanifold inside the \mathbb{CP}^3 , while preserving $\mathcal{N} = 3$ supersymmetry (see also [138, 139, 140, 141] for different setups with D6-branes in Chern-Simons-matter theories). When the number of flavors is small one can study the system in the quenched approximation, in which the D6-branes are considered as probes in the $AdS_4 \times \mathbb{CP}^3$ background. This quenched approach has been adopted in refs. [142, 143, 144], where different observables of the Chern-Simons-matter theory with flavor have been analyzed.

4.1.1 The ABJM solution

In this subsection, we discuss in detail the IIA supergravity solution dual to the ABJM theory. Apart from setting the notation, we write the solution in a system of coordinates that will be very useful for later purposes.

We use throughout all the chapter units where $g_s = 1, \alpha' = 1$. The metric of the ABJM background is given, in string frame, by:

$$ds^2 = L^2 ds_{AdS_4}^2 + 4L^2 ds_{\mathbb{CP}^3}^2, \quad (4.1.2)$$

where $ds_{AdS_4}^2$ and $ds_{\mathbb{CP}^3}^2$ are respectively the AdS_4 and \mathbb{CP}^3 metrics. The former, in Poincaré coordinates, is given by:

$$ds_{AdS_4}^2 = r^2 dx_{1,2}^2 + \frac{dr^2}{r^2}, \quad (4.1.3)$$

with $dx_{1,2}^2$ being the Minkowski metric in 2+1 dimensions. This solution depends on two integers N and k which represent, in the gauge theory dual, the rank of the gauge groups and the Chern-Simons level, respectively. In string units, the AdS_4 radius L can be written in terms of N and k as:

$$L^4 = 2\pi^2 \frac{N}{k} \quad (4.1.4)$$

Moreover, for this background the dilaton Φ is constant and given by:

$$e^\Phi = \frac{2L}{k} = 2\sqrt{\pi} \left(\frac{2N}{k^5} \right)^{\frac{1}{4}}. \quad (4.1.5)$$

This solution of type IIA supergravity is also³ endowed with a RR two-form F_2 and a RR

³Actually, as explained by [145], there should also be a non-trivial B-field. This is unimportant for the supergravity calculations in the large N limit we will do.

four-form F_4 , whose expression can be written as:

$$F_2 = 2k J, \quad F_4 = \frac{3}{2} k L^2 \omega_{\text{Vol}(AdS_4)} = \frac{3\pi}{\sqrt{2}} (kN)^{\frac{1}{2}} \omega_{\text{Vol}(AdS_4)}, \quad (4.1.6)$$

with J being the Kähler form of \mathbb{CP}^3 and $\omega_{\text{Vol}(AdS_4)}$ the volume element of the AdS_4 metric (4.1.3). This solution is a good gravity dual of the Chern-Simons-matter theory when the AdS radius is large in string units and the string coupling e^Φ is small. By looking at equations (4.1.4) and (4.1.5), this amounts to the condition $N^{\frac{1}{5}} \ll k \ll N$.

The \mathbb{CP}^3 metric in (4.1.2) is the canonical Fubini-Study metric. In the context of the ABJM solution, the \mathbb{CP}^3 space is usually represented as foliated by the $T^{1,1} \sim \mathbb{S}^2 \times \mathbb{S}^3$ manifold. Here we write the \mathbb{CP}^3 metric in a form which is more convenient for our purposes. We will regard \mathbb{CP}^3 as an \mathbb{S}^2 -bundle over \mathbb{S}^4 , with the fibration constructed by using the self-dual $SU(2)$ instanton on the four-sphere. Explicitly, $ds_{\mathbb{CP}^3}^2$ will be written as:

$$ds_{\mathbb{CP}^3}^2 = \frac{1}{4} \left[ds_{\mathbb{S}^4}^2 + (dx^i + \epsilon^{ijk} A^j x^k)^2 \right], \quad (4.1.7)$$

where $ds_{\mathbb{S}^4}^2$ is the standard metric for the unit four-sphere, x^i ($i = 1, 2, 3$) are Cartesian coordinates that parameterize the unit two-sphere ($\sum_i (x^i)^2 = 1$), and A^i are the components of the non-Abelian one-form connection corresponding to the $\mathfrak{su}(2)$ instanton. Mathematically, the representation (4.1.7) is obtained when \mathbb{CP}^3 is constructed as the twistor space of the four-sphere. We shall now introduce a specific system of coordinates to represent the metric (4.1.7). First of all, let $\bar{\omega}^i$ ($i = 1, 2, 3$) be the $\mathfrak{su}(2)$ left-invariant one-forms which satisfy $d\bar{\omega}^i = \frac{1}{2} \epsilon_{ijk} \bar{\omega}^j \wedge \bar{\omega}^k$. Notice that the sign of the $\mathfrak{su}(2)$ algebra is inverted with respect to (3.2.6). We can write down an explicit representation of the $\bar{\omega}^i$'s in terms of angular coordinates $\bar{\theta}, \bar{\varphi}, \bar{\psi}$ as

$$\begin{aligned} \bar{\omega}^1 &= \cos \bar{\psi} d\bar{\theta} + \sin \bar{\psi} \sin \bar{\theta} d\bar{\varphi}, \\ \bar{\omega}^2 &= \sin \bar{\psi} d\bar{\theta} - \cos \bar{\psi} \sin \bar{\theta} d\bar{\varphi}, \\ \bar{\omega}^3 &= d\bar{\psi} + \cos \bar{\theta} d\bar{\varphi}, \end{aligned} \quad (4.1.8)$$

with $0 \leq \bar{\theta} \leq \pi$, $0 \leq \bar{\varphi} < 2\pi$, $0 \leq \bar{\psi} \leq 4\pi$. Together with a new coordinate ξ , the $\bar{\omega}^i$'s can be used to parameterize the metric of a four-sphere \mathbb{S}^4 as:

$$ds_{\mathbb{S}^4}^2 = \frac{4}{(1 + \xi^2)^2} \left[d\xi^2 + \frac{\xi^2}{4} \left((\bar{\omega}^1)^2 + (\bar{\omega}^2)^2 + (\bar{\omega}^3)^2 \right) \right], \quad (4.1.9)$$

where $0 \leq \xi < +\infty$ is a non-compact coordinate. The $\mathfrak{su}(2)$ instanton one-forms A^i can be written in these coordinates as:

$$A^i = -\frac{\xi^2}{1 + \xi^2} \bar{\omega}^i. \quad (4.1.10)$$

Let us next parameterize the x^i coordinates of the \mathbb{S}^2 by means of two angles θ and φ ($0 \leq \theta < \pi$, $0 \leq \varphi < 2\pi$), namely:

$$x^1 = \sin \theta \cos \varphi, \quad x^2 = \sin \theta \sin \varphi, \quad x^3 = \cos \theta. \quad (4.1.11)$$

Then, one can easily prove that:

$$(\mathrm{d}x^i + \epsilon^{ijk} A^j x^k)^2 = (E^1)^2 + (E^2)^2, \quad (4.1.12)$$

where E^1 and E^2 are the following one-forms:

$$\begin{aligned} E^1 &= d\theta + \frac{\xi^2}{1+\xi^2} (\sin \varphi \bar{\omega}^1 - \cos \varphi \bar{\omega}^2), \\ E^2 &= \sin \theta \left(d\varphi - \frac{\xi^2}{1+\xi^2} \bar{\omega}^3 \right) + \frac{\xi^2}{1+\xi^2} \cos \theta (\cos \varphi \bar{\omega}^1 + \sin \varphi \bar{\omega}^2). \end{aligned} \quad (4.1.13)$$

Therefore, the canonical Fubini-Study metric of \mathbb{CP}^3 can be written in terms of the one-forms defined above as:

$$\mathrm{d}s_{\mathbb{CP}^3}^2 = \frac{1}{4} \left[\mathrm{d}s_{\mathbb{S}^4}^2 + (E^1)^2 + (E^2)^2 \right]. \quad (4.1.14)$$

As a check, one can verify that the volume of \mathbb{CP}^3 obtained from the above metric is $\pi^3/6$. We shall now consider a rotated version of the forms $\bar{\omega}^i$ by the two angles θ and φ . Accordingly, we define three new one-forms S^i ($i = 1, 2, 3$) as:

$$\begin{aligned} S^1 &= \sin \varphi \bar{\omega}^1 - \cos \varphi \bar{\omega}^2, \\ S^2 &= \sin \theta \bar{\omega}^3 - \cos \theta (\cos \varphi \bar{\omega}^1 + \sin \varphi \bar{\omega}^2), \\ S^3 &= -\cos \theta \bar{\omega}^3 - \sin \theta (\cos \varphi \bar{\omega}^1 + \sin \varphi \bar{\omega}^2). \end{aligned} \quad (4.1.15)$$

In terms of the forms defined in (4.1.15) the line element of the four-sphere is just obtained by substituting $\bar{\omega}^i \rightarrow S^i$ in (4.1.9). Let us next define the one-forms \mathcal{S}^ξ and \mathcal{S}^i as:

$$\mathcal{S}^\xi = \frac{2}{1+\xi^2} \mathrm{d}\xi, \quad \mathcal{S}^i = \frac{\xi}{1+\xi^2} S^i, \quad (i = 1, 2, 3), \quad (4.1.16)$$

in terms of which the metric of the four-sphere is just $\mathrm{d}s_{\mathbb{S}^4}^2 = (\mathcal{S}^\xi)^2 + \sum_i (\mathcal{S}^i)^2$. The RR two-form F_2 can be written in terms of the one-forms defined in (4.1.13) and (4.1.16) as:

$$F_2 = \frac{k}{2} \left(E^1 \wedge E^2 - (\mathcal{S}^\xi \wedge \mathcal{S}^3 + \mathcal{S}^1 \wedge \mathcal{S}^2) \right). \quad (4.1.17)$$

Notice that F_2 is a closed two-form due to the relation:

$$\begin{aligned} \mathrm{d}(E^1 \wedge E^2) &= \mathrm{d}(\mathcal{S}^\xi \wedge \mathcal{S}^3 + \mathcal{S}^1 \wedge \mathcal{S}^2) = \\ &= E^1 \wedge (\mathcal{S}^\xi \wedge \mathcal{S}^2 - \mathcal{S}^1 \wedge \mathcal{S}^3) + E^2 \wedge (\mathcal{S}^\xi \wedge \mathcal{S}^1 + \mathcal{S}^2 \wedge \mathcal{S}^3). \end{aligned} \quad (4.1.18)$$

4.1.2 ABJM geometry

Let us collect in this subsection some basic facts of the geometry of the ABJM solution in our coordinates. We first focus on displaying the non-trivial cycles of \mathbb{CP}^3 in our coordinates. We illustrate why they are important by using them to extract relevant physical quantities of the dual field theory.

There is a non-trivial $\mathbb{CP}^1 = \mathbb{S}^2$ in the geometry, which in our coordinates is parameterized by the angles θ and φ at a fixed point in the base \mathbb{S}^4 . As one can readily verify by a simple calculation from (4.1.17), the flux of the RR two-form F_2 through this \mathbb{CP}^1 is given by:

$$\frac{1}{2\pi} \int_{\mathbb{CP}^1} F_2 = k. \quad (4.1.19)$$

Equation (4.1.19) is essential to understand the meaning of k as the Chern-Simons level of the gauge theory. Indeed, let us consider a fractional D2-brane, *i.e.* a D4-brane wrapping a \mathbb{CP}^1 two-cycle and extended along the Minkowski directions. For such a brane there is a coupling to the worldvolume gauge field \mathcal{A} of the type $\int_{\text{Mink}_{1,2}} \mathcal{A} \wedge d\mathcal{A} \int_{\mathbb{CP}^1} F_2$ which, taking into account (4.1.19), clearly induces a Chern-Simons coupling for the gauge field \mathcal{A} with level k .

We can also find a non-trivial four-cycle corresponding to a \mathbb{CP}^2 , whose embedding, in our coordinates, is obtained by taking the \mathbb{S}^2 angles θ and φ to be constant and given by:

$$\varphi = \theta = \frac{\pi}{2}. \quad (4.1.20)$$

In such a case the pullbacks of E^1 and E^2 are given by:

$$\hat{E}^1 = \frac{\xi^2}{1 + \xi^2} \bar{\omega}^1, \quad \hat{E}^2 = -\frac{\xi^2}{1 + \xi^2} \bar{\omega}^3. \quad (4.1.21)$$

Then, the pullback of the \mathbb{CP}^3 metric (4.1.14) is just:

$$\frac{d\xi^2}{(1 + \xi^2)^2} + \frac{\xi^2}{4(1 + \xi^2)} \left((\bar{\omega}^1)^2 + (\bar{\omega}^3)^2 \right) + \frac{\xi^2}{4(1 + \xi^2)^2} (\bar{\omega}^2)^2. \quad (4.1.22)$$

Introducing the new angle χ as:

$$\xi = \cot\left(\frac{\chi}{2}\right), \quad 0 \leq \chi \leq \pi, \quad (4.1.23)$$

we can rewrite the above metric as:

$$\frac{1}{4} \left[(d\chi)^2 + \cos^2 \frac{\chi}{2} \left((\bar{\omega}^1)^2 + (\bar{\omega}^3)^2 + \sin^2 \frac{\chi}{2} (\bar{\omega}^2)^2 \right) \right], \quad (4.1.24)$$

which is, indeed, the Fubini-Study metric of \mathbb{CP}^2 . Notice that the total volume for this metric is just $\pi^2/2$. As an application of this result, let us consider now a D4-brane wrapped on the \mathbb{CP}^2 . Its mass is given by:

$$m_{D4} = T_{D4} \text{Vol}(\mathbb{CP}^2), \quad (4.1.25)$$

where T_{D4} and $\text{Vol}(\mathbb{CP}^2)$ are:

$$T_{D4} = \frac{1}{(2\pi)^4 e^\Phi}, \quad \text{Vol}(\mathbb{CP}^2) = \frac{\pi^2}{2} L^4. \quad (4.1.26)$$

The dilaton has been written in (4.1.5) and L is the AdS_4 radius for the ABJM solution displayed in (4.1.4). Using these values of g_s and L , we get:

$$m_{D4} = \frac{1}{2\sqrt{\pi}} \left(\frac{kN^3}{2} \right)^{\frac{1}{4}}. \quad (4.1.27)$$

From the mass of this wrapped D4-brane, it is possible to extract the conformal dimension Δ_{D4} of the dual operator through the dictionary as:

$$\Delta_{D4} = m_{D4} L = \frac{N}{2}. \quad (4.1.28)$$

This is the expected result since these branes are dual to dibaryon operators (see [116]) which are products of N bifundamental fields, each of them of dimension $1/2$.

Let us now show how the uplifted solution in M-theory corresponds to the space $AdS_4 \times \mathbb{S}^7/\mathbb{Z}_k$, where the \mathbb{S}^7 is realized as an \mathbb{S}^3 -bundle over \mathbb{S}^4 . The corresponding uplifting formula for the metric is:

$$ds_{11}^2 = e^{-\frac{2\Phi}{3}} ds_{10}^2 + e^{\frac{4\Phi}{3}} (dx_{11} - A_1)^2, \quad (4.1.29)$$

where the eleven-dimensional coordinate x_{11} takes values in the range $x_{11} \in [0, 2\pi)$ and A_1 is the one-form potential for the type IIA field strength F_2 :

$$F_2 = dA_1. \quad (4.1.30)$$

For the ABJM solution of section 4.1.1, the actual value of A_1 is:

$$A_1 = -\frac{k}{2} \left(\cos \theta d\varphi + \xi \mathcal{S}^3 \right), \quad (4.1.31)$$

where \mathcal{S}^3 has been defined in (4.1.16). Let us next define a new angular variable ψ as:

$$\psi := \frac{2}{k} x_{11}, \quad \psi \in \left[0, \frac{4\pi}{k} \right), \quad (4.1.32)$$

as well as a new one-form E^3 as:

$$E^3 := d\psi + \cos \theta d\varphi + \xi \mathcal{S}^3. \quad (4.1.33)$$

Then, the uplifted metric (4.1.29) can be written as the one corresponding to the product space $AdS_4 \times \mathbb{S}^7/\mathbb{Z}_k$, namely :

$$ds_{11}^2 = \frac{R^2}{4} ds_{AdS_4}^2 + R^2 ds_{\mathbb{S}^7/\mathbb{Z}_k}^2, \quad (4.1.34)$$

where the eleven-dimensional radius R is given by

$$R^6 = 2^5 \pi^2 N k, \quad (4.1.35)$$

and the $\mathbb{S}^7/\mathbb{Z}_k$ metric is:

$$ds_{\mathbb{S}^7/\mathbb{Z}_k}^2 = \frac{1}{4} \left[ds_{\mathbb{S}^4}^2 + (E^1)^2 + (E^2)^2 + (E^3)^2 \right], \quad (4.1.36)$$

where $ds_{\mathbb{S}^4}^2$ is the metric of the four-sphere written in (4.1.9). As a check one can verify that the eight-dimensional cone with metric $dr^2 + r^2 ds_{\mathbb{S}^7/\mathbb{Z}_k}^2$ is locally flat. Moreover, the metric (4.1.36) can be written as an \mathbb{S}^3 -bundle over \mathbb{S}^4 . Indeed, let $\tilde{\omega}^i$ ($i = 1, 2, 3$) be a second set of left-invariant one-forms, defined in terms of the angles θ , φ and ψ as:

$$\begin{aligned}\tilde{\omega}^1 &= -\sin \varphi d\theta + \cos \varphi \sin \theta d\psi, \\ \tilde{\omega}^2 &= \cos \varphi d\theta + \sin \varphi \sin \theta d\psi, \\ \tilde{\omega}^3 &= d\varphi + \cos \theta d\psi.\end{aligned}\tag{4.1.37}$$

These forms satisfy $d\tilde{\omega}^i = \frac{1}{2} \epsilon^{ijk} \tilde{\omega}^j \wedge \tilde{\omega}^k$. In terms of the $\tilde{\omega}^i$ the metric (4.1.36) takes the form

$$ds_{\mathbb{S}^7/\mathbb{Z}_k}^2 = \frac{1}{4} \left[ds_{\mathbb{S}^4}^2 + \sum_i (\tilde{\omega}^i + A^i)^2 \right],\tag{4.1.38}$$

that makes explicit the structure of \mathbb{S}^7 as an \mathbb{S}^3 -bundle over \mathbb{S}^4 , where the one-forms A^i are the components of the $\mathfrak{su}(2)$ instanton connection written in (4.1.10).

4.1.3 The Ooguri-Park solution

There are two supersymmetric seven-spheres. One is the beloved round sphere \mathbb{S}^7 , and the other one is the squashed seven-sphere, that we denote by $\overline{\mathbb{S}}^7$. The metric of the latter reads

$$ds_{\overline{\mathbb{S}}^7/\mathbb{Z}_k}^2 = \frac{1}{4} \left[\frac{9}{5} ds_{\mathbb{S}^4}^2 + \frac{9}{25} \sum_i (\tilde{\omega}^i + A^i)^2 \right],\tag{4.1.39}$$

where $\tilde{\omega}^i, A^i$ were defined in (4.1.37) and (4.1.10) respectively. It is natural to wonder what is the field theory dual to the $\mathcal{N} = 1$ solution of eleven-dimensional supergravity $AdS_4 \times \overline{\mathbb{S}}^7/\mathbb{Z}_k$. This question was answered in [135], where it was proposed that this background was the gravity dual of an $\mathcal{N} = 1$ superconformal Chern-Simons-matter gauge theory with $Sp(2) \times U(1) \cong SO(5) \times U(1)$ global symmetry, since that is the isometry group of $\overline{\mathbb{S}}^7/\mathbb{Z}_k$.

To see that, one follows the same procedure as for the construction of the ABJM theory. Start with a three-dimensional Chern-Simons-matter theory with gauge group $U(N) \times U(N)$, and four complex fields C_I , ($I = 1, \dots, 4$) transforming in the bifundamental representation $(\mathbf{N}, \overline{\mathbf{N}})$, plus their complex conjugates. Now what we want is an $\mathcal{N} = 1$ supersymmetric extension of the Chern-Simons-matter theory with an $SO(5) \times U(1)$ R-symmetry. Again, requiring that this extension has no dimensionful parameters, there is only one possibility, and its action was written in [135].

The theory still has the ABJM quiver (see figure 4.1), but the superpotential is now more complicated. The action is conformally invariant at the classical level, and this invariance is not broken by quantum effects (the arguments are essentially the same as for the ABJM case).

The interest we have in the Ooguri-Park solution comes from the fact that its isometry group $SO(5) \times U(1)$ is the same as the one we will have in the solutions we present in the next section, that we later use to introduce flavors. This means that the Chern-Simons-matter

theories dual to the solutions we find in section 4.3 will share some similarities with the Ooguri-Park theory.

Let us write the supergravity solution. In eleven dimensions, it looks like (4.1.34), replacing the round sphere by the squashed sphere:

$$ds_{11}^2 = \frac{\bar{R}^2}{4} ds_{AdS_4}^2 + \bar{R}^2 \left[\frac{9}{20} ds_{\mathbb{S}^4}^2 + \frac{9}{100} \left((E^1)^2 + (E^2)^2 + (E^3)^2 \right) \right], \quad (4.1.40)$$

where the eleven-dimensional radius \bar{R} is given by

$$\bar{R}^6 = \frac{2^5 5^5}{3^7} \pi^2 N k. \quad (4.1.41)$$

When reducing to type IIA supegravity, the resulting ten-dimensional metric takes the form:

$$ds_{10}^2 = \bar{L}^2 ds_{AdS_4}^2 + \frac{36}{25} \bar{L}^2 ds_{\mathbb{CP}^3}^2, \quad (4.1.42)$$

where $ds_{\mathbb{CP}^3}^2$ is the metric of a squashed \mathbb{CP}^3 (\mathbb{CP}^3 is the base of the $U(1)$ -fibration of $\bar{\mathbb{S}}^7$), given by:

$$ds_{\mathbb{CP}^3}^2 = \frac{5}{4} ds_{\mathbb{S}^4}^2 + \frac{1}{4} \left((E^1)^2 + (E^2)^2 \right), \quad (4.1.43)$$

and the Anti-de-Sitter radius \bar{L} is given by:

$$\bar{L}^4 = \frac{9}{400} \frac{\bar{R}^6}{k^2} = \frac{250}{243} \pi^2 \frac{N}{k}. \quad (4.1.44)$$

The RR two-form F_2 is as in (4.1.17), while the RR four-form F_4 for this solution is given by:

$$F_4 = \frac{5}{2} k \bar{L}^2 \omega_{\text{Vol}(AdS_4)} = \frac{25 \pi}{18} \sqrt{\frac{10}{3}} \left(k N \right)^{\frac{1}{2}} \omega_{\text{Vol}(AdS_4)}, \quad (4.1.45)$$

and the dilaton is

$$e^\Phi = 2\sqrt{\pi} \left(\frac{2}{15} \frac{N}{k^5} \right)^{\frac{1}{4}}. \quad (4.1.46)$$

4.2 Deforming the ABJM background

We now analyze a generalization of the ABJM background obtained by performing a certain deformation of the metric which preserves some amount of supersymmetry. In general, the reduction will be from $\mathcal{N} = 6$ superconformal symmetry to $\mathcal{N} = 1$ supersymmetry in three dimensions (two supercharges). The interest of this deformation is that it will allow to accommodate the backreaction of the flavor branes when we introduce them later in section 4.3.

We shall consider a ten-dimensional string frame metric of the form:

$$ds_{10}^2 = h^{-\frac{1}{2}} dx_{1,2}^2 + h^{\frac{1}{2}} ds_7^2, \quad (4.2.1)$$

where h is a warp factor and ds_7^2 is a seven-dimensional metric containing an \mathbb{S}^2 fibered over an \mathbb{S}^4 in the same way as in the \mathbb{CP}^3 metric (4.1.14), namely:

$$ds_7^2 = dr^2 + e^{2f} ds_{\mathbb{S}^4}^2 + e^{2g} \left((E^1)^2 + (E^2)^2 \right), \quad (4.2.2)$$

with h , f and g being functions of the radial variable r . We choose the following vielbein:

$$\begin{aligned} e^\mu &= h^{-\frac{1}{4}} dx^\mu, \quad (\mu = 0, 1, 2), & e^3 &= h^{\frac{1}{4}} dr, & e^4 &= h^{\frac{1}{4}} e^f \mathcal{S}^\xi, \\ e^5 &= h^{\frac{1}{4}} e^f \mathcal{S}^1, & e^6 &= h^{\frac{1}{4}} e^f \mathcal{S}^2, & e^7 &= h^{\frac{1}{4}} e^f \mathcal{S}^3, \\ e^8 &= h^{\frac{1}{4}} e^g E^1, & e^9 &= h^{\frac{1}{4}} e^g E^2. \end{aligned} \quad (4.2.3)$$

Notice that f and g determine the sizes of the \mathbb{S}^4 and \mathbb{S}^2 of the internal \mathbb{CP}^3 manifold. If $f \neq g$ we say that the \mathbb{CP}^3 is *squashed*. We verify below that this squashing is compatible with supersymmetry when the functions of the ansatz satisfy certain first-order BPS equations.

The background is completed with a dilaton $\Phi = \Phi(r)$, and some fluxes. The type IIA supergravity solutions we are looking for are endowed with a RR two-form F_2 , for which we adopt the same ansatz as in (4.1.17). In addition, as it is always the case for the solutions associated to D2-branes, there is a RR four-form F_4 given by:

$$F_4 = K(r) dx^3 \wedge dr, \quad (4.2.4)$$

where $K(r)$ is a function of the radial coordinate r . Notice that the Bianchi identities $dF_2 = dF_4 = 0$ are automatically satisfied. Moreover, the Hodge dual of F_4 is equal to:

$$*F_4 = -K h^2 e^{4f+2g} \omega_{\text{Vol}(\mathbb{S}^4)} \wedge E^1 \wedge E^2, \quad (4.2.5)$$

and, thus, the equation of motion of the four-form F_4 (namely $d * F_4 = 0$), leads to:

$$K h^2 e^{4f+2g} = \text{constant} =: \beta \quad \implies \quad K = \beta h^{-2} e^{-4f-2g}. \quad (4.2.6)$$

The constant β should be determined from a quantization condition for F_4 :

$$\frac{1}{2\kappa_{10}^2} \int_{M_6} *F_4 = \pm N T_{\text{D2}}, \quad (4.2.7)$$

where M_6 is the six-dimensional angular manifold enclosing the D2-brane. Using our ansatz this quantization condition is converted into:

$$\frac{1}{2\kappa_{10}^2 T_{\text{D2}}} \int_{M_6} *F_4 = -\frac{1}{(2\pi)^5} \int_{M_6} K h^2 e^{4f+2g} \omega_{\text{Vol}(\mathbb{S}^4)} \wedge \omega_{\text{Vol}(\mathbb{S}^2)} = -\frac{\beta}{3\pi^2}. \quad (4.2.8)$$

Therefore, the coefficient β should be related to the number of D2-branes as:

$$\beta = 3\pi^2 N \quad \implies \quad K = 3\pi^2 N h^{-2} e^{-4f-2g}. \quad (4.2.9)$$

4.2.1 Supersymmetry analysis

We will determine the functions entering our ansatz by requiring that our background preserves (at least) two supersymmetries. This requirement can be expressed compactly in the language of generalized calibrations. We impose the following projections on the Killing spinors (recall our frame basis (4.2.3)):

$$\Gamma_{47} \epsilon = \Gamma_{56} \epsilon = \Gamma_{89} \epsilon, \quad \Gamma_{012} \epsilon = -\epsilon, \quad \Gamma_{3458} \epsilon = -\epsilon. \quad (4.2.10)$$

Then the BPS system can be written in terms of two calibration forms: a three-form $\tilde{\mathcal{K}}$ (natural for a background D2-branes) and a seven-form \mathcal{K} (natural for accommodating D6-branes) defined as:

$$\mathcal{K} = \frac{1}{7!} \mathcal{K}_{a_0 \dots a_6} e^{a_0 \dots a_6}, \quad \tilde{\mathcal{K}} = \frac{1}{3!} \tilde{\mathcal{K}}_{a_0 a_1 a_2} e^{a_0 a_1 a_2}, \quad (4.2.11)$$

where the components are fermionic bilinears:

$$\mathcal{K}_{a_0 \dots a_6} = e^{\frac{\Phi}{3}} h^{\frac{1}{4}} \epsilon^\dagger \Gamma_{a_0 \dots a_6} \epsilon, \quad \tilde{\mathcal{K}}_{a_0 a_1 a_2} = e^{\frac{\Phi}{3}} h^{\frac{1}{4}} \epsilon^\dagger \Gamma_{a_0 a_1 a_2} \epsilon, \quad (4.2.12)$$

with ϵ being a Killing spinor of the background, and the prefactor in (4.2.12) is included to account for the proper normalization of ϵ (see (4.A.23)). Using the projections satisfied by ϵ , one can verify that \mathcal{K} and $\tilde{\mathcal{K}}$ are given by:

$$\mathcal{K} = -e^{012} \wedge (e^{3458} - e^{3469} + e^{3579} + e^{3678} + e^{4567} + e^{4789} + e^{5689}), \quad (4.2.13)$$

$$\tilde{\mathcal{K}} = e^{012}. \quad (4.2.14)$$

The BPS equations read:

$$*F_2 = -d(e^{-\Phi} \mathcal{K}), \quad d(e^{-\Phi} h^{-\frac{1}{2}} * \mathcal{K}) = 0, \quad F_4 = -d(e^{-\Phi} \tilde{\mathcal{K}}). \quad (4.2.15)$$

These equations are fulfilled if the dilaton Φ , the warp factor h and the functions f and g satisfy the following system of first-order BPS equations:

$$\begin{aligned} \Phi' &= -\frac{3k}{8} e^\Phi h^{-\frac{1}{4}} (e^{-2g} - 2e^{-2f}) - \frac{e^\Phi}{4} K h^{\frac{3}{4}}, \\ h' &= \frac{k}{2} e^\Phi h^{\frac{3}{4}} (e^{-2g} + 2e^{-2f}) - e^\Phi K h^{\frac{7}{4}}, \\ f' &= \frac{k}{4} h^{-\frac{1}{4}} e^\Phi [e^{-2f} + e^{-2g}] + e^{-2f+g}, \\ g' &= \frac{k}{2} e^\Phi h^{-\frac{1}{4}} e^{-2f} + e^{-g} - e^{-2f+g}. \end{aligned} \quad (4.2.16)$$

In the first two equations of the system (4.2.16) the function K should be understood as given by (4.2.9). In appendix 4.A, we have verified that imposing supersymmetry through the method of supersymmetry variations also leads to the BPS system (4.2.16).

Partial integration

Let us now carry out some simple manipulations of the BPS system (4.2.16), which will allow us to perform a partial integration. First of all, let us define the function Λ as follows:

$$e^\Lambda := e^\Phi h^{-\frac{1}{4}}. \quad (4.2.17)$$

One can easily see that Λ , f and g close the following system of first-order differential equations:

$$\begin{aligned} \Lambda' &= k e^{\Lambda-2f} - \frac{k}{2} e^{\Lambda-2g}, \\ f' &= \frac{k}{4} e^{\Lambda-2f} - \frac{k}{4} e^{\Lambda-2g} + e^{-2f+g}, \\ g' &= \frac{k}{2} e^{\Lambda-2f} + e^{-g} - e^{-2f+g}. \end{aligned} \quad (4.2.18)$$

Notice that the function K has disappeared from the system (4.2.18) and that Φ and h only appear through the combination Λ . One can recover K as:

$$K = \frac{d}{dr} \left(e^{-\Phi} h^{-\frac{3}{4}} \right), \quad (4.2.19)$$

and the warp factor h through

$$h' + h \Lambda' = -3\pi^2 N e^{\Lambda-4f-2g}, \quad (4.2.20)$$

that can be solved by the method of variation of constants, giving:

$$h(r) = e^{-\Lambda(r)} \left[\alpha - 3\pi^2 N \int^r dz e^{2\Lambda(z)-4f(z)-2g(z)} \right], \quad (4.2.21)$$

where α is a constant of integration that should be adjusted appropriately. We have not been able to integrate the BPS system (4.2.18) in general. However, we have found some important particular solutions which we discuss in the next two subsections. In the solutions of the first subsection the supersymmetry is enhanced with respect to the two supersymmetries preserved by the generic solution of (4.2.18).

4.2.2 Anti-de-Sitter solutions

We are mostly interested in backgrounds with the Anti-de-Sitter geometry and in their corresponding deformations. In order to find these solutions systematically, let us now introduce a new radial variable τ , related to r as follows:

$$e^f \frac{d}{dr} = \frac{d}{d\tau}. \quad (4.2.22)$$

If the dot denotes derivative with respect to τ , the system of equations (4.2.18) reduces to:

$$\begin{aligned} \dot{\Lambda} &= k e^{\Lambda-f} - \frac{k}{2} e^{\Lambda+f-2g}, \\ \dot{f} &= \frac{k}{4} e^{\Lambda-f} - \frac{k}{4} e^{\Lambda+f-2g} + e^{-f+g}, \\ \dot{g} &= \frac{k}{2} e^{\Lambda-f} + e^{f-g} - e^{-f+g}. \end{aligned} \quad (4.2.23)$$

Let us next define the following combination of functions:

$$\Sigma := \Lambda - f, \quad \Delta := f - g. \quad (4.2.24)$$

Notice that Δ measures the squashing of the \mathbb{S}^4 and \mathbb{S}^2 internal directions. Actually, the right-hand-side of the equations in (4.2.23) depends only on Σ and Δ and it is straightforward to find the following system of two equations involving Σ and Δ :

$$\begin{aligned} \dot{\Sigma} &= \frac{k}{4} e^{\Sigma} (3 - e^{2\Delta}) - e^{-\Delta}, \\ \dot{\Delta} &= -\frac{k}{4} e^{\Sigma} (1 + e^{2\Delta}) - e^{\Delta} + 2e^{-\Delta}. \end{aligned} \quad (4.2.25)$$

One can take Σ , Δ and (say) g as independent functions. In fact, g can be obtained by simple integration once Σ and Δ are known, due to the equation:

$$\dot{g} = \frac{k}{2} e^{\Sigma} + e^{\Delta} - e^{-\Delta}. \quad (4.2.26)$$

We have thus reduced the full BPS system to a set of two coupled differential equations for the functions Σ and Δ .

Let us now obtain some particular solutions of (4.2.26) in which the squashing factor Δ is constant, as expected for an AdS background. It follows from the second equation in (4.2.25) that, in this case, Σ must be also constant. Actually, we can eliminate Σ from the equations $\dot{\Sigma} = \dot{\Delta} = 0$ and get a simple algebraic equation for Δ . In order to express this equation in simple terms, let us define the quantity q as:

$$q := e^{2\Delta} = e^{2f-2g}. \quad (4.2.27)$$

Then, $\dot{\Sigma} = \dot{\Delta} = 0$ implies the following quadratic equation for q :

$$q^2 - 6q + 5 = 0, \quad (4.2.28)$$

which has two solutions, namely:

$$q = 1, \quad q = 5. \quad (4.2.29)$$

Notice that $q = 1$ corresponds⁴ to the $\mathcal{N} = 6$ ABJM background, while $q = 5$ describes the Ooguri-Park solution of reduced supersymmetry that we discussed in section 4.1.3.

⁴One can easily check that $q = e^{2\Delta} = 1$ leads to $e^{\Sigma} = \frac{2}{k}$. Going back to the original variables one gets $e^f = e^g = r$, $h = \frac{2\pi^2 N}{k} \frac{1}{r^4}$, $K = \frac{3k^2}{4\pi^2 N} r^2$. Rescaling the Minkowski coordinates as $x^\mu \rightarrow \pi \sqrt{\frac{N}{2k}} x^\mu$, one can verify that, indeed, the metric and RR four-form for this solution coincide with the ones in (4.1.2) and (4.1.6). One can proceed similarly for the $q = 5$ solution, but in this case one must take $k \rightarrow -k$ to recover the expressions of section 4.1.3.

4.2.3 Running solutions

Anti-de-Sitter solutions are dual to conformal field theories, and therefore they represent the fixed points of the RG flow. In the previous subsection, we have found that our deformation admits two Anti-de-Sitter solutions, with the fixed points being the ABJM theory and the Ooguri-Park theory. A natural question to ask is whether we can find solutions dual to non-trivial RG flows. In what follows, we give a positive answer to this question, by finding a family of solutions that flow in the IR to the ABJM theory, and another family of different solutions that flow in the UV to the Ooguri-Park theory. It would be very interesting to see whether one can find an interpolating solution connecting these two flows.

An IR fixed point

Instead of trying to solve analytically the BPS system (4.2.18), we can also solve it in a power series expansion in the radial coordinate r . The aim is to find new solutions that approach the $AdS_4 \times \mathbb{CP}^3$ background in the IR limit $r \rightarrow 0$. We begin by rewriting the system (4.2.18) in a more convenient form. Let us define the new function F as:

$$F = \frac{k}{2} e^\Lambda. \quad (4.2.30)$$

Then, one can recast (4.2.18) as:

$$\begin{aligned} F' &= F^2 (2e^{-2f} - e^{-2g}), \\ (e^f)' &= \frac{F}{2} (e^{-f} - e^{f-2g}) + e^{g-f}, \\ (e^g)' &= F e^{g-2f} + 1 - e^{2g-2f}. \end{aligned} \quad (4.2.31)$$

The $\mathcal{N} = 6$ ABJM solution (without squashing) can be simply written as $F = e^f = e^g = r$. To solve (4.2.31) in a series expansion in powers of r , we propose that the solution looks like:

$$F = r[1 + a_1 r + a_2 r^2 + \dots], \quad e^f = r[1 + b_1 r + b_2 r^2 + \dots], \quad e^g = r[1 + c_1 r + c_2 r^2 + \dots]. \quad (4.2.32)$$

By substituting this ansatz on the system (4.2.31) and solving for the different powers of r up to third order, one can find the following solution:

$$\begin{aligned} F &= r [1 + 3c r + 8c^2 r^2 + 20c^3 r^3 + \dots], \\ e^f &= r \left[1 + \frac{c}{2} r + \frac{7}{8} c^2 r^2 + \frac{25}{16} c^3 r^3 + \dots \right], \\ e^g &= r [1 + c r + 2c^2 r^2 + 4c^3 r^3 + \dots], \end{aligned} \quad (4.2.33)$$

where c is an arbitrary constant (if $c = 0$ we come back to the $AdS_4 \times \mathbb{CP}^3$ solution). Plugging the expansions (4.2.33) into the right-hand side of (4.2.21) and adjusting the integration constants in such a way that h vanishes at $r = \infty$, one gets the following expression of the warp factor h :

$$h = \frac{2\pi^2 N}{k} \left[\frac{1}{r^4} + \frac{c^2}{r^2} - \frac{23c^3 + 12c^3 \log(r)}{r} + \dots \right]. \quad (4.2.34)$$

Similarly, the dilaton runs as:

$$e^\Phi = 2\sqrt{\pi} \left(\frac{2N}{k^5} \right)^{\frac{1}{4}} \left[1 + 3c r + \frac{33c^2 r^2}{4} + 3c^3 \left(5 - \log(r) \right) r^3 + \dots \right], \quad (4.2.35)$$

whereas the function K is given by:

$$K = \frac{3k^2}{4\pi^2 N} r^2 \left(1 - 4c r + 2c^3 (29 + 12 \log(r)) r^3 + \dots \right). \quad (4.2.36)$$

Notice that when the constant c is non-vanishing, the geometry is not Anti-de-Sitter and the internal space is squashed by an r -dependent function.

An UV fixed point

Let us see that there exists a consistent truncation of the reduced unflavored BPS system (4.2.25) that allows to find other non-trivial analytic solutions. In these truncations Σ and Δ are related as:

$$e^\Sigma = A e^{-\Delta}, \quad (4.2.37)$$

with A being a constant. To have a natural interpretation of this truncation, let us look at the metric obtained after uplifting to eleven dimensions. This metric is given by (4.1.29). For our explicit ansatz (4.2.1)-(4.2.2) the uplifted eleven-dimensional metric has the form:

$$\begin{aligned} ds_{11}^2 = & e^{-\frac{2\Phi}{3}} h^{-\frac{1}{2}} dx_{1,2}^2 + e^{-\frac{2\Phi}{3}} h^{\frac{1}{2}} dr^2 + e^{-\frac{2\Phi}{3}} h^{\frac{1}{2}} e^{2f} ds_{\mathbb{S}^4}^2 + \\ & + e^{-\frac{2\Phi}{3}} h^{\frac{1}{2}} e^{2g} \left((E^1)^2 + (E^2)^2 \right) + e^{\frac{4\Phi}{3}} (dx_{11} - A_1)^2. \end{aligned} \quad (4.2.38)$$

Notice that the relative coefficient between the $U(1)$ fiber and the E^1, E^2 parts of ds_{11}^2 (the last two terms in (4.2.38)) is given by $e^{2\Phi} h^{-\frac{1}{2}} e^{-2g} = e^{2\Sigma+2\Delta}$, which is constant if the truncation condition (4.2.37) holds. Therefore, when (4.2.37) is satisfied these two parts of the metric can give rise to the metric of a three-sphere.

Substituting the relation (4.2.37) on the right-hand side of the system (4.2.25), we get the following two equations:

$$\begin{aligned} \dot{\Sigma} &= \left(\frac{3kA}{4} - 1 \right) e^{-\Delta} - \frac{kA}{4} e^\Delta, \\ \dot{\Delta} &= \left(2 - \frac{kA}{4} \right) e^{-\Delta} - \left(1 + \frac{kA}{4} \right) e^\Delta. \end{aligned} \quad (4.2.39)$$

The truncation condition (4.2.37) implies that $\dot{\Sigma} = -\dot{\Delta}$ which in turn leads to:

$$\left(\frac{kA}{2} + 1 \right) \left(e^{-\Delta} - e^\Delta \right) = 0, \quad (4.2.40)$$

There are two possible ways to solve (4.2.40). The first one is by imposing that $e^\Delta = e^{-\Delta}$, which would lead to $e^{2\Delta} = 1$, *i.e.* $\Delta = 0$, that corresponds to the ABJM solution. The other possibility to solve (4.2.40) consists in taking $kA = -2$, namely:

$$A = -\frac{2}{k}, \quad (4.2.41)$$

which implies that

$$e^\Sigma = -\frac{2}{k} e^{-\Delta}. \quad (4.2.42)$$

Notice that k must be negative in this case. In this solution the squashing can vary with the radial coordinate. To continue with the analysis of this case it is much more convenient to come back to the original system (4.2.18) in terms of the radial variable r and the functions Λ , f and g . Actually, from the definitions of Σ and Δ , the truncation (4.2.42) is equivalent to:

$$e^\Lambda = -\frac{2}{k} e^g. \quad (4.2.43)$$

After using (4.2.43), the equations for f and g in (4.2.18) become:

$$\begin{aligned} f' &= \frac{1}{2} e^{g-2f} + \frac{1}{2} e^{-g}, \\ g' &= -2 e^{g-2f} + e^{-g}. \end{aligned} \quad (4.2.44)$$

This can be immediately integrated to give the following solution for f and g :

$$e^{2f} = \frac{9}{5} \rho^2 \left[1 - \left(\frac{\mu}{\rho} \right)^{\frac{5}{3}} \right], \quad e^{2g} = \frac{9}{25} \rho^2 \left[1 - \left(\frac{\mu}{\rho} \right)^{\frac{5}{3}} \right]^2, \quad (4.2.45)$$

where μ is a constant, and the new radial variable ρ is just a shift of the old one: $\rho = r + \text{constant}$. The squashing corresponding to this solution is:

$$e^{2\Delta} = \frac{5}{1 - \left(\frac{\mu}{\rho} \right)^{\frac{5}{3}}}, \quad (4.2.46)$$

which varies with the radial coordinate except when the constant μ is chosen to vanish. In this last case one gets the Ooguri-Park gravity dual. Taking into account that for this solution, one has

$$e^\Lambda = \frac{6}{5|k|} \rho \left(1 - \left(\frac{\mu}{\rho} \right)^{\frac{5}{3}} \right), \quad (4.2.47)$$

the warp factor h will be:

$$h(\rho) = -\frac{27}{400} \frac{\bar{R}^6}{k^2} \frac{1}{\rho \left(1 - \left(\frac{\mu}{\rho} \right)^{\frac{5}{3}} \right)} \int_{\rho_0}^{\rho} \frac{d\xi}{\xi^4 \left(1 - \left(\frac{\mu}{\xi} \right)^{\frac{5}{3}} \right)}, \quad (4.2.48)$$

where ρ_0 is a constant that should be determined. The dilaton ϕ for this solution can be obtained simply from the relation $e^\Phi = e^\Lambda h^{\frac{1}{4}}$, which follows from the definition of Λ in (4.2.17). Similarly, the function K which parametrizes the RR four-form F_4 can be obtained from (4.2.6). The UV fixed point of this one-parameter family of solutions, attained as $\rho \rightarrow \infty$, is the Ooguri-Park theory.

4.3 Adding flavors

We want to study now the holographic dual of the ABJM theory with unquenched flavor. For this, we use the tools described in section 3.3.1. So we study the backreaction induced by a smeared continuous distribution of a large number N_f of flavor branes. As we said at the beginning of the chapter, the ABJM theory remains conformally invariant after the addition of flavor. We then expect the presence of an AdS_4 factor in the backreacted metric.

An important point to notice is that, *contrary to the majority of the cases, a gravity solution for the case where the flavor branes are localized and coincident is known!* For a stack D6-branes, the corresponding gravity dual in M-theory is a purely geometric background which, in the near horizon limit, is a space of the type $AdS_4 \times \mathcal{M}_7$, where \mathcal{M}_7 is a tri-Sasakian seven-dimensional manifold whose cone is an eight-dimensional hyperKähler manifold [146]. This is quite impressive, but unfortunately the tri-Sasakian metric of \mathcal{M}_7 has, in general, a very complicated structure which makes it difficult to use it for many purposes. For this reason, it would be still very nice to look for a simpler solution accounting for the presence of fundamental matter. The smearing technique is ideal for this.

Recall that when the branes are smeared, they are not coincident anymore and, therefore, the flavor symmetry for N_f flavors is $U(1)^{N_f}$ rather than $U(N_f)$. Moreover, the solutions with smeared unquenched flavor are generically less supersymmetric than the ones with localized flavor, due to the fact that we are superposing branes with different orientations in the internal space. Indeed, in our flavored ABJM case the solutions will be $\mathcal{N} = 1$ supersymmetric instead of being $\mathcal{N} = 3$ (as the localized ones).

What we will find in this section is that the backreaction of the flavor branes induces a deformation of the unquenched solution which, in particular, results in a suitable squashing of the metric. In order to determine precisely this flavor deformation one has to write the metric in a way such that it can be squashed without breaking all supersymmetry. We argue below that for the ABJM case in the type IIA description the convenient way of writing the \mathbb{CP}^3 metric is as S^2 -bundle over S^4 .

The three steps we have to follow to implement the smearing technique are:

1. Write an ansatz for the geometry that can accommodate the backreaction of the flavor branes. We have already taken care of this in section 4.2.
2. Find supersymmetric embeddings for flavor branes in the geometry above.
3. Write a good ansatz for the smearing form Ξ , and compute it with our favorite method.

The flavor deformation will just amount to squashing the S^2 fiber with respect to the S^4 base, as well as to changing the radii of both AdS_4 and \mathbb{CP}^3 factors of the metric.

Since the first point is solved, let us move to the second one and study where the flavor D6-branes can be placed preserving some supersymmetry.

4.3.1 Supersymmetric embeddings of flavor D6-branes

In this subsection we study the addition of flavor D6-branes to a background of the type studied in section 4.2. We analyze certain configurations in which the D6-branes preserve

some amount of supersymmetry of the background. We work in the probe approximation, corresponding to having quenched quarks on the field theory side, in which the background supergravity solution is not affected by the presence of the flavor D6-branes. The effect of the backreaction will be considered in detail in sections 4.3.2 and 4.3.4.

Generically, we consider configurations corresponding to massless quarks which extend along the three Minkowski directions x^μ , the radial coordinate r and that wrap a three-dimensional cycle of \mathbb{CP}^3 . On general grounds [136, 137] it is expected that this three-cycle of \mathbb{CP}^3 is a special Lagrangian cycle which can be identified with \mathbb{RP}^3 . Let us show how this \mathbb{RP}^3 arises in our coordinates. Recall the definition of the $\mathfrak{su}(2)$ left invariant one-forms $\bar{\omega}_i$ of the four-sphere metric (4.1.9), that we gave in (4.1.8) in terms of three angles $0 \leq \bar{\theta} \leq \pi$, $0 \leq \bar{\varphi} < 2\pi$, $0 \leq \bar{\psi} \leq 4\pi$. In order to write down a coordinate description of the D6-brane configuration, let us choose the following set of worldvolume coordinates:

$$\zeta^\alpha = (x^\mu, r, \xi, \bar{\psi}, \varphi). \quad (4.3.1)$$

In these coordinates our embedding is defined by the conditions:

$$\bar{\theta}, \bar{\varphi} = \text{constant}, \quad \theta = \frac{\pi}{2}. \quad (4.3.2)$$

Notice that ξ and $\bar{\psi}$ vary inside the \mathbb{S}^4 , whereas φ varies inside the \mathbb{S}^2 . Actually, ξ and $\bar{\psi}$ parameterize an $\mathbb{S}^2 \subset \mathbb{S}^4$, while $\theta = \frac{\pi}{2}$ is a maximal $\mathbb{S}^1 \subset \mathbb{S}^2$. The induced worldvolume metric is:

$$d\hat{s}_7^2 = h^{-\frac{1}{2}} dx_{1,2}^2 + h^{\frac{1}{2}} dr^2 + ds_3^2, \quad (4.3.3)$$

where the metric ds_3^2 of the three-cycle is given by:

$$ds_3^2 = 4 h^{\frac{1}{2}} e^{2g} \left[q \left(\frac{d\xi^2}{(1+\xi^2)^2} + \frac{\xi^2}{4(1+\xi^2)^2} d\bar{\psi}^2 \right) + \frac{1}{4} \left(d\varphi - \frac{\xi^2}{1+\xi^2} d\bar{\psi} \right)^2 \right], \quad (4.3.4)$$

with q being the squashing factor defined in (4.2.27). Let us verify that this three-dimensional metric corresponds to (a squashed) $\mathbb{RP}^3 = \mathbb{S}^3/\mathbb{Z}_2$. We first perform the following change of variable from ξ to a new angular variable α , defined as:

$$\xi = \tan\left(\frac{\alpha}{2}\right), \quad 0 \leq \alpha < \pi. \quad (4.3.5)$$

In terms of α the metric ds_3^2 becomes:

$$ds_3^2 = h^{\frac{1}{2}} e^{2g} \left[q d\alpha^2 + q \sin^2 \alpha \left(\frac{d\bar{\psi}}{2} \right)^2 + \left(d\varphi + \frac{1}{2} (\cos \alpha - 1) d\bar{\psi} \right)^2 \right]. \quad (4.3.6)$$

Let us next define new angles β and ψ as:

$$\beta := \frac{\bar{\psi}}{2}, \quad \psi := \varphi = \frac{\bar{\psi}}{2}. \quad (4.3.7)$$

Then, the metric (4.3.6) becomes:

$$ds_3^2 = h^{\frac{1}{2}} e^{2g} \left[q d\alpha^2 + q \sin^2 \alpha d\beta^2 + (d\psi + \cos \alpha d\beta)^2 \right]. \quad (4.3.8)$$

It is clear from (4.3.7) that $0 \leq \beta < 2\pi$. Moreover, by comparing the volume obtained with the metric (4.3.6) with the one obtained with (4.3.8), one concludes that $0 \leq \psi < 2\pi$ and that our three-cycle is indeed a squashed \mathbb{RP}^3 manifold inside \mathbb{CP}^3 .

Let us now verify that the cycle (4.3.2) preserves some amount of supersymmetry. First of all, let us note that the embedding ι defined by (4.3.2) can be characterized by the three differential conditions:

$$\iota^*(\mathcal{S}^1) = \iota^*(\mathcal{S})^3 = \iota^*(E^1) = 0, \quad (4.3.9)$$

which are integrable due to Frobenius theorem since $d\mathcal{S}^1 = d\mathcal{S}^3 = dE^1 = 0$ when (4.3.9) holds and $\theta = \pi/2$. From this result one can verify that the cycle is calibrated by the form \mathcal{K} for a metric given by the general form (4.2.1) and (4.2.2). Indeed, the only non-zero component of the pullback of \mathcal{K} is the one containing e^{3469} in (4.2.13) and one has:

$$\iota^*(\mathcal{K}) = \frac{2\xi}{(1+\xi^2)^2} h^{\frac{1}{4}} e^{2f+g} d^3x \wedge dr \wedge d\xi \wedge d\psi \wedge d\varphi, \quad (4.3.10)$$

which one can easily show that coincides with the volume form derived from the worldvolume metric (4.3.3), satisfying the condition (3.2.3). Therefore, the embedding defined by (4.3.2) in the geometry (4.2.1) is supersymmetric. A generalization of this embedding is easy to find for the case in which θ is not constant. If $\theta = \theta(r)$, the supersymmetric configurations are those where the following first-order BPS equation is satisfied:

$$e^g \frac{d\theta}{dr} = \cot \theta. \quad (4.3.11)$$

Notice that, indeed, the solutions of (4.3.11) with constant θ must necessarily have $\theta = \pi/2$. Moreover, one can easily show by analyzing (4.3.11) that, when θ is not constant, the radial coordinate reaches a minimal value r_* in the corresponding brane embedding. Therefore, one can interpret these D6-brane configurations with varying θ as flavor branes that add massive flavors to the Chern-Simons-matter theory. The corresponding quark mass is related to the minimal distance r_* .

In the language of section 3.3.1, we have found a representative embedding, and the whole continuous family of embeddings over which we will place the D6-branes can be generated by acting with the different isometries of the metric. We are then ready to compute explicitly the backreaction of such a smeared set of flavor branes.

4.3.2 Backreacted massless flavor

Now that we have the supersymmetric embeddings, we can place D6-branes along them. The smearing form Ξ tells us how they are distributed. To compute the smearing form, we use equation (3.3.10). In our case, we have a violation of the Bianchi identity of F_2 that reads as:

$$dF_2 = 2\pi \Xi, \quad (4.3.12)$$

where we have used the fact that, in our units, we have $2\kappa_{10}^2 T_{D6} = 2\pi$. Of course, our ansatz (4.1.17) for F_2 must be modified in order to satisfy (4.3.12). Looking at (4.1.18), it is easy to find the appropriate modification. Indeed, the two-form F_2 written in (4.1.17) is closed

because there is a precise balance between the term $E^1 \wedge E^2$ (along the fibered \mathbb{S}^2) and the two other terms with components along the \mathbb{S}^4 . Clearly, to get a non-closed two-form F_2 without distorting much the \mathbb{S}^2 - \mathbb{S}^4 structure of our ansatz, one should squash the two type of terms in (4.1.17) by means of some squashing factor η . Accordingly, we adopt the following ansatz for F_2 in this flavored case:

$$F_2 = \frac{k}{2} \left[E^1 \wedge E^2 - \eta (\mathcal{S}^\xi \wedge \mathcal{S}^3 + \mathcal{S}^1 \wedge \mathcal{S}^2) \right]. \quad (4.3.13)$$

Notice that equation (4.1.19) is still satisfied and, therefore, the constant k continues to be the Chern-Simons level of the gauge theory. In this section we consider the case of massless flavors, which corresponds to taking η constant (see section 4.3.4 for the case of massive flavors). The precise relation between η and the number of flavors can be obtained through the hybrid method described at the end of section 3.3.1.

The first thing to do is to compute Ξ . This is quickly done by computing the exterior derivative of the two-form written in (4.3.13), which yields:

$$\Xi = \frac{k}{4\pi} (1 - \eta) \left[E^1 \wedge (\mathcal{S}^\xi \wedge \mathcal{S}^2 - \mathcal{S}^1 \wedge \mathcal{S}^3) + E^2 \wedge (\mathcal{S}^\xi \wedge \mathcal{S}^1 + \mathcal{S}^2 \wedge \mathcal{S}^3) \right]. \quad (4.3.14)$$

We can remark the following interesting fact, that points to this smearing form being the correct one for a collection of flavor branes embedded as in section 4.3.1, giving rise to massless flavors. Notice that the smearing form should contain the volume element of the space transverse to the brane worldvolume. In the case of the set of embeddings (4.3.2) this space should be spanned by the three one-forms \mathcal{S}^1 , \mathcal{S}^3 and E^1 (see equation (4.3.9)). Thus, one naively expects to have a term of the type $E^1 \wedge \mathcal{S}^1 \wedge \mathcal{S}^3$ in Ξ , which is indeed contained in our ansatz (4.3.14). It is also easy to find embeddings with $E^2 = \mathcal{S}^2 = \mathcal{S}^3 = 0$, which contribute to the $E^2 \wedge \mathcal{S}^2 \wedge \mathcal{S}^3$ component of Ξ . Presumably, there are other embeddings generating the other components of the charge-density three-form written in (4.3.14).

In order to relate the squashing coefficient η to the number of flavors N_f , we use equation (3.3.21) and compare the smeared DBI action with the DBI action of a single brane. The former is given by:

$$S_{\text{DBI}}^{\text{smeared}} = -T_{\text{D6}} \int_{\mathcal{M}_{10}} e^{-\Phi} \mathcal{K} \wedge \Xi, \quad (4.3.15)$$

where we have taken into account that \mathcal{K} is a calibration form for the D6-brane worldvolume. By using the explicit expression of \mathcal{K} (equation (4.2.13)) and our ansatz for Ξ , we get:

$$\mathcal{K} \wedge \Xi = \frac{k(1 - \eta)}{\pi} h^{\frac{1}{4}} e^{2f+g} d^3x \wedge dr \wedge \omega_{\text{Vol}(\mathbb{S}^4)} \wedge \omega_{\text{Vol}(\mathbb{S}^2)}. \quad (4.3.16)$$

Integrating over \mathbb{S}^4 and \mathbb{S}^2 gives a factor $32\pi^3/3$ and we can write the smeared DBI action as:

$$S_{\text{DBI}}^{\text{smeared}} = \int d^3x dr \mathcal{L}_{\text{DBI}}^{\text{smeared}}, \quad (4.3.17)$$

where the DBI Lagrangian density of the smeared set of flavor branes is:

$$\mathcal{L}_{\text{DBI}}^{\text{smeared}} = -\frac{32\pi^2 k (1 - \eta)}{3} T_{\text{D6}} e^{-\Phi} h^{\frac{1}{4}} e^{2f+g}. \quad (4.3.18)$$

Now we compute the action of a single representative brane, which we choose to be one sitting along the embedding (4.3.2). In terms of the angular coordinates defined in (4.3.5) and (4.3.7) the DBI action for the embedding can be written as:

$$S_{\text{DBI}}^{\text{single}} = -T_{\text{D6}} \int d^3x dr d\alpha d\beta d\psi e^{-\Phi} \sqrt{-\det[\hat{g}_7]} =: \int d^3x dr \mathcal{L}_{\text{DBI}}^{\text{single}}, \quad (4.3.19)$$

where \hat{g}_7 is the induced metric written in (4.3.3) and (4.3.8). By integrating over the angular variables one easily gets the effective Lagrangian density for the representative embedding, namely:

$$\mathcal{L}_{\text{DBI}}^{\text{single}} = -8\pi^2 T_{\text{D6}} e^{-\Phi} h^{\frac{1}{4}} e^{2f+g}. \quad (4.3.20)$$

Imposing then

$$\mathcal{L}_{\text{DBI}}^{\text{smeared}} = N_f \mathcal{L}_{\text{DBI}}^{\text{single}}, \quad (4.3.21)$$

on the Lagrangian densities (4.3.18) and (4.3.20), it is straightforward to find the precise relation between the squashing factor η and the number of flavors N_f . One gets:

$$\eta = 1 + \frac{3N_f}{4k}. \quad (4.3.22)$$

Notice that η depends linearly on the deformation parameter ε , defined as:

$$\varepsilon := \frac{N_f}{k}. \quad (4.3.23)$$

Indeed, it follows from (4.3.22) that $\eta = 1 + 3\varepsilon/4$. Interestingly, ε can be rewritten in terms of gauge theory quantities as:

$$\varepsilon = \frac{N_f}{N} \lambda, \quad (4.3.24)$$

where $\lambda = N/k$ is the 't Hooft coupling of the Chern-Simons-matter theory. As we will show below, the deformations of the metric, dilaton and RR four-form will also depend on ε , similarly to what happens in other flavored backgrounds such as the D3-D7 system (see [109] for a review and further references).

Flavored BPS system

We are now in the position of addressing the central problem of this section, namely finding the backgrounds dual to Chern-Simons-matter theories with flavors. We adopt an ansatz for the metric as the one written in (4.2.1) and (4.2.2), in which the line element is parameterized by a warp factor h and two squashing functions f and g . Moreover, the RR four-form F_4 will depend on the function K as in (4.2.4), while F_2 will be given by (4.3.13). By imposing on the Killing spinors the projection conditions (4.2.10), one can find a system of first-order BPS equations for the different functions of the ansatz. Actually, these BPS equations imposed by supersymmetry are readily obtained from (4.2.16) by performing the substitution:

$$k e^{-2f} \rightarrow k \eta e^{-2f}. \quad (4.3.25)$$

In this way, one gets:

$$\begin{aligned}
\Phi' &= -\frac{3k}{8} e^\Phi h^{-\frac{1}{4}} (e^{-2g} - 2\eta e^{-2f}) - \frac{e^\Phi}{4} K h^{\frac{3}{4}}, \\
h' &= \frac{k}{2} e^\Phi h^{\frac{3}{4}} (e^{-2g} - 2\eta e^{-2f}) - e^\Phi K h^{\frac{7}{4}}, \\
f' &= \frac{k}{4} h^{-\frac{1}{4}} e^\Phi (\eta e^{-2f} - e^{-2g}) + e^{-2f+g}, \\
g' &= \frac{k}{2} e^\Phi h^{-\frac{1}{4}} \eta e^{-2f} + e^{-g} - e^{-2f+g}.
\end{aligned} \tag{4.3.26}$$

The fulfillment of the system (4.3.26) guarantees the preservation of two supercharges, which corresponds to $\mathcal{N} = 1$ supersymmetry in three dimensions. Moreover, one can show that the BPS system can be rewritten as in (4.2.15), in terms of the calibration forms \mathcal{K} and $\tilde{\mathcal{K}}$, which are written in (4.2.13) and (4.2.14) in the frame basis.

The system (4.3.26) is very similar to the unflavored one in (4.2.16). Therefore, we can follow the same procedure as in section 4.2 to perform a partial integration of the system of differential equations and to find some of its particular solutions. With the same definitions we made there, one arrives to

$$\begin{aligned}
\dot{\Sigma} &= \frac{k}{4} e^\Sigma (3\eta - e^{2\Delta}) - e^{-\Delta}, \\
\dot{\Delta} &= -\frac{k}{4} e^\Sigma (\eta + e^{2\Delta}) - e^\Delta + 2e^{-\Delta}.
\end{aligned} \tag{4.3.27}$$

Equations (4.2.19), (4.2.9) and (4.2.20) still hold. The system (4.3.27) admits a particular solution which leads to the Anti-de-Sitter geometry in this flavored case. We study it in the next subsection.

4.3.3 Flavored Anti-de-Sitter solutions

In close analogy with the study carried out in section 4.2.2, let us consider solutions of the reduced system (4.3.27) in which the functions Σ and Δ are constant. Notice that, according to the definition in (4.2.27), constant Δ implies that the squashing parameter $q = e^{2\Delta}$ is also constant. Actually, by imposing $\dot{\Sigma} = \dot{\Delta} = 0$ in (4.3.27) one can straightforwardly prove that q must satisfy the following quadratic equation:

$$q^2 - 3(1 + \eta)q + 5\eta = 0, \tag{4.3.28}$$

which reduces to (4.2.28) when $\eta = 1$. The relation (4.3.28) can be regarded as the relation between the deformation η of the RR two-form and the internal deformation of the \mathbb{CP}^3 metric, parameterized by the squashing factor q . Both parameters are related to the number of flavors or, to be more precise, to the deformation parameter ε defined in (4.3.23). Actually, by solving (4.3.28) as a quadratic equation in q , one gets:

$$q = \frac{3(1 + \eta) \pm \sqrt{9\eta^2 - 2\eta + 9}}{2}. \tag{4.3.29}$$

By using (4.3.22) one can obtain the squashing factor q in terms of N_f and k , namely:

$$q = 3 + \frac{9}{8} \frac{N_f}{k} \pm 2 \sqrt{1 + \frac{3}{4} \frac{N_f}{k} + \left(\frac{3}{4}\right)^4 \left(\frac{N_f}{k}\right)^2}. \quad (4.3.30)$$

The two signs in (4.3.29) give rise to the two possible branches. The minus sign in (4.3.29) corresponds to the flavored ABJM model (it reduces to $q = 1$ when $\eta = 1$), while the plus sign corresponds to the Ooguri-Park model discussed in 4.1.3. Notice that the discriminant in (4.3.29) is never negative and, therefore, the parameter η can be arbitrary. Actually, when $\eta \rightarrow \infty$ one has the following behavior in the two branches:

$$\lim_{\eta \rightarrow \infty} q = \begin{cases} 5/3, & \text{for the } - \text{ branch,} \\ \infty, & \text{for the } + \text{ branch.} \end{cases} \quad (4.3.31)$$

Similarly, one can compute the squashing factor for the case in which N_f is small. At second order in N_f/k , one gets:

$$q \approx \begin{cases} 1 + \frac{3}{8} \frac{N_f}{k} - \frac{45}{256} \left(\frac{N_f}{k}\right)^2, & \text{for the } - \text{ branch,} \\ 5 + \frac{15}{8} \frac{N_f}{k} + \frac{45}{256} \left(\frac{N_f}{k}\right)^2, & \text{for the } + \text{ branch.} \end{cases} \quad (4.3.32)$$

It is interesting to point out that, in the two branches in (4.3.30), the squashing factor q takes values in ranges that are disjoint. In the flavored ABJM case $1 \leq q \leq 5/3$, whereas $q \geq 5$ in the other branch. In what follows we restrict ourselves to the ABJM model with flavor and thus q should be understood as the right-hand-side of (4.3.30) with the minus sign. Let us write the complete supergravity solution in this case. First of all, it follows from the system (4.3.27) that Σ is given by:

$$\frac{k}{2} e^\Sigma = \frac{2}{\sqrt{q}} \frac{2-q}{\eta+q}. \quad (4.3.33)$$

Moreover, the equation for g in (4.3.26) can be rewritten as:

$$\frac{d}{dr} (e^g) = \frac{1}{\sqrt{q}} \left[\frac{k\eta}{2} e^\Sigma + \sqrt{q} - \frac{1}{\sqrt{q}} \right]. \quad (4.3.34)$$

Since the right-hand side of (4.3.34) is constant, it follows that e^g is a linear function of r . Actually, by making use of (4.3.33) one can prove that g and f can be written as:

$$e^g = \frac{r}{b}, \quad e^f = \frac{\sqrt{q}}{b} r, \quad (4.3.35)$$

with the coefficient b being given in terms of the squashing parameters η and q by:

$$b = \frac{q(\eta+q)}{2(q+\eta q-\eta)}. \quad (4.3.36)$$

Let us next compute the warp factor h by using the general expression (4.2.21). A glance at the right-hand side of (4.2.21) reveals that we have to compute the function Λ first. However,

it follows from the definition (4.2.24) that $e^\Lambda = e^\Sigma e^f$ and, therefore, we can obtain e^Λ from (4.3.33) and (4.3.35). One gets:

$$e^\Lambda = \frac{8}{k} \frac{2-q}{q(\eta+q)^2} [q + \eta q - \eta] r. \quad (4.3.37)$$

Taking into account this result, we can write the warp factor h as:

$$h = \frac{\beta}{24k} \frac{q^3 (\eta+q)^4 (2-q)}{(q + \eta q - \eta)^5} \frac{1}{r^4}, \quad (4.3.38)$$

where we have adjusted the integration constant in (4.2.21) by requiring that h vanishes at $r \rightarrow \infty$. Notice that, as $h \sim r^{-4}$, this solution does indeed lead to an Anti-de-Sitter metric. Actually, the AdS_4 radius L is related to the warp factor h as:

$$L^4 = r^4 h. \quad (4.3.39)$$

From (4.3.38) we can extract the expression of L , which can be written as:

$$L^4 = 2\pi^2 \frac{N}{k} \frac{(2-q)b^4}{q(q + \eta q - \eta)}. \quad (4.3.40)$$

Using these results we can represent the ten-dimensional metric for this solution as:

$$ds^2 = L^2 ds_{AdS_4}^2 + \frac{L^2}{b^2} \left(q ds_{\mathbb{S}^4}^2 + (E^1)^2 + (E^2)^2 \right). \quad (4.3.41)$$

In order to write the AdS_4 part of the metric as in (4.1.3) we have to rescale the Minkowski coordinates as $x^\mu \rightarrow L^2 x^\mu$, where L is the same as in (4.3.40). From (4.3.41) the interpretation of the parameter b is rather clear: it represents the relative squashing, due to the flavor, of the \mathbb{CP}^3 part of the metric with respect to the AdS_4 part. It is also interesting to rewrite the metric (4.3.41) in terms of the variables used in (4.1.9). One has:

$$ds^2 = L^2 ds_{AdS_4}^2 + ds_6^2, \quad (4.3.42)$$

where ds_6^2 is the metric of the deformed internal six-dimensional manifold, written in terms of the $\mathfrak{su}(2)$ instanton on the four-sphere, as:

$$ds_6^2 = \frac{L^2}{b^2} \left[q ds_{\mathbb{S}^4}^2 + (dx^i + \epsilon^{ijk} A^j x^k)^2 \right]. \quad (4.3.43)$$

Let us now obtain the remaining non-vanishing fields for this solution. First of all, the constant dilaton can be found by using (4.2.17). One gets:

$$e^\Phi = \frac{4\sqrt{\pi}}{\eta+q} \frac{(2-q)^{\frac{5}{4}}}{[q(q + \eta q - \eta)]^{\frac{1}{4}}} \left(\frac{2N}{k^5} \right)^{\frac{1}{4}}. \quad (4.3.44)$$

This expression can be rewritten in a more compact form as:

$$e^{-\Phi} = \frac{b}{4} \frac{\eta+q}{2-q} \frac{k}{L}. \quad (4.3.45)$$

Finally, let us write the four-form F_4 for these solutions. After rescaling the Minkowski coordinates as before, we can write F_4 as proportional to the volume element $\omega_{\text{Vol}(AdS_4)}$ of AdS_4 , namely:

$$F_4 = \frac{L^6 K}{r^2} \omega_{\text{Vol}(AdS_4)} . \quad (4.3.46)$$

The function K was written in (4.2.6) in terms of h , f and g . Taking into account that $e^{2f} = q e^{2g}$ and the relation (4.3.39), one can rewrite F_4 as:

$$F_4 = \frac{\beta}{q^2} \frac{r^6 e^{-6g}}{L^2} \omega_{\text{Vol}(AdS_4)} . \quad (4.3.47)$$

Using the expressions of g and L in (4.3.35) and (4.3.40) and the one for β written in (4.2.9), we arrive at:

$$F_4 = \frac{3\pi}{16\sqrt{2}} \frac{q^{\frac{5}{2}} (\eta + q)^4}{(q + \eta q - \eta)^{\frac{7}{2}} \sqrt{2 - q}} \sqrt{k N} \omega_{\text{Vol}(AdS_4)} . \quad (4.3.48)$$

We can rewrite this result more compactly as:

$$F_4 = \frac{3k}{4} \frac{(\eta + q)b}{2 - q} L^2 \omega_{\text{Vol}(AdS_4)} . \quad (4.3.49)$$

Eqs. (4.3.42) and (4.3.43) are the flavored generalization of the ABJM metric written in (4.1.2) and (4.1.7). Notice that the radius L is not the same in both cases (compare (4.1.4) and (4.3.40)) and, in addition, the flavored metric is deformed by the parameters b and q . The RR two-form F_2 for the flavored solution was written in (4.3.13) (it was our starting point) and, together with the F_4 written in (4.3.48), generalize (4.1.6). Finally, the constant dilaton also gets corrected by the effect of the matter fields, as one can see by comparing equations (4.3.44) and (4.1.5).

Critical analysis of the approximations made

Let us finish this section by discussing the regime of validity of our supergravity dual. On general grounds we must require that the curvature of the space is small in string units (or, equivalently, that the curvature radius is large) and that the string coupling e^Φ is small (otherwise we should describe the system in eleven-dimensional supergravity). Thus, the two conditions that make our type IIA supergravity approximation valid are:

$$L \gg 1, \quad e^\Phi \ll 1. \quad (4.3.50)$$

Let us analyze the two conditions in (4.3.50) in two different regimes of the deformation parameter $\varepsilon = N_f/k$. If ε is of the order one or less, the squashing parameters are also of this same order and they do not modify the order of magnitude of L and e^Φ . Therefore, (4.3.50) leads to the same conditions as in the unflavored case, namely:

$$N^{\frac{1}{5}} \ll k \ll N, \quad (4.3.51)$$

with N_f being, at most, of the order of the Chern-Simons level k . Let us consider next the opposite limit, namely when $N_f \gg k$. In this case, as q remains finite (see (4.3.31)) and η is large, it follows from (4.3.40) that:

$$L^4 \approx 2\pi^2 \frac{N}{k} \frac{(2-q)b^4}{q(q-1)} \frac{1}{\eta}. \quad (4.3.52)$$

Moreover, since $\eta \sim \frac{N_f}{k}$ in this limit, one has:

$$L^4 \sim \frac{N}{N_f}. \quad (4.3.53)$$

Similarly, for $N_f \gg k$ the dilaton behaves as:

$$e^\Phi \approx 4\sqrt{\pi} \left(\frac{2N}{k^5}\right)^{\frac{1}{4}} \frac{(2-q)^{\frac{5}{4}}}{q^{\frac{1}{4}}(q-1)^{\frac{1}{4}}} \eta^{-\frac{5}{4}} \sim \left(\frac{N}{N_f^5}\right)^{\frac{1}{4}}. \quad (4.3.54)$$

Thus, the conditions (4.3.50) for $N_f \gg k$ are equivalent to:

$$N^{\frac{1}{5}} \ll N_f \ll N. \quad (4.3.55)$$

Notice that conditions similar to (4.3.51) and (4.3.55) were found in ref. [137] for general tri-Sasakian manifolds.

Let us now discuss the regime of validity of the DBI+WZ action used to describe the flavor branes⁵. In principle the DBI action is considered to be valid when $g_s N_f$ is small [147]. Indeed, $g_s N_f$ is the effective coupling for the process in which an open string ends on the N_f branes. However, as argued in refs. [111, 92], when the flavor branes are smeared the situation is more subtle and the effective coupling $g_s N_f$ is further suppressed due to the fact that the branes are separated a large distance in $\sqrt{\alpha'}$ units and only a small fraction of the N_f branes will be available for an open string process. In general, if R denotes the typical radius of an internal dimension of the geometry in $\sqrt{\alpha'}$ units, the number of flavor branes involved in a typical process will be of order N_f/R^d , where d is the codimension of the flavor branes in the internal space. Thus, we should require that $g_s N_f/R^d$ be small. In our case $d = 3$ and R is just the radius L . Therefore, we should require that $e^\Phi N_f/L^3$ be small. When $\varepsilon = N_f/k$ is small this condition is satisfied if (4.3.51) holds since $e^\Phi N_f/L^3 \sim \varepsilon \sqrt{k/N}$ in this case. In the opposite large ε regime, L and e^Φ behave as in (4.3.53) and (4.3.54) respectively and one has:

$$\frac{e^\Phi N_f}{L^3} \sim \sqrt{\frac{N_f}{N}}. \quad (4.3.56)$$

Thus, we should require that $N_f \ll N$, which is the same condition obtained by imposing that the curvature is small in string units. Notice also that the typical separation scale between two D6-branes is:

$$D \sim \frac{L}{N_f^{\frac{1}{3}}}. \quad (4.3.57)$$

⁵We are grateful to A. Cotrone for discussions on what follows.

For consistency we should require that the distribution of branes is dense enough to be described by a continuous charge density. This condition amounts to require that $D \ll L$, which is clearly satisfied if N_f is large. On the other hand, in accordance with our discussion above, we should also require that D must be greater than 1 (in $\sqrt{\alpha'}$ units) which, for large N_f , leads to the condition $N_f \ll N^{\frac{3}{7}}$. Notice that this requirement is more restrictive than the one written in (4.3.55).

4.3.4 Backreaction with massive flavors

Let us write an ansatz for the backreacted background in the case that the quarks introduced by the flavor D6-branes are massive. According to what happens in other setups [109] analyzed with the smearing technique, we modify the ansatz of F_2 by substituting N_f by $N_f p(r)$, where $p(r)$ is a function of the radial coordinate to be determined. This new function should satisfy the following conditions:

$$p(r) = 0 \quad \text{if } r < r_*, \quad \lim_{r \rightarrow \infty} p(r) = 1, \quad (4.3.58)$$

where r_* is related to the mass of the quarks. Therefore, the new ansatz for F_2 is:

$$F_2 = \frac{k}{2} E^1 \wedge E^2 - \frac{1}{2} \left(k + \frac{3N_f}{4} p(r) \right) (\mathcal{S}^\xi \wedge \mathcal{S}^3 + \mathcal{S}^1 \wedge \mathcal{S}^2). \quad (4.3.59)$$

Now, the smearing form $\Xi = dF_2/2\pi$ casts as:

$$\begin{aligned} \Xi = & -\frac{3N_f}{16\pi} p(r) \left[E^1 \wedge (\mathcal{S}^\xi \wedge \mathcal{S}^2 - \mathcal{S}^1 \wedge \mathcal{S}^3) + E^2 \wedge (\mathcal{S}^\xi \wedge \mathcal{S}^1 + \mathcal{S}^2 \wedge \mathcal{S}^3) \right] - \\ & -\frac{3N_f}{16\pi} p'(r) dr \wedge (\mathcal{S}^\xi \wedge \mathcal{S}^3 + \mathcal{S}^1 \wedge \mathcal{S}^2), \end{aligned} \quad (4.3.60)$$

and has new components (the last line in (4.3.60)) which were not present in the massless case. Notice, however, that the BPS equations for this massive case can be simply obtained by changing:

$$k\eta \rightarrow k + \frac{3N_f}{4} p(r), \quad (4.3.61)$$

in the system for massless matter (4.3.26).

To obtain the function $p(r)$, we use again the hybrid method of comparing the smeared WZ action of the D6-brane with the one corresponding to a single massive embedding, which was characterized by (4.3.11). First of all we notice that, with our new expression (4.3.60) for the smearing form Ξ , we get:

$$\mathcal{K} \wedge \Xi = \frac{3N_f}{4\pi} \left[p(r) + \frac{1}{2} e^g p'(r) \right] h^{\frac{1}{4}} e^{2f+g} d^3x \wedge dr \wedge \text{Vol}(\mathbb{S}^4) \wedge \text{Vol}(\mathbb{S}^2). \quad (4.3.62)$$

By integrating over the \mathbb{S}^4 and \mathbb{S}^2 (which amounts to multiplying by $32\pi^3/3$) and taking into account that $C_7 = e^{-\Phi} \mathcal{K}$, we get effective WZ Lagrangian density in the x^μ and r variables, namely:

$$\mathcal{L}_{WZ} = 8\pi^2 N_f T_{D6} e^{-\Phi} h^{\frac{1}{4}} e^{2f+g} \left[p(r) + \frac{1}{2} e^g p'(r) \right]. \quad (4.3.63)$$

The WZ Lagrangian density of the single massive brane embedding (4.3.11) is:

$$\mathcal{L}_{WZ} = 8\pi^2 T_{D6} e^{-\phi} h^{\frac{1}{4}} e^{2f+g} \sin \theta \left[\sin \theta + \cos \theta e^g \theta' \right]. \quad (4.3.64)$$

Comparing with the Lagrangian (4.3.64) multiplied by N_f , we get that one can identify $p(r)$ with:

$$p(r) = (\sin \theta(r))^2 \Theta(r - r_*). \quad (4.3.65)$$

Integrating (4.3.11), we can rewrite this as:

$$p(r) = \left[1 - \exp \left(-2 \int_{r_*}^r dz e^{-g(z)} \right) \right] \Theta(r - r_*), \quad (4.3.66)$$

Equation (4.3.66) is most general solution of the following differential equation:

$$e^g p'(r) + 2p(r) = 2. \quad (4.3.67)$$

One then realizes that, in this massive case, it is quite convenient to introduce a new radial variable ρ such that:

$$\frac{d\rho}{dr} = e^{-g}. \quad (4.3.68)$$

Denoting by a dot the derivative with respect to ρ , one finds that the first-order differential equation (4.3.67) becomes:

$$\dot{p} + 2p = 2, \quad (\rho > \rho_*), \quad (4.3.69)$$

where ρ_* is the value of the ρ coordinate that corresponds to the minimal value r_* of r . Equation (4.3.69) can be solved as:

$$p(\rho) = \left[1 - e^{2(\rho_* - \rho)} \right] \Theta(\rho - \rho_*), \quad (4.3.70)$$

where we have required the continuity of $p(\rho)$ at $\rho = \rho_*$. Therefore, in the ρ variable the function $p(\rho)$ is known and, in order to determine the background, one has to integrate the system:

$$\begin{aligned} \dot{\Lambda} &= \left(k + \frac{3N_f}{4} p(\rho) \right) e^{\Lambda-2f+g} - \frac{k}{2} e^{\Lambda-g}, \\ \dot{f} &= \frac{1}{4} \left(k + \frac{3N_f}{4} p(\rho) \right) e^{\Lambda-2f+g} - \frac{k}{4} e^{\Lambda-g} + e^{-2f+2g}, \\ \dot{g} &= \frac{1}{2} \left(k + \frac{3N_f}{4} p(\rho) \right) e^{\Lambda-2f+g} + 1 - e^{-2f+2g}. \end{aligned} \quad (4.3.71)$$

This is a very interesting system, and when the mass is non-zero one can hope to find solutions of (4.3.71) that interpolate between two *AdS* spaces, namely, the original unflavored ABJM geometry in the IR and our flavored *AdS* space in the deep UV. However, we do not attempt to do this here, as we go back to the solutions of massless flavors, and use the presence of an *AdS* solution there to play the *AdS*/CFT game.

4.4 Some flavor effects in the dual field theory

Having a simple supergravity solution with no evident pathologies for the unquenched flavor gives us a great opportunity to explore the effects of dynamical matter in several observables. Moreover, since for the case of *massless flavors* (on which we focus in this section) our solution is an Anti-de-Sitter background, we have at our disposal several techniques and holographic prescriptions to evaluate the observables of the unquenched theory in a neat form. Furthermore, some of these observables can also be computed for the localized flavor solutions, which gives us a unique chance to compare with our results and to explore the effects of the smearing technique. In the next subsections we will analyze these flavor effects for some of these observables. We will show that, although the two setups (localized and smeared) have different amount of supersymmetry and flavor group, the results are very similar and, in the case of some observable such as the free energy, they are amazingly close. This is an indication of the fact that the $\mathcal{N} = 3 \rightarrow \mathcal{N} = 1$ breaking introduced by the smearing is, in fact, rather mild.

4.4.1 Free energy on the sphere

Let us consider the euclidean version of the conformal field theory formulated in a three-sphere. The corresponding free energy is given by:

$$F(\mathbb{S}^3) = -\log |Z_{\mathbb{S}^3}|, \quad (4.4.1)$$

where $Z_{\mathbb{S}^3}$ is the euclidean path integral. The holographic calculation of this quantity in AdS_4 gives [148]:

$$F(\mathbb{S}^3) = \frac{\pi L^2}{2G_N}, \quad (4.4.2)$$

where L is the AdS_4 radius and G_N is the effective four-dimensional Newton constant. In our case, G_N is related to the ten-dimensional Newton constant G_{10} by means of the equation:

$$\frac{1}{G_N} = \frac{1}{G_{10}} e^{-2\Phi} \text{Vol}(\mathcal{M}_6), \quad (4.4.3)$$

where \mathcal{M}_6 is the internal manifold and $\text{Vol}(\mathcal{M}_6)$ its volume. For our flavored Anti-de-Sitter solutions this volume can be readily computed from the metric of \mathcal{M}_6 written in (4.3.43) and is equal to:

$$\text{Vol}(\mathcal{M}_6) = \frac{32\pi^3}{3} \frac{q^2 L^6}{b^6}. \quad (4.4.4)$$

Taking into account that, in our units, the ten-dimensional Newton constant G_{10} is given by $G_{10} = 8\pi^6$, and using the value of the dilaton for our solution (equation (4.3.45)), we get:

$$F(\mathbb{S}^3) = \frac{k^2}{24\pi^2} \frac{q^2(\eta + q)^2}{(2 - q)^2 b^4} L^6. \quad (4.4.5)$$

Using the value of the AdS radius L for our geometry written in (4.3.40), we get that $F(\mathbb{S}^3)$ can be represented as:

$$F(\mathbb{S}^3) = \frac{\pi\sqrt{2}}{3} k^{\frac{1}{2}} N^{\frac{3}{2}} \xi\left(\frac{N_f}{k}\right), \quad (4.4.6)$$

where $\xi\left(\frac{N_f}{k}\right)$ is given by:

$$\xi\left(\frac{N_f}{k}\right) \equiv \frac{1}{16} \frac{q^{\frac{5}{2}} (\eta + q)^4}{(2 - q)^{\frac{1}{2}} (q + \eta q - \eta)^{\frac{7}{2}}}. \quad (4.4.7)$$

Notice that $\xi = 1$ for the unflavored case and we recover the ABJM result, namely:

$$F_{ABJM}(\mathbb{S}^3) = \frac{\pi\sqrt{2}}{3} k^{\frac{1}{2}} N^{\frac{3}{2}} = \frac{\pi\sqrt{2}}{3} \frac{N^2}{\sqrt{\lambda}}, \quad (4.4.8)$$

where, in the last step, we have written the result in terms of the 't Hooft coupling $\lambda = N/k$. For small values of N_f/k we can expand ξ as:

$$\xi = 1 + \frac{3}{4} \frac{N_f}{k} - \frac{9}{64} \left(\frac{N_f}{k}\right)^2 + \mathcal{O}\left(\left(\frac{N_f}{k}\right)^3\right). \quad (4.4.9)$$

Thus, the free energy of the flavored theory can be expanded in powers of N_f/k as:

$$F(\mathbb{S}^3) = \frac{\pi\sqrt{2}}{3} \frac{N^2}{\sqrt{\lambda}} + \frac{\pi\sqrt{2}}{4} N_f N \sqrt{\lambda} - \frac{3\pi\sqrt{2}}{64} N_f^2 \lambda^{\frac{3}{2}} + \dots \quad (4.4.10)$$

If, on the contrary, N_f/k is large, one can verify that, at leading order, ξ behaves as:

$$\xi \sim \frac{225}{256} \sqrt{\frac{5}{2}} \sqrt{\frac{N_f}{k}} \approx 1.389 \sqrt{\frac{N_f}{k}}, \quad (4.4.11)$$

and, therefore, the free energy in this large N_f case becomes:

$$F(\mathbb{S}^3) \sim \frac{75\sqrt{5}\pi}{256} N_f^{\frac{1}{2}} N^{\frac{3}{2}}. \quad (4.4.12)$$

Let us next compare our results with the ones obtained with the $\mathcal{N} = 3$ tri-Sasakian geometry that corresponds to a localized stack of flavor D6-branes. In M-theory these geometries are obtained as the base $X_7(\mathbf{t})$ of a hyperkähler cone $\mathcal{M}_8(\mathbf{t})$, labelled by three natural numbers $\mathbf{t} = (t_1, t_2, t_3)$. These cones are obtained as hyperkähler quotients of the form $\mathbb{H}^3//U(1)$, where the $U(1)$ action is characterized by the three charges \mathbf{t} . The dual to the $\mathcal{N} = 3$ Chern-Simons-matter theories with N_f fundamentals has charges $\mathbf{t} = (N_f, N_f, k)$ (see [137]). The volume of $X_7(\mathbf{t})$ has been computed in [149] by using localization techniques. From this result one can obtain the corresponding free energy $F(\mathbb{S}^3)$ [137], which matches the matrix model field theory calculation [150]. One gets an expression like (4.4.6) with a flavor correction factor ξ simply given by:

$$\xi^{3-S} = \frac{1 + \frac{N_f}{k}}{\sqrt{1 + \frac{N_f}{2k}}}. \quad (4.4.13)$$

Let us expand ξ^{3-S} in powers of N_f/k , namely:

$$\xi^{3-S} = 1 + \frac{3}{4} \frac{N_f}{k} - \frac{5}{32} \left(\frac{N_f}{k} \right)^2 + \mathcal{O} \left(\left(\frac{N_f}{k} \right)^3 \right). \quad (4.4.14)$$

This result is indeed very similar to our result (4.4.9). For large N_f/k one has:

$$\xi^{3-S} \sim \sqrt{2} \sqrt{\frac{N_f}{k}}, \quad (4.4.15)$$

which is again amazingly close to the value we have found in (4.4.11). Actually, one can plot together the two functions ξ written in (4.4.7) and (4.4.13) and check that the two curves are, indeed, almost identical (see figure 4.2).

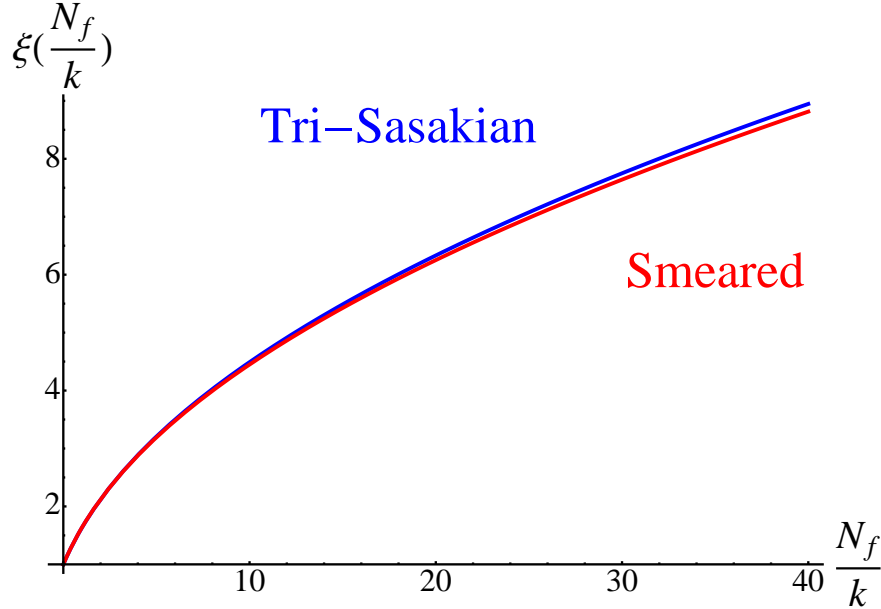


Figure 4.2: Comparison of the flavor correction factor ξ obtained with our smeared setup (lower red curve) and the one corresponding to the tri-Sasakian geometry (upper blue curve).

4.4.2 Wilson loops and quark-antiquark potentials

Most of the results derived for Wilson loops in $\mathcal{N} = 4$ super-Yang-Mills in four dimensions can be adapted to our flavored setup. To illustrate this fact let us consider the calculation of the quark-antiquark static potential. Due to conformal invariance, the quark-antiquark potential must be Coulombic, namely of the form:

$$V_{q\bar{q}} = -\frac{Q}{d}, \quad (4.4.16)$$

where d is the distance between the quark and the antiquark and the coefficient Q measures the strength of the Coulombic potential. The holographic calculation of Q is just the same as the one performed in [73, 151] and yields the result:

$$Q = \frac{4\pi^2 L^2}{\left[\Gamma\left(\frac{1}{4}\right)\right]^4}. \quad (4.4.17)$$

Using the value of the AdS radius L (see (4.3.40)), one can write Q as:

$$Q = \frac{4\pi^3 \sqrt{2\lambda}}{\left[\Gamma\left(\frac{1}{4}\right)\right]^4} \sigma, \quad (4.4.18)$$

where σ parameterizes the screening effects due to dynamical quarks, and is given by:

$$\sigma = \sqrt{\frac{2-q}{q(q-\eta q-\eta)}} b^2 = \frac{1}{4} \frac{q^{\frac{3}{2}} (\eta+q)^2 (2-q)^{\frac{1}{2}}}{(q+\eta q-\eta)^{\frac{5}{2}}}. \quad (4.4.19)$$

For small N_f/k , one can expand σ as:

$$\sigma = 1 - \frac{3}{8} \frac{N_f}{k} + \frac{9}{64} \left(\frac{N_f}{k}\right)^2 + \dots \quad (4.4.20)$$

Clearly, the fact that the first correction is negative means that the screening makes the Coulombic attraction between the quark and the antiquark smaller, as expected on physical grounds. In the opposite limit, when N_f/k is large, σ is small. Actually, one gets:

$$\sigma \rightarrow \frac{1}{4} \frac{q^{\frac{3}{2}} (2-q)^{\frac{1}{2}}}{(q-1)^{\frac{5}{2}}} \eta^{-\frac{1}{2}} = \sqrt{\frac{125}{128}} \sqrt{\frac{k}{N_f}}, \quad \text{for } \frac{N_f}{k} \gg 1. \quad (4.4.21)$$

Similarly, the calculation of the circular Wilson loop can be done by applying the same techniques as in the $AdS_5 \times S^5$ background (see [152]). The result depends on the AdS radius L , namely:

$$\langle W \rangle \sim e^{L^2} \quad (4.4.22)$$

Using our value of L , we get:

$$\langle W \rangle \sim e^{\pi\sqrt{2\lambda}\sigma}, \quad (4.4.23)$$

and, as before, the screening effects are encoded in σ . It is interesting to compare again our results with the ones found in refs. [137, 150] from the tri-Sasakian geometry. The corresponding screening factor σ is given by:

$$\sigma^{3-S} = \frac{1}{\sqrt{1 + \frac{N_f}{2k}}} \approx \begin{cases} 1 - \frac{1}{4} \frac{N_f}{k}, & \text{for } N_f \ll k, \\ \sqrt{2} \sqrt{\frac{k}{N_f}}, & \text{for } N_f \gg k. \end{cases} \quad (4.4.24)$$

By comparing the right-hand side of (4.4.24) with (4.4.20) and (4.4.21) we conclude that our result is qualitatively similar to the one of [137, 150], although our smeared setup gives rise to a larger screening effect.

4.4.3 Dimensions of scalar meson operators

Let us analyze how the dimensions of the meson operators (bilinears in the fundamental fields) change when the effect of dynamical unquenched matter is taken into account. With this purpose, let us consider a D6-brane probe in the flavored background which fluctuates around the static BPS configuration (4.3.2). The induced metric on the D6-brane worldvolume for this static configuration is given by:

$$\mathcal{G}_{\alpha\beta} d\zeta^\alpha d\zeta^\beta = L^2 ds_{AdS_4}^2 + \frac{L^2}{b^2} \left[q (d\alpha)^2 + q \sin^2 \alpha (d\beta)^2 + (d\psi + \cos \alpha d\beta)^2 \right]. \quad (4.4.25)$$

For simplicity we will concentrate on the case in which only the angle θ varies with respect to the value written in (4.3.2) and we will consider a perturbed configuration in which the angle θ is given by:

$$\theta(r) = \frac{\pi}{2} + \lambda(r), \quad (4.4.26)$$

with $\lambda(r)$ being a small fluctuation of the transverse scalars of the BPS embedding (4.3.2) (it should not be confused with the 't Hooft coupling). In order to study the equation of motion for λ let us compute the worldvolume induced metric g_7 at second order in λ . We represent g_7 as:

$$g_7 = \mathcal{G} + g', \quad (4.4.27)$$

where \mathcal{G} is the metric (4.4.25). At second order in λ the metric perturbation g' is the following:

$$g'_{\alpha\beta} d\zeta^\alpha d\zeta^\beta = \frac{L^2}{b^2} \left[\lambda^2 (d\psi + \cos \alpha d\beta)^2 + (\lambda')^2 (dr)^2 \right], \quad (4.4.28)$$

with $\lambda' = d\lambda/dr$. The DBI Lagrangian density for the flavor D6-brane is just:

$$\mathcal{L}_{\text{DBI}} = -T_{\text{D6}} e^{-\Phi} \sqrt{-\det[g_7]}. \quad (4.4.29)$$

By plugging the results written above for g_7 , one gets the following second-order result:

$$\mathcal{L}_{\text{DBI}} = -T_{\text{D6}} e^{-\Phi} \sqrt{-\det[\mathcal{G}]} \left[\frac{r^2}{2b^2} (\lambda')^2 - \frac{1}{2} \lambda^2 \right]. \quad (4.4.30)$$

Similarly, the WZ term of the Lagrangian is:

$$S_{\text{WZ}} = T_{\text{D6}} \int_{\mathcal{M}_7} e^{-\Phi} \hat{\mathcal{K}}, \quad (4.4.31)$$

with \mathcal{K} being the calibration form and $\hat{\mathcal{K}}$ its pullback to the D6-brane worldvolume \mathcal{M}_7 . One can easily show that, at second order, one has:

$$\hat{\mathcal{K}} = \left(1 - \lambda^2 - \frac{r}{b} \lambda \lambda' \right) \text{Vol}(\mathcal{M}_7), \quad (4.4.32)$$

where $\text{Vol}(\mathcal{M}_7)$ is the volume form of the metric \mathcal{G} . After integrating by parts, we can write the langrangian density for the WZ part of the action as:

$$\mathcal{L}_{\text{WZ}} = -T_{\text{D6}} e^{-\Phi} \sqrt{-\det[\mathcal{G}]} \left[\left(1 - \frac{3}{2b} \right) \lambda^2 \right]. \quad (4.4.33)$$

The total Lagrangian density is thus:

$$\mathcal{L} = -T_{D6} e^{-\Phi} \sqrt{-\det[\mathcal{G}]} \left[\frac{r^2}{2b^2} (\lambda')^2 + \frac{1}{2} \left(1 - \frac{3}{b}\right) \lambda^2 \right], \quad (4.4.34)$$

and the corresponding equation of motion for λ is:

$$\frac{1}{r^2} \partial_r [r^4 \partial_r \lambda] + b(3 - b) \lambda = 0. \quad (4.4.35)$$

Let us assume that the fluctuation $\lambda(r)$ in AdS_4 behaves for large r as:

$$\lambda \sim c_1 r^{-2a_1} + c_2 r^{-2a_2}, \quad a_2 > a_1, \quad (4.4.36)$$

where a_1 (a_2) corresponds to the non-normalizable (normalizable) mode. The associated conformal dimension of the dual operator $\bar{\psi}\psi$ is:

$$\Delta = \dim(\bar{\psi}\psi) = \frac{3}{2} + a_2 - a_1. \quad (4.4.37)$$

In order to find the values of the exponents a_1 and a_2 in our case, let us assume that there is a solution of the fluctuation equation (4.4.35) in the form:

$$\lambda \sim r^\alpha. \quad (4.4.38)$$

It is now straightforward to show that the exponent α can take the values $\alpha = -b, b - 3$. It follows that a_1 and a_2 are given by:

$$a_1 = \frac{b}{2}, \quad a_2 = \frac{3 - b}{2}. \quad (4.4.39)$$

Thus, it follows from (4.4.37) that the dimension Δ is just given by:

$$\dim(\bar{\psi}\psi) = 3 - b. \quad (4.4.40)$$

Let us expand this result in the number of flavors. As the parameter b written in (4.3.36) is given by the following power series in N_f/k :

$$b = 1 + \frac{3}{16} \frac{N_f}{k} - \frac{63}{512} \left(\frac{N_f}{k}\right)^2 + \dots, \quad (4.4.41)$$

the dimension of the dual operator is:

$$\dim(\bar{\psi}\psi) = 2 - \frac{3}{16} \frac{N_f}{k} + \frac{63}{512} \left(\frac{N_f}{k}\right)^2 + \dots. \quad (4.4.42)$$

This equation shows how the canonical dimension $\dim(\bar{\psi}\psi) = 2$ is corrected by the addition of dynamical quarks in the regime in which N_f/k is not large. Let us consider next the opposite limit in which N_f/k is large. In this case one can easily verify that:

$$b \rightarrow \frac{5}{4}, \quad \left(\frac{N_f}{k} \rightarrow \infty\right), \quad (4.4.43)$$

and therefore

$$\dim(\bar{\psi}\psi) \rightarrow \frac{7}{4}, \quad \left(\frac{N_f}{k} \rightarrow \infty\right). \quad (4.4.44)$$

4.4.4 Dimensions of high spin operators

A high spin operator can be holographically realized as a rotating string [153]. The anomalous dimension Δ of such operator can be computed in the large λ limit. Indeed, the calculation is just the same as in [153] and the result for the difference between the dimension Δ and the spin S can be written as:

$$\Delta - S = f(\lambda, \varepsilon) \log S, \quad (4.4.45)$$

with $f(\lambda, \varepsilon)$ being the so-called cusp anomalous dimension which depends on the 't Hooft coupling λ and on the flavor deformation parameter ε (the unflavored result was obtained in [116]). From the calculations in [153], we have:

$$f(\lambda, \varepsilon) = \frac{L^2}{\pi}. \quad (4.4.46)$$

In terms of the gauge theory parameters the cusp anomalous dimension can be written as:

$$f(\lambda, \varepsilon) = \sqrt{2\lambda} \sigma, \quad (4.4.47)$$

where σ is the screening factor of the quark-antiquark potential defined in (4.4.19), which also encodes the effects of the unquenched quarks on the anomalous dimensions of high spin operators.

4.4.5 Particle-like branes

As our final example let us analyze how quark loops effects change the dimensions of the operators dual to some particle-like brane configurations. In general, the conformal dimension of the operator dual to an object of mass m in the AdS_4 space of radius L is given by:

$$\Delta = m L. \quad (4.4.48)$$

First of all, let us consider the case of D0-branes which, according to [116], are dual to di-monopole operators with charges $(1, 1)$ under the two gauge groups. These operators are equivalent to Wilson line operators carrying k fundamental indices of one group and k anti-fundamental indices of the other group. From the value of the dilaton in (4.3.44) we immediately obtain the mass of a D0-brane ($m_{D0} = 1/g_s$):

$$m_{D0} = \frac{\eta + q}{4\sqrt{\pi}} \frac{q^{\frac{1}{4}} (q + \eta q - \eta)^{\frac{1}{4}}}{(2 - q)^{\frac{5}{4}}} \left(\frac{k^5}{2N} \right)^{\frac{1}{4}}. \quad (4.4.49)$$

The conformal dimension of the gauge dual is just obtained by applying (4.4.48). We get:

$$\Delta_{D0} = \frac{1}{8} \frac{q (\eta + q)^2}{(q + \eta q - \eta) (2 - q)} k. \quad (4.4.50)$$

As a check, we notice that (4.4.50) reduces to $k/2$ for $\eta = q = 1$, which is the value expected for an operator which is the product of k bi-fundamentals of dimension $1/2$.

In reference [137] it was argued from the field theory side that the dimension of the di-monopole operators of an $\mathcal{N} = 3$ Chern-Simons-matter theory is corrected by the fundamentals as $\Delta_{D0} \rightarrow \Delta_{D0} + \frac{N_f}{2}$. In order to compare this result with our expression (4.4.50), let us evaluate Δ_{D0} for N_f small and large with respect to the Chern-Simons-Level k . One gets:

$$\Delta_{D0} \approx \begin{cases} \frac{k}{2} + \frac{9N_f}{16} & \text{for } N_f \ll k, \\ \frac{45}{64} N_f & \text{for } N_f \gg k. \end{cases} \quad (4.4.51)$$

Notice that (4.4.51) is not very different from the result obtained in [137], specially for small N_f (although both results refer to theories with different amount of supersymmetry and flavor group).

We now consider di-baryons in the flavored geometry. They should correspond to D4-branes wrapped on (deformed) \mathbb{CP}^2 , which we will take to be given by the same angular embedding as in the unflavored case in (4.1.20), namely it will be defined by $\varphi = \theta = \pi/2$. In terms of the angle χ defined in (4.1.23), the induced metric in the four-cycle is given by the following deformation of the Fubini-Study metric:

$$\frac{L^2}{b^2} \left[(d\chi)^2 + \cos^2 \frac{\chi}{2} \left((1 + (q-1) \sin^2 \frac{\chi}{2}) ((\bar{\omega}^1)^2 + (\bar{\omega}^3)^2) + q \sin^2 \frac{\chi}{2} (\bar{\omega}^2)^2 \right) \right]. \quad (4.4.52)$$

The volume V_4 of this cycle can be immediately obtained by integration, namely:

$$V_4 = \frac{8\pi^2}{3} \frac{(2+q)L^4}{b^4}, \quad (4.4.53)$$

and the mass of the wrapped D4-brane is:

$$m_{D4} = \frac{e^{-\Phi}}{(2\pi)^4} V_4 = \frac{L^3}{24\pi^2 b} \frac{(2+q)(\eta+q)}{2-q} k. \quad (4.4.54)$$

The corresponding conformal dimension $\Delta_{D4} = m_{D4} L$ is just:

$$\Delta_{D4} = \frac{1}{96} \frac{q^2 (\eta+q)^4 (2+\eta)}{(q+\eta q - \eta)^4} N. \quad (4.4.55)$$

As a check of the formula (4.4.55) one can verify that its right-hand side reduces to the unflavored value $N/2$ when $N_f = 0$. Actually, the dimension Δ_{D4} does not vary much with the number of flavors. For small N_f/k one can expand

$$\Delta_{D4} = \left(1 + \frac{1}{8} \frac{N_f}{k} + \frac{33}{256} \left(\frac{N_f}{k} \right)^2 + \dots \right) \frac{N}{2}. \quad (4.4.56)$$

Moreover, for large N_f/k the dimension approaches the following constant asymptotic limit:

$$\Delta_{D4} \rightarrow \frac{125}{256} N. \quad (4.4.57)$$

which is very close to the unflavored value $N/2$. Actually, it was argued in [149, 138] from the analysis of the tri-Sasakian geometry dual to $\mathcal{N} = 3$ theories that Δ_{D4} should not be changed when fundamentals are added. Again, we see that the results obtained with our smeared geometry are not very different from the ones found with the localized $\mathcal{N} = 3$ backgrounds.

4.A The method of supersymmetry variations

In this appendix we rederive the system of BPS first-order equations satisfied by our supergravity solutions, as well as the corresponding Killing spinors, using the supersymmetry variations approach. In order to do that, we use the supersymmetric variations of the dilatino λ and the gravitino ψ_μ of the type IIA supergravity in string frame (which we take from [154]):

$$\delta \lambda = \left[\frac{1}{2} \Gamma^\mu \partial_\mu \Phi + \frac{3}{8} \frac{e^\Phi}{2!} F_{\mu\nu}^{(2)} \Gamma^{\mu\nu} \Gamma_{11} - \frac{1}{8} \frac{e^\Phi}{4!} F_{\mu\nu\rho\sigma}^{(4)} \Gamma^{\mu\nu\rho\sigma} \right] \epsilon, \quad (4.A.1)$$

$$\delta \psi_\mu = \left[\nabla_\mu + \frac{e^\Phi}{8} \frac{1}{2!} F_{\rho\sigma}^{(2)} \Gamma^{\rho\sigma} \Gamma_{11} \Gamma_\mu + \frac{e^\Phi}{8} \frac{1}{4!} F_{\mu\nu\rho\sigma}^{(4)} \Gamma^{\mu\nu\rho\sigma} \Gamma_\mu \right] \epsilon. \quad (4.A.2)$$

In order to study the supersymmetric metrics of form (4.2.1), recall that we had chosen the basis of frame one-forms in (4.2.3), that we repeat here for convenience:

$$\begin{aligned} e^\mu &= h^{-\frac{1}{4}} dx^\mu, \quad (\mu = 0, 1, 2), & e^3 &= h^{\frac{1}{4}} dr, & e^4 &= h^{\frac{1}{4}} e^f \mathcal{S}^\xi, \\ e^5 &= h^{\frac{1}{4}} e^f \mathcal{S}^1, & e^6 &= h^{\frac{1}{4}} e^f \mathcal{S}^2, & e^7 &= h^{\frac{1}{4}} e^f \mathcal{S}^3, \\ e^8 &= h^{\frac{1}{4}} e^g E^1, & e^9 &= h^{\frac{1}{4}} e^g E^2. \end{aligned} \quad (4.A.3)$$

Let us first compute the dilatino variation. One gets:

$$\begin{aligned} \delta \lambda &= \left[\frac{1}{2} h^{-\frac{1}{4}} \Gamma_3 \Phi' + \frac{3k}{16} e^\Phi h^{-\frac{1}{2}} \left(e^{-2g} \Gamma_{89} - \eta e^{-2f} \Gamma_{47} - \eta e^{-2f} \Gamma_{56} \right) \Gamma_{11} + \right. \\ &\quad \left. + \frac{e^\Phi}{8} K h^{\frac{1}{2}} \Gamma_{012} \Gamma_3 \right] \epsilon. \end{aligned} \quad (4.A.4)$$

We will first impose the following projection conditions:

$$\Gamma_{47} \epsilon = \Gamma_{56} \epsilon = \Gamma_{89} \epsilon. \quad (4.A.5)$$

Then, the vanishing of the dilatino variation, $\delta \lambda = 0$, leads to the following equation:

$$\Phi' \epsilon + \frac{3k}{8} e^\Phi h^{-\frac{1}{4}} (e^{-2g} - 2\eta e^{-2f}) \Gamma_{389} \Gamma_{11} \epsilon - \frac{e^\Phi}{4} K h^{\frac{3}{4}} \Gamma_{012} \epsilon = 0. \quad (4.A.6)$$

Let us next impose the following projection on ϵ :

$$\Gamma_{012} \epsilon = -\epsilon. \quad (4.A.7)$$

Notice that, as Γ_{11} is defined as:

$$\Gamma_{11} = \Gamma_{01\dots 9}, \quad (4.A.8)$$

the two matrices appearing on (4.A.6) are related, namely:

$$\Gamma_{389} \Gamma_{11} = \Gamma_{012} \Gamma_{4567}. \quad (4.A.9)$$

Since $\Gamma_{4567} \epsilon = -\epsilon$ (see equation (4.A.5)), one has that the projection (4.A.7) implies that:

$$\Gamma_{389} \Gamma_{11} \epsilon = \epsilon. \quad (4.A.10)$$

Using these projections, the dilatino equation becomes the following first-order differential equation:

$$\Phi' = -\frac{3k}{8} e^\Phi h^{-\frac{1}{4}} (e^{-2g} - 2\eta e^{-2f}) - \frac{e^\Phi}{4} K h^{\frac{3}{4}}. \quad (4.A.11)$$

The variation of the components of the gravitino along the Minkowski directions leads to the equations:

$$h^{\frac{3}{2}} \partial_{x^\mu} \epsilon - \frac{h'}{8} \Gamma_{\mu 3} \epsilon - \frac{1}{8} \left[\frac{k}{2} e^\Phi h^{\frac{3}{4}} (e^{-2g} - 2\eta e^{-2f}) - e^\Phi K h^{\frac{7}{4}} \right] \Gamma_{\mu 3} \Gamma_{012} \epsilon = 0. \quad (4.A.12)$$

When the projection (4.A.7) is imposed, (4.A.12) can be solved by means of a spinor which does not depend on the Cartesian coordinates x^μ . Indeed, if $\partial_{x^\mu} \epsilon = 0$ equation (4.A.12) leads to the following differential equation for h :

$$h' = \frac{k}{2} e^\Phi h^{\frac{3}{4}} (e^{-2g} - 2\eta e^{-2f}) - e^\Phi K h^{\frac{7}{4}}. \quad (4.A.13)$$

Let us now consider the equation obtained from the supersymmetry variation of the component of the gravitino along the direction 4. After using the projections (4.A.5) and imposing that the spinor does not depend on the internal coordinates, one arrives at the following equation:

$$(h' + 4hf') \epsilon + 4h e^{-2f+g} \Gamma_{3458} \epsilon - \frac{1}{2} h^{\frac{3}{4}} e^\Phi (k e^{-2g} + 2hK) \Gamma_{012} \epsilon = 0. \quad (4.A.14)$$

In order to solve this equation, let us impose a new projection:

$$\Gamma_{3458} \epsilon = -\epsilon. \quad (4.A.15)$$

Using this projection, together with the one in (4.A.7), leads to the differential equation:

$$h' + 4hf' = -\frac{k}{2} h^{\frac{3}{4}} e^\Phi e^{-2g} - e^\Phi K h^{\frac{7}{4}} + 4h e^{-2f+g}. \quad (4.A.16)$$

By combining equations (4.A.13) and (4.A.16) one can easily prove that:

$$f' = \frac{k}{4} h^{-\frac{1}{4}} e^\Phi [\eta e^{-2f} - e^{-2g}] + e^{-2f+g}. \quad (4.A.17)$$

Let us next consider the equation obtained from $\delta\psi_8 = 0$. Again, after imposing (4.A.5) and the independence of the spinor on the internal coordinates, one arrives at:

$$(h' + 4hg') \epsilon + 4h (e^{-g} - e^{-2f+g}) \Gamma_{3458} \epsilon + \frac{1}{2} h^{\frac{3}{4}} e^\Phi (2k\eta e^{-2f} + k e^{-2g} - 2Kh) \Gamma_{012} \epsilon = 0. \quad (4.A.18)$$

By using again the projections (4.A.7) and (4.A.15), we get:

$$h' + 4hg' = \frac{k}{2} e^\Phi h^{\frac{3}{4}} (e^{-2g} + 2\eta e^{-2f}) - e^\Phi K h^{\frac{7}{4}} + 4h (e^{-g} - e^{-2f+g}). \quad (4.A.19)$$

Eliminating h' from (4.A.13) we arrive at:

$$g' = \frac{k}{2} e^\Phi h^{-\frac{1}{4}} \eta e^{-2f} + e^{-g} - e^{-2f+g}. \quad (4.A.20)$$

Let us finally analyze the supersymmetry variation of the gravitino component along the radial direction. After imposing (4.A.5) one arrives at the following equation:

$$\partial_r \epsilon = -\frac{1}{6} e^\Phi h^{\frac{3}{4}} K \Gamma_{012} \epsilon. \quad (4.A.21)$$

This equation can be easily integrated. First of all we impose (4.A.7). Secondly, as shown in section 4.2.1, from the equations derived above the function K can be written in terms of Φ and h as in (4.2.19) and one can show that:

$$e^\Phi h^{\frac{3}{4}} K = -\frac{d}{dr} \log \left(e^\Phi h^{\frac{3}{4}} \right). \quad (4.A.22)$$

Therefore, the Killing spinor equation (4.A.21) can be integrated as:

$$\epsilon = e^{-\frac{\Phi}{6}} h^{-\frac{1}{8}} \epsilon_0, \quad (4.A.23)$$

where ϵ_0 is a constant spinor satisfying the same projections as ϵ .

Eqs. (4.A.11), (4.A.13), (4.A.17) and (4.A.20) constitute the system of first-order BPS equations (4.3.26). They have been obtained by imposing the projections (4.2.10) and ensure the preservation of two supercharges, both in the unflavored and flavored theories. As we will show in the next subsection, the actual number of supersymmetries is increased for certain particular solutions of the BPS equations due to the fact that some of the projections which are imposed in the generic case are not needed in these special solutions. In particular, for the case of AdS solutions of sections 4.2.2 and 4.3.2, the projection (4.A.7) is not needed and there are four Killing spinors (as it corresponds to $\mathcal{N} = 1$ superconformal supersymmetry in three dimensions). Moreover, for the unflavored ABJM solution one can solve the BPS equations without imposing any of the projections written in (4.2.10) and, after a detailed study, one can show that there are 24 Killing spinors, as it corresponds to $\mathcal{N} = 6$ in three dimensions.

4.A.1 Supersymmetry for the Anti-de Sitter solutions

Let us consider the particular solution of the BPS equations which leads to the AdS_4 metric. Since the dilaton Φ is constant in this case, it follows from (4.A.11) that the following relation holds:

$$2\eta e^{-2f} - e^{-2g} = \frac{2Kh}{3k}. \quad (4.A.24)$$

Actually, by using (4.A.24) and (4.A.9) one can show that (4.A.6) is satisfied by imposing only the projections (4.A.5), without requiring the condition (4.A.7). Moreover, by plugging (4.A.24) into (4.A.12) one gets:

$$\partial_{x^\mu} \epsilon = \frac{1}{8} h^{-\frac{3}{2}} h' \Gamma_{\mu 3} \epsilon - \frac{1}{6} h^{\frac{1}{4}} e^\Phi K \Gamma_{\mu 3} \Gamma_{012} \epsilon. \quad (4.A.25)$$

Furthermore, when Φ is constant (4.A.22) can be used to relate K to h' . This relation can be written as:

$$e^\Phi K = -\frac{3}{4} h^{-\frac{7}{4}} h'. \quad (4.A.26)$$

By eliminating K on the right-hand side of (4.A.25), one gets:

$$\partial_{x^\mu} \epsilon = \frac{1}{8} h^{-\frac{3}{2}} h' \Gamma_{\mu 3} (1 + \Gamma_{012}) \epsilon. \quad (4.A.27)$$

Since for these solutions $h = L^4/r^4$, where L is the AdS_4 radius, we can rewrite (4.A.27) as:

$$\partial_{x^\mu} \epsilon = -\frac{r}{2L^2} \Gamma_{\mu 3} (1 + \Gamma_{012}) \epsilon. \quad (4.A.28)$$

We can now combine this equation with (4.A.21) to obtain the dependence of the Killing spinors on the AdS_4 coordinates. Indeed, by using (4.A.26) in (4.A.21) it is straightforward to prove that:

$$\partial_r \epsilon = -\frac{1}{2r} \Gamma_{012} \epsilon. \quad (4.A.29)$$

It is now easy to integrate (4.A.28) and (4.A.29) following [155]. One gets:

$$\epsilon = r^{-\frac{\Gamma_{012}}{2}} \left(1 + \frac{1}{2L^2} x^\mu \Gamma_\mu \Gamma_3 (1 + \Gamma_{012}) \right) \epsilon_0, \quad (4.A.30)$$

where ϵ_0 is a constant spinor satisfying the projection conditions (4.A.5). Notice that the spinors ϵ in (4.A.30) with $\Gamma_{012}\epsilon_0 = -\epsilon_0$ satisfy (4.A.7) and are independent of the Cartesian coordinates. On the contrary, if we choose an ϵ_0 such that $\Gamma_{012}\epsilon_0 = \epsilon_0$, the resulting Killing spinors ϵ do depend on the Cartesian coordinates and do not have a well-defined eigenvalue of Γ_{012} . Moreover, since for these AdS solutions $h' + 4hf' = h' + 4hg' = 0$, one can easily verify that the equations obtained from the variation of the gravitino along the internal directions (*i.e.* equations (4.A.14) and (4.A.18)) are satisfied if the following projection:

$$\Gamma_{012} \Gamma_{3458} \epsilon = \epsilon, \quad (4.A.31)$$

is imposed on ϵ . Notice that the matrix on the left-hand side of (4.A.31) commutes with the one multiplying the constant spinor ϵ_0 in (4.A.30). Thus, ϵ_0 must also satisfy (4.A.31) and these AdS backgrounds preserve four supercharges, as claimed.

Interestingly, the BPS equations for the AdS solutions can be recast as the ones corresponding to a compactification with fluxes in an internal manifold with an $SU(3)$ -structure (see [156] for a review). To verify this fact, let us define the fundamental two-form \mathcal{J} as:

$$\mathcal{J} = h^{-\frac{1}{2}} e^{-2f} \left(e^4 \wedge e^7 + e^5 \wedge e^6 + e^8 \wedge e^9 \right), \quad (4.A.32)$$

where the one-forms e^4, \dots, e^9 are the ones written in (4.A.3). Moreover, let Ω be the holomorphic three-form defined as:

$$i\Omega = h^{-\frac{3}{2}} e^{-3f} (e^4 + ie^7) \wedge (e^5 + ie^6) \wedge (e^8 + ie^9). \quad (4.A.33)$$

One can check that these forms satisfy:

$$d\mathcal{J} = \frac{3}{2} \mathcal{W}_1 \text{Im}(\Omega), \quad (4.A.34)$$

$$d\Omega = -\mathcal{W}_1 \mathcal{J} \wedge \mathcal{J} = \mathcal{W}_2 \wedge \mathcal{J}, \quad (4.A.35)$$

where \mathcal{W}_1 and \mathcal{W}_2 are the so-called torsion classes which, for our solutions with $e^g = e^f / \sqrt{q}$, are given by:

$$\begin{aligned} \mathcal{W}_1 &= \frac{2}{3} \frac{q+1}{\sqrt{q}}, \\ h^{\frac{1}{2}} e^{2f} \mathcal{W}_2 &= \frac{2}{3} \frac{2-q}{\sqrt{q}} \left(e^4 \wedge e^7 + e^5 \wedge e^6 - 2 e^8 \wedge e^9 \right). \end{aligned} \quad (4.A.36)$$

Notice that, in terms of the one-forms in (4.A.3), our ansatz (4.3.13) for F_2 can be written as:

$$h^{\frac{1}{2}} e^{2f} F_2 = -\frac{k}{2} \left[\eta (e^4 \wedge e^7 + e^5 \wedge e^6) - \sqrt{q} e^8 \wedge e^9 \right]. \quad (4.A.37)$$

Then, one can check that, if the squashing factors q and η are related as in (4.3.28), the two-form F_2 is also given in terms of the torsion classes and of the fundamental form by:

$$F_2 = -\frac{\sqrt{q}}{3-q} \eta k \left[\frac{1}{4} \mathcal{W}_1 \mathcal{J} - *_6(\mathcal{W}_2 \wedge \mathcal{J}) \right], \quad (4.A.38)$$

where the \mathcal{W}_i are given in (4.A.36) and $*_6$ denotes the Hodge dual with respect to the six-dimensional internal metric $h^{-1/2} e^{2f} ((e^4)^2 + \dots + (e^9)^2)$.

4.A.2 Supersymmetry for the unflavored ABJM solution

For the ABJM unflavored solution the squashing factors q and η are equal to one. Moreover, in this solution $K h e^{2g} = 3k/2$, and one can easily verify that the projections (4.A.5) are not needed to solve the dilatino equation $\delta\lambda = 0$. Indeed, it is straightforward to show from (4.A.4) that the equation for the supersymmetry variation of the dilatino leads to:

$$\epsilon = (\Gamma_{4756} - \Gamma_{5689} - \Gamma_{4789}) \epsilon. \quad (4.A.39)$$

In order to study the solutions of this equation let us work on a representation of the Dirac algebra in which the spinors are characterized by their ± 1 eigenvalue of the following complete commuting set of matrices: $\{\Gamma_{01}, i\Gamma_{23}, i\Gamma_{47}, i\Gamma_{56}, i\Gamma_{89}\}$. In this representation the matrices on the right-hand side of (4.A.39) will also act diagonally. Let us parametrize their eigenvalues as:

$$\Gamma_{4756} \epsilon = s_1 \epsilon, \quad \Gamma_{5689} \epsilon = s_2 \epsilon, \quad \Gamma_{4789} \epsilon = -s_1 s_2 \epsilon. \quad (4.A.40)$$

One immediately shows that (4.A.39) is equivalent to the following condition on s_1 and s_2 :

$$s_1 - s_2 + s_1 s_2 = 1. \quad (4.A.41)$$

Since only three of the four possible values of (s_1, s_2) satisfy (4.A.41), the projection (4.A.39) preserves 3/4 of the supercharges, *i.e.* 24 of them. This is, indeed, the amount of supersymmetry of an $\mathcal{N} = 6$ supersymmetric theory in three dimensions. Moreover, one can show that the remaining equations for ϵ can also be solved without imposing any additional projection.

Chapter 5

Flavor Physics in $\mathcal{N} = 1$ theories

Contextualizing this chapter

From the setup of the previous chapter, which was ideal from a theoretical point of view, we move on to a more phenomenological four-dimensional setup. The application of the ideas of the gauge/gravity correspondence is less clean, but still quite robust. From a phenomenological point of view, the golden goal of the gauge/gravity correspondence would be to find a gravity solution encoding some non-perturbative IR physics of QCD, an essentially untractable problem with field theory tools (the main insight comes from simulations on the lattice). A step in this direction was taken in [108], where a type IIB supergravity solution was found encoding the IR dynamics of a SQCD-like theory. This solution has unfortunately a singularity which does not allow to fully trust the gravity predictions.

In this chapter, we discuss the results published in [23], where the singularity was resolved by finding a new (regular everywhere) supergravity solution that encodes the effects of having massive quarks in the field theory. The solution was found using the smearing technique, and this work also clarified the connection between the microscopic and macroscopic approaches (discussed in section 3.3.1). After that, these solutions can be “rotated”, as done in [24, 25], to give new type IIB solutions dual to purely four-dimensional theories with a very rich dynamics. We also discuss how these dynamics could model some Beyond-the-Standard-Model physics.

5.1 The CNP solution

The many achievements of the MN solution have been praised already in section 3.2.2. This supergravity solution successfully encodes many IR features we expect to find in $\mathcal{N} = 1$ pure SYM. But along the main line of this second part of the thesis, we are interested in field theories with fundamental matter. The object of interest would be then a gravity dual to $\mathcal{N} = 1$ SQCD. In 2006, Casero, Núñez, and Paredes used the smearing technique (for the first time in this context) to incorporate flavor branes into the MN solution. The geometry is of course altered by the backreaction of these branes, and the new solution, referred to as the CNP solution [108], encodes the dynamics of quarks in an $\mathcal{N} = 1$ SQCD-like theory. The “-like” embodies a few technicalities that we discuss along the way in this section.

5.1.1 The type IIB background

Using the techniques described in 3.3.1, CNP introduced a smeared set of N_f ($\sim N_c$) D5-branes into the type IIB supergravity background that was generated by wrapping a large number N_c of D5-branes on a two-sphere inside a Calabi-Yau three-fold, the MN solution. As the latter, the CNP background is still characterized by only a metric $g_{\mu\nu}$, a RR three-form flux F_3 , and a dilaton Φ , but the three of them change (with respect to the MN solution) to accommodate the effect of the flavor branes. Let us characterize the CNP solution precisely:

In Einstein frame, and with the conventions¹ $\alpha' = 1, g_s = 1$, the metric, RR three-form and dilaton cast as:

$$ds^2 = e^{\frac{\Phi}{2}} dx_{1,3}^2 + N_c ds_6^2, \quad (5.1.1)$$

$$ds_6^2 = e^{\frac{\Phi}{2}} \left[e^{2k} dr^2 + e^{2h} (\sigma_1^2 + \sigma_2^2) + \frac{e^{2g}}{4} ((\omega_1 - A_1)^2 + (\omega_2 - A_2)^2) + \frac{e^{2k}}{4} (\omega_3 - A_3)^2 \right], \quad (5.1.2)$$

$$F_3 = -\frac{N_c}{4} \bigwedge_{i=1}^3 (\omega_i - B_i) + \frac{N_c}{4} \sum_{i=1}^3 G_i \wedge (\omega_i - B_i) - \frac{N_f}{4} \sigma_1 \wedge \sigma_2 \wedge (\omega_3 - B_3), \quad (5.1.3)$$

where g, h, k are all functions of the radial/holographic coordinate $r_0 \leq r < \infty$ ($r = r_0$ is called the “origin of the space”); $\sigma_{1,2}$ are one-forms that parameterize a two-sphere \mathbb{S}^2 and $\omega_{1,2,3}$ are the one-forms written in (3.2.7), that parameterize a three-sphere \mathbb{S}^3 . The topology of the internal space, with metric ds_6^2 , is that of a cone over an $\mathbb{S}^2 \times \mathbb{S}^3$ base (the spheres being fibered). The set of \mathbb{S}^2 one-forms $\sigma_{1,2}$ can be completed with a third one σ_3 , such that they mimic the \mathbb{S}^3 Maurer-Cartan algebra, $d\sigma_i = -\frac{1}{2}\epsilon_{ijk}\sigma_j \wedge \sigma_k$, although they are obviously not independent. The one-forms A_i, B_i entering the fibration and the RR form then read:

$$A_{1,2} = a \sigma_{1,2}, \quad A_3 = \sigma_3 \quad ; \quad B_{1,2} = b \sigma_{1,2}, \quad B_3 = \sigma_3, \quad (5.1.4)$$

where a, b are also functions of r . Finally the two-forms G_i appearing in F_3 can be written as a gauge field-strength for B_i :

$$G_i = dB_i + \frac{1}{2}\epsilon_{ijk} B_j \wedge B_k. \quad (5.1.5)$$

We use the following coordinate representation for the one-forms described above. Choosing the usual coordinate system for the \mathbb{S}^2 and \mathbb{S}^3 , $\{\theta, \varphi\}$ and $\{\tilde{\theta}, \tilde{\phi}, \psi\}$ respectively, we have:

$$\begin{aligned} \sigma_1 &= -d\theta, & \omega_1 &= \cos\psi d\tilde{\theta} + \sin\psi d\tilde{\phi}, \\ \sigma_2 &= \sin\theta d\phi, & \omega_2 &= -\sin\psi d\tilde{\theta} + \cos\psi d\tilde{\phi}, \\ \sigma_3 &= -\cos\theta d\phi, & \omega_3 &= d\psi + \cos\tilde{\theta} d\tilde{\phi}. \end{aligned} \quad (5.1.6)$$

The color branes have dissolved into flux, and the fact that we had N_c of them is encoded in the flux quantization condition

$$-N_c = \frac{1}{2\kappa_{10}^2 T_{D5}} \int_{\mathbb{S}^3} i^*(F_3), \quad (5.1.7)$$

¹Anytime you want to restore units, just substitute N_c, N_f by $g_s \alpha' N_c, g_s \alpha' N_f$.

where the 3-sphere \mathbb{S}^3 is the one parameterized by the ω_i , and $2\kappa_{10}^2 T_{D5} = 4\pi^2$ in our units. The distribution of flavor branes can be inferred from the violation of the Bianchi identity:

$$dF_3 = -2\kappa_{10}^2 T_{D5} \frac{N_f}{\text{Vol}(\mathbb{S}^2 \times \mathbb{S}^2)} \omega_{\text{Vol}(\mathbb{S}^2 \times \mathbb{S}^2)} = -\frac{N_f}{4} \sin \theta \sin \tilde{\theta} d\theta \wedge d\phi \wedge d\tilde{\theta} \wedge d\tilde{\phi} \quad (5.1.8)$$

that tells us that each of the flavor branes is extended, in the internal space, in the (r, ψ) directions, and placed at arbitrary values of the other coordinates $\theta_0, \phi_0, \tilde{\theta}_0, \tilde{\phi}_0$. The smearing takes place in the “orthogonal” $\mathbb{S}^2 \times \mathbb{S}^2$ parameterized by these. The CNP background is 1/8-supersymmetric. That means that it preserves just four of the thirty-two supercharges of type IIB supergravity. Consequently, it has four Killing spinors, that satisfy the following projections:

$$\epsilon = \tau_1 \epsilon, \quad \Gamma_{12} \epsilon = \Gamma_{34} \epsilon, \quad \Gamma_{r345} \epsilon = \cos \alpha \epsilon + \sin \alpha \Gamma_{24} \epsilon, \quad (5.1.9)$$

where $\alpha = \alpha(r)$ is a new function in the ansatz, and we use the following vielbein frame for the metric (5.1.1):

$$\begin{aligned} e^{x^i} &= e^{\frac{\Phi}{2}} dx^i, \quad (i = 0, 1, 2, 3), & e^r &= e^{\frac{\Phi}{2}+k} dr, \\ e^1 &= e^{\frac{\Phi}{2}+h} \sigma_1, & e^2 &= e^{\frac{\Phi}{2}+h} \sigma_2, \\ e^3 &= \frac{e^{\frac{\Phi}{2}+g}}{2} (\omega_1 - A_1), & e^4 &= \frac{e^{\frac{\Phi}{2}+g}}{2} (\omega_2 - A_2), & e^5 &= \frac{e^{\frac{\Phi}{2}+k}}{2} (\omega_3 - A_3). \end{aligned} \quad (5.1.10)$$

The functions $\Phi, g, h, k, a, b, \alpha$ characterizing the background are known² as the solution of a BPS system of first-order ordinary differential equations. This system can be nicely recast in terms of the two fundamental forms of the underlying geometric $SU(3)$ -structure of the internal complex manifold, central concept of the next subsection. These forms are the $(1, 1)$ two-form J and the holomorphic $(3, 0)$ three-form Ω , which are defined in terms of fermionic bilinears as:

$$J = \frac{i}{2!} \epsilon^\dagger \Gamma_{a_1 a_2} \epsilon e^{a_1 a_2}, \quad \Omega = \frac{e^{\frac{5\Phi}{2}}}{3!} \epsilon^T \Gamma_{a_1 a_2 a_3} \epsilon e^{a_1 a_2 a_3}, \quad (5.1.11)$$

where ϵ is a Killing spinor normalized as $\epsilon^\dagger \epsilon = 1$. Using the projections (5.1.9) satisfied by ϵ one can express the $SU(3)$ -structure forms as:

$$\begin{aligned} J &= e^{r^5} + (\cos \alpha e^2 + \sin \alpha e^4) \wedge e^1 + (-\sin \alpha e^2 + \cos \alpha e^4) \wedge e^3, \\ \Omega &= e^{3f+\Phi/2} (e^r + i e^5) \wedge ((\cos \alpha e^2 + \sin \alpha e^4) + i e^1) \wedge ((-\sin \alpha e^2 + \cos \alpha e^4) + i e^3). \end{aligned} \quad (5.1.12)$$

The conditions imposed by the preservation of $\mathcal{N} = 1$ supersymmetry can be written as the following set of equations to be satisfied by the structure forms [157]:

$$\begin{aligned} e^{-\Phi} d(e^{\frac{3\Phi}{2}} J) &= -e^\Phi *_6 F_3, \\ d\Omega &= 0, \\ d(e^\Phi J \wedge J) &= 0, \end{aligned} \quad (5.1.13)$$

²For general N_c, N_f , the full solutions are only known numerically. Only the asymptotic UV and IR behaviors are known analytically.

where $*_6$ denotes the Hodge dual with respect to the internal part of the metric (5.1.2). The conditions in (5.1.13) translate into a system of first-order differential equations for the functions g, h, k, a, b, α : the BPS system. This system can be partially integrated and reduced to a second-order ordinary differential equation, which we call “master equation” since, once it is solved, all the previous functions follow. This master equation is simpler if we perform the reparameterization of the ansatz that was originally proposed in [92]. After this reparameterization, the geometry is not as transparent as in (5.1.1)-(5.1.2), where we can clearly see an \mathbb{S}^3 fibered over an \mathbb{S}^2 , but in turn, the analytic treatment of the solution is much simpler. The change of variables reads as follows:

$$\begin{aligned} e^{2h} &= \frac{1}{4} \frac{P^2 - Q^2}{P \cosh \tau - Q}, & a &= \frac{P \sinh \tau}{P \cosh \tau - Q}, & \cos \alpha &= \frac{P - Q \cosh \tau}{P \cosh \tau - Q}, \\ e^{2g} &= P \cosh \tau - Q, & b &= \frac{\sigma}{N_c}, & \sin \alpha &= -\frac{\sinh \tau \sqrt{P^2 - Q^2}}{P \cosh \tau - Q}, \\ e^{2k} &= 4Y, & e^{2\Phi} &= \frac{D}{Y^{1/2}(P^2 - Q^2)}, \end{aligned} \quad (5.1.14)$$

where, of course, the new functions P, Q, Y, τ, σ, D depend only on r . Notice there is one function less than before. This occurs because α could be written in terms of the others as a consequence of supersymmetry:

$$\frac{a^2 - 1}{4} e^{2g} - e^{2h} = e^{h+g} a \cot \alpha. \quad (5.1.15)$$

In the new variables, all but one of the equations that follow from (5.1.13) can be integrated, and the CNP solution reads:

$$\begin{aligned} \sigma &= \tanh \tau \left(Q + \frac{2-v}{2} \right), & \sinh \tau &= \frac{1}{\sinh(2r - 2r_0)}, \\ D &= e^{2\Phi_0} \sqrt{P^2 - Q^2} \cosh(2r_0) \sinh(2r - 2r_0)/2, & Y &= \frac{1}{8} (P' + v), \\ Q &= \left(Q_0 + \frac{2-v}{2} \right) \coth(2r - 2r_0) + \frac{2-v}{2} (2r \coth(2r - 2r_0) - 1), \end{aligned} \quad (5.1.16)$$

where the prime denotes differentiation with respect to r , the terms with a zero subindex are constants, and P is the solution of the following second-order differential equation:

$$P'' + (P' + v) \left(\frac{P' + Q' + 2v}{P - Q} + \frac{P' - Q' + 2v}{P + Q} - 4 \coth(2r - 2r_0) \right) = 0. \quad (5.1.17)$$

We introduced the dimensionless parameter v , that characterizes the Veneziano limit we are taking:

$$v = \frac{N_f}{N_c}. \quad (5.1.18)$$

This is not the standard notation in the CNP literature, where one absorbs the N_c factor in the internal metric (5.1.1). The choice of notation we are making is closer in spirit to

the original examples of the AdS/CFT correspondence, where the main role of the number of colors of the dual field theory is to tune the radii of the geometry (in this way, small curvatures imply large N_c). Furthermore, it will help to clarify the restoration of units, and the fact that the solution really depends on the ratio v , rather than on N_c and N_f separately. The reader more familiar with CNP can use the following simple prescription to switch notations:

$$P_{\text{CNP}} = N_c P_{\text{here}}, \quad Q_{\text{CNP}} = N_c Q_{\text{here}}, \quad (5.1.19)$$

together with the definition (5.1.18). It is straightforward to see that the master equation in CNP notation would be:

$$P''_{\text{CNP}} + (P'_{\text{CNP}} + N_f) \left(\frac{P'_{\text{CNP}} + Q'_{\text{CNP}} + 2N_f}{P_{\text{CNP}} - Q_{\text{CNP}}} + \frac{P'_{\text{CNP}} - Q'_{\text{CNP}} + 2N_f}{P_{\text{CNP}} + Q_{\text{CNP}}} - 4 \coth(2r - 2r_0) \right) = 0. \quad (5.1.20)$$

Let us stress again how remarkable it is that all the geometry is characterized by a simple second-order differential equation, that deservedly receives the name of master equation. We analyze its solutions later in sections 5.1.3 and 5.1.4.

5.1.2 Some complex geometry

Before moving on to describe the physics the background (5.1.1)-(5.1.3) is encoding, it is worth it to spend some time exploring more in detail its mathematical structure. This will prove invaluable for later purposes.

As we discussed in section 3.2, the fact that the background (5.1.1)-(5.1.3) preserves four supercharges amounts to the internal manifold having an $SU(3)$ -structure. The metric of the internal manifold, ds_6^2 , read from (5.1.2), is:

$$ds_6^2 = e^{\Phi(r)/2} \left[e^{2k(r)} dr^2 + e^{2h(r)} (d\theta^2 + \sin^2 \theta d\phi^2) + \frac{e^{2g(r)}}{4} ((\omega_1 + a(r) d\theta)^2 + (\omega_2 - a(r) \sin \theta d\phi)^2) + \frac{e^{2k(r)}}{4} (\omega_3 + \cos \theta d\phi)^2 \right], \quad (5.1.21)$$

with the functions Φ, k, h, g, a being given as the solution to the BPS system (5.1.13). Having an $SU(3)$ -structure implies that the internal manifold is complex. In particular, we can find a set of complex coordinates for it. For a six-dimensional manifold, one expects to have three complex coordinates. However, it will be more useful for us to describe our manifold (5.1.21) with four complex coordinates (of course not independent), mimicking the structure of the conifold [158]. The symmetries will be explicit proceeding this way, and this will be key later on (recall the connection between smearing and isometries made in section 3.3.1).

Let us then begin by introducing a set of four complex variables z_i ($i = 1, \dots, 4$), that as a matter of fact parameterize a deformed conifold³, *i.e.* they satisfy the following quadratic equation:

$$z_1 z_2 - z_3 z_4 = 1. \quad (5.1.22)$$

³In virtue of (5.1.1), the internal metric is dimensionless, so the deformation parameter of this deformed conifold should be dimensionless, as well, and we choose it to be 1.

The radial variable r is related to the z_i by:

$$\sum_{i=1}^4 |z_i|^2 = 2 \cosh(2r). \quad (5.1.23)$$

In order to find a useful parameterization of the z_i , let us arrange them as the following 2×2 complex matrix Z :

$$Z = \begin{pmatrix} z_3 & z_2 \\ -z_1 & -z_4 \end{pmatrix}. \quad (5.1.24)$$

Then, the defining equations (5.1.22) and (5.1.23) can be conveniently written in matrix form as:

$$\det[Z] = 1, \quad \text{tr}(Z Z^\dagger) = 2 \cosh(2r). \quad (5.1.25)$$

It is immediate to verify that the matrix

$$Z_0 = \begin{pmatrix} 0 & e^r \\ -e^{-r} & 0 \end{pmatrix} \quad (5.1.26)$$

is a particular solution of (5.1.25). The general solution of this equation can be found by realizing that the equations in (5.1.25) exhibit the following $SU(2)_L \times SU(2)_R$ symmetry:

$$Z \rightarrow L Z R^\dagger, \quad L \in SU(2)_L, \quad R \in SU(2)_R. \quad (5.1.27)$$

A generic point in the conifold can be obtained by acting with isometries on the point (5.1.26). If we parameterize the $SU(2)$ matrices above in terms of Euler angles as:

$$L = \begin{pmatrix} a & -\bar{b} \\ b & \bar{a} \end{pmatrix} \quad \begin{matrix} a = \cos \frac{\theta}{2} e^{i\frac{\psi_1 + \phi}{2}} \\ b = \sin \frac{\theta}{2} e^{i\frac{\psi_1 - \phi}{2}} \end{matrix} \quad \text{and} \quad R = \begin{pmatrix} k & -\bar{l} \\ l & \bar{k} \end{pmatrix} \quad \begin{matrix} k = \cos \frac{\tilde{\theta}}{2} e^{i\frac{\psi_2 + \tilde{\phi}}{2}} \\ l = -\sin \frac{\tilde{\theta}}{2} e^{i\frac{\psi_2 - \tilde{\phi}}{2}} \end{matrix}, \quad (5.1.28)$$

then, the four complex variables z_1, z_2, z_3, z_4 that solve (5.1.25) are given by:

$$\begin{aligned} z_1 &= -e^{-\frac{i}{2}(\phi + \tilde{\phi})} \left(e^{r+i\frac{\psi}{2}} \sin \frac{\theta}{2} \sin \frac{\tilde{\theta}}{2} - e^{-r-i\frac{\psi}{2}} \cos \frac{\theta}{2} \cos \frac{\tilde{\theta}}{2} \right), \\ z_2 &= e^{\frac{i}{2}(\phi + \tilde{\phi})} \left(e^{r+i\frac{\psi}{2}} \cos \frac{\theta}{2} \cos \frac{\tilde{\theta}}{2} - e^{-r-i\frac{\psi}{2}} \sin \frac{\theta}{2} \sin \frac{\tilde{\theta}}{2} \right), \\ z_3 &= e^{\frac{i}{2}(\phi - \tilde{\phi})} \left(e^{r+i\frac{\psi}{2}} \cos \frac{\theta}{2} \sin \frac{\tilde{\theta}}{2} + e^{-r-i\frac{\psi}{2}} \sin \frac{\theta}{2} \cos \frac{\tilde{\theta}}{2} \right), \\ z_4 &= -e^{-\frac{i}{2}(\phi - \tilde{\phi})} \left(e^{r+i\frac{\psi}{2}} \sin \frac{\theta}{2} \cos \frac{\tilde{\theta}}{2} + e^{-r-i\frac{\psi}{2}} \cos \frac{\theta}{2} \sin \frac{\tilde{\theta}}{2} \right), \end{aligned} \quad (5.1.29)$$

where $\psi = \psi_1 + \psi_2$. Let us now check that these complex variables z_i are indeed good holomorphic coordinates for the internal manifold. For that we have to verify two things.

The first one is that the fundamental two-form J written in (5.1.11) should be a $(1, 1)$ -form, which means that it can be written as:

$$J = \frac{i}{2} h_{\alpha\bar{\beta}} dz^\alpha \wedge d\bar{z}^{\bar{\beta}}, \quad (5.1.30)$$

and that the metric (5.1.21) should be cast as:

$$ds_6^2 = \frac{1}{2} h_{\alpha\bar{\beta}} (dz^\alpha \otimes d\bar{z}^{\bar{\beta}} + d\bar{z}^{\bar{\beta}} \otimes dz^\alpha). \quad (5.1.31)$$

To check this, it is useful to rewrite the J in (5.1.11) as

$$\begin{aligned} e^{-\frac{\Phi}{2}} J = & \frac{e^{2k}}{2} dr \wedge (\omega_3 + \cos \theta d\phi) + \frac{e^{2g}}{4} \frac{a \cosh(2r - 2r_0) - 1}{\sinh(2r - 2r_0)} (d\theta \wedge \omega_2 + \sin \theta d\phi \wedge \omega_1) - \\ & - \frac{e^{2g}}{4} \left(\frac{a \cosh(4r) - \cosh(2r - 2r_0)}{\sinh(2r - 2r_0)} \sin \theta d\theta \wedge d\phi + \frac{\cosh(2r - 2r_0) - a}{\sinh(2r - 2r_0)} \sin \tilde{\theta} d\tilde{\theta} \wedge d\tilde{\phi} \right), \end{aligned} \quad (5.1.32)$$

where we used the explicit value of the angle α in (5.1.15). Some simple (but tedious) algebra shows that the coefficients appearing in (5.1.30) and (5.1.31) do coincide. The second check is that the Ω of (5.1.11) is indeed a $(3, 0)$ -form. We have that

$$\Omega = -\frac{1}{\sinh(2r - 2r_0)} e^{2\Phi+g+h+k} \frac{1}{z_3} dz_1 \wedge dz_2 \wedge dz_3, \quad (5.1.33)$$

for the complex coordinates in (5.1.29). Since it follows from (5.1.14) and (5.1.16) that

$$e^{-2\Phi} = 2e^{-2\Phi_0} \frac{e^{h+g+k}}{\sinh(2r - 2r_0) \cosh(2r_0)}, \quad (5.1.34)$$

the three-form Ω in (5.1.33) is of the $(3, 0)$ type. Thus, the complex coordinates in (5.1.29) do correspond to the $SU(3)$ -structure of our internal manifold.

In order to make the $SO(4) = SU(2)_L \times SU(2)_R$ symmetry of the background more explicit, it is useful to introduce a new set of complex variables w_i , related to the z_i by means of the following linear combinations:

$$w_1 = \frac{z_1 + z_2}{2}, \quad w_2 = \frac{z_1 - z_2}{2i}, \quad w_3 = \frac{z_3 - z_4}{2}, \quad w_4 = \frac{z_3 + z_4}{2i}. \quad (5.1.35)$$

These variables satisfy:

$$(w_1)^2 + (w_2)^2 + (w_3)^2 + (w_4)^2 = 1, \quad (5.1.36)$$

and there is an obvious $SO(4)$ invariance that is obtained by rotating the w_i . It is then easy to build all the possible $SO(4)$ -invariant $(1, 1)$ -forms of this complex structure [159]:

$$\eta_1 = \delta^{ij} dw_i \wedge d\bar{w}_j, \quad \eta_2 = (\delta^{ij} w_i d\bar{w}_j) \wedge (\delta^{kl} \bar{w}_k dw_l), \quad \eta_3 = \epsilon^{ijkl} w_i \bar{w}_j d\bar{w}_k \wedge dw_l. \quad (5.1.37)$$

In terms of the radial and angular coordinates, these forms are given by:

$$\begin{aligned}\eta_1 &= -i \left(\cosh(2r) dr \wedge (\omega_3 + \cos \theta d\phi) - \frac{1}{2} \sinh(2r) \left(\sin \theta d\theta \wedge d\phi + \sin \tilde{\theta} d\tilde{\theta} \wedge d\tilde{\phi} \right) \right), \\ \eta_2 &= i \sinh^2(2r) dr \wedge (\omega_3 + \cos \theta d\phi), \\ \eta_3 &= -i \left(\frac{1}{4} \sinh(4r) \left(\sin \theta d\theta \wedge d\phi - \sin \tilde{\theta} d\tilde{\theta} \wedge d\tilde{\phi} \right) - \frac{1}{2} \sinh(2r) (d\theta \wedge \omega_2 + \sin \theta d\phi \wedge \omega_1) \right).\end{aligned}\tag{5.1.38}$$

These $SO(4)$ -invariant $(1, 1)$ -forms will be heavily used posteriorly in section 5.2.

So in summary, our internal manifold (5.1.21) shares several features with the deformed conifold, regarding their complex structures. We have seen that it has the same complex coordinates, and more importantly the same isometries. The isometry group is $SO(4) = SU(2)_L \times SU(2)_R$, acting as specified in (5.1.27), and it is really a vestige of the fact that the base of the usual conifold is the coset space $\frac{SU(2) \times SU(2)}{U(1)}$. This sharing of common features between our internal manifold and the conifold is no coincidence, and the reason for that is the metric of the deformed conifold can be written exactly as in (5.1.21), but with different values for the radial functions Φ, h, g, k, a (see equation (3.2.17)). We will come back to this point in section 5.4.1. Now we are done with the mathematics of the CNP solution, we turn our attention to its physics.

5.1.3 Physics of CNP

The flavor D5-branes introduce fundamental matter in the MN theory of section 3.2.2. How is the field theory modified? Let us forget for a moment about the smearing and introduce flavors by means of pairs of chiral multiplets Q and \tilde{Q} transforming in the fundamental and antifundamental representations of both the gauge group $SU(N_c)$ and a flavor group $SU(N_f)$. The natural Lagrangian for the (Q, \tilde{Q}) fields is given by the usual kinetic terms and a Yukawa interaction between the quarks and the KK modes, which can be schematically written as:

$$L_{Q, \tilde{Q}} = \int d^4\theta (Q^\dagger e^{-V} Q + \tilde{Q}^\dagger e^V \tilde{Q}) + \int d^2\theta \tilde{Q} \Phi_k Q + \text{h.c.} \tag{5.1.39}$$

This should be added to (3.2.13), resulting a Lagrangian

$$\int d^4\theta \left(\sum_k \Phi_k^\dagger e^V \Phi_k + Q^\dagger e^{-V} Q + \tilde{Q}^\dagger e^V \tilde{Q} \right) + \int d^2\theta \left(\mathcal{W} + \sum_k \left(\tilde{Q} \Phi_k Q + W(\Phi_k) \right) \right) + \text{h.c.} \tag{5.1.40}$$

Let us consider an effective superpotential of the form

$$W(\Phi_k) = m_k \Phi_k^2 + \mathcal{O}(\Phi_k^3), \tag{5.1.41}$$

where the first is a mass term and the higher-order terms are not important for the following reason. The integration-out of the KK modes Φ_k yields, in the large N_c limit, the following IR Lagrangian

$$\mathcal{L}_{\text{IR}} = \int d^4\theta (Q^\dagger e^{-V} Q + \tilde{Q}^\dagger e^V \tilde{Q}) + \int d^2\theta (\mathcal{W} + \kappa \text{Tr} [(\tilde{Q} Q \tilde{Q} Q)]) + \text{h.c.}, \tag{5.1.42}$$

where we have omitted in the second integrand terms going like $\sim (\bar{Q}Q)^3$, generated by the higher-order terms in (5.1.42) and which are irrelevant in the IR. This is the Lagrangian of $\mathcal{N} = 1$ SQCD with a quartic superpotential for the quark fields, where κ^{-1} is a mass scale (the integration-out happens below the KK scale, which is also the confinement scale, so it is not a very clean process as the theory is strongly coupled).

The reasoning above is quite generic, and the smearing will just change the details of the superpotential. This is not very significant; as we saw in the previous chapter, the smeared solution captures all the qualitative features of the localized solution. Therefore, *the CNP supergravity solution should capture the IR physics of $\mathcal{N} = 1$ SQCD with a quartic superpotential.* Let us show some evidence for it.

Solutions of the master equation

In section 5.1.1 we only wrote the ansatz for the type IIB supergravity solution. The full background is completely determined by the solutions of the master equation (5.1.17). For $v \neq 0$, there are no known analytical solutions giving a singularity-free geometry. Thus, one has to solve in series expansion around the asymptotic values of the radial coordinate r . These two asymptotics solutions are then connected with a numerical solution. For most purposes, this is almost as good as having an exact solution.

The expansion around $r = \infty$ corresponds to an UV expansion. One could have expected, in the presence of flavors, a Landau pole that would make the geometry singular at some finite value of r ; as we discuss later, this does not happen. The IR expansion does not necessarily have to be around $r = r_0$, as the solution can end at a finite $r_{\text{IR}} > r_0$ (in such a case r_{IR} would be the new origin of the space). An exhaustive study of all the possible expansions can be found in [92].

Here we just mention that there are two possible UV expansions. One is characterized by linearly growing P and Φ , and the other one by an exponentially growing P , and an asymptotically constant dilaton. The behavior of the other metric functions is gathered in table 5.1. In the IR, there are three possible expansions. Since all of these expansions lead to singular solutions, we do not present details about them here.

It must be noted that, *despite the presence of an IR singularity, IR physics can be still extracted from the backgrounds.* Since such type of curvature singularities is relatively common in gauge/gravity constructions, several criteria have been developed in the literature for determining the case in which the singularity does not hinder the application of the gauge/gravity techniques. A very general criterium is the one developed in [85], which says that whenever the time-time component of the metric tensor $g_{x^0 x^0}$ is bounded when approaching the singularity, sensible results can be obtained for IR observables. In such a case, *the singularity is called a “good” singularity.* The CNP IR singularity (for the three different IRs) is of the good type. Indeed, when computing many IR observables, typically the different singular components of the metric combine in such a way that the singular behavior is cancelled out. However, this does not happen for all IR observables, and as we comment later (see the remarks on Wilson loops) even in the cases where sensible results are obtained, the strings propagating close to the curvature singularity still display an unphysical behavior. Thus, it is not clear how much we can trust the results obtained, and a resolution of the

singularity is desirable.

N_f	linear P	exponential P
$< 2N_c$	$P \sim Q \sim 2 - v r$ $e^{2h} \sim \left(1 - \frac{v}{2}\right) r$ $e^{2g} \sim 1$ $e^{2k} \sim 1$ $e^{4(\Phi - \Phi_0)} \sim \frac{\cosh^2(2r_0)}{8(2-v)} \frac{e^{4(r-r_0)}}{r}$ $a \sim 2(2-v) e^{-2(r-r_0)} r$	
$> 2N_c$	$P \sim -Q \sim 2 - v r$ $e^{2h} \sim \frac{1}{4}(v - 1)$ $e^{2g} \sim \frac{1}{2}(v - 2) r$ $e^{2k} \sim v - 1$ $e^{4(\Phi - \Phi_0)} \sim \frac{\cosh^2(2r_0)}{2(v-1)^2(v-2)} \frac{e^{4(r-r_0)}}{r}$ $a \sim e^{-2(r-r_0)} r$	$P \sim c_+ e^{4r/3}$ $e^{2h} \sim \frac{1}{4} c_+ e^{4r/3}$ $e^{2g} \sim c_+ e^{4r/3}$ $e^{2k} \sim \frac{2}{3} c_+ e^{4r/3}$ $e^{4(\Phi - \Phi_0)} \sim \frac{3}{8c_+^3}$ $a \sim 2e^{-2(r-r_0)}$
$= 2N_c$	$P \sim (\text{constant}) = \frac{8}{(4-\xi)\xi}, \quad 0 < \xi < 4$ $e^{2h} \sim \frac{1}{\xi}$ $e^{2g} \sim \frac{4}{4-\xi}$ $e^{2k} \sim 1$ $e^{4(\Phi - \Phi_0)} \sim e^{4(r-r_0)} \cosh^2(2r_0) \frac{(4-\xi)\xi}{16}$ $a \sim \frac{4}{\xi} e^{-2(r-r_0)}$	

Table 5.1: The two classes of leading UV behaviors.

Meaning of the different expansions

All the physics of the CNP background, for a given v , is really codified in the function P , solution of the master equation (5.1.17). Then, the different expansions we found above must represent different physics. This is indeed the case, as the careful analyses in [160, 92] have shown.

The two different UV expansions represent two different UV completions of the theory. Recall that an UV completion must exist because the field theory is coupled to an infinite tower of KK modes and becomes higher-dimensional at high energies. The UV completion provided by the solutions with a linearly growing P is similar to the UV completion of the MN field theory. The dilaton also grows unbounded, an S-duality becomes necessary, and the UV completion should involve Little String Theory (as for MN, although the smearing here makes the picture less clear). The solutions with an exponentially growing P and a bounded dilaton provide a different UV completion, where the theory couples to gravity. The UV of these solutions for different values of v is qualitatively the same, and the analysis can be done for $v = 0$, which we do in section 5.1.4. Although the background is dual to

$\mathcal{N} = 1$ SQCD with a quartic superpotential rigorously only in the IR, the solutions with a linearly growing P will capture some UV features of the theory (the same as in MN, with the reason being the same as in there; see section 5.1.4). Therefore, *in all but the last section of this chapter, we are only interested in the solutions with a linearly growing P .*

Regarding the three IR expansions, they have been connected with the different phases of a non-Abelian gauge theory. One can also study the phase transitions between them and obtain results that match the field theory expectations. These phases can be characterized by the possible expectation values of Wilson and 't Hooft loops⁴ at long distances. Since these expectation values are dual to string-like objects within the gauge/gravity correspondence, they are easy to compute from the supergravity solution. However, as we say later, string-like objects behave strangely close to the IR singularity and again it is unclear whether one should trust these results.

Seiberg duality

Gauge theories with four supercharges and a non-trivial fundamental (or bi-fundamental) matter content enjoy a very interesting non-perturbative duality first unraveled in the seminal work of Seiberg [161]. In his original paper, Seiberg argued that the IR dynamics of SQCD could be understood with the usual “electric” description, that of an $SU(N_c)$ gauge theory with N_f flavors; or alternatively via a “magnetic” description, consisting of an $SU(N_f - N_c)$ gauge theory with N_f flavors interacting with some gauge singlets. The global anomalies of both the electric and magnetic theory match, a precise dictionary between gauge-invariant primary operators can be found (in particular the gauge singlets of the magnetic theory are related to the mesons of the electric theory) so that the 't Hooft anomaly matching conditions are satisfied, and the deformations of the two moduli spaces can be put in correspondence.

Since the gauge/gravity correspondence gives access to non-perturbative physics of gauge theories, it is a very non-trivial check that the CNP supergravity solution encodes Seiberg duality, which is realized in a very beautiful geometrical way, that we promptly describe.

First a caveat. The dual field theory to CNP is not exactly SQCD, but rather SQCD plus an effective superpotential. This superpotential is proposed to be quartic in the fundamental fields ($W \sim \kappa \tilde{Q}Q\tilde{Q}Q$ as in (5.1.42)). Some features of these field theories were very nicely discussed in [98], where it was shown that Seiberg duality acted in an *exact* way, meaning that the duality holds along all the RG flow. The idea is that the $\tilde{Q}Q\tilde{Q}Q$ term of the electric theory becomes a mass term for the gauge singlets (mesons) M of the magnetic theory.

$$W \sim \kappa \tilde{Q}Q\tilde{Q}Q = \kappa MM \rightarrow W_{\text{dual}} \sim \kappa MM + \frac{1}{\mu} \bar{q} M q, \quad (5.1.43)$$

where q stand for the quarks of the “magnetic” theory, and μ parameterizes their coupling with the mesons. In the resulting theory, the mesons are therefore massive and can be integrated out. Doing so leaves a SQCD theory with a quartic superpotential $W_{\text{dual}} \sim \frac{1}{\mu} q\bar{q}q\bar{q}$, as the electric one.

So how does one see Seiberg duality in the CNP background? We should ask ourselves how does one extract the number of colors N_c and flavors N_f from the geometry. For N_c , we

⁴The 't Hooft loop can be roughly thought of as the “Wilson loop for monopoles”.

used equation (5.1.7), and for N_f we looked at the violation of the Bianchi identity (5.1.8). If we stop to think about it, (5.1.7) is somewhat ambiguous, and the ambiguity resides in how we choose the \mathbb{S}^3 over which we are integrating.

What we want is a three-sphere that collects all the RR flux emitted by the color branes. We are choosing the one spanned by $\{\tilde{\theta}, \tilde{\phi}, \psi\}$. But since the color branes are wrapping the Bertolini-Merlatti cycle, which is a 2-cycle mixed among the two two-spheres present in the problem, $\{\theta, \phi\}$ and $\{\tilde{\theta}, \tilde{\phi}\}$; we are clearly discriminating one of the two two-spheres for our choice of the \mathbb{S}^3 . The three-sphere spanned by $\{\theta, \phi, \psi\}$ (call it $\tilde{\mathbb{S}}^3$) would be an equally good choice.

Sticking to this second choice we would read the number of colors \tilde{N}_c as:

$$\frac{1}{2\kappa_{10}^2 T_{D5}} \int_{\tilde{\mathbb{S}}^3} \iota^*(F_3) = -\tilde{N}_c = -(N_f - N_c). \quad (5.1.44)$$

The Bianchi identity does respect the symmetry between the two two-spheres, and therefore this interchange of two-spheres does not affect the number of flavors, *i.e.*

$$\tilde{N}_f = N_f. \quad (5.1.45)$$

So it looks like this ambiguity in the way one extracts the number of colors and flavors produces the same numerology as Seiberg duality. Indeed, we can be more explicit as to how our background can be read in two different ways. Looking at the ansatz (5.1.1), we see that N_c appears explicitly as a prefactor in front of the internal metric. Let us multiply this prefactor by $v - 1$, and divide the internal metric over $v - 1$. We have done nothing. These changes amount to:

$$N_c \rightarrow N_f - N_c, \quad e^{2k} \rightarrow \frac{e^{2k}}{v-1}, \quad e^{2h} \rightarrow \frac{e^{2h}}{v-1}, \quad e^{2g} \rightarrow \frac{e^{2g}}{v-1}. \quad (5.1.46)$$

In the formalism of the master equation we can see that they would read as:

$$v \rightarrow \frac{v}{v-1}, \quad P \rightarrow \frac{P}{v-1}, \quad Q \rightarrow -\frac{Q}{v-1}. \quad (5.1.47)$$

If we go back to the master equation (5.1.17), we see that under these changes, the master equation remains invariant⁵!

In summary, what we are seeing is that *the very same supergravity solution can describe two different theories*. One has gauge group $SU(N_c)$ and N_f flavors, and the other one has gauge group $SU(\tilde{N}_c = N_f - N_c)$ and $\tilde{N}_f = N_f$ flavors. Through the gauge/gravity correspondence, one flips the claim, and what we are saying is that these two theories have the same dynamics (not just long-distance dynamics), and this is the statement of exact Seiberg duality! Since the two possible descriptions of the same supergravity solution correspond to swapping the two two-spheres present in the geometry, we can say that *the geometrical realization of Seiberg duality is the interchange of two two-spheres*.

⁵The CNP parameterization (5.1.19) is more natural for seeing Seiberg duality. The symmetry of the correspondent master equation (5.1.20) is just $Q_{\text{CNP}} \rightarrow -Q_{\text{CNP}}$.

Of course, we just described the most simple numerology of Seiberg duality, and the prescription of the swap of the two-spheres would actually work for any solution with the same ansatz as here, supersymmetric or not. To check that this is really Seiberg duality one has to see that R-symmetry anomalies of the pair of dual theories, that can be computed in the supergravity picture, do actually match. A careful account of these topics can be found in [160].

Wilson loops and other string-like objects

A fundamental observable of the long-distance physics of a theory is the Wilson loop in the fundamental representation. Its expectation value is related to the exponential of the quark-antiquark potential. An analogous quantity is the 't Hooft loop, that gives the potential between monopoles; and one can also consider a loop giving the dyon-antidyon potential (a dyon is an object with both electric and magnetic charge). All these loops are represented by string-like objects in the gravity dual, which probe the ten-dimensional geometry, sitting in the most favorable configuration. The “effective tension” of this configuration determines the potential between the test charges. We will be more detailed in section 5.3.3.

A Wilson loop is proposed to be dual to a fundamental string hanging from the UV boundary, while both the 't Hooft loop and the dyon-antidyon loop are dual to wrapped D3-branes. In the case of the 't Hooft loop, the D3-brane wraps the Bertolini-Merlatti cycle [160], and for the dyon-antidyon one has to incorporate an additional world-volume gauge field [92]. The analysis of these quantities yields the different potentials, that are useful to determine in which phase the dual non-Abelian gauge theory is. This computation runs fine and, despite the IR curvature singularity, one observes a string breaking phenomenon for Wilson loops and obtains finite results for the effective tensions of the other two. The phenomenon of string breaking, realized as a maximum length for the string, is expected in the presence of quarks ($N_f \neq 0$). For long separations, the flux tube between the quarks can decay into mesons: $\bar{Q}Q \rightarrow (\bar{Q}q) + (\bar{q}Q)$.

These results come with a forewarning. As shown in the careful study of [162] for the Wilson loop, the IR singularity of the background makes the strings behave unphysically as we approach to it: except for the case of $v = 2$, the string seems to want to sit at the origin of the space, as for the MN background, but at some point it falls into the singularity, whose gravitational attraction generates a spike of infinite curvature in the string. Presumably, the same situation holds for the other string-like objects (the computation is much more difficult and has not been done in the literature), implying that all these computations, although giving sensible results, should be taken with a grain of salt.

Another quantity that could be computed via string-like objects is the k -string, but the IR singularity wrecks the computation. For more details, see section 5.3.4, where we come back to it once the singularity is resolved.

Domain walls and gaugino condensation

As for SYM, the $U(1)$ R-symmetry of SQCD with N_f flavors self-interacting via a quartic superpotential is broken by quantum effects, $U(1) \rightarrow \mathbb{Z}_{2N_c - N_f}$. The same computation done in the MN model (the analysis of C_2 under large gauge transformations) works in this case

too, and one obtains the aforementioned breaking. Actually, the full breaking sequence is $U(1) \rightarrow \mathbb{Z}_{2N_c - N_f} \rightarrow \mathbb{Z}_2$, again analogously to the MN model. The reason for the last breaking is the formation of a gaugino condensate, and the identification $a \sim < \lambda^2 > \sim \left(\frac{\Lambda_{QCD}}{\mu} \right)^3$, as in MN, holds. This gives the following radius-energy relation for large values of r :

$$\frac{\mu}{\Lambda_{QCD}} \underset{r \gg 1}{\approx} e^{\frac{2}{3}r}. \quad (5.1.48)$$

The last step of the breaking is spontaneous and has the consequence of generating BPS domains walls. Once more, the parallelism with MN is evident, and the tension of these objects can be computed in the same way (namely wrapping a D5-brane on the \mathbb{S}^3 parameterized by $\{\tilde{\theta}, \tilde{\phi}, \psi\}$), and is non-vanishing at the origin of the space.

Beta function

As we will argue in the next subsection, the CNP background with a linearly growing dilaton captures some short-distance physics of the dual theory. In particular, as it happened for MN, the β -function of the theory is a good example of this physics. Since the theory is $\mathcal{N} = 1$ supersymmetric, we have the exact NVSZ beta-function:

$$\beta_{\tilde{g}} = \frac{d\tilde{g}}{d \log \left(\frac{\mu}{\Lambda_{QCD}} \right)} = -\frac{\tilde{g}^2}{1 - \tilde{g}} (3N_c - N_f (1 - \gamma_f)), \quad \tilde{g} = \frac{g^2}{8\pi^2}, \quad (5.1.49)$$

where γ_f is the anomalous dimension of the quark superfield. To extract the gauge coupling from the background, one can use the same probe computation as in MN [95, 96], to obtain⁶

$$\frac{8\pi^2}{g^2} = 2N_c \left(e^{2h} + \frac{e^{2g}}{4}(a-1)^2 \right) = N_c \frac{\cosh(2r - 2r_0) - 1}{\sinh(2r - 2r_0)} P \underset{r \gg 1}{\approx} N_c P. \quad (5.1.50)$$

Notice the naturality of the master equation formalism: the function P is essentially the inverse of the gauge coupling! To compare with (5.1.49), we plug the expansion for the linearly growing P of table 5.1, and neglecting exponentially suppressed terms we get

$$\beta_{\tilde{g}} = -\frac{3}{2} |2N_c - N_f| \frac{\tilde{g}^2}{1 - \tilde{g}} \implies \begin{cases} \gamma_f = -\frac{1}{2} & \text{for } N_f < 2N_c, \\ \gamma_f = \frac{5}{2} & \text{for } \tilde{N}_f < 2\tilde{N}_c \Leftrightarrow N_f > 2N_c. \end{cases} \quad (5.1.51)$$

In the second case, $N_f > 2N_c$, we have to use the Seiberg dual description to match (5.1.49). The huge difference between the anomalous dimensions of the quark superfield in the two cases $N_f < 2N_c$ and $N_f > 2N_c$ is due to the fact that they are quite different theories as the quartic superpotential is irrelevant for the second theory. Still, the two theories can be connected flowing to the case $N_f = 2N_c$, and moving along the space of theories parameterized by the ξ of table 5.1 (which is dual to the quartic coupling κ). A quite detailed account of the story, and more robust arguments to accept the anomalous dimensions

⁶We remind the reader that we are using units where $g_s = 1, \alpha' = 1$, and if we restore units in (5.1.50) the expression would remain invariant, as it corresponds for the dimensionless coupling g .

in (5.1.51), can be found in [160]. The gravity results match the field theory expectations [163, 98]. From (5.1.51), one can notice two additional interesting things.

One is that the theory never develops a Landau pole. A Landau pole is a point in the energy scale where the gauge coupling becomes infinite. For example QED has a Landau pole in the UV. In general, for $\mathcal{N} = 1$ theories one expects a Landau pole for a large number of flavors N_f , where the β -function (5.1.51) would become positive (this is a pathology of D3-D7 systems, *e.g.* [110, 164, 165]). However, one must be careful as non-perturbative effects can hugely modify the anomalous dimensions, as it happens here for $N_f > 2N_c$, rendering the argument invalid.

The other interesting thing is that in the case $N_f = 2N_c$ the coupling does not run asymptotically. Even better, if we take $r_0 \rightarrow -\infty$ in the corresponding expansion of table 5.1, the UV expansion there becomes an exact solution, and the coupling does not run at all. It is possible to check that actually none of the couplings in the theory run. The theory is conformal. However, this is not reflected in the presence of an AdS_5 factor in the metric. The reason might be that the theory still becomes six-dimensional at high energies.

Finally, let us mention that the β -function (5.1.51) gives access to non-perturbative information which might be impossible to grasp with the actual field-theoretical techniques. A relevant question is for instance the existence of a Banks-Zaks mechanism, that would be implied by having two fixed points, one in the IR and another in the UV, where the β -function would vanish. This has been recently investigated in [166], where the IR singularity had to be avoided, and therefore the solutions that we are present in the next sections had to be used.

In summary, the CNP supergravity solution successfully encodes many features we would expect to find in a SQCD-like theory. The main lament one can have about this solution is that it has a curvature singularity at the origin of the space (it is an IR singularity). This singularity hinders the application of gauge/gravity techniques in this region in a fully controlled and trustable manner. It was already clear to the CNP authors in 2006 that this singularity could be resolved by turning on masses for the quarks, but for several years this issue remained unsolved, in contrast to many other setups, like the conifold-related ones [111, 110, 164]. The purpose of the next section is to show how it is possible to get rid of this singularity. Before, let us allow ourselves to make a small digression for the next subsection, where we comment on the solutions on the right column of table 5.1.

5.1.4 Physics of a solution without flavors

The reason for the IR singularity of CNP is the presence of flavor branes. If we remove them, *i.e.* if we put $N_f = 0$, it should disappear. One could expect that this takes us back to the MN solution of section 3.2.2. However, because the ansatz (5.1.1) is more general than (3.2.4), there are additional $\mathcal{N} = 1$ supersymmetric solutions, first found in [108] and then recast in the master equation formalism in [92]. *We call these additional solutions “the exponential solutions”*, for reasons that will become clear below. Let us describe them here.

From the supergravity side

These exponential solutions are known only numerically, unlike the case of the MN solution. The solutions are best expressed in the language of the master equation. The MN solution reads as

$$P = 2r. \quad (5.1.52)$$

The other family of solutions can be characterized by a real parameter β . Solving the master equation with $N_f = 0$, one sees that they have the following expansion close to $r = 0$:

$$P(r) = 2\beta \left[r + \frac{4}{15} \left(1 - \frac{1}{\beta^2} \right) r^3 + \frac{16}{525} \left(1 - \frac{1}{3\beta^2} - \frac{2}{3\beta^4} \right) r^5 + \mathcal{O}(r^7) \right], \quad (5.1.53)$$

where $\beta > 1$. The case $\beta = 1$ truncates to the solution (5.1.52). The parameter h_1 found in [92] is related to β by $h_1 = 2\beta$. The different functions of the ansatz behave for this solution near $r = 0$ as:

$$\begin{aligned} e^{2h} &= \left[\beta r^2 + \frac{4}{45\beta} (-12\beta^2 + 15\beta - 8) r^4 + \mathcal{O}(r^6) \right], \\ e^{2g} &= \left[\beta + \frac{4}{15\beta} (6\beta^2 - 5\beta - 1) r^2 + \frac{16}{1575\beta^3} (3\beta^4 + 35\beta^3 - 36\beta^2 - 2) r^4 + \mathcal{O}(r^6) \right], \\ e^{2k} &= \left[\beta + \frac{4}{5\beta} (\beta^2 - 1) r^2 + \frac{16}{315\beta^3} (3\beta^4 - \beta^2 - 2) r^4 + \mathcal{O}(r^6) \right], \\ e^{4\Phi} &= \frac{4e^{4\Phi_0}}{\beta^3} \left[1 + \frac{4r^2}{9\beta^2} (9r^2 + 4) + \frac{16r^4}{405\beta^4} (135\beta^4 + 150\beta^2 + 62) r^4 + \mathcal{O}(r^6) \right], \\ a &= 1 + \left(-2 + \frac{4}{3\beta} \right) r^2 + \frac{2}{45\beta^3} (75\beta^3 - 116\beta^2 + 40\beta + 8) r^4 + \mathcal{O}(r^6). \end{aligned} \quad (5.1.54)$$

This solution, as the MN one, is regular in the IR. Near $r = 0$, the different curvature invariants are:

$$\begin{aligned} R &= \frac{4e^{-\Phi_0/2}}{3N_c} \beta^{-21/8} + \mathcal{O}(r^2), \\ R_{\mu\nu} R^{\mu\nu} &= \frac{248e^{-\Phi_0}}{27N_c^2} \beta^{-21/4} + \mathcal{O}(r), \\ R_{\mu\nu\rho\sigma} R^{\mu\nu\rho\sigma} &= \frac{16e^{-\Phi_0}}{135N_c^2} \beta^{-21/4} (648\beta^4 - 576\beta^2 + 173) + \mathcal{O}(r). \end{aligned} \quad (5.1.55)$$

Notice that there is only one integration constant in (5.1.53), while the master equation is a second-order equation. It is possible to have another integration constant P_0 such that $P(0) = P_0 \neq 0$ (if so, the function P behaves like $P \sim P_0 + \mathcal{O}(r^3)$). This makes the solution singular, so we are not interested in it here. This solution is useful for other purposes though, such as for modeling walking technicolor models [167, 168].

The function P grows linearly close to $r = 0$, according to (5.1.53), and at some point $r = r_*$ it starts to grow exponentially. *Up to this scale r_* , this solution is very similar to the MN one.* The expansion of P in the UV has the form:

$$P = c_+ e^{4r/3} + \frac{4N_c^2}{c_+} \left(r^2 - r + \frac{13}{16} \right) e^{-4r/3} + \left(c_- - \frac{8c_+}{3} r \right) e^{-8r/3} + \mathcal{O}(e^{-4r}), \quad (5.1.56)$$

where $c_+ > 0$ and c_- are two integration constants. These integration constants are not independent from the ones of the IR expansion, although the relation between them cannot be expressed in a closed analytical form. However it is known that requiring $P(0) = 0$ as in (5.1.53) kills both the integration constant P_0 in the IR and c_- in the UV. The rest of the functions of the metric behave as in the second column of table 5.1. The important point to notice is that the dilaton asymptotes to a constant.

From the field theory side

The key feature of the exponential solutions is the UV-asymptotically constant dilaton. This implies that one does not need to perform the S-duality to go to Little String Theory anymore. These solutions are providing a different UV completion for $\mathcal{N} = 1$ SYM (*i.e.* different from the one provided by the MN solution). Thinking of the dilaton as a sort of warp factor (since it is in front of the metric (5.1.1)), the fact that it goes to a constant can be interpreted as if we were not taking the near-horizon limit⁷. The metric actually becomes asymptotically the metric of the deformed conifold [108]. This means that the UV completion is through gravity.

By studying this different UV completion of $\mathcal{N} = 1$ SYM one can actually learn things about the original MN solution. Besides, the dual theory is not becoming higher-dimensional anymore, and it can be analyzed as a four-dimensional theory. It can be seen [169] that the UV of the theory is driven by an irrelevant operator of dimension eight, whose coupling is c_+^2 . This operator “kicks in” at the scale $r = r_*$, which explains why for $r < r_*$ MN and exponential solutions are similar.

Notice that the scale r_* can be tuned, and increasing it yields a limiting series of exponential solutions that approach the MN solution. One can think of the latter as a solution where the kick-in is delayed forever. In particular, this allows to explain why the MN solution captures the exact NVSZ β -function of $\mathcal{N} = 1$ SYM. If one does the probe computation of [96] in this solution without flavors, one gets far in the UV a β -function completely different from the NVSZ one. However going to a scale below r_* , but still far from the IR, the solution is the MN one and one does get the NVSZ function. This explains “the miracle” of the β -function computation in the MN solution.

So the, the dual theory to these exponential solutions is an $\mathcal{N} = 1$ four-dimensional $SU(N_c)$ theory, which looks like $\mathcal{N} = 1$ SYM in the IR, but contains several operators that can deform both the UV and the IR. Looking at the expansion for P in (5.1.56), the two integration constants c_- and c_+ can be interpreted, in the *AdS/CFT* spirit, as a VEV

⁷In the case of the Maldacena duality, the solution for D3-branes has a warp factor $h = 1 + \frac{Q}{r^4}$. In the near-horizon limit one only keeps the second term $h \sim \frac{Q}{r^4}$, and the warp factor does not go to a constant at infinity anymore.

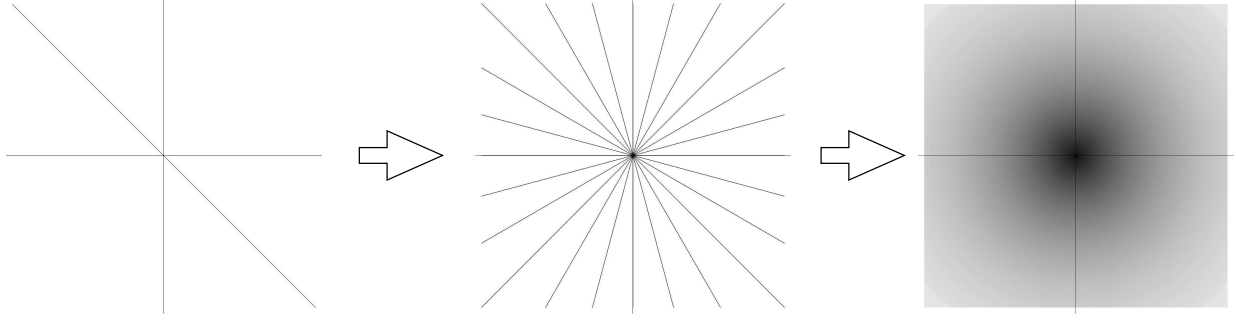


Figure 5.1: Sketch of the smearing procedure for massless flavor branes. Each of the flavor branes passes through the origin of the space. When we smear an infinite number of them (the isometry group in this sketch is simply the rotation group), we generate an infinite mass density at the origin.

for a dimension-two operator (that generates a phenomenon of walking and modifies the IR introducing a singularity there), and as the coupling of a dimension-eight operator that deforms the UV respectively. The latter puts the theory in need of a UV completion which is non field-theoretical. Very interestingly, the theory can be UV-completed in a different way, so that the dimension-eight operator is killed and the completion is four-dimensional. This UV-completion works in very much the same way as how the Standard model completes the Fermi Theory of Weak interactions. We come back to this point in section 5.4.1.

5.2 De-singularizing CNP

From the supergravity point of view, the IR singularity seems to have a unique culprit: an infinite mass density of flavor branes at the origin of the space. Recall that all the N_f flavor branes were extended along the coordinate x^μ, r, ψ , and localized at different transverse coordinates $\theta, \phi, \tilde{\theta}, \tilde{\phi}$. Therefore, at $r = 0$ they all intersect. Since N_f is very large, this generates a mass-density peak that causes a curvature singularity after the backreaction⁸. This is schematically illustrated in figure 5.1. Notice however that this does not always happen. We saw in the previous chapter an example of a configuration of massless flavor branes which did not generate any singularity. The reason was that their backreaction generated an *AdS* space, and $r = 0$ was the bottom of the throat. Since the throat is infinite, the flavor branes crossing there pose no problem.

Then, a way to remove this curvature singularity seems to be to avoid the intersection of all flavor branes. This can be achieved by making the flavor branes pass at a certain distance r_q from the origin of the space, as we show in figure 5.2. Considering what we argued in the introduction, this distance is roughly translated by the dictionary into the mass of the

⁸Another argument, explained to me by Francesco Bigazzi, for the presence of the singularity is the fact that the smeared action we use (see (3.3.3)) is based on using the Abelian DBI action for each of the flavor branes. When they all intersect, this action ceases to be valid as there should be non-Abelian effects to take into account.

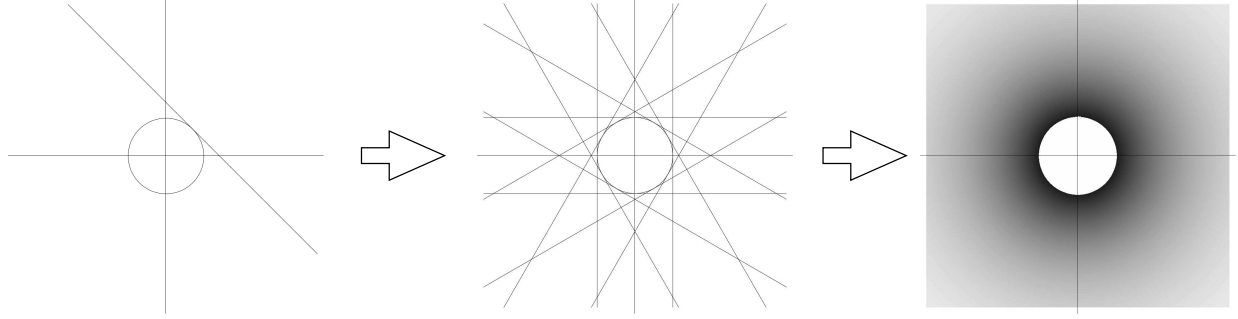


Figure 5.2: Smearing procedure when the flavor branes are “massive”. This means they pass at a certain distance from the origin. There is no point where all the branes intersect.

quarks introduced by the flavor branes: $m_q \sim r_q$. So we conclude that the way to resolve the IR singularity in CNP is by turning on masses for the quarks.

In what follows, we show how this can be technically done, as the problem of computing the backreaction from a smeared set of flavor branes is not trivial at all. We discuss the two approaches to the problem (macroscopic and microscopic), illustrating the ideas presented in section 3.3.1.

5.2.1 The macroscopic approach

Recall that the idea in this approach is to find a suitable modification of the CNP ansatz (5.1.1)-(5.1.3), that accounts for the backreaction of the flavor branes, *i.e.* that solves the equations of motion derived from the action

$$S = S_{\text{IIB}} + S_{\text{flavor branes}} . \quad (5.2.1)$$

This modification can be found in great generality using the power of G-structures [78]. One can then wonder what is the most general ansatz compatible with an $SU(3)$ -structure characterized by:

- the Killing spinors (5.1.9) with α given by (5.1.15),
- a cone-like metric for the internal manifold (*i.e.* with the metric functions depending only on the holographic coordinate),
- having just F_3 flux.

Such generalized ansatz is just a slight modification on the CNP ansatz, where two new components can be added to the RR three-form. It turns out that, after some algebra, this deformation for F_3 can be conveniently written as

$$F_3 = -\frac{N_c}{4} \bigwedge_i (\omega_i - B_i) + \frac{N_c}{4} \sum_i \left(G_i + g_i^{(f)} \right) \wedge (\omega_i - B_i) , \quad (5.2.2)$$

where B_i and G_i are still given as in CNP (see equations (5.1.4)-(5.1.5)):

$$B_1 = -b d\theta, \quad B_2 = b \sin \theta d\phi, \quad B_3 = -\cos \theta d\phi, \quad (5.2.3)$$

$$G_1 = -b' dr \wedge d\theta, \quad G_2 = b' \sin \theta dr \wedge d\phi, \quad G_3 = (1 - b^2) \sin \theta d\theta \wedge d\phi, \quad (5.2.4)$$

and the ansatz for $g_i^{(f)}$ parallels that of G_i :

$$\begin{aligned} g_1^{(f)} &= -\frac{N_f}{2N_c} \frac{S'(r)}{\cosh(2r)} dr \wedge d\theta, & g_2^{(f)} &= \frac{N_f}{2N_c} \frac{S'(r)}{\cosh(2r)} \sin \theta dr \wedge d\phi, \\ g_3^{(f)} &= -\frac{N_f}{N_c} S(r) \sin \theta d\theta \wedge d\phi, \end{aligned} \quad (5.2.5)$$

with $S(r)$ being a new unknown function to be determined. Notice that if S grows slower than e^{2r} (as it will be the case), in the UV (large r), the two-forms $g_i^{(f)}$ that implement the flavor deformation of F_3 are non-vanishing only along the third $\mathfrak{su}(2)$ direction, while the other two components are excited when we move towards the IR. Interestingly, this structure is reminiscent of the way in which the singularity of Abelian MN solution (reviewed in section 3.2.2) is resolved, namely by turning on the function $a(r)$ and making the two-form F_i the field strength of a non-Abelian magnetic monopole.

Therefore, the more general deformation of the CNP solution, preserving its $SU(3)$ -structure as specified above, can be encoded in the addition of a new piece to F_3 , involving just a new function $S(r)$. This is a quite strong statement, made possible by the use of the G-structures machinery. Unfortunately, G-structures tell us nothing about the physics driving this deformation. Is it massive flavor, or are we turning on some other operators in the dual field theory?

In order to answer rigorously this question, which is always posed in the macroscopic approach, we will have to find later (in the next subsection) a microscopic interpretation of our ansatz. For the moment, we content ourselves with delving into this macroscopic approach, finding some hints that the deformation is indeed due to massive flavor. For that, let us first gather together the pieces of the new ansatz, written in Einstein frame. The metric is

$$\begin{aligned} ds^2 = e^{\frac{\Phi}{2}} &\left[dx_{1,3}^2 + N_c \left(e^{2k} dr^2 + e^{2h} (d\theta^2 + \sin^2 \theta d\phi^2) + \right. \right. \\ &\left. \left. + \frac{e^{2g}}{4} ((\omega_1 + a d\theta)^2 + (\omega_2 - a \sin \theta d\phi)^2) + \frac{e^{2k}}{4} (\omega_3 + \cos \theta d\phi)^2 \right) \right], \end{aligned} \quad (5.2.6)$$

as in (5.1.2). We are using the same notation as there, although we take $r_0 = 0$ in what follows⁹. The RR three-form, written above in (5.2.2)-(5.2.5), can be recast in flat coordinates (with reference to the vielbein (5.1.10)) as:

$$F_3 = e^{-\frac{3}{4}\Phi} [f_1 e^{345} + f_2 e^{125} + f_3 (e^{145} + e^{235}) + f_4 (-e^{r13} + e^{r24})], \quad (5.2.7)$$

⁹It turns out that r_0 is not relevant for the solution with massive flavors we are looking for. r_0 just shifts the origin of the space, as in the MN solution, and can be therefore put to zero. The fact that it was relevant for CNP was related to the possibility of having different IRs, which is only attainable when we allow the IR to be singular.

with

$$\begin{aligned} f_1 &= -2N_c e^{-k-2g}, & f_2 &= \frac{N_c}{2} e^{-k-2h} (a^2 - 2ab + 1 - v S), \\ f_3 &= N_c e^{-k-h-g} (a - b), & f_4 &= \frac{N_c}{2} e^{-k-h-g} \left(b' + \frac{v S'}{2 \cosh(2r)} \right). \end{aligned} \quad (5.2.8)$$

Recall $v = N_f/N_c$. From here, the smearing form $\Xi = (2\kappa_{10}^2 T_{D5})^{-1} dF_3$ can be immediately written:

$$\begin{aligned} \Xi &= \frac{N_f}{16\pi^2} \sin \theta d\theta \wedge d\phi \wedge \left[S \omega_1 \wedge \omega_2 - S' dr \wedge \omega_3 \right] + \\ &+ \frac{N_f}{32\pi^2} \frac{S'}{\cosh(2r)} dr \wedge \left[d\theta \wedge \omega_2 \wedge \omega_3 + d\phi \wedge \left(\sin \theta \omega_1 \wedge \omega_3 + \cos \theta d\theta \wedge \omega_2 \right) \right]. \end{aligned} \quad (5.2.9)$$

The first hint that the deformation introduced by S corresponds to massive flavor is ready. In the backgrounds where it is known how to add massive flavors, this is typically done by replacing $N_f \rightarrow N_f S(r)$ in the ansatz for massless flavors. In particular, setting $S = 1$ in the solution for massive flavors should take us to the solution for massless flavors. The latter statement holds (set $S = 1$ in (5.2.9) to recover, taking into account the factor $2\kappa_{10}^2 T_{D5} = 4\pi^2$, (5.1.8)), but the first one does not (observe that the ansatz (5.2.7)-(5.2.8) for F_3 contains S').

This is a somewhat surprising fact. More light can be shed on the issue if we adopt the formalism of the master equation (5.1.14)-(5.1.17). This formalism can be implemented for our new solution including S in very much the same fashion as for CNP. Let us shortcut the derivation of this formalism here (see [23] for details).

As a consequence of supersymmetry, the function b parameterizing the one-forms B_i can be written as:

$$b(r) = \frac{2r + \eta(r)}{\sinh(2r)}, \quad (5.2.10)$$

where $\eta(r)$ is defined as the following integral involving S :

$$\eta(r) = -\frac{v}{2} \left[\tanh(2r) S(r) + 2 \int_0^r d\rho \tanh^2(2\rho) S(\rho) \right]. \quad (5.2.11)$$

One can also integrate partially the BPS system for some of the functions of the metric in terms of $S(r)$. The dilaton can be related to the other functions h , g and k as:

$$e^{-2\Phi} = 2e^{-2\Phi_0} \frac{e^{h+g+k}}{\sinh(2r)}, \quad (5.2.12)$$

where Φ_0 is a constant. If we define the functions $P(r)$ and $Q(r)$ in terms of a and g as in CNP:

$$Q = (a \cosh(2r) - 1) e^{2g}, \quad P = a e^{2g} \sinh(2r), \quad (5.2.13)$$

whose inverse relation is:

$$e^{2g} = P \coth(2r) - Q, \quad a = \frac{P}{P \cosh(2r) - Q \sinh(2r)}, \quad (5.2.14)$$

it turns out that one can express h and k in terms of P , Q and S , namely:

$$e^{2h} = \frac{1}{4} \frac{P^2 - Q^2}{P \coth(2r) - Q}, \quad e^{2k} = \frac{P' + v S(r)}{2}. \quad (5.2.15)$$

So it follows from equations (5.2.12)-(5.2.15) that all the functions of the ansatz are determined in terms of P , Q and S . And what is more, the function Q can be integrated in terms of S as:

$$Q = \coth(2r) \left[\int_0^r d\rho \frac{2 - v S(\rho)}{\coth^2(2\rho)} + q_0 \right], \quad (5.2.16)$$

where q_0 is another constant of integration, that we will fix to zero later to avoid singularities. It only remains to specify what P and S are, and for that we find the new master equation:

$$P'' + v S' + (P' + v S) \left(\frac{P' - Q' + 2v S}{P + Q} + \frac{P' + Q' + 2v S}{P - Q} - 4 \coth(2r) \right) = 0. \quad (5.2.17)$$

Again, once this master equation is solved, the type IIB background is completely characterized. In our pursue to identify the sort of modification S is introducing, the second hint is provided by comparing (5.2.17) with (5.1.17). Putting $r_0 = 0$ and replacing $P'' \rightarrow (P' + v)'$ in the latter, we see that to move from the CNP master equation to the new master equation, the only change needed would be

$$v \rightarrow v S(r) \quad \Leftrightarrow \quad N_f \rightarrow N_f S(r). \quad (5.2.18)$$

Of course the replacement $P'' \rightarrow (P' + v)'$ is done in hindsight, but it comes quite naturally in the master equation formalism. As we said, the change (5.2.18) on the massless ansatz typically amounts to giving mass to the quarks of the theory. This seems to indicate that S should be related to the distribution of flavor branes, and the mass/charge density they generate. For this reason, we will generically use the term *profile* for the function $S(r)$. Through the dictionary, the profile $S(r)$ is sort of counting the fraction of massless degrees of freedom at a given energy scale $\mu \sim r$. Then, on general grounds, one expects $S(\text{deep IR}) = 0$, corresponding to the fact that in the IR all the massive flavors are integrated out, and $S(\text{far UV}) = 1$, since at very high energies any massive quark will look massless. Actually, we expect S to vanish for values of r smaller than a certain scale related to the mass of the quarks. Moreover, S should be an increasing function, in harmony with the idea that degrees of freedom disappear as we move along the RG flow (from short to long distances).

In summary, the macroscopic approach has yielded, as the most general deformation of CNP preserving its $SU(3)$ -structure, a system governed by a master equation involving just two unknown functions P and S , and presumably describing the physics of massive quarks in the CNP theory. Since we only have one equation for two functions, the system is under-determined, *i.e.* one of the functions is completely free. That is the function S , presumably related to how we distribute the flavor branes in the geometry, and about which the macroscopic approach tells us nothing other than some generic features it should possess.

In the next subsection we show how this S can be computed from a microscopic approach, identifying the embeddings where the flavor branes sit, and performing the integral giving the resulting mass/charge density of the smeared system. Once this is done, we just have to input this S back in (5.2.17), and solve the master equation to obtain all the physics we want.

5.2.2 The microscopic approach

We want to find a family of supersymmetric embeddings such that when we smear flavor branes along this family, the backreaction they generate on the geometry is of the form assumed in our ansatz (5.2.6), and the RR charge they induce is compatible with the ansatz for F_3 written in (5.2.7). By construction, we require that all branes are mutually supersymmetric, so that they do not exert force on each other, and the configuration is stable. We then have two tasks:

- one is finding families of supersymmetric embeddings,
- and the other one is checking that their backreaction is compatible with our ansatz.

Both tasks are highly simplified by the tools of complex geometry described in section 5.1.2, which translate directly from the CNP background to ours since they share the same holomorphic structure.

Traditionally, the way of exploring the flora of supersymmetric embeddings of flavor branes has been by looking at the realization of kappa symmetry for probe D-branes. For the MN background of sections 3.2.2, this method was successfully carried out in [114], and it yielded some interesting supersymmetric embeddings. In particular, the ones where the flavor branes are sitting in the CNP background were first found there. Unfortunately, the analysis of kappa symmetry has to be performed in terms of explicit “real” coordinates for the metric, and this becomes very cumbersome for our metric (5.2.6). We clearly need a more systematic approach, where the symmetries of the problem come naturally. This framework is provided by the holomorphic structure of the background.

First of all, we need to identify what is the symmetry operating behind the smearing. We have already done it in (5.1.27): the isometry group of the background is $SU(2)_L \times SU(2)_R$. Thus, once an embedding, called representative or fiducial embedding, is found, the full family follows by simply acting with the isometry group on it. We can then focus on individual embeddings instead of families of them.

In [114] a connection between holomorphy and supersymmetry was made. We can improve it and make a very general claim: *any embedding defined with holomorphic functions of the complex coordinates is supersymmetric*. It is actually straightforward to show this.

We particularize to the case that occupies us now, with complex coordinates defined in (5.1.29), and study the case of an embedding for a D5-brane, extended in the Minkowski directions, and wrapping a two-cycle in the internal space defined in the following way:

$$z_2 = F(z_1), \quad z_3 = G(z_1), \quad \bar{z}_2 = \bar{F}(\bar{z}_1), \quad \bar{z}_3 = \bar{G}(\bar{z}_1), \quad (5.2.19)$$

where, for definiteness, we have chosen z_1 and \bar{z}_1 as world-volume coordinates in the internal space. Recall that $z_4 = z_3^{-1}(z_1 z_2 - 1)$. The calibration form \mathcal{K} for a D5-brane in Einstein frame is given by:

$$\mathcal{K} = e^\Phi d^4x \wedge J. \quad (5.2.20)$$

By using (5.1.30) one can easily get the pullback of this calibration form on the world-volume of the embedding, namely:

$$i^*(\mathcal{K}) = i e^\Phi K d^4x \wedge dz_1 \wedge d\bar{z}_1, \quad (5.2.21)$$

where we have defined the function K as:

$$K = \frac{1}{2} (h_{1\bar{1}} + \bar{F}' h_{1\bar{2}} + \bar{G}' h_{1\bar{3}} + F' h_{2\bar{1}} + F' \bar{F}' h_{2\bar{2}} + F' \bar{G}' h_{2\bar{3}} + G' h_{3\bar{1}} + G' \bar{F}' h_{3\bar{2}} + G' \bar{G}' h_{3\bar{3}}) . \quad (5.2.22)$$

Now, we look at the induced metric $d\hat{s}_6^2$ on the world-volume of the embedding. We get from (5.1.31):

$$d\hat{s}_6^2 = e^{\Phi/2} dx_{1,3}^2 + 2K dz_1 d\bar{z}_1 . \quad (5.2.23)$$

Therefore, $\det [\hat{g}] = e^{2\Phi} K^2$, and one has

$$\sqrt{-\det [\hat{g}]} d^4x \wedge dz_1 \wedge d\bar{z}_1 = i e^{\Phi} K d^4x \wedge dz_1 \wedge d\bar{z}_1 = i^* (\mathcal{K}) , \quad (5.2.24)$$

where $d^4x = dx^0 \wedge dx^1 \wedge dx^2 \wedge dx^3$. This means that the embedding is supersymmetric, proving explicitly that all holomorphic embeddings are supersymmetric.

Now that we have a very general characterization of supersymmetric embeddings, we can tackle the second task of analyzing which of those generate a backreaction compatible with our ansatz. In principle, given a family we should compute the smearing form it would generate through the integral (3.3.13), and compare it with the one derived from our ansatz (5.2.9). This is nothing short of a Herculean task, as a brief look to the computation in 5.A will convince you of. We need a faster method.

It was already discussed in the final part of section 3.3.1 that the families of embeddings “getting along” with our ansatz can be characterized by the compatibility conditions (3.3.27)-(3.3.28). This is much easier than performing the microscopic average, and it is the method we embrace in this subsection. Recall that this compatibility condition arised from the comparison between the action for the whole set of N_f flavor branes and the one corresponding to a representative embedding. Let us show how this condition looks like for our present case.

We choose to work with the WZ actions. Then, we need to impose equation (3.3.24). And for that, we need to know the RR six-form potential C_6 , which is determined from supersymmetry. Indeed, since $F_7 = -e^{\Phi} * F_3 = dC_6$, it follows from the first of the BPS conditions in (5.1.13) that C_6 can be written in terms of the form J as

$$C_6 = e^{\frac{3\Phi}{2}} d^4x \wedge J . \quad (5.2.25)$$

Recall we wrote J explicitly in (5.1.32). The actions we have to compute are

$$S_{\text{WZ}}^{\text{smearred}} = T_{\text{D5}} \int_{\mathcal{M}_{10}} C_6 \wedge \Xi , \quad S_{\text{WZ}}^{\text{single}} = T_{\text{D5}} \int_{\text{D5}} i^* (C_6) . \quad (5.2.26)$$

The one on the left can be readily obtained by plugging the expressions of Ξ and C_6 written in (5.2.9) and (5.2.25) respectively. After integrating over the angular coordinates, one gets a remarkably simple expression, namely:

$$S_{\text{WZ}}^{\text{smearred}} = 2\pi N_f T_{\text{D5}} \int d^4x dr e^{2\Phi} \left(e^{2k} S + \frac{1}{2} e^{2g} \tanh(2r) S' \right) . \quad (5.2.27)$$

To compute the WZ action of a single brane, we notice that the non-compact two-cycle \mathcal{C}_2 that the flavor D5-branes wrap can be parameterized by the radial coordinate r and an angular variable. After integrating over the latter, the WZ action can be represented as:

$$S_{\text{WZ}}^{\text{single}} = 2\pi T_{\text{D5}} \int d^4x dr e^{2\Phi} \mathcal{S}(r), \quad (5.2.28)$$

where the function $\mathcal{S}(r)$ is related to the integral of the pullback of J along the two-cycle by:

$$\int_{\mathcal{C}_2} i^*(J) = 2\pi \int dr e^{\frac{\Phi}{2}} \mathcal{S}(r). \quad (5.2.29)$$

By plugging (5.2.27) and (5.2.28) into (3.3.24) we arrive at the following relation between the profile $S(r)$ and the function $\mathcal{S}(r)$:

$$e^{2k} S + \frac{1}{2} e^{2g} \tanh(2r) S' = \mathcal{S}(r). \quad (5.2.30)$$

The function \mathcal{S} appearing on the right-hand side of (5.2.30) depends both on the embedding and on the different functions of our ansatz. As the compatibility condition (3.3.27) says, it will be only possible to obtain the profile function S from (5.2.30) in the case in which \mathcal{S} depends only on the functions k and g , and this dependence is the same as on the left-hand side of (5.2.30). This is a highly non-trivial condition which most families of embeddings do not satisfy (see appendix 5.A for more details). Let us present in what follows one that does the job¹⁰.

A class of compatible embeddings

In terms of the holomorphic coordinates (5.1.29) the simplest embeddings one can think of are those characterized by two linear relations of the z_i . The representative embedding we want to focus on can be written in terms of the holomorphic coordinates (5.1.29) as the following two linear equations:

$$z_3 = A z_1, \quad z_4 = B z_2, \quad (5.2.31)$$

where A and B are two complex constants. We can parameterize the two-surface defined by (5.2.31) in terms of, for example, z_1 :

$$z_2 = \frac{1}{1 - AB} \frac{1}{z_1}, \quad z_3 = A z_1, \quad z_4 = \frac{B}{1 - AB} \frac{1}{z_1}. \quad (5.2.32)$$

This allows us to get the relation between r and z_1 :

$$2 \cosh(2r) = (1 + |A|^2) |z_1|^2 + \frac{1 + |B|^2}{|1 - AB|^2} \frac{1}{|z_1|^2}, \quad (5.2.33)$$

¹⁰This is actually the only one we have found. But it needs not be unique, and actually we found embeddings which yield different UV asymptotics for S . Unfortunately, these embeddings only work for the Abelian version of the background; although it is likely that there exists their non-Abelian generalization.

where we have used the relation between r and the holomorphic coordinates written in (5.1.23). From (5.2.33) we can compute the minimum distance r_q that this embedding reaches, namely:

$$\cosh(2r_q) = \frac{\sqrt{1+|A|^2}\sqrt{1+|B|^2}}{|1-AB|}. \quad (5.2.34)$$

Notice that this minimum distance depends on the modulus of the constants A and B , as well as on the phase of AB . In order to compute the function $\mathcal{S}(r)$ for these embeddings, we have to compute the pullback of J . For this, it is essential that we use the $(1,1)$ -forms defined in (5.1.38). Since J is invariant under the $SO(4)$ isometry group, it is possible to express it in terms of the η_i of (5.1.37) as:

$$e^{-\frac{\Phi}{2}} J = \frac{1}{2i} \left[\frac{e^{2k}}{\sinh^2(2r)} \eta_2 - a e^{2g} \left(\eta_1 + \frac{\cosh(2r)}{\sinh^2(2r)} \eta_2 \right) + e^{2g} \frac{a \cosh(2r) - 1}{\sinh^2(2r)} \eta_3 \right]. \quad (5.2.35)$$

Another relevant quantity that should be also invariant under the $SO(4)$ isometry is the smearing form Ξ in (5.2.9), since it is giving us the charge distribution of the system. It is a $(2,2)$ -form which can be cast in terms of $(1,1)$ -forms as follows:

$$16\pi^2 \Xi = -\frac{2N_f S}{\sinh^2 2r} \eta_1 \wedge \left(\eta_1 + \frac{2 \cosh(2r)}{\sinh^2 2r} \eta_2 \right) + \frac{N_f S'}{\sinh^3 2r} \eta_2 \wedge \left(\eta_1 - \frac{1}{\cosh(2r)} \eta_3 \right). \quad (5.2.36)$$

Using the complex coordinates z_i to obtain first the pullback of the η_i forms:

$$\begin{aligned} i^*(\eta_1) &= \frac{1}{2} \left((1+|A|^2)|z_1|^2 + \frac{1+|B|^2}{|1-AB|^2} \frac{1}{|z_1|^2} \right) \frac{dz_1 \wedge d\bar{z}_1}{|z_1|^2} = \cosh(2r) \frac{dz_1 \wedge d\bar{z}_1}{|z_1|^2}, \\ i^*(\eta_2) &= -\frac{1}{4} \frac{((1+|B|^2) - (1+|A|^2)|1-AB|^2|z_1|^2) dz_1 \wedge d\bar{z}_1}{|1-AB|^4 |z_1|^4} = \\ &= (\cosh^2(2r_q) - \cosh^2(2r)) \frac{dz_1 \wedge d\bar{z}_1}{|z_1|^2}, \\ i^*(\eta_3) &= \frac{|A+\bar{B}|^2}{|1-AB|^2} \frac{dz_1 \wedge d\bar{z}_1}{|z_1|^2} = \cosh^2(2r_q) \frac{dz_1 \wedge d\bar{z}_1}{|z_1|^2}, \end{aligned} \quad (5.2.37)$$

the pullback of J is readily computed:

$$e^{-\frac{\Phi}{2}} i^*(J) = \left(e^{2k} \frac{\cosh(4r) + 1 - 2 \cosh^2(2r_q)}{\sinh^2(2r)} + e^{2g} \frac{2 \cosh^2(2r_q) - 2}{\sinh^2(2r)} \right) \frac{i}{4} \frac{dz_1 \wedge d\bar{z}_1}{|z_1|^2}. \quad (5.2.38)$$

Magically, the pullback of J only contains the functions e^{2g} and e^{2k} , and it is ready for comparison with the smeared action. In order to obtain the actual value of $\mathcal{S}(r)$ we need to express $dz_1 \wedge d\bar{z}_1 = dr \wedge d(\text{angular})$. With this purpose in mind we will parameterize z_1 as:

$$z_1 = u e^{i\theta}. \quad (5.2.39)$$

Then, one has:

$$\frac{dz_1 \wedge d\bar{z}_1}{|z_1|^2} = -2i \frac{du}{u} \wedge d\theta, \quad (5.2.40)$$

and since from (5.2.33) it follows that:

$$\frac{du}{u} = \pm \frac{\sinh(2r)}{\sqrt{\cosh^2(2r) - \cosh^2(2r_q)}}, \quad (5.2.41)$$

we can write:

$$\int_{\mathcal{C}_2} i^*(J) = 2\pi \int dr e^{\frac{\Phi}{2}} \left(e^{2k} \frac{\sqrt{\cosh(4r) - \cosh(4r_q)}}{\sqrt{2} \sinh(2r)} + e^{2g} \frac{\sqrt{2} \tanh(2r) \cosh(2r) \sinh^2(2r_q)}{\sinh^2(2r) \sqrt{\cosh(4r) - \cosh(4r_q)}} \right). \quad (5.2.42)$$

Thus, the function $\mathcal{S}(r)$ in this case is given by:

$$\mathcal{S} = e^{2k} \frac{\sqrt{\cosh(4r) - \cosh(4r_q)}}{\sqrt{2} \sinh(2r)} + e^{2g} \tanh(2r) \frac{\sqrt{2} \cosh(2r) \sinh^2(2r_q)}{\sinh^2(2r) \sqrt{\cosh(4r) - \cosh(4r_q)}}. \quad (5.2.43)$$

Looking at (5.2.30), we can verify the compatibility condition (3.3.28), and confirm that the coefficients of e^{2k} and $e^{2g} \tanh 2r$ are related by a derivative:

$$\frac{d}{dr} \left[\frac{\sqrt{\cosh(4r) - \cosh(4r_q)}}{\sqrt{2} \sinh(2r)} \right] = 2 \frac{\sqrt{2} \cosh(2r) \sinh^2(2r_q)}{\sinh^2(2r) \sqrt{\cosh(4r) - \cosh(4r_q)}}. \quad (5.2.44)$$

Finally, we get that the profile function $S(r)$ for this family is simply given by:

$$S(r) = \frac{\sqrt{\cosh(4r) - \cosh(4r_q)}}{\sqrt{2} \sinh(2r)} \Theta(r - r_q) = \sqrt{1 - \frac{\sinh^2(2r_q)}{\sinh^2(2r)}} \Theta(r - r_q), \quad (5.2.45)$$

where we have taken into account that $r \geq r_q$ on the cycle. Notice that this S has the qualitative properties we expect it to have: it is an increasing function from $S(0) = 0$ to $S(r) \rightarrow 1$ as $r \rightarrow \infty$, where the massive solution becomes the solution of [108] in the far UV. Notice also that $S(r) = 1$ in (5.2.45) for the massless case $r_q = 0$ and, therefore, we recover the results of [108] in this case. We confirm in appendix 5.A that this is the resulting S of the brane configuration we have, where we perform an explicit microscopic calculation in the UV region of large r of the charge density four-form Ξ generated by such a configuration.

5.2.3 Analysis of singularities

The aim of this section was to get rid of the IR singularity that agitated our souls in CNP. We proposed a way to do that, turning on a mass for the flavors, and we found the corresponding supergravity solution that implemented it. The obvious question is then: has the IR singularity disappeared?

The proper way of characterizing singularities of a geometry is by looking at its invariant quantities, that are obtained as contractions of the Riemann tensor. In particular, we can look at the Ricci tensor of our background, that is determined by the Einstein equations¹¹

¹¹The Einstein equations involve the Einstein tensor $G_{\mu\nu} = R_{\mu\nu} - \frac{1}{2}g_{\mu\nu}R$, rather than the Ricci tensor $R_{\mu\nu}$. But it is easy to obtain one from the other. In ten dimensions, $R = -\frac{1}{4}G_{\mu\nu}g^{\mu\nu}$, and therefore $R_{\mu\nu} = G_{\mu\nu} - \frac{1}{8}g_{\mu\nu}g^{\rho\sigma}G_{\rho\sigma}$.

(see appendix B of [23]):

$$R_{\mu\nu} - \frac{1}{2}g_{\mu\nu}R = \frac{1}{2}\partial_\mu\Phi\partial_\nu\Phi - \frac{1}{4}g_{\mu\nu}\partial_\rho\Phi\partial_\rho\Phi + \frac{1}{24}e^\Phi(6F_{\mu\rho\sigma}F_\nu{}^{\rho\sigma} - g_{\mu\nu}F_3^2) + T_{\mu\nu}^{\text{sources}}, \quad (5.2.46)$$

where $T_{\mu\nu}^{\text{sources}}$ has the schematic form:

$$T_{\mu\nu}^{\text{sources}} = (\text{metric functions}) S + (\text{metric functions}) S'. \quad (5.2.47)$$

Disclosing some information that will be clearer in the next section, it happens that the most singular function on the RHS of (5.2.46) is S' , and for profiles that are identically zero in a neighborhood of $r = 0$, the solution in this region is the same as the unflavored one. The latter has no IR singularity (there are no flavor branes intersecting there to create it), so our solution will not have it either.

So indeed, the IR singularity is not present in the solutions with massive flavors. However, the massive solutions with S given by (5.2.45) exhibit a singularity at $r = r_q$, because the profile there vanishes as:

$$S(r) \sim 2\sqrt{\cosh(2r_q)} \sqrt{r - r_q}, \quad (5.2.48)$$

which means that $S(r)$ is continuous at $r = r_q$, but $S'(r)$ diverges. As we said, it follows from Einstein's equations that this divergence will induce the divergence of the Ricci tensor at $r = r_q$. This divergence is due to the hard-wall effect that we are introducing in our configuration when the flavor branes are added and it should be thought as the gravitational analogue of the threshold effects of field theory. Let us propose a way to resolve this singularity in our string duals.

The idea is to consider branes whose tips reach different radial positions and perform an average over the value r_q of the radial coordinate of the tip of the flavor branes. If we consider branes along compatible embeddings, the backreaction of this new configuration will be also compatible with our ansatz. Actually, this is the way in which the threshold singularity is removed in the Klebanov-Strassler model with massive flavors studied in [164] (see appendix D of [23] for a reconsideration this last model with the tools described in this chapter).

So we will allow r_q to vary on a certain finite interval and we will weight the different values of r_q with a non-negative measure function $\rho(r_q)$, which should be conveniently normalized. In this way the hard wall at $r = r_q$ will be substituted by a shell of non-vanishing width. *If the resulting profile function S and its first radial derivative are continuous the geometry will be free of threshold singularities.* As we will see explicitly below, if the measure function is smooth enough the resulting profile will fulfill the conditions to have a regular supergravity solution.

For convenience let us redefine the radial coordinate as:

$$x = \cosh(4r), \quad x \geq 1. \quad (5.2.49)$$

We also denote $x_q = \cosh(4r_q)$. We consider distributions of branes having x_q in the interval $x_Q \leq x_q \leq x_Q + \delta$, which corresponds in principle to having quarks of different masses. The

way we distribute the tips is characterized by a measure function $\rho(x_q)$ that must obey the normalization condition:

$$\int_1^\infty dx_q \rho(x_q) = 1. \quad (5.2.50)$$

To obtain the profile S for this configuration, we have to modify slightly (3.3.24). Taking into account that the resulting charge density distribution is additive, this modification should be:

$$\left(\int \left(\text{non-radial} \atop \text{coord. of } \mathcal{M}_{10} \right) \mathcal{L}_{\text{smeared}}^{\text{WZ}} \right) (x) = N_f \int_{x_Q}^x dx_q \rho(x_q) \int \left(\text{non-radial} \atop \text{coord. of } \mathbb{D}p \right) \mathcal{L}_{\text{single}}^{\text{WZ}} |_{x_q}, \quad (5.2.51)$$

where $\mathcal{L}_{\text{single}}^{\text{WZ}} |_{x_q}$ is the Lagrangian density for a brane whose tip is at x_q . meaning by this equation that for a given radial distance x , we should compare the smeared action with the sum of the actions of only the flavor branes whose tips x_q are smaller than x . It is then easy to obtain:

$$S(x) = \int_{x_Q}^x dx_q \rho(x_q) \frac{\sqrt{x - x_q}}{\sqrt{x - 1}}. \quad (5.2.52)$$

It is also easy to see from here how the behavior of ρ at the endpoints $x_Q, x_Q + \delta$ translates into the behavior of S there:

$$\begin{aligned} \rho \sim (x - x_Q)^\alpha \quad \text{near} \quad x_Q, & \implies S \sim (x - x_Q)^{\alpha + \frac{3}{2}} \quad \text{near} \quad x_Q, \\ \rho \sim (x - x_Q - \delta)^\beta \quad \text{near} \quad x_Q + \delta. & \implies S \sim (x - x_Q - \delta)^{\beta + \frac{3}{2}} \quad \text{near} \quad x_Q + \delta. \end{aligned} \quad (5.2.53)$$

Thus a measure function with $\delta > 0$, $\alpha, \beta \geq 0$ will guarantee a profile S with continuous first derivative S' . With hindsight, we see that the name of “profile” for the function S might not be the best choice. Equation (5.2.52) shows that S is sort of a functional transform of the function ρ , the latter being really the distribution or profile of the tips of the flavor branes. Actually, (5.2.52) is very closely related to an Abel transform. As shown by [166], in the case $x_Q = 1$, the derivative of S is related to an Abel transform \mathfrak{A} of ρ as:

$$2\partial_x (\sqrt{x - 1} S(x)) = \mathfrak{A}[\rho(x)] = \int_1^x dx_q \frac{\rho(x_q)}{\sqrt{x - x_q}}. \quad (5.2.54)$$

In particular, this allows to invert the relation using the inverse Abel transform, and express ρ in terms of S :

$$\rho(x_q) = \frac{2}{\pi} \partial_{x_q} \int_1^{x_q} dx \frac{(\sqrt{x - 1} S(x))}{\sqrt{x_q - x}}. \quad (5.2.55)$$

What measure ρ to choose

When the measure ρ is a δ -function of the type $\rho(x_q) = \delta(x_q - x_{\bar{q}})$ the profile (5.2.52) reduces to (5.2.45) which, as we have seen, leads to a background with a threshold singularity. To resolve this singularity we just consider measures with a finite width δ and we regard δ as a regularization parameter of the threshold effect. As $\delta \rightarrow 0$ we recover (5.2.45).

Since we are completely free to choose the distribution ρ , or free to choose a reasonable S if you want, one would expect this choice not to be very relevant for the physics derived from the corresponding supergravity solution. This is indeed the case, and one sees that once the parameters x_Q and δ are fixed, the plot of S varies very little for different choices of ρ (see right plot of figure 5.3). For the rest of this chapter, we focus on two particular choices:

- One that is simple in ρ , but yields a not so simple S . This is more natural from the supergravity point of view.
- One that is simple in S , although more complicated in ρ . This is more convenient for numerical purposes, and therefore more natural from a phenomenological point of view.

The first choice for the weighting measure arises from considering the situation in which all the embeddings with different tips in the interval $x_Q \leq x_q \leq x_Q + \delta$ weight the same. This election corresponds to choosing a rectangular step function in the interval $x_Q \leq x_q \leq x_Q + \delta$ which, conveniently normalized, reads:

$$\rho(x_q) = \frac{\Theta(x_q - x_Q) - \Theta(x_q - x_Q - \delta)}{\delta}. \quad (5.2.56)$$

We will refer to this measure as the “flat measure”. Performing the integral (5.2.52) for this measure, we get:

$$\begin{aligned} S(x) &= \frac{2}{3} \frac{(x - x_Q)^{3/2}}{\delta \sqrt{x - 1}} \quad \text{when } x_Q \leq x \leq x_Q + \delta, \\ S(x) &= \frac{2}{3} \frac{(x - x_Q)^{3/2} - (x - x_Q - \delta)^{3/2}}{\delta \sqrt{x - 1}} \quad \text{when } x \geq x_Q + \delta, \end{aligned} \quad (5.2.57)$$

and it is understood that $S(x) = 0$ for $x \leq x_Q$. In figure 5.3 (left) we have plotted the function $S(x)$ for different values of the width δ . As shown in this figure, when δ is increased, $S(x)$ grows slower in the transition region and, thus, $S(x)$ is a milder function of x . It can be straightforwardly checked that S and its first derivative are continuous everywhere¹². Thus, this profile function gives rise to a solution without threshold singularities, as we desired.

The second choice comes from selecting a measure that gives a simple S . By simple we mean, for instance, that the integral (5.2.16) can be explicitly performed. In the case $x_Q = 1$, a very nice possibility is [166]:

$$S = \tanh(2r)^4 = \left(1 - \frac{2}{1+x}\right)^2. \quad (5.2.58)$$

¹²The second derivative S'' does actually have a singular behavior at the threshold points $x_Q, x_Q + \delta$. This would make derivatives of the Ricci tensor singular. Nonetheless, at the level we are working on the supergravity approximation, these terms are neglected in the supergravity action (they are higher order in α'). Including them would change the type IIB action, and therefore the whole background would change as well.

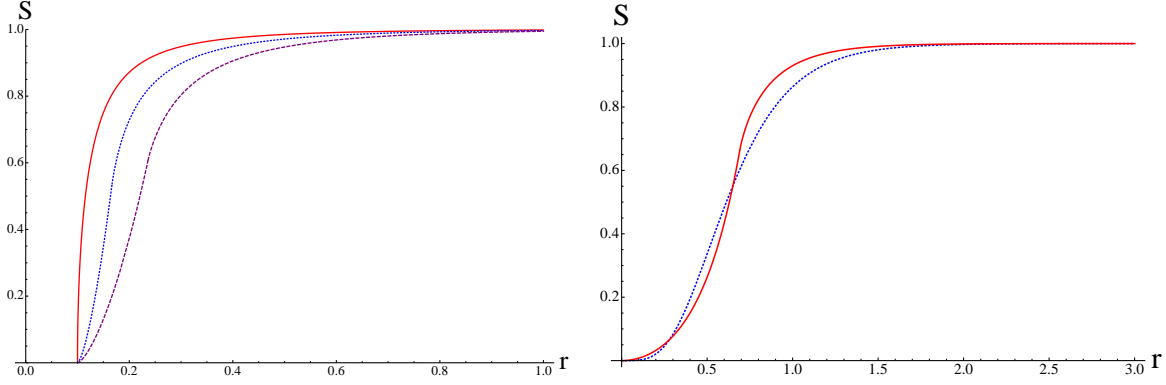


Figure 5.3: We show plots of the function S for the flat measure on the left. The red solid curve is the singular profile, the blue dotted one is for $\delta = 0.15$ and the purple dashed one is for $\delta = 0.4$. On the right we plot S for the two different choices in the text. The red solid line corresponds to (5.2.57) and the blue dotted one to (5.2.58). Despite the very different measures giving rise to them, we see that the profiles are very similar.

This comes from a bit unnatural measure

$$\rho(x_q) = \frac{15(x_q - 1)}{\sqrt{2}(1 + x_q)^{\frac{7}{2}}}, \quad (5.2.59)$$

where the tips are spreaded all the way from $r = 0$ to $r = \infty$, but concentrated around $r = \operatorname{arccoth}\left(\sqrt{\frac{7+2\sqrt{10}}{3}}\right)$, as one could see by plotting S' . From there, it is possible to define a sense of width δ for this distribution as well. For this second choice, S and all of its derivatives are smooth, making the corresponding supergravity background free of singularities as well.

What is the mass of the flavors?

Recapitulating, we have been able to resolve the IR singularity of CNP by giving a mass to the quarks introduced via flavor branes in the supergravity picture. This is done by placing the branes along embeddings that do not reach the origin, *i.e.* their tip is at a finite radial distance. The isometries of the background are used to smear the branes. In addition, in order not to have threshold singularities, all branes must not reach the same minimal distance, and we also have to distribute their tips on a shell. This distribution is characterized by a measure we are free to choose, and any “reasonable” distribution with a finite width yields a non-singular geometry.

The need for this tip-spreading procedure is clear from the supergravity point of view. However, it is a bit unclear from the field theory point of view. The dictionary says that the mass of a quark introduced by a flavor brane is equal to the minimal energy an open string hanging from it can have. We present a possible interpretation right after equation (5.3.1). Equipped with the way to produce regular backgrounds we have described hitherto in this chapter, we move on to the task of finding them explicitly, *i.e.* solving the master equation, and then use them to describe the physics of some $\mathcal{N} = 1$ theories.

5.3 Physics of SQCD with massive flavors

In this section, we focus on the most direct application of the formalism described above. That is to build a holographic dual to SQCD with massive quarks. More precisely, the dual field theory we are adding mass to is the one described in 5.1.3. The way we are adding the mass for the fundamentals through the distribution of flavor branes can be interpreted in two ways:

- As the addition of radius-energy-dependent masses for the flavors in the dual field theory — the profile of masses is somewhat related to $S(r)$.
- Recalling that the CNP field theory couples to the flavors according to the superpotential

$$W \sim \tilde{Q}^\dagger \Phi_k Q, \quad (5.3.1)$$

where (\tilde{Q}) Q are the (anti) quark superfields introduced by the sources and Φ_k is a generic KK massive chiral multiplet. The profile is understood as an energy-dependent VEV for the fields Φ_k , that effectively generates an energy-dependent mass term for the flavor multiplets.

While the outcome in both cases is an energy-dependent “distribution of mass”. The second interpretation implements it without breaking the R-symmetry, hence making it our choice.

To study the dynamics of this theory via the gauge/gravity correspondence, we have to find the explicit type IIB supergravity solutions. As we have already said many times, it is enough with solving the master equation.

5.3.1 Solutions of the master equation

The master equation (5.2.17) involves the profile $S(r)$ and the function $Q(r)$ (see (5.2.16)). Notice that in the cases $S = 0$ and $S = 1$, this master equation has been extensively studied in the literature (see especially [92]), and we have briefly reviewed them in section 5.1.3. These cases are precisely the IR and UV limits of the type of profiles $S(r)$ we are interested in, so then the small- and large-radius asymptotics of our solutions are already known. What we have to find is a smooth matching between them.

Recall that in the small- r region ($S = 0$) there is only one type of expansion yielding a regular background; and for the large- r region ($S = 1$) there are two possible UV behaviors, one characterized by a linearly growing P , and another one by an exponentially growing P (recall table 5.1). As we argued in section 5.1.3, the two expansions correspond to different UV dynamics of the field theory, and we are interested in the first one. We just need a solution that interpolates between these two asymptotic behaviors.

We cannot provide an exact analytical solution of the master equation, but we can give analytical expansions in the relevant regions (around $r = 0$, $r = r_Q$ where S starts to grow, and $r = \infty$), and solve numerically in between them.

Analytical matching

On general grounds we expect $S(r)$ to be null up to a certain point $r = r_Q$, where we have enough energy to start seeing the effects of virtual quarks running in the loops. Then it starts growing because as the energy increases it is easier to produce the quarks. It should eventually stabilize around $S(r) = 1$ since at very high energies all the flavors appear to be massless. Although we know the specific functional form of $S(r)$ in some cases, let us keep the discussion more general and assume that $S(r)$ can be expanded in a kind of power series around r_Q as the one below:

$$S(r) = \Theta(r - r_Q) [S_1(r - r_Q)^{1/2} + S_2(r - r_Q) + S_3(r - r_Q)^{3/2} + \mathcal{O}((r - r_Q)^2)] . \quad (5.3.2)$$

It is important to notice that, according to this expansion, although $S(r)$ is continuous, the $\left[\frac{n+1}{2}\right]$ -th derivative will not be, if S_n is the first non-zero coefficient of the expansion. Note that the two profiles displayed in the previous section (given by (5.2.57) and (5.2.58)) are included in this expansion (we only have the odd coefficients for the former, and the even ones for the latter¹³).

Of course up to $r = r_Q$ the solution of the master equation will be the unflavored one, that we can denote by $P_{\text{unfl}}(r)$. There is only one known solution of it yielding a singularity-free geometry. This solution requires taking $q_0 = 0$ in (5.2.16), and we discussed its details in section 5.1.4. Recall that the solution (5.1.53) was characterized by a real parameter $\beta \geq 1$.

From r_Q on, $S \neq 0$, and the master equation must be solved with initial conditions given by the unflavored solution: $P(r_Q) = P_{\text{unfl}}(r_Q)$, $P'(r_Q) = P'_{\text{unfl}}(r_Q)$. The form of the solution will depend on the form of $S(r)$ around $r = r_Q$.

To solve the master equation in power series close to the matching point $r = r_Q$, we need to know the expression for $Q(r)$, which can be obtained from (5.2.16):

$$\begin{aligned} Q(r) = & 2r_Q \coth(2r_Q) - 1 + \frac{\sinh(4r_Q) - 4r_Q}{\sinh^2(2r_Q)}(r - r_Q) - \frac{2v}{3} S_1 \tanh(2r_Q)(r - r_Q)^{3/2} + \\ & + \left(\frac{4(2r_Q \coth(2r_Q) - 1)}{\sinh^2(2r_Q)} - \frac{v}{2} \tanh(2r_Q) S_2 \right) (r - r_Q)^2 + \mathcal{O}((r - r_Q)^{5/2}) . \end{aligned} \quad (5.3.3)$$

As no term is singular in the master equation at $r = r_Q$, the uniqueness and existence theorem for ordinary differential equations guarantees the existence of a unique smooth solution (actually as smooth as $\int dr S$) for this second order differential equation. Therefore, let us propose an expansion for $P(r)$ as:

$$\begin{aligned} P(r) = & P_{\text{unfl}}(r_Q) + P'_{\text{unfl}}(r_Q)(r - r_Q) + P_3(r - r_Q)^{3/2} + P_4(r - r_Q)^2 + \\ & + P_5(r - r_Q)^{5/2} + \mathcal{O}((r - r_Q)^3) . \end{aligned} \quad (5.3.4)$$

Plugging the expansions (5.3.2), (5.3.3) and (5.3.4) in the master equation (5.2.17), we obtain

¹³In equation (5.2.58) we used $r_Q = 0$, but one could think of reinstating a finite r_Q by having something like $S = \Theta(r - r_Q) \tanh^4(2r - 2r_Q)$.

the following solution:

$$\begin{aligned} P_3 &= -\frac{2v}{3}S_1, \\ P_4 &= \frac{1}{2}(P''_{\text{unfl}}(r_Q) - vS_2), \\ P_5 &= -\frac{2v}{5}S_3 + \frac{8v}{15}S_1 P'_{\text{unfl}}(r_Q) \frac{P_{\text{unfl}}(r_Q) - 2r_Q + \tanh(2r_Q)}{(2r_Q \coth(2r_Q) - 1)^2 - P_{\text{unfl}}^2(r_Q)}. \end{aligned} \quad (5.3.5)$$

Since the metric functions are obtained as combinations of P, P', Q, S , they will be clearly continuous at $r = r_Q$. The curvature of our space involves second derivatives of these metric functions. One would then expect to find P''' and S'' in the curvature invariants, and they would be the most dangerous terms. There is a little subtlety though: because of the form of the master equation (5.2.17), the combination $P' + vS$ is less singular than P' and S separately; indeed, $P' + vS$ is as smooth as $\iint dr S$. Because P''' and S'' enter in the curvature invariants precisely through the combination $P''' + vS''$, it turns out that these invariants will be as smooth as $P'' \sim S'$, as we claimed in section 5.2.3. This can be clearer if we power-expand these invariants around $r = r_Q$. Let us illustrate this for instance for the scalar curvature R :

$$R = (\text{constant}) \frac{S_1 \Theta(r - r_Q)}{(r - r_Q)^{\frac{1}{2}}} + (\text{constant}) + (\text{constant}) S_2 \Theta(r - r_Q) + \mathcal{O}\left((r - r_Q)^{\frac{1}{2}}\right). \quad (5.3.6)$$

Clearly our background will present no curvature discontinuity as long as $S_1 = 0, S_2 = 0$, which is the same as saying that P'' is continuous, as we claimed above.

So for our backgrounds, with a function S characterized near r_Q as (5.3.2), no curvature threshold singularity will amount to having $S_1 = 0 = S_2$.

Finally, we characterize the large-radius behavior of the solutions. In the UV we have $S \rightarrow 1$. The asymptotic value $S = 1$ will be reached in a fashion that depends on the particular details of the measure used to compute S . Typically this will be exponentially, *i.e.* $S = 1 - e^{-(\text{number} > 0)r}$. Then, if we neglect the exponentially suppressed terms, we have the same asymptotic expansions as for CNP (for the solutions with a linearly growing P). Quoting the results in [92], we have for the asymptotics of P :

$$P = Q + v \left(\frac{1}{v} + \frac{1}{4Q} + \frac{v-2}{8Q^2} + \frac{16-19v+5v^2}{32Q^3} \right) + \mathcal{O}(Q^{-4}), \quad N_f < 2N_c, \quad (5.3.7)$$

$$P = -Q + v(v-1) \left(\frac{1}{v} - \frac{1}{4Q} - \frac{v-2}{8Q^2} - \frac{16-13v+2v^2}{32Q^3} \right) + \mathcal{O}(Q^{-4}), \quad N_f > 2N_c, \quad (5.3.8)$$

$$P = (\text{constant}) + \mathcal{O}(e^{-\min\{4, (\text{number} > 0)\}r}), \quad N_f = 2N_c. \quad (5.3.9)$$

Notice that to pass from (5.3.7) to (5.3.8) one just has to apply the changes (5.1.47), as the two regimes $N_f < 2N_c$ and $N_f > 2N_c$ are interchanged by Seiberg duality. The asymptotics these expansions generate for the metric functions were already gathered in table 5.1. In the UV, our solution is essentially the same one as the CNP one, corresponding to the fact that at very high-energy any massive quark can be very well approximated by a massless one.

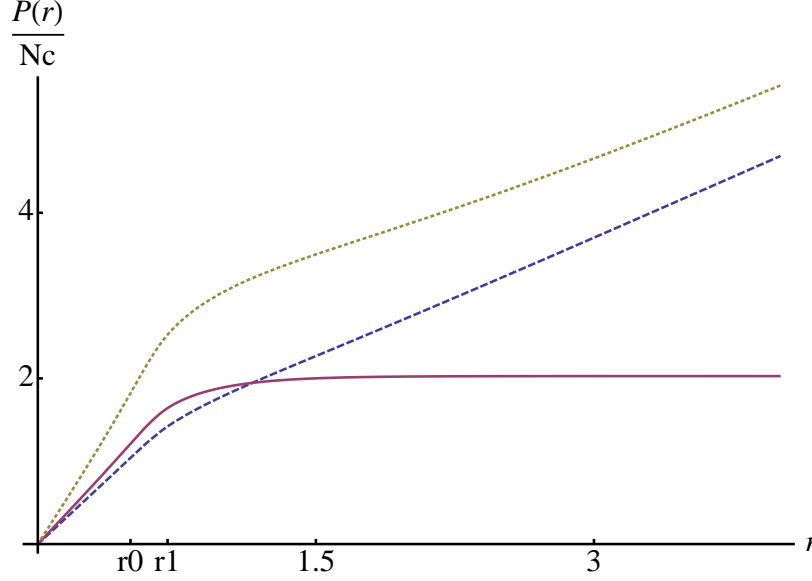


Figure 5.4: Numerical solutions for P for different values of v , keeping fixed the profile (flat measure) and r_Q and δ (in the plot, $\cosh(4r_1) = \cosh(4r_Q) + \delta$). The blue dashed line corresponds to $v = 1$. The purple line corresponds to the conformal case $v = 2$. And the olive dotted line corresponds to $v = 3$. Notice the expected UV asymptotic behaviors.

Numerical matching

If we solve the master equation (5.2.17) numerically, we find, regardless of the specific profile $S(r)$ we use, two qualitatively different behaviors as we go to $r \rightarrow \infty$, which are in correspondence with the two classes of UV that can be found for the CNP solution (recall table 5.1). We have checked that our numerical solutions comply with the UV asymptotic behaviors of equations (5.3.7)-(5.3.9).

In order to solve numerically the master equation, we solve it first in the unflavored region ($r < r_Q$, where $S = 0$) with initial conditions given by the asymptotics (5.1.53). Then we solve again in the flavored region ($r > r_Q$, where $S \neq 0$). In the last step we use as initial conditions $P_{\text{unfl}}(r_Q)$, $P'_{\text{unfl}}(r_Q)$, so that the two solutions, flavored and unflavored can be glued together.

We find that in general the flavored solution only glues nicely (meaning that the solution will reach infinity) with P_{unfl} if we choose β to be bigger than some critical value β_c , which is only known numerically (see figure 5.5) and bigger than 1. This means in particular that the unflavored solution cannot be that of MN, (5.1.52). We observe the following:

Assume the unflavored P up to r_Q is given by the numerical solution characterized in the IR by (5.1.53). Then there exists a β_c such that:

- For $\beta < \beta_c$, P will eventually start decreasing, crossing Q at some finite value of the radial coordinate and making $e^{2h} = 0$ at that point. This solution is then singular.
- For $\beta = \beta_c$, P will reach infinity linearly. This solution has precisely the asymptotics (5.3.7)-(5.3.9), characterized by a linearly growing P and a linearly growing dilaton.

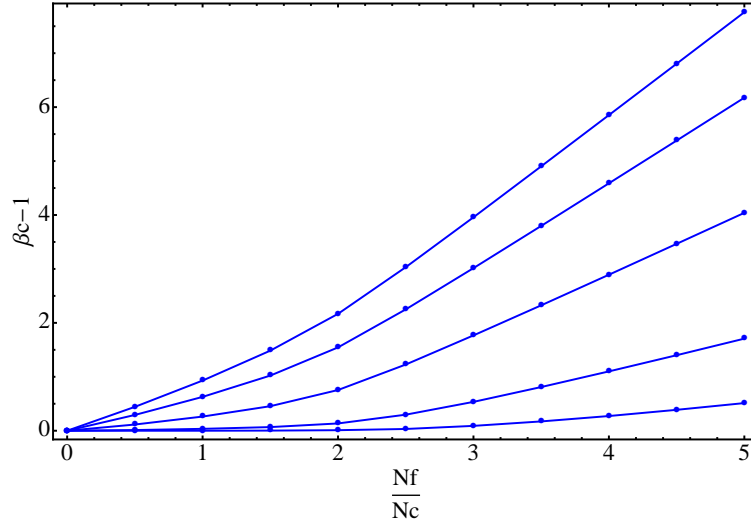


Figure 5.5: We plot the different values of $\beta_c - 1$ as one varies v . The different curves are for different quark masses: moving from the upper curves to the lower ones, the values used are $r_Q = 0, 0.15, 0.3, 0.7, 1.2$; and fixed width $\delta = 0.2$ for the flat measure profile. Notice that as the r_Q increases (the mass increases), the growth of β_c with v is less and less noticeable, and the solution in the unflavored region is almost that of [88] ($\beta_c \simeq 1$). This was to be expected since the more massive the flavors, the less they affect the IR dynamics.

- For $\beta > \beta_c$, P will reach infinity exponentially. This solution possesses the asymptotics characterized by an exponentially growing P , and an asymptotically constant dilaton.

So the IR expansion (5.1.53) can be connected with any of the two known UV behaviors as long as we choose the parameter β appropriately. For an interpretation of our solutions as gravity duals of $\mathcal{N} = 1$ SQCD we are interested in the ones with asymptotically linear dilaton, *i.e.* the ones which have $\beta = \beta_c$. Notice that the IR effects of the flavors will be codified in the dependence of β_c with v . We can then regard β_c as a measure of the deformation induced by the flavors in the IR. In figure 5.5 we explore the dependence of β_c on the number of flavors and their mass.

Even if we fix $\beta = \beta_c$, and for a given ratio v , we can still play with several parameters in the profile $S(r)$, like r_Q , δ or even with the functional form of S itself. The reader may wonder what would be the effect of that. We find that the qualitative behavior of the metric functions does not change. For instance, varying the width of the mass distribution of the quarks δ , just makes more or less sharp the transition from the unflavored region to the flavored one. We gathered in figure 5.6 the plots of the various metric functions for some particular values of the parameters, just to exhibit explicitly this transition from unflavored to flavored background that happens around r_Q .

The solution for massless flavors

Let us take $r_Q \rightarrow 0$ in our expressions, keeping a finite width δ for the measure (recall that also taking $\delta \rightarrow 0$ gives back the singular CNP solution). We still have a profile $S(r)$ for the

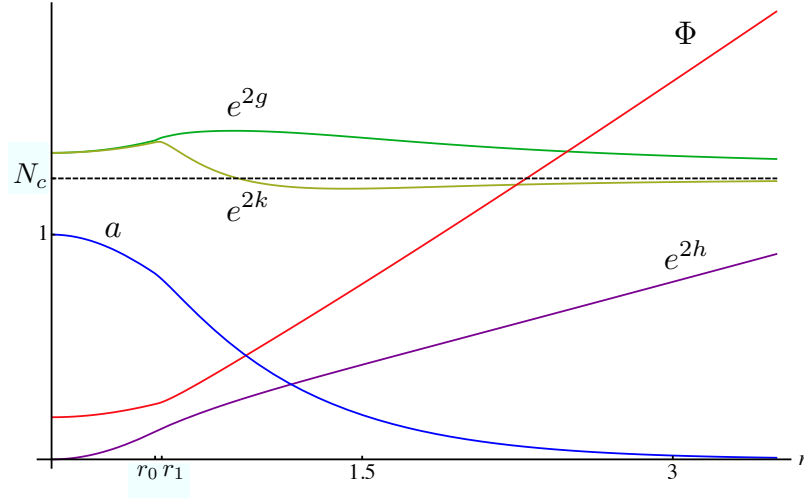


Figure 5.6: Metric functions for a case with $v \neq 2$. We have used the flat measure profile with $r_Q = 0.5$, $\delta = 0.5$. All the functions have the expected asymptotics. Notice in particular the linearly growing dilaton, in red.

flavors, so this solution is not a typical massless-flavor solution, as in [108].

Let us consider the following expansion for the profile function $S(r)$:

$$S(r) = S_1 r + S_2 r^2 + S_3 r^3 + \mathcal{O}(r^4). \quad (5.3.10)$$

We set the first coefficient to zero because we are imposing $S(0) = 0$. This expansion encompasses the results coming from the two measures we chose in section 5.2.3. For this $S(r)$, we have to integrate the differential equation for Q in a series expansion. We get:

$$Q(r) = \frac{4}{3} r^2 - \frac{v}{2} S_1 r^3 - \left(\frac{16v}{45} + \frac{2v}{5} S_2 \right) r^4 + \left(\frac{2v}{9} S_1 - \frac{v}{3} S_3 \right) r^5 + \mathcal{O}(r^6). \quad (5.3.11)$$

The expansion we obtain for P now is:

$$\begin{aligned} P = & 2\beta r - \frac{5v}{4} S_1 r^2 + \frac{8\beta}{15} \left(1 - \frac{9v}{8} S_2 - \frac{1}{\beta^2} + \frac{9v_2}{256\beta^2} S_1^2 \right) r^3 + \\ & + \left(-\frac{7v}{18} S_3 + v S_1 \left(-\frac{34}{135} + \frac{7}{27\beta} + \frac{7v^2}{360\beta} S_2 - \frac{7}{45\beta^2} + \frac{7v^2}{1280\beta^2} S_1^2 \right) \right) r^4 + \mathcal{O}(r^5), \end{aligned} \quad (5.3.12)$$

where β is a free parameter, denoted so by analogy with (5.1.53). We find the following IR asymptotics for the metric functions and the dilaton:

$$\begin{aligned} e^{2h} &= \beta r^2 - \frac{5v}{8} S_1 r^3 - \frac{16\beta}{15} \left(1 - \frac{5}{4\beta} + \frac{9v}{32\beta} S_2 + \frac{2}{3\beta^2} - \frac{9v^2}{1024\beta^2} S_1^2 \right) r^4 + \mathcal{O}(r^5), \\ e^{2g} &= 1 - \frac{5v}{8} S_1 r + \frac{8\beta}{5} \left(1 - \frac{5}{6\beta} - \frac{3v}{16\beta} S_2 - \frac{1}{6\beta^2} + \frac{3v^2}{512\beta^2} S_1^2 \right) r^2 + \mathcal{O}(r^3), \end{aligned}$$

$$\begin{aligned}
e^{2k} &= 1 - \frac{3v}{4} S_1 r + \frac{4\beta}{5} \left(1 - \frac{v}{2\beta} S_2 - \frac{1}{\beta^2} + \frac{9v^2}{256\beta^2} S_1^2 \right) r^2 + \mathcal{O}(r^3) , \\
e^{4(\Phi - \Phi_0)} &= \frac{4}{\beta^3} \left[1 + \frac{2v}{\beta} S_1 r + \left(4 + \frac{v}{\beta} S_2 + \frac{16}{9\beta^2} + \frac{21v^2}{8\beta^2} S_1^2 \right) r^2 + \mathcal{O}(r^3) \right] , \\
a &= 1 - \left(2 - \frac{4}{3\beta} \right) r^2 - \frac{v}{6\beta} \left(3 - \frac{5}{\beta} \right) S_1 r^3 + \mathcal{O}(r^4) .
\end{aligned} \tag{5.3.13}$$

Solving the master equation numerically, we find the same UV behaviors as in the previous analysis, that is, P grows either linearly or exponentially as $r \rightarrow \infty$. Again, the linear behavior can only be reached by choosing β equal to a critical value β_c (see the uppermost curve in 5.5).

We have checked that the solution above presents no curvature singularity in the IR if we choose $S_1 = 0$. For instance, the Ricci scalar near $r = 0$ is given by:

$$R = \frac{3e^{-\Phi_0/2} v S_1}{2N_c \beta^{13/8}} \frac{1}{r} + \mathcal{O}(r^0) , \tag{5.3.14}$$

and the metric is clearly singular at $r = 0$ if $S_1 \neq 0$.

What is done in this subsection *might* be thought as a regular way to introduce massless flavors, as opposite to what happens in [108], where the geometry is singular in the far IR. Nonetheless, we still have a function $S(r)$ related to a non-trivial RG flow. The way we proposed the masses to be generated (around equation (5.3.1)), involving the KK dynamics may hold the key for a clear explanation, that we do not have at the moment.

We can say now that we have solved the problem of finding a regular supersymmetric solution for unquenched massive quarks. It is time to extract the physics holographically encoded in these backgrounds. Our solution should capture those flavor effects for which the fact that the fundamentals are massive is important. Since in the UV our solution reduces to CNP, we expect our formalism to be relevant in the description of the IR physics of the model. In particular, we should be able to address the computation of observables that were haunted by the IR singularity in CNP, like Wilson loops and tensions of k-strings. We should be able to explain also any other feature for which the fact that the quarks are massive is important, like Seiberg duality. Let us deal with these issues in the following subsections.

5.3.2 Seiberg duality

Seiberg duality is an interesting feature of $\mathcal{N} = 1$ four-dimensional gauge theories with flavors. In this section, we briefly comment on the particularities of Seiberg duality in the presence of massive flavors, and explain how these features are realized in our holographic setup.

As discussed in Seiberg's original work [161], to understand the effect of giving a mass to the fundamentals, we can just give a mass to, say, the N_f -th quark flavor. We can now think what happens to the IR theory both in the electric and in the magnetic picture. In the electric picture, the massive flavor will be integrated out in the IR, so that the effective electric theory will have N_c colors and $N_f - 1$ flavors. From the magnetic perspective, the

mass term becomes, after working out the F-term equation of the gauge singlets, a VEV for the magnetic N_f -th quark. The gauge group $SU(N_f - N_c)$ is then broken down through the Higgs mechanism to $SU(N_f - N_c - 1)$, and consequently the IR theory will have $N_f - N_c - 1$ colors and $N_f - 1$ flavors. This magnetic effective description is precisely the (usual) Seiberg dual of the effective electric one just described.

The lesson we should extract is that Seiberg duality in the presence of massive flavors works very much like in the case of massless flavors, but instead of the usual duality relation $(N_c, N_f) \rightarrow (N_f - N_c, N_f)$, one should have $(N_c, N_f^{\text{eff}}) \rightarrow (N_f^{\text{eff}} - N_c, N_f^{\text{eff}})$, where N_f^{eff} is the number of massless flavors. Let us see how this feature is codified in our holographic dual.

We should stress again that the field theory whose dynamics our supergravity background is capturing is not exactly SQCD, but rather SQCD plus a quartic superpotential, and the theory is thus Seiberg self-dual with the same numerology as the usual Seiberg duality of SQCD. As discussed in section 5.1.3, a quick way of detecting this Seiberg self-duality was by realizing that the background was invariant under the change $(N_c, N_f) \rightarrow (N_f - N_c, N_f)$. In the master equation formalism, this corresponded to the changes (5.1.47) leaving the master equation invariant.

In order to see a symmetry like this in our solution for massive flavors, it is better to absorb N_c in the internal part of the metric in (5.1.1), which could be achieved by conveniently re-defining P and Q as:

$$P \rightarrow P_{\text{conv}} = N_c P, \quad Q \rightarrow Q_{\text{conv}} = N_c Q = \coth(2r) \left[\int_0^r d\rho \frac{2N_c - N_f S(\rho)}{\coth^2(2\rho)} \right]. \quad (5.3.15)$$

This is essentially going back to CNP notation (see (5.1.19)). The master equation for these convenient functions is

$$0 = P''_{\text{conv}} + N_f S' + (P'_{\text{conv}} + N_f S) \left(\frac{P'_{\text{conv}} + Q'_{\text{conv}} + 2N_f S}{P_{\text{conv}} - Q_{\text{conv}}} + \frac{P'_{\text{conv}} - Q'_{\text{conv}} + 2N_f S}{P_{\text{conv}} + Q_{\text{conv}}} - 4 \coth(2r) \right). \quad (5.3.16)$$

This equation is invariant under the change $(N_c, N_f S(r)) \rightarrow (N_f S(r) - N_c, N_f S(r))$, that takes $Q_{\text{conv}} \rightarrow -Q_{\text{conv}}$. Taking into account that $N_f S(r)$ is precisely counting how many flavors are effectively massless at a given energy scale, this is exactly what we were expecting to find from the discussion above. Note that the change $(N_c, N_f) \rightarrow (N_f - N_c, N_f)$ is NOT a symmetry of the master equation (5.3.16).

5.3.3 Wilson loops

Let us look now at the behavior of the quark-antiquark potential in the field theory dual to our supergravity solution, that can be studied within the gauge/gravity correspondence. This topic has been treated already in [108] for the case of massless flavors, and extended in [170] to the case of massive flavors. The interest of revisiting this last calculation is the following:

The authors in [170] proposed to use a gravity solution built out of a flavorless solution and a solution with massless flavors, glued at some finite $r = r_Q$, modeling a mass $m_Q \sim r_Q$ for the quarks. This solution would correspond to taking in our formalism $S = \Theta(r - r_Q)$, which would not be singular in the IR, but it would have a very ugly curvature singularity at $r = r_Q$.

With our gravity solution at hand, we can address the study of the quark-antiquark potential in a singularity-free context. Before going on, let us state that the results we obtain are in qualitative agreement with those of [170], where they found that the “connected part” of the static potential between two non-dynamical quarks (i.e. without taking into account the decay into mesons) went from a Coulomb-like law at short separation distances to a confining behavior in the IR. Moreover, depending on the mass of the quarks m_Q , there was a first-order phase transition between these two different behaviors for masses below a certain critical mass m_c .

The quark-antiquark potential can be extracted from the expectation value of a Wilson loop, and the procedure for computing the latter within the gauge/gravity correspondence is well known. The idea is to introduce a probe flavor brane at $r = \infty$ (so that the probe quarks have infinite mass and are non-dynamical) extended along the Minkowski directions as well as wrapping a certain two-cycle¹⁴ in the internal manifold. We attach then a string to this brane, that will hang into the ten-dimensional geometry, reaching a minimum radial distance r_{\min} . We have to compute the energy E of the string and the separation L of the quarks at the end-points of the string for different r_{\min} . We briefly summarize the relevant formulae. For details one can have a look at [162]. Defining:

$$\hat{f}^2 := g_{x^0 x^0} g_{x^i x^i} = e^{2\Phi}, \quad \hat{g}^2 := g_{x^0 x^0} g_{rr} = e^{2\Phi+2k}, \quad \hat{V} := \frac{\hat{f}}{C\hat{g}} \sqrt{\hat{f}^2 - C^2}, \quad (5.3.17)$$

where $C = \hat{f}(r_{\min})$ and we are using string frame, we have that

$$L = 2 \int_{r_{\min}}^{\infty} \frac{dr}{\hat{V}}, \quad E = 2 \int_{r_{\min}}^{\infty} dr \frac{\hat{g} \hat{f}}{\sqrt{\hat{f}^2 - C^2}} - 2 \int_0^{\infty} dr \hat{g}. \quad (5.3.18)$$

Attaching a string to the probe flavor brane we are introducing can be done whenever it is possible to impose Dirichlet conditions on the string end-points. For our geometry, as discussed in [162], this is possible when $\lim_{r \rightarrow \infty} \hat{V}(r) = \infty$. Since for large r , $\hat{V} \sim e^{\Phi-k}$, this conditions holds only for the solutions with an asymptotic linear dilaton. For these solutions we plot the results in figure 5.7.

As mentioned above, the quark-antiquark potential exhibits two different behaviors: an inverse-power law in the UV, and a confining linear behavior in the IR, where the massive quarks have been integrated out, and the dynamics of the unflavored theory is recovered. The transition between these two behaviors can be smooth as in the plot on the right, or a first-order phase transition (the derivative of the energy has a finite jump), as in the plot on the left. As explained in [170], this behavior could be expected whenever we have two scales

¹⁴One can take for instance the limit $r_q \rightarrow \infty$ of our embeddings (5.2.31). One possibility is to take $A = 1 = B$, and the resulting embedding can be characterized in coordinates by $r = \infty$, $\theta = 3\pi/4$, $\phi = 0$.

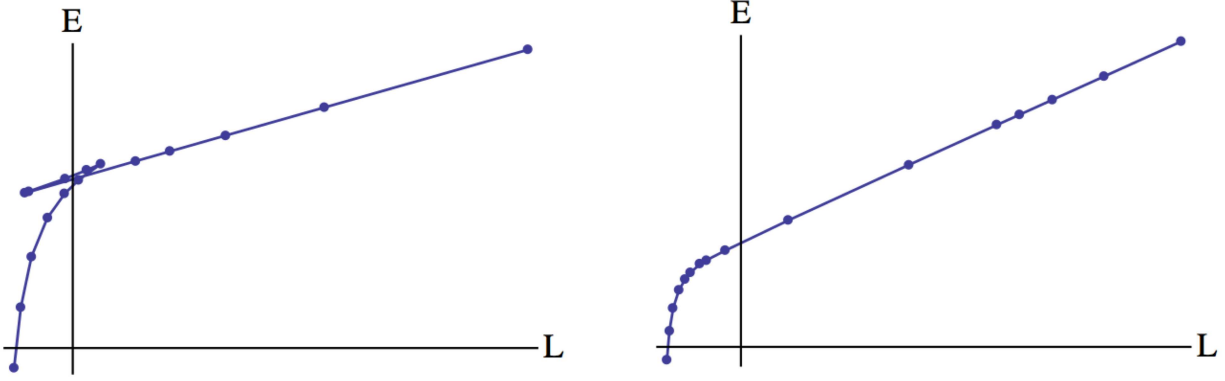


Figure 5.7: We plot the energy of the Wilson loop E vs. the quark separation L . We have fixed $v = 1$, $r_Q = 0.05$ and we use the flat measure profile. For small widths of the brane distribution we have the plot on the left, where we observe a first-order phase transition. As we increase the width, the mass of the heaviest quark becomes of the order of Λ_{QCD} , and the phase transition disappears, as shown in the plot on the right. Notice the similarity between these curves and the G-P (Gibbs free energy vs. pressure) curves of the Van der Waals gas.

in the theory. In the present case, these scales are the gaugino condensate and the mass of the quarks. More precisely, our background does not have a sharp value for the mass of the quarks, but rather a distribution of masses with a certain width. The phase transition shows up when the mass “of the heaviest quark” ($\sim \text{arccoth}(4r_Q + \delta)$) is smaller than a certain critical mass m_c , set by the gaugino condensate.

We could have pursued a more detailed study of these phenomena, like analyzing the dependence of m_c with the number of flavors, their masses, and their distribution, or exploring the decay into mesons characterized by the string breaking length. A fast analysis revealed that the way we distribute the quarks is not very relevant for these observables, and that other features follow qualitatively the behavior described in [170]. We would like to stress though, that the present calculations are performed in a background without any pathology, giving them a more solid foundation.

5.3.4 k-string tensions

One of the most interesting features of the IR physics of confining $\mathcal{N} = 1$ theories is the existence of the so-called k-string states, *i.e.* of flux tubes induced by sources with k fundamental indices (which can be thought as a bound state of k fundamental strings). It was argued in [171] that such a state can be described by D3-branes extended along one of the Minkowski spatial directions, time and wrapping a two-sphere in the IR geometry. For the unflavored MN geometry of section 3.2.2, the tensions of these k-strings obey a sine law.

It is important to notice that, in order to get the results of [171], it is crucial to find the RR two-form potential C_2 . In the approach of [171] the potential C_2 is converted into an NSNS two-form B_2 by means of an S-duality transformation and, then, the flux stabilization mechanism of [172] is applied to determine the configurations that minimize the energy and

to obtain the corresponding tensions. In our flavored background the Bianchi identity of F_3 is violated due to the presence of D5-brane sources (see equation (5.2.9)) and, accordingly, one cannot define the RR potential in regions where Ξ is different from zero. However, in our massive flavored case, the probe D3-brane only explores the deep IR region near $r = 0$, where there are no flavor brane sources since the profile function $S(r)$ always vanishes there. For this reason we can define the potential C_2 in this region and proceed with the analysis of the k-string states. Notice also that, in our low-energy analysis, one would not expect to find k-string breaking due to quark-antiquark pair production. However, we will clearly find screening effects due to quark loops which will modify the tensions.

Let us begin our analysis by studying the IR geometry near $r = 0$. Following [108], we consider the submanifold [96] defined by the conditions $\tilde{\theta} = \theta$, $\tilde{\phi} = 2\pi - \phi$ at $r = 0$. From the IR behavior (5.1.54) of our solutions it is straightforward to verify that the induced metric on this submanifold, in string frame, takes the form:

$$ds^2 = e^{\Phi(0)} \left[dx_{1,3}^2 + N_c \beta \left(d\chi^2 + \sin^2 \chi \left(d\theta^2 + \sin^2 \theta d\phi^2 \right) \right) \right], \quad (5.3.19)$$

where the angle χ is related to the coordinate ψ , which is fixed, by means of the relation: $\chi = (\psi - \pi)/2$. Clearly, the angles χ , θ and ϕ parameterize a non-collapsing three-sphere at the origin $r = 0$, and we should take χ to vary in the range $0 \leq \chi \leq \pi$. Notice also that the constant β characterizes the size of this three-sphere. At $r = 0$ the charge density of the flavor branes vanishes and, as a consequence, there is no violation of the Bianchi identity of F_3 . Therefore, it is possible to represent at this point F_3 in terms of a two-form potential C_2 ($F_3 = dC_2$). It is straightforward to check that C_2 at $r = 0$ in these coordinates takes the form:

$$C_2 = -N_c C(\chi) \sin \theta d\theta \wedge d\phi, \quad C(\chi) = -\chi + \frac{\sin(2\chi)}{2}. \quad (5.3.20)$$

Contrary to the approach followed in [171], we perform our analysis directly in the D5-brane background, without performing the S-duality transformation (see also [173]). Accordingly, let us now consider a probe D3-brane moving in our background. Its dynamics is governed by the action:

$$S_{D3} = -T_{D3} \int_{D3} d^4 \xi e^{-\Phi} \sqrt{-\det[\hat{g} + \mathcal{F}]} + T_{D3} \int_{D3} \mathcal{F} \wedge i^*(C_2), \quad (5.3.21)$$

with \hat{g} being the induced metric on the world-volume of the D3-brane, and \mathcal{F} the world-volume gauge field. We now consider that the D3-brane is extended in (t, x, θ, ϕ) in the metric (5.3.19) at $r = 0$, and at fixed values of χ and of the other two Minkowski coordinates. We also assume that there exists an electric world-volume gauge field \mathcal{F}_{0x} along the Minkowski direction. In this case, the D3-brane action can be written as:

$$S_{D3} = \int dt dx \mathcal{L}, \quad (5.3.22)$$

where we have integrated over the angles (θ, ϕ) and \mathcal{L} is the effective Lagrangian density, given by:

$$\mathcal{L} = -4\pi T_{D3} N_c \left[\beta \sin^2 \chi \sqrt{e^{2\Phi(0)} - \mathcal{F}_{0x}^2} + \mathcal{F}_{0x} C(\chi) \right]. \quad (5.3.23)$$

The equation of motion for the electric world-volume field is:

$$\frac{\partial \mathcal{L}}{\partial \mathcal{F}_{0x}} = \text{constant}, \quad (5.3.24)$$

which is nothing but Gauss' law. Following [174], the constant on the right-hand side of (5.3.24) is fixed by imposing the quantization condition corresponding to having k fundamental strings along the x direction:

$$\frac{\partial \mathcal{L}}{\partial \mathcal{F}_{0x}} = k T_f, \quad k \in \mathbb{Z}, \quad (5.3.25)$$

where $T_f = 1/(2\pi\alpha')$ is the tension of the fundamental string. This condition determines the electric field in terms of the angle χ . Indeed, let us define a new function $\mathcal{C}(\chi)$ as:

$$\mathcal{C}(\chi) \equiv C(\chi) + \frac{\pi k}{N_c}. \quad (5.3.26)$$

Then, one has:

$$\mathcal{F}_{0x} = \frac{e^{\Phi(0)} \mathcal{C}(\chi)}{\sqrt{\beta^2 \sin^4 \chi + \mathcal{C}(\chi)^2}}. \quad (5.3.27)$$

Notice that \mathcal{F}_{0x} is the momentum of a cyclic coordinate that can be eliminated from the Lagrangian. The correct way to do this is by performing the Legendre transformation and computing the Hamiltonian as:

$$H = \int dx \left[\mathcal{F}_{0x} \frac{\partial \mathcal{L}}{\partial \mathcal{F}_{0x}} - \mathcal{L} \right] = 4\pi T_{D3} e^{\Phi(0)} N_c \int dx \sqrt{\beta^2 \sin^4 \chi + \mathcal{C}^2(\chi)}. \quad (5.3.28)$$

Let us minimize the energy with respect to χ . For this purpose it is interesting to notice that the function $\mathcal{C}(\chi)$ satisfies $d\mathcal{C}/d\chi = -2\sin^2 \chi$. Using this property of \mathcal{C} it is straightforward to prove that, for a given integer k , the energy is minimized for the χ_k which satisfies:

$$\mathcal{C}(\chi_k) = \frac{\beta^2}{2} \sin(2\chi_k) \quad \Leftrightarrow \quad \chi_k - \frac{\pi k}{N_c} + \frac{\beta^2 - 1}{2} \sin(2\chi_k) = 0, \quad (5.3.29)$$

which is the equation written in [171] with β instead of the b of [171]. It is also immediate to find the tension of the k -string object, namely:

$$T_k = \frac{e^{\Phi(0)} N_c}{2\pi^2 \alpha'} \beta \sin \chi_k \sqrt{1 + (\beta^2 - 1) \cos^2 \chi_k}. \quad (5.3.30)$$

It is interesting to point out that (5.3.29) does not change under the transformation $k \rightarrow N_c - k$ and $\chi_k \rightarrow \pi - \chi_k$. One can also check that the tension in (5.3.30) does not change under this transformation. Notice also that in the unflavored case reviewed in section 3.2.2 one has $\beta = 1$ and we recover the results in [171, 173, 174]. The case with $\beta \neq 1$ for the generalized unflavored models with the IR behavior (5.1.54) was considered in [108]. Notice that, in our case, the parameter β is related to the mass of the quarks and to the number of flavors by means of the matching conditions discussed in section 5.3.1.

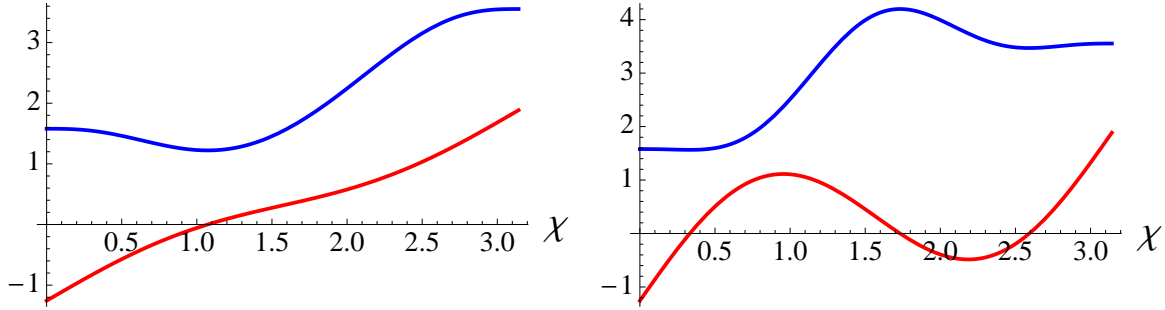


Figure 5.8: The (lower) red curves correspond to the function on the left-hand side of (5.3.29), whose zeros are the angles that extremize the energy (5.3.28). The (upper) blue curves are plots of the energy. We are taking in all cases $k/N_c = 0.4$. On the left, we plot these curves for $\beta = 1.2$ and we see only one zero, which corresponds to the minimum of the energy. On the right, for $\beta = 2$, we notice the appearance of two new zeros, one corresponding to a maximum of the energy, and the other one to a metastable configuration. The true minimum, however, moves towards $\chi = 0$, that is towards the north pole of the sphere, as β is increased.

Let us look at the tension of the k -string as a function of k/N_c , for different values of β . First, we need to solve (5.3.29). Depending on the value of β and k/N_c , we find that there can be up to three different solutions. We then have to check which one corresponds to the true minimum of the energy (5.3.28). We notice that for $k/N_c < 1/2$, the minimum of the energy is given by the solution for χ_k closest to 0 as we can see in figure 5.8, while for $k/N_c > 1/2$, it is the solution closest to π .

Knowing the correct value of χ_k for each β and k/N_c , we can go on and plot the tension (5.3.30) as a function of k/N_c for various values of β , as shown in figure 5.9. When β is close to 1 (which is the smallest value it can reach, corresponding to the unflavored case), the tension of the k -string can be approximated by:

$$T_k \sim \frac{e^{\Phi(0)} N_c}{2\pi^2 \alpha'} \beta \sin\left(\frac{\pi k}{N_c}\right). \quad (5.3.31)$$

Thus, in this low β case, the screening effect due to the flavor is manifested in the tensions by just multiplying the sine formula by the deformation parameter β . In turn, β can be related to the number of flavors and their masses by means of the matching condition studied in section 5.3.1. Notice that, for a given number of strings k , the tension of the flavored k -string is higher than the one corresponding to the unflavored theory. Actually, this is what is expected on general grounds since the screening reduces the (negative) binding energy and, therefore, it increases the total energy (*i.e.* the tension).

As β goes to infinity, the binding energy becomes smaller and smaller and the tension of a k -string is a linear function of k . In this case one can analytically obtain the approximate solution of (5.3.29) which corresponds to the minimum of the energy. Indeed, if β is large the only possibility to solve (5.3.29) is by having $\sin(2\chi_k)$ small. One can show that when $k/N_c < 1/2$ this equation is solved for $\chi_k \approx \pi k / \beta^2 N_c$, while for $k/N_c > 1/2$ the energy is

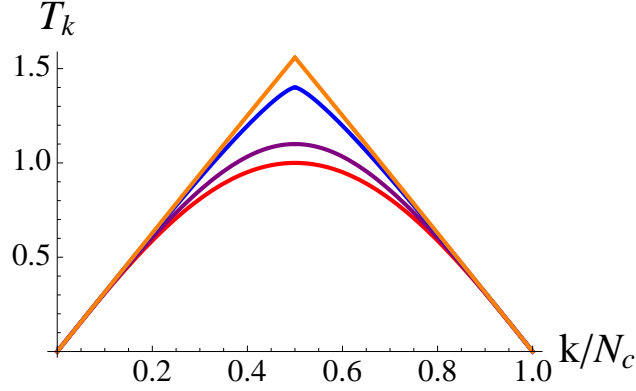


Figure 5.9: This plot corresponds to the tension of the k -string as a function of k/N_c . The values for β are 1 for red, 1.1 for purple, 1.4 for blue and 2 for orange.

minimized for $\chi_k \approx \pi - \pi (N_c - k)/\beta^2 N_c$. The corresponding tensions in these two cases are:

$$e^{-\Phi(0)} T_k \sim \begin{cases} k T_f, & \text{for } 0 \leq k \leq N_c/2, \\ (N_c - k) T_f, & \text{for } N_c/2 \leq k \leq N_c, \end{cases} \quad (5.3.32)$$

which shows that, when β is large, the screening effects are so large that the binding energy is very small and one can regard the flux tube as composed by non-interacting strings with vanishing binding energy. One can visualize this behavior as β is increased in figure 5.9.

5.4 Physics of cascading theories

The techniques presented in section 5.2 not only allow to build type IIB supergravity solutions dual to SQCD-like theories, but also solutions dual to more generic $\mathcal{N} = 1$ theories. Actually, these more general solutions can be obtained from the ones we have already found by “rotating” them in a way we describe in the following subsection. They include non-trivial fluxes F_5 and B_2 , and the dual theories are quiver gauge theories related to the Klebanov-Strassler theory (see section 3.2.3). The phenomenology of these theories is quite rich (a generic feature is the presence of a cascade of Seiberg dualities), and the fact that they are UV-complete and strongly coupled all along the RG flow makes them very interesting objects to study via the gauge/gravity correspondence.

The purpose of this section is then to illustrate how one can construct new supergravity solutions, dual to cascading gauge theories, by rotating the solutions described hitherto in this chapter. The spirit is to write down the equations just for a concrete example of such a construction admitting an exact analytic description, and to describe with words the general case. We want to focus on the physics these backgrounds could encode. Plenty of details on the construction itself, and its many subtleties, can be found in [24], and some nice numerics run for the general case in [25].

5.4.1 The rotation

There are two paramount examples of using the gauge/gravity correspondence to study four-dimensional $\mathcal{N} = 1$ theories. We discussed them in the introduction: the KS solution (section 3.2.3) coming from placing D3-branes on the tip of the deformed conifold, and the MN system (section 3.2.2) obtained when wrapping N_c D5-branes on the two-cycle of the resolved conifold. In this section, *we will refer for convenience to the dual field theories to the KS and MN solutions as the “KS theory” and the “MN theory” respectively.*

Recall the KS theory is a quiver theory with gauge group $SU(n + N_c) \times SU(n)$ and bi-fundamental matter multiplets A_i, B_α with $i, \alpha = 1, 2$. The global symmetries are¹⁵

$$SU(2)_L \times SU(2)_R \times U(1)_B \times U(1)_R. \quad (5.4.1)$$

There is also a superpotential of the form $W = \frac{1}{\mu} \epsilon_{ij} \epsilon_{\alpha\beta} \text{Tr} [A_i B_\alpha A_j B_\beta]$. The field theory is taken to be close to a strongly coupled fixed point at high energies. The dual description, as we said, is given by the Klebanov-Strassler background [84] and its generalizations [100].

The MN field theory [90, 91] has one gauge group $SU(N_c)$ and the global symmetries are those of equation (5.4.1), except for the baryonic symmetry that is not present in this system. The $SU(2)_L \times SU(2)_R$ symmetry is not as explicit (at the Lagrangian level) as in the KS case, since it involves knowing the precise way the KK modes interact.

These two theories, apparently so different, can be connected at the perturbative level as discussed in [175] and [169] via Higgsing. Indeed, giving a particular (classical) baryonic VEV to the fields (A_i, B_α) and expanding around it, the field content and degeneracies of the MN field theory are reproduced (see [175]). This weakly coupled field theory connection has its non-perturbative counterpart in the type IIB solutions dual to each of the field theories. Indeed, it is possible to connect the KS and MN backgrounds using U-duality [175]. This connection was further studied in [169, 176, 177, 178, 179, 180]. A generic way to uncover this connection between different type IIB supergravity backgrounds, is by obtaining one from the other via an algebraic procedure called rotation, that we readily explain.

The *rotation* is a solution-generating technique that, given a solution of the type IIB supergravity equations of motion endowed with an $SU(3)$ -structure, returns a family of different solutions of type IIB supergravity with different $SU(3)$ -structures. In most cases, this procedure is equivalent to the chain of U-dualities originally discussed in [175], where it was shown how to build a family of type IIB supergravity solutions that interpolate between the KS and MN solutions. When one translates this chain of U-dualities into the language of G-structures, it turns out that the procedure is actually a rotation in the space of Killing spinors [176]. Hence the name of rotation. This rotation of G-structures is more general than the chain of U-dualities. The most interesting thing about this generalization is that it allows to rotate solutions with sources, which is what we will do here. It is actually possible to rotate solutions with different G-structures (see [181] for a study of the rotation of G_2 -structures), but our interest is focused just on $SU(3)$ -structures. For these, the rotation works as follows.

Take a solution of type IIB supergravity with metric (5.2.6) (and vielbein (5.1.10)) and RR three-form (5.2.7)-(5.2.8). This means that the functions h, g, k, a, b, Φ are related via

¹⁵The R-symmetry is anomalous, breaking $U(1)_R \rightarrow Z_{2N_c}$.

equations (5.2.10)-(5.2.15) to functions P, Q and S , where Q is known through (5.2.16) (we take $q_0 = 0$), and P satisfies the master equation (5.2.17). The function S is, at the level of the equations, unconstrained. Then one can generate a family of new solutions of type IIB supergravity that we characterize with a vielbein:

$$\begin{aligned} e^{x^i} &= e^{\frac{\Phi}{4}} \hat{h}^{-\frac{1}{4}} dx^i & e^r &= N_c e^{\frac{\Phi}{4}+k} \hat{h}^{\frac{1}{4}} dr, \\ e^\theta &= N_c e^{\frac{\Phi}{4}+h} \hat{h}^{\frac{1}{4}} d\theta, & e^\phi &= N_c e^{\frac{\Phi}{4}+h} \hat{h}^{\frac{1}{4}} \sin \theta d\phi, \\ e^1 &= \frac{N_c}{2} e^{\frac{\Phi}{4}+g} \hat{h}^{\frac{1}{4}} (\omega_1 + a d\theta), & e^2 &= \frac{N_c}{2} e^{\frac{\Phi}{4}+g} \hat{h}^{\frac{1}{4}} (\omega_2 - a \sin \theta d\phi), \\ e^3 &= \frac{N_c}{2} e^{\frac{\Phi}{4}+k} \hat{h}^{\frac{1}{4}} (\omega_3 + \cos \theta d\phi). \end{aligned} \quad (5.4.2)$$

where h, g, k, a, b, Φ remain the same (as before the rotation). Recall the one-forms ω_i were defined in (5.1.6). Keeping also the same f_1, f_2, f_3, f_4 we defined in (5.2.8), the newly generated metric, RR and NSNS fields are

$$\begin{aligned} ds_E^2 &= \sum_{i=1}^{10} (e^i)^2, \\ F_3 &= \frac{e^{-\frac{3}{4}\Phi}}{\hat{h}^{3/4}} \left[f_1 e^{123} + f_2 e^{\theta\phi 3} + f_3 (e^{\theta 23} + e^{\phi 13}) + f_4 (e^{r1\theta} + e^{r\phi 2}) \right], \\ B_2 &= \kappa \frac{e^{\frac{3}{2}\Phi}}{\hat{h}^{1/2}} \left[e^{r3} - \cos \alpha (e^{\theta\phi} + e^{12}) - \sin \alpha (e^{\theta 2} + e^{\phi 1}) \right], \\ H_3 &= -\kappa \frac{e^{\frac{5}{4}\Phi}}{\hat{h}^{3/4}} \left[-f_1 e^{\theta\phi r} - f_2 e^{r12} - f_3 (e^{\theta 2r} + e^{\phi 1r}) + f_4 (e^{1\theta 3} + e^{\phi 23}) \right], \\ C_4 &= -\kappa \frac{e^{2\Phi}}{\hat{h}} dx^0 \wedge dx^1 \wedge dx^2 \wedge dx^3, \\ F_5 &= \kappa e^{-\frac{5}{4}\Phi-k} \hat{h}^{\frac{3}{4}} \partial_r \left(\frac{e^{2\Phi}}{\hat{h}} \right) \left[e^{\theta\phi 123} - e^{x^0 x^1 x^2 x^3 r} \right]. \end{aligned} \quad (5.4.3)$$

We have defined

$$\cos \alpha = \frac{\cosh(2r) - a}{\sinh(2r)}, \quad \sin \alpha = -\frac{2e^{h-g}}{\sinh(2r)}, \quad \hat{h} = 1 - \kappa^2 e^{2\Phi}, \quad (5.4.4)$$

and κ is a positive constant whose absolute value is bounded from above by $e^{-\Phi(\infty)}$. This constant κ is related to the angle of rotation in the space of G-structures, and it is the only free parameter in the rotation. Notice that the last definition in (5.4.4) implies that the rotation can only be performed on solutions with a bounded dilaton. The solutions of the master equation we mainly discussed in the previous section had a linearly growing dilaton, so they do not fulfill this condition, and *precisely the solutions we left out, with an exponentially growing P and asymptotically constant dilaton, are the ones that will be interesting in this section.*

We focus just on a particular solution of the family presented above, which is the one that saturates the bound for κ ; *i.e.* we choose

$$\kappa = e^{-\Phi(\infty)}. \quad (5.4.5)$$

The rationale for this choice is discussed below. The background in equation (5.4.3) has the same form as the one describing the baryonic branch of KS [100]. Indeed, one can check that the BPS equations written in [100] are exactly equivalent to our master equation. Another way of understanding this connection was explained in [176]: what relates the background of the previous section (given in (5.2.6), (5.2.7)-(5.2.8)) with the new one (5.4.3) is a rescaling of the almost-Kähler and complex-structure forms describing the six-dimensional internal space.

Rotating old solutions

The rotation, described above, is a really powerful tool. Finding supergravity solutions with many fluxes turned on is a challenging problem, and the rotation gives a way to do it “just knowing” some simple solution with a single flux. It immediately comes to mind trying the rotation on the MN solution. This cannot be done, since the dilaton is not bounded in that solution, but we can use the closely related exponential solution described in section 5.1.4. A very detailed study of what happens when we rotate the exponential solutions can be found in [169]. Let us briefly summarize it here:

The solutions that come out after the rotation are very similar the supergravity solutions dual to the baryonic branch of the KS theory. To identify the difference, one needs to perform the standard AdS/CFT analysis (that works even though the resulting solutions have no AdS factor). One reduces the ten-dimensional action to a five-dimensional one, identifies the energy scale (exactly as it is done for the MN solution, using the gaugino condensation phenomenon, see equation (5.1.48)), and then studies the UV expansion of the fields. From there, one can extract information about what type of VEVs and operators are turned on. The most relevant ones are the following:

- **Dimension-two VEV.** This is the VEV \mathcal{U} that we mentioned in 3.2.3, that characterizes the baryonic branch. It happens that $\mathcal{U} \sim \frac{1}{c_+}$.
- **Dimension-six VEV.** This appears with a non-zero value for the constant c_- of (5.1.56). This VEV generates a walking behavior.
- **Dimension-eight operator.** We already discussed it in section 5.1.4. The coupling was proportional to c_+^2 .

In the KS baryonic branch, we expect that the two final elements are not present. As we said, the dimension-six VEV can be killed by choosing $c_- = 0$, that amounts to choose $P(0) = 0$ in the IR. The killing of the dimension-eight operator is less obvious, but it can be done with a specific choice of the rotation constant κ , namely (5.4.5). This is easy to see from the expansions written in [169], but it can be motivated by saying that what we want is to get a warp factor that vanishes at large r , which eventually gives a dual QFT that is UV-complete, as it happens for the $AdS_5 \times S^5$ case. Looking at the last equation in (5.4.4), it is clear that the choice (5.4.5) will do the job.

The final conclusion is that we start with an exponential solution, dual to an $SU(N_c)$ gauge theory that is UV-incomplete, and we UV-complete it with an appropriate rotation. The final theory is the cascading KS theory in its baryonic branch. This is a quiver theory

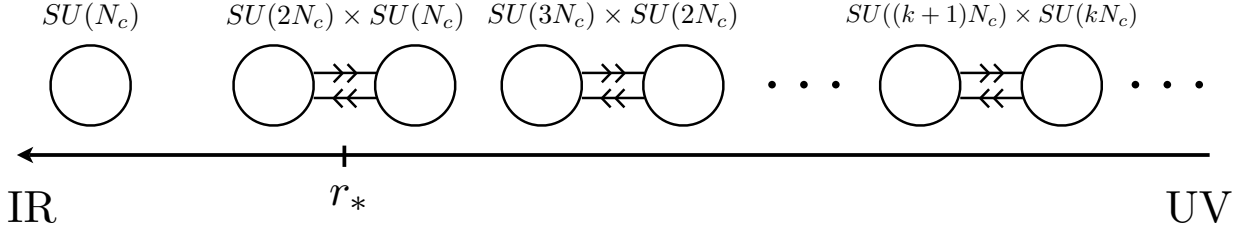


Figure 5.10: Sketch of the RG flow of the theory we obtained after the rotation. The UV completion needed in the unrotated theory above the energy scale given by r_* is provided by the KS cascade. The KS theory is in the baryonic branch.

with gauge group $SU((k+1)N_c) \times SU(kN_c)$, where $k \in \mathbb{Z}$ decreases along the RG flow, becoming equal to zero at the scale $r = r_*$ (see figure 5.10).

Notice that *what we the rotation is doing is UV-completing the theory by un-Higgsing a gauge group*. This is exactly what one does in the Standard model¹⁶, where one takes the Fermi theory, which has a non-renormalizable vertex $\sim G_F \bar{\psi}\psi\bar{\psi}\psi$, and interprets G_F as the inverse squared mass of a very massive gauge field of a new gauge sector. This mass is generated by a VEV v for the Higgs field so that $G_F \sim \frac{1}{v^2}$. This is precisely the relation we got for the dimension-eight operator and the dimension-two VEV discussed above! Moreover, the fact that values of κ different from (5.4.5) do not yield a UV-complete theory can be interpreted, within this analogy, as a bad choice for the matter content of the would-be-UV-completion.

The rotation also works if we try to perform it on a solution with sources, although flavor branes are transformed into a different kind of branes that are not necessarily flavor branes in the dual rotated theory. Then the natural question is what happens when we rotate the CNP solution with the exponential P . This is what [176] tried to answer.

The CNP solution contains only D5 sources, N_f of them. After the rotation, we can consider that we have both D5 and D3 sources, since the presence of the NSNS B_2 field induces D3-brane charge on the D5 flavor branes after the rotation. The D5s are not flavor branes anymore. The proposal in [176] is that the dual field theory is the quiver

$$SU((k+1)N_c + n_f) \times SU(kN_c + n_f + \frac{N_f}{2}), \quad (5.4.6)$$

where n_f is the number of D3-branes induced by the sources, and the field content and superpotential are those of the KS field theory. It was also proposed that the field theory was on a *mesonic branch*. Notice however that this is NOT the mesonic branch of KS, as the rotated theory is wildly different from the KS theory in the UV. Let us see this from the supergravity perspective.

Due to the presence of N_f D5 sources the function P gets a contribution at large values of the radial coordinate (compare with equation (5.1.56)):

$$P(r) = c_+ e^{4r/3} + \frac{9v}{8} + \mathcal{O}(e^{-4r/3}). \quad (5.4.7)$$

¹⁶This beautiful analogy was first explained to me by Carlos Núñez.

One finds that this new term impacts the large-radius asymptotics of the warp factor for the rotated background as

$$\hat{h} = v e^{-4r/3} + \frac{(2-v)^2}{2c_+} r e^{-8r/3} + \mathcal{O}(e^{-8r/3}). \quad (5.4.8)$$

The KS system only has the $e^{-8r/3}$ term, that represents its cascading behavior. This behavior is overcome by the presence of the D3 and D5 sources, and the system is then deviated from the “near AdS_5 ” UV.

The situation in the IR is not much better, as the presence of the small- r singular behavior of the background (inherited from the singularity in the unrotated CNP background), implies that we should not trust the IR dynamics as read from the geometry. As it was clearly stated in [176], a resolution of the singularity was very desirable as it would allow to trust the low energy dynamics of the field theory read from the type IIB background with sources.

It turns out that *these two problems can be solved by introducing the sources with a profile*, as we have just showed how to do in section 5.2. In the next subsections, we perform the rotation of the solutions with profiles, and then proceed to interpret the dual field theory.

5.4.2 Solving the master equation again

We are interested in rotating a background, with a metric (5.2.6) and a RR three-form (5.2.7)-(5.2.8), characterized by a solution of the master equation (5.2.17) that reads as:

$$P \sim c_+ e^{\frac{4r}{3}}, \quad (5.4.9)$$

for large values of r . For the moment we keep a generic profile $S(r)$, with the only initial assumption that it vanishes at the origin $r = 0$ in such a way that there is no IR singularity. This implies that the rotated solution will also be singularity-free. The IR expansion of such a solution is given by (5.1.53).

Since we do not know the solutions of the master equation in analytical form, we have to content ourselves with finding them as numerical interpolations connecting series expansions at the IR and UV that can be computed analytically. Such expansions have been written down in [24]. To illustrate the main differences between rotating solutions with sources introduced with a nice profile and solutions with sources introduced with $S = 1$, as in [176], we do not need those expansions. It is enough with solving the master equation in the limit $c_+ \rightarrow \infty$, where moreover the solution can be written down analytically. Recall that the VEV of the baryonic branch was $\mathcal{U} \propto \frac{1}{c_+}$. Therefore, this limit corresponds to turning off this VEV. In addition, to make sense of this limit, we also have to take $N_f \rightarrow 0 \Leftrightarrow v \rightarrow 0$ in such a way that the product

$$c_+ v =: \nu, \quad (5.4.10)$$

is kept finite. This is done in order to have a well-defined metric in the limit, and it amounts to having D3 sources, but no D5 sources in the background.

Let us work out the derivation of the supergravity solutions in this limit. The master equation (5.2.17) can be rewritten as

$$\partial_r \left(\frac{(P^2 - Q^2)}{\sinh^2(2r)} (P' + v S) \right) + \frac{4}{\sinh^2(2r)} (P' + v S) (Q Q' + P v S) = 0. \quad (5.4.11)$$

Then, we can take this last equation and integrate it twice, to get

$$P^3 - 3PQ^2 + 3 \int_0^r d\tilde{r} (2PQ Q' + v S(P^2 - Q^2)) - \\ - 12 \int_0^r d\tilde{r} \sinh^2(2\tilde{r}) \int_{\tilde{r}}^\infty d\hat{r} \frac{(P' + v S)}{\sinh^2(2\hat{r})} (Q Q' + P v S) = 4\lambda^3 \epsilon^4 \int_0^r d\tilde{r} \sinh^2(2\tilde{r}), \quad (5.4.12)$$

where we have taken into account the IR and UV asymptotics (5.1.53) and (5.4.9), and we have defined the constant λ as:

$$\lambda = 2^{\frac{2}{3}} \frac{N_c}{\epsilon^{\frac{4}{3}}} c_+. \quad (5.4.13)$$

Here ϵ is a dimensionful parameter, such that $\epsilon^{4/3}$ has dimension of length squared, so that (restoring units of $g_s \alpha'$) λ is also a dimensionless parameter. We have introduced ϵ for later convenience, when it will be identified with the deformation parameter of the deformed conifold. *Notice that λ is essentially c_+ , with just some numerical factors in between.* So $c_+ \rightarrow \infty \Leftrightarrow \lambda \rightarrow \infty$. We now propose a solution in an inverse series expansion in λ :

$$P = \lambda P_1 + P_0 + \frac{P_{-1}}{\lambda} + \frac{P_{-2}}{\lambda^2} + \frac{P_{-3}}{\lambda^3} + \dots \quad (5.4.14)$$

Equating factors of λ we get,

$$P_1 = \frac{1}{N_c} \left(4\epsilon^4 \int_0^r d\tilde{r} \sinh^2(2\tilde{r}) \right)^{1/3} = \frac{\epsilon^{\frac{4}{3}}}{2^{\frac{1}{3}} N_c} (\sinh(4r) - 4r)^{1/3}, \\ P_0 = -\frac{v}{P_1^2} \left(\int_0^r d\tilde{r} P_1^2 S - 4 \int_0^r d\tilde{r} \sinh^2(2\tilde{r}) \int_{\tilde{r}}^\infty d\hat{r} \frac{P_1 P_1' S}{\sinh^2(2\hat{r})} \right), \\ P_{-1} = -\frac{1}{P_1^2} \left(P_1(P_0^2 - Q^2) + 2 \int_0^r d\tilde{r} P_1 (v P_0 S + Q Q') - \right. \\ \left. - 4 \int_0^r d\tilde{r} \sinh^2(2\tilde{r}) \int_{\tilde{r}}^\infty d\hat{r} \frac{v P_1 S (v S + P_0') + P_1' (v P_0 S + Q Q')}{\sinh^2(2\hat{r})} \right). \quad (5.4.15)$$

With this, the functions of the ansatz become:

$$e^{2h} = \lambda \frac{\tanh(2r)}{4} P_1(r) + \frac{\tanh(2r)}{4} (P_0 + Q \tanh(2r)) + \\ + \frac{\tanh(2r)}{4 P_1 \lambda} (P_1 P_{-1} - \frac{Q^2}{\cosh^2(2r)}) + \mathcal{O}(\lambda^{-2}), \\ \frac{e^{2g}}{4} = \lambda \frac{\coth(2r) P_1}{4} + \frac{1}{4} (P_0 \coth(2r) - Q) + \frac{P_{-1} \coth(2r)}{4 \lambda} + \mathcal{O}(\lambda^{-2}), \\ \frac{e^{2k}}{4} = \lambda \frac{P_1'}{8} + \frac{v S(r) + P_0'}{8} + \frac{P_{-1}'}{8 \lambda} + \mathcal{O}(\lambda^{-2}), \\ a = \frac{1}{\cosh(2r)} + \frac{Q \tanh(2r)}{P_1 \cosh(2r) \lambda} + \frac{Q \tanh(2r)}{P_1 \lambda^2} (Q \sinh(2r) - P_0 \cosh(2r)) + \mathcal{O}(\lambda^{-3}), \\ e^{4\Phi - 4\Phi_0} = \frac{2 \sinh^2(2r)}{\lambda^3 P_1^2 P_1'} - \frac{2 \sinh^2(2r)}{\lambda^4 P_1^3 P_1'^2} (P_1 (v S + P_0') + 2 P_0 P_1') +$$

$$\begin{aligned}
& + \frac{2 \sinh(2r)^2}{P_1^4 P_1'^3 \lambda^5} (P_1(P'_0 + vS)(2P'_0 P_1 + 2P_0 P'_1 + vP_1 S) - P_0'^2 P_1'^2 + \\
& + P_1'(3P_0'^2 P_1' + P_1' Q^2 - 2P_1 P_1' P_{-1} - P_1^2 P_{-1}')) + \mathcal{O}(\lambda^{-6}), \\
\hat{h} = 1 - \frac{\kappa^2 e^{2\Phi_0}}{\lambda^{3/2}} & \sqrt{\frac{2 \sinh^2(2r)}{P_1^2 P_1'}} + \frac{\hat{h}_f}{\lambda^{5/2}} + \frac{\hat{h}_c}{\lambda^{7/2}} + \mathcal{O}(\lambda^{-9/2}), \tag{5.4.16}
\end{aligned}$$

where we have defined

$$\begin{aligned}
\hat{h}_f &= \frac{\kappa^2 e^{2\Phi_0}}{2P_1 P_1'} \sqrt{\frac{2 \sinh^2(2r)}{P_1^2 P_1'}} (2P_0 P_1' + P_1(vS + P'_0)), \\
\hat{h}_c &= \frac{\kappa^2 e^{2\Phi_0}}{8P_1'^2 P_1^2} \sqrt{\frac{2 \sinh^2(2r)}{P_1^2 P_1'}} \left[-4P_1'^2(2P_0^2 + Q^2) + 4P_1 P_1'(2P_{-1} P_1' - P_0 P'_0) + \right. \\
& \left. + P_1^2(4P_1' P_{-1}' - 3P_0'^2) - 2vP_1 S[3P_1 P'_0 + 2P_0 P_1'] - 3v^2 P_1^2 S^2 \right]. \tag{5.4.17}
\end{aligned}$$

Notice that the expressions for $Q(r), b(r)$ do not change from those in equations (5.2.16) and (5.2.10) respectively. Taking into account the value of $e^{4\Phi(\infty)}$ that can be extracted from (5.4.16), and the choice (5.4.5) we have made, we can write the constant κ as

$$3N_c^3 \kappa^4 = 2\epsilon^4 \lambda^3 e^{-4\Phi_0}. \tag{5.4.18}$$

Now, the limits we have to take are:

$$\lambda \rightarrow \infty, \quad v \rightarrow 0, \quad v \lambda \rightarrow \frac{2^{2/3} N_c}{\epsilon^{4/3}} \nu. \tag{5.4.19}$$

Taking these limits greatly simplify the expansions in (5.4.16).

$$\begin{aligned}
e^{2h} &= \lambda \frac{\tanh(2r)}{4} P_1 + \mathcal{O}(\lambda^0), \quad \frac{e^{2k}}{4} = \frac{P_1' \lambda}{8} + \mathcal{O}(\lambda^0), \\
\frac{e^{2g}}{4} &= \lambda \frac{\coth(2r)}{4} P_1 + \mathcal{O}(\lambda^0), \quad a = \frac{1}{\cosh(2r)} + \mathcal{O}(\lambda^{-1}), \quad e^{4\Phi} = \frac{3e^{4\Phi_0}}{2\epsilon^4 \lambda^3} + \mathcal{O}(\lambda^{-4}), \\
Q &= 2r \coth(2r) - 1 + \mathcal{O}(\lambda^{-1}), \quad b = \frac{2r}{\sinh(2r)} + \mathcal{O}(\lambda^{-1}). \tag{5.4.20}
\end{aligned}$$

And on the function \hat{h} this has two interesting effects. On the one hand, taking $v \rightarrow 0$ considerably simplifies the expression for \hat{h}_c, \hat{h}_f in (5.4.17). On the other hand the scaling $v \lambda = 2^{2/3} N_c \epsilon^{-4/3} \nu$ makes the term $\lambda^{-5/2} \hat{h}_f$ scale like $\lambda^{-7/2} \hat{h}_c$ (that is as λ^{-2}). Indeed in the limit (5.4.19), $\lambda^{-5/2} \hat{h}_f$ becomes

$$\frac{\hat{h}_f}{\lambda^{5/2}} = \frac{4N_c^2}{\lambda^2 \epsilon^{8/3}} \nu \int_r^\infty dx \frac{S(x)}{(\sinh(4x) - 4x)^{1/3}}, \tag{5.4.21}$$

while \hat{h}_c reads as

$$\frac{\hat{h}_c}{\lambda^{7/2}} = \frac{2^{5/3}}{\lambda^2 \epsilon^{8/3}} N_c^2 \int_r^\infty dx \frac{(\sinh(4x) - 4x)^{1/3} (2x \coth(2x) - 1)}{\sinh^2(2x)} + \mathcal{O}(\lambda^{-3}) = \frac{\hat{h}_{KS}}{\lambda^2} + \mathcal{O}(\lambda^{-3}), \tag{5.4.22}$$

where \hat{h}_{KS} is the warp factor of the Klebanov-Strassler solution that we wrote in (3.2.16). Notice that we dropped terms that are suppressed like $\frac{\nu^2}{\lambda^2}$ in the previous expression. Finally, rescaling the Minkowski coordinates $x_i \rightarrow \lambda^{-1/2}x_i$ we have a metric that is independent of the parameter λ . Noticing that

$$\frac{P'_1}{P_1} = \frac{8 \sinh^2(2r)}{3(\sinh(4r) - 4r)}, \quad (5.4.23)$$

we see that the internal space metric is going to be the deformed conifold (3.2.17). Let us write the full background that is obtained in the limit (5.4.19).

The exact and analytic solution

Combining the equations (5.4.21) and (5.4.22), and taking into account the rescaling $x_i \rightarrow \lambda^{-1/2}x_i$, we can write the warp factor as

$$\hat{H} = \frac{4N_c^2}{\epsilon^{8/3}} \nu \int_r^\infty dx \frac{S(x)}{(\sinh(4x) - 4x)^{1/3}} + \hat{h}_{KS}. \quad (5.4.24)$$

The dilaton is constant and we choose it to be:

$$e^\Phi = e^{\Phi(\infty)} = 1. \quad (5.4.25)$$

The full configuration reads

$$\begin{aligned} ds^2 &= \hat{H}^{-1/2} dx_{1,3}^2 + \hat{H}^{1/2} ds_6^2, \\ ds_6^2 &= \frac{\epsilon^{4/3}}{2^{1/3}} (\sinh(4r) - 4r)^{\frac{1}{3}} \left[\frac{4 \sinh^2(2r)}{3(\sinh(4r) - 4r)} \left(dr^2 + \frac{1}{4} (\omega_3 + \cos \theta d\phi)^2 \right) + \right. \\ &\quad \left. + \frac{\tanh(2r)}{4} (d\theta^2 + \sin^2 \theta d\phi^2) + \coth(2r) ((\omega_1 + a d\theta)^2 + (\omega_2 - a \sin \theta d\phi)^2) \right], \\ B_2 &= -\frac{N_c}{4} \frac{2r \coth(2r) - 1}{\sinh(2r)} \left[\cosh(2r) (\sin \theta d\theta \wedge d\phi - \sin \tilde{\theta} d\tilde{\theta} \wedge d\tilde{\phi}) - \sin \theta d\phi \wedge \omega_1 - d\theta \wedge \omega_2 \right], \\ H_3 &= dB_2, \quad F_3 = *_6 H_3, \\ F_5 &= -(1 + *) \left(\partial_r \hat{H}^{-1} dx_0 \wedge dx_1 \wedge dx_2 \wedge dx_3 \wedge dr \right), \\ a &= \frac{1}{\cosh(2r)}. \end{aligned} \quad (5.4.26)$$

To arrive here, there is a little subtlety when taking the limit for B_2 : expanding it in terms of inverse powers of λ , one gets

$$B_2 = \lambda \frac{\epsilon^2 \sinh(2r)}{2\sqrt{3}\kappa P_1 \sqrt{P'_1}} d\left(P_1(\omega_3 + \cos \theta d\phi)\right) - (B_2)_{KS} + \mathcal{O}(\lambda^{-1}), \quad (5.4.27)$$

where $(B_2)_{KS}$ was written in (3.2.18). Using the equation (5.4.15) for P_1 , the overall factor in front of the total derivative in the previous expression is a constant. So the leading order term

in B_2 can be gauged away because it is exact. Then one is left with $B_2 = -(B_2)_{KS} + \mathcal{O}(\lambda^{-1})$ as desired (the sign difference between our result and the one of Klebanov-Strassler comes from a different choice of orientation).

The system (5.4.24)-(5.4.26) is precisely the KS one except for the term proportional to ν in the warp factor. Let us stress that taking $S = 0$ in (5.4.26) (*i.e.* removing the sources) yields exactly the Klebanov-Strassler background. *This is the non-perturbative connection between the KS theory and the MN theory* we announced in section 5.4.1: one starts with the solution of section 5.1.4, dual to the UV-incomplete MN field theory, and UV-completes with the rotation. The UV completion turns out to be given by the KS field theory, which is the baryonic branch of the KS solution (here we only showed the explicit equivalence for the special point where the baryonic VEV $\mathcal{U} = 0$).

Let us now study what is the modification of the KS system introduced by the flavors. Serendipitously, we write the warp factor as

$$\hat{h} = \hat{h}_{KS} + \frac{4N_c^2}{\epsilon^{8/3}} \nu \int_r^\infty dx \frac{S(x) (-4x + \sinh(4x))^{1/3}}{(-4x + \sinh(4x))^{2/3}}. \quad (5.4.28)$$

The function

$$G(r) = \int_r^\infty dx \frac{1}{(-4x + \sinh(4x))^{2/3}}, \quad (5.4.29)$$

is sort of a Green function for the deformed conifold, and indicates that the solution above is just the solution to the Laplace equation (for the function \hat{h}) in the presence of fluxes F_5, H_3, F_3 and D3 sources (see equation (101) in [84]). So, *we have the KS geometry being deformed by a distribution of source D3-branes*

$$n_f \sim \nu S(r) (\sinh(4r) - 4r)^{1/3}, \quad (5.4.30)$$

that are supersymmetric when placed on the deformed conifold¹⁷. Notice the exponentially growing behavior of the second factor in (5.4.30); for the profiles S we have used, such that $S \rightarrow 1$ as $r \rightarrow \infty$, the D3-branes will pile up exponentially as we move along the radial coordinate. We come back to this point in the next subsection.

This exact and analytical solution could have been written without going over all this effort of rotating, just assuming the strange distribution of D3 sources in equation (5.4.30). As we pointed out after equation (5.4.29), this solution was already known in [84], and it is not new. This is not the case for the solutions with λ, N_f finite, whose expansions we do not present here. We comment on them in what follows.

Generic features of the solutions

Recall that the parameter λ is, for $N_f = 0$, the one moving between different VEVs for the baryon and anti-baryon operators. For non-zero values of N_f , an interpretation of the parameter λ was given in [176]. When we do not take the limit $\lambda \rightarrow \infty$, that corresponds to turning off the VEV in the $N_f = 0$ case, the series expansion (5.4.14) is not truncated, and

¹⁷In the language of equation (5.2.19), the embeddings correspond to take $z_1, z_2, z_3 = \text{constant}$, and constant functions are holomorphic, and consequently the embeddings supersymmetric.

one needs all the terms in the power series to describe the background. Another possibility is to study directly the IR and UV expansions for the functions of the background. Both possibilities were studied in detail in [24], and the following are generic features of these solutions, which can actually be read from the exact solution (5.4.24)-(5.4.26).

From the supergravity side, the interesting point to analyze is how the singularities of the solution of [176] are modified by the presence of a non-trivial profile S .

The most immediate one is the IR singularity. The presence of this singularity is not modified by the rotation. *So if one rotates an IR-singular (-regular) solution, the result is another IR-singular (-regular) solution.* Therefore, as in section 5.2.3, to avoid the small- r singularity we have to choose a profile $S(r)$ that makes the number of sources suitably decrease towards $r = 0$. Then, the backgrounds constructed present no pathology at $r \sim 0$, and hence the low-energy strong dynamics of the dual field theory can be calculated using the gauge/gravity correspondence in a trustable manner.

What about the UV of [176], where the sources were driving the system out of its near-conformal point? According to what we wrote in equation (5.4.30), after the rotation, the induced source D3-branes are distributed in such a way that they pile up exponentially towards large values of the radial coordinate as $n_f \sim e^{4r/3}$. This is precisely what produces the solutions' departure from the four-dimensional behavior of the KS cascade. This large pile-up of D3-branes dominates the UV dynamics and is equivalent to the insertion of a dimension-six operator into the Lagrangian, as we can see by expanding the warp factor \hat{h} in equation (5.4.24) giving as a result the one in equation (5.4.8). We analyze in the next subsection how to get rid of this undesirable behavior.

Finally, let us comment on the change of meaning of the function $S(r)$ with the rotation. The function $S(r)$ originated in the supergravity background dual to the MN field theory with D5-brane sources. Its meaning there was that of a profile for the D5-brane charge present in the background. We placed several D5-branes on the geometry, each of them reaching a minimal radial distance. These minimal distances were distributed on a shell¹⁸ with a measure ρ . S is a functional transform of this ρ (see equation (5.2.54)).

This interpretation of $S(r)$ as a profile for the D5-brane charge is however lost after the rotation. We gave an interpretation of $S(r)$ for the exact solution of equation (5.4.26). As explained after equation (5.4.29), in this new solution $S(r)$ accounts for how the D3-branes are distributed in the geometry. So, for this exact solution, $S(r)$ represents a distribution of D3-branes. More precisely, the distribution is given by $S(r) (\sinh(4r) - 4r)^{1/3}$.

5.4.3 Field theory comments

For definiteness, let us focus our attention on backgrounds in the limit $\lambda \rightarrow \infty$ (the one in equation (5.4.26)), but the lessons are valid as well for the backgrounds with finite λ . For the

¹⁸An electrostatic analogue of this situation is given by the electric field created by a hollow cavity with a thick charged shell. In this case $S(r)$ would count the effective radial charge. Inside the cavity $S(r) = 0$ as there is no electric field. As we cross the shell, $S(r)$ increases, and stabilizes to the total charge away from the shell. The electric field outside the shell, will be that of a point charge. Had the shell null thickness, the electric field would display a jump. Away from the shell, $S(r \rightarrow \infty) \sim 1$ in coincidence with the $S(r)$ generated by “massless” sources.

latter, although there are no exact solutions available, the relevant quantities, like the ranks of the gauge groups and the holographic c -function (that “counts” the degrees of freedom of the theory), can be defined in terms of supegravity quantities and studied numerically. The generic conclusions we draw in this subsection can be confirmed in this way for these backgrounds. For details, we refer to the more complete papers [24, 25].

There are two works in the literature that can help us to explain what is happening in the field theory dual to the backgrounds we are considering. One of the works is [99], where Dymarsky et al. studied non-perturbatively the KS theory. They explain that one may think the moduli space for the quiver

$$SU((k+1)N_c + l) \times SU(kN_c + l), \quad (l < N_c), \quad (5.4.31)$$

as l D3-branes free to move on the deformed conifold with $((k+1)N_c)$ D5 together with kN_c anti-D5-branes forming a bound state at the tip. The ways of distributing the l D3-branes give rise to a symmetric product of deformed conifolds as moduli space. *When $l = 0$, the theory is said to be in the baryonic branch, and when $l \neq 0$, this theory describes the mesonic branch of the KS field theory.* It is possible to move from the mesonic branch to the baryonic branch by a process of Higgsings:

$$\begin{aligned} SU((k+1)N_c + l) \times SU(kN_c + l) &\rightarrow SU((k+1)N_c + l - 1) \times SU(kN_c + l - 1) \times U(1) \rightarrow \\ &\rightarrow \dots \dots SU((k+1)N_c) \times SU(kN_c) \times U(1)^l. \end{aligned} \quad (5.4.32)$$

The quiver at the final step has the numerology to fit the baryonic branch of the KS field theory. One must be careful though, as noticed by [99], where they made the point that the $U(1)_{\text{baryonic}}$ is *gauged* as it mixes with the $U(1)^l$. We later reflect on how this is captured by the supergravity solutions.

The other work that is relevant for us is [182], where it was shown that each of the Higgsing processes in (5.4.32) happens, from the gravity side point of view, each time we cross one of the l D3-branes of the background as we move along the radial coordinate towards $r = 0$. This is all the information we need to extract the physics our backgrounds are encoding.

The dual theory at high energies

Let us consider the background of equations (5.4.24)-(5.4.26), with a function $S(r)$ that vanishes for $r \leq r_Q$ and stabilizes to $S(r) \rightarrow 1$ for large values of the the radial coordinate. Getting inspiration in [176], we propose that the dual quiver is of the form

$$SU(n + n_f + N_c) \times SU(n + n_f), \quad n = kN_c, \quad (5.4.33)$$

where k is an integer number that decreases along the RG flow, and n_f is the number of D3-branes (5.4.30). The precise definitions of the charges n and n_f is, in the general case with λ finite:

$$n = \left(\frac{1}{2\kappa_{10}^2} \int_{\Sigma_5} i^*(F_5) \right) \Big|_{v=0}, \quad n_f = \frac{1}{2\kappa_{10}^2} \int_{\Sigma_5} i^*(F_5) - \frac{1}{2\kappa_{10}^2} \left(\int_{\Sigma_5} i^*(F_5) \right) \Big|_{v=0}, \quad (5.4.34)$$

where Σ_5 is the five-dimensional manifold of coordinates $(\theta, \varphi, \tilde{\theta}, \tilde{\varphi}, \psi)$. For the the background of equations (5.4.24)-(5.4.26), one can check that this quantitative definition of n_f coincides with our qualitative expectations (5.4.30). Indeed, the computation of n_f with (5.4.34) yields

$$n_f = 2^{\frac{1}{3}} \pi \nu \frac{S(r) (\sinh(4r) - 4r)^{\frac{1}{3}}}{\tanh(2r)}. \quad (5.4.35)$$

The field theory is in the mesonic branch for $r > r_Q$, where the function $S(r) \sim 1$. As already explained in [176], there we can find two competing processes, as we move down the RG flow. One is the usual cascade of the KS system, represented by the \hat{h}_{KS} in the warp factor of equation (5.4.28). The other one is a Higgsing process, happening because we are crossing D3-branes distributed according to equation (5.4.35), and represented by the term proportional to ν in equation (5.4.28). In the new radial coordinate $z \sim e^{2r/3}$,

$$\hat{h}|_{r \rightarrow \infty} \sim \frac{\nu z^2 + 3N_c^2 \log z}{z^4}, \quad (5.4.36)$$

we see clearly the superposition of the cascade and the Higgsing. The presence of an exponentially increasing number of source D3s effectively behaves as the insertion of an irrelevant operator of dimension six¹⁹, deforming the UV dynamics out of the near-conformal KS dynamics. This indicates the need for a UV completion.

The dual theory at low energies

Flowing towards the IR the Higgsing and cascading lower down the ranks of the groups. The Higgsing acts in such a way that eventually, and close to $r \sim r_Q$, we reach the numerology of the baryonic branch

$$\begin{aligned} & SU(n_f + (k+1)N_c) \times SU(n_f + kN_c) \rightarrow \\ & SU(n_f + (k+1)N_c - 1) \times SU(n_f + kN_c - 1) \times U(1) \rightarrow \\ & \rightarrow \dots \rightarrow SU((k+1)N_c) \times SU(kN_c) \times U(1)^{n_f}. \end{aligned} \quad (5.4.37)$$

The main difference with respect to the usual baryonic branch is, as we already said, the fact that the baryon symmetry is in this case gauged. This symmetry being gauged impacts the low-energy phenomenology. Gauge symmetries do not generate Goldstone bosons, unlike spontaneously broken ones. We can check in the case of the background in equation (5.4.26), that the massless excitation described in [101], dual to a Goldstone boson, is not a solution to the equations of motion. This agrees with the proposal that the theory is on a mesonic branch. For the rest, with a suitable choice of $S(r)$ vanishing conveniently fast at $r = r_Q$, the phenomenology of the low-energy field theory is very similar to that of the Klebanov-Strassler theory, as both backgrounds are quite similar. The computation of various IR quantities will give qualitatively similar results to those computed with the backgrounds of [84] and [100].

¹⁹Notice that $h \sim \nu z^{-2}$, which according to the dictionary means that ν is the coupling of an operator of dimension Δ , with $4 - \Delta = -2 \implies \Delta = 6$.

How to improve the UV behavior: a phenomenological approach

We would like to stop the growing number of D3 sources responsible for the pile-up of Higging processes, and ultimately for the deviation from the nearly conformal behavior. A way to do so would be to choose a profile for the sources that somewhat recovers the cascade behavior. In the case of the background in equation (5.4.26) this is an easy task because, as we are distributing the D3 sources on the deformed conifold, the solution preserves supersymmetry for any $S(r)$. This suggests that we should choose (at least at a phenomenological level) a distribution function behaving as $S(r) \sim e^{-4r/3}$ for large values of r . A profile that does the job of fixing all the IR and UV problems is

$$S(r) = \tanh(2r)^4 e^{-4r/3}, \quad (5.4.38)$$

which is a convenient choice for numerical purposes. Using this distribution function²⁰, one can compute the new warp factor using equation (5.4.28). Doing so, one obtains a smooth IR geometry and a cascade behavior in the far UV.

In principle, it seems that we should only require that the distribution of D3-brane sources is either constant or vanishing for large values of r . So one could try different profiles vanishing as a generic power $e^{-(\frac{4}{3}+\epsilon)r}$. However, *if we want this distribution of sources to have a positive mass density everywhere, it seems that the only possibility is to have profiles decreasing exactly as $e^{-4r/3}$* . See appendix C of [24] for details.

Then we have constraints coming from the field theory side that require the function S to decay at least as $e^{-4r/3}$, and constraints coming from the supergravity side requiring that it does not decay faster than that. The number $\frac{4}{3}$ seems to be very special. Notice that a curious fact is that the “physically sensible” $S(r)$ for the unrotated background (which asymptotes $S \sim 1$), is pathological for the rotated configuration as the number of D3-branes grows exponentially with r , inducing an irrelevant deformation. Conversely, for a physically sensible $S(r)$ in the rotated background (vanishing at infinity as $e^{-4/3r}$), we cannot give (at present) a microscopic interpretation in terms of the usual flavor D5-branes in the unrotated solution. Since S is, as we discussed in the previous section, sort of counting the number of flavor degrees of freedom, this would mean that we are “integrating them in” along the RG flow. From the gravity perspective, this situation is very strange as well, as $S(r)$ is somewhat counting what fraction of the tips r_q of the branes fall in the region $r_q < r$. This quantity should never decrease with r . A clarification of this point would be very desirable.

5.4.4 Towards applications

In this last subsection we give some reasons why the type of solutions we have just built is interesting and might be relevant for phenomenology and model-building in high-energy Physics. To do that, we first summarize the picture we have obtained for the dual field theory of our backgrounds (for generic λ, N_f), that were obtained rotating solutions of the master equation (5.2.17), using a profile which is only non-vanishing in a region $r_Q < r < r_S$

²⁰The function $S(r)$ in (5.4.38) starts growing for small r , reaches a maximum, and then decreases exponentially for large values of the holographic coordinate. Of course, one could tune it a little bit so that it starts growing at some $r_Q > 0$ and becomes zero at some finite value $r_S > r_Q$.

(inspired by (5.4.38)), and with asymptotics (5.4.9). Before rotating them, the dual theory to these solutions is UV-incomplete as there is an irrelevant operator of dimension-eight that kicks in at a scale r_* . The rotation provides a UV completion. How does this completion look like?

First of all, notice that (besides the confinement scale Λ_{QCD} related to the end of space in the geometry) there are three dynamical scales in the theory. One is the scale r_* , controlled by the parameter c_+ in equation (5.4.9), which is related to a dimension-two VEV in the rotated theory, as explained in [169]. In the absence of sources, below such scale the theory is best described as a generalization of the one-site MN field theory, while above this scale the rotation procedure yields a background that is dual to a two-site quiver realizing the (baryonic branch of the) KS duality cascade. There are then the two other scales r_Q and r_S , $r_Q < r_S$, such that the function S has support in the range between them. There is no obvious relation between r_* and these other two scales, but for reasons of simplicity we assume in this discussion that $r_* \simeq r_S$. Different cases can be discussed along the same lines, in a case-by-case analysis that adds nothing to the main physical points we want to make. The physics in between these scales is as follows:

- In the far UV, for $r > r_S \sim r_*$, the theory resembles the KS cascade: the theory is flowing close to a line of fixed points, each of which is an $\mathcal{N} = 1$ Klebanov-Witten fixed point, but it never falls in any of them because of a small imbalance between the ranks of the two gauge groups. The flow towards the UV goes up a cascade of Seiberg dualities which continues indefinitely towards $r \rightarrow +\infty$, and the theory is said to be nearly conformal.
- There is an intermediate range $r_Q < r < r_S \sim r_*$ over which the function S is non-trivial. At the scale r_* the duality cascade stops, due to the Higgsing induced by the dimension-two condensate \mathcal{U} appearing, that precipitates the theory towards the last stages of the duality cascade, yielding an $SU(n_f + N_c)$ theory. On the other hand, because in this range the function S is non-trivial, another cascade starts, which has a completely different interpretation: it is a cascade of Higgsings of the gauge theory.
- Below the scale controlled by the value of r_Q , the Higgsing cascade stops, and with it most of the dynamical features related to N_f (up to subtleties which have been discussed earlier), because S vanishes. The theory now looks like a generalization of the single-quiver MN field theory, with gauge group $SU(N_c)$ and the same type of dynamics.
- At very low scales (near the end of space $r = 0$ of the geometry), the theory shows the appearance of a non-trivial gaugino condensate, and confines in the usual sense of producing an area law for the Wilson loop.

Notice that one might as well take r_* to be very small, near the end of space: in this case the duality cascade would continue all the way to very small energies, in particular extending over the second and third of the four ranges described above. In this case, there would be a regime in which both Higgsing cascade and duality cascade coexist. This is illustrated in figure 5.11.

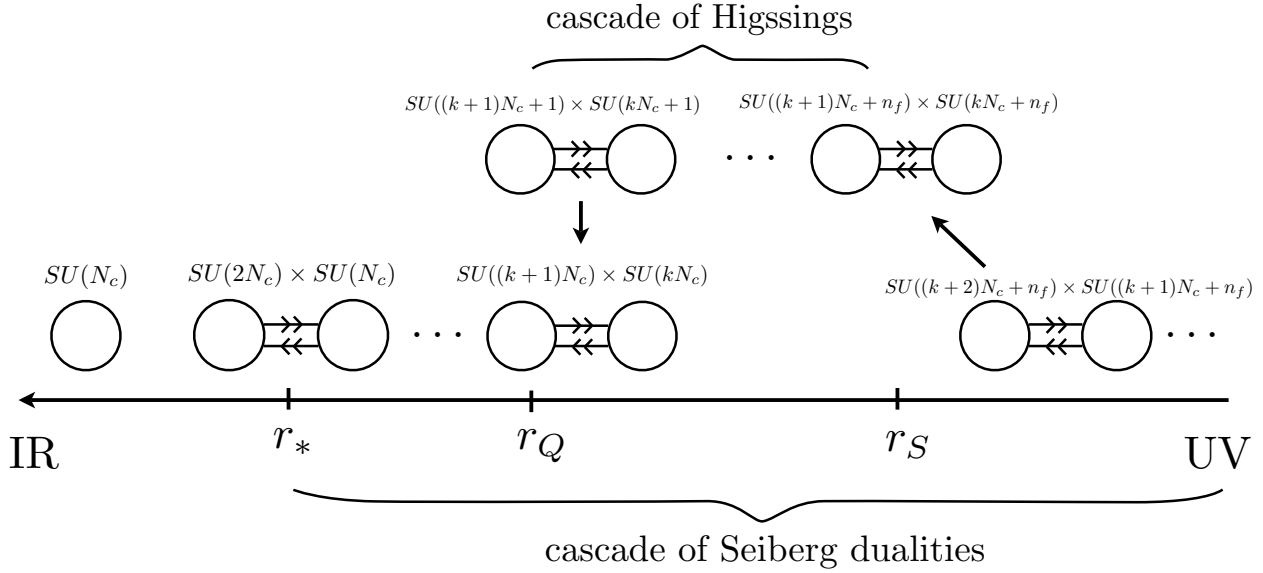


Figure 5.11: The addition of sources introduces a new cascade: that of consecutive Higgsings. It can coexist with the KS cascades. The Higgsings happen when crossing source D3-branes, therefore they only take place in the region $r_Q < r < r_S$. Above the scale r_Q , the theory is in a mesonic branch.

The physics taking place in the field theory at the second of the four stages (for $r_Q < r < r_S \sim r_*$) is very peculiar, and even more peculiar is the fact that such a behavior appears only over a finite range of energies. The question is: what kind of theoretical models exhibit features that are qualitatively similar to the one discussed here, and what kind of possible physical systems can they describe? In other words: are there conceivable applications of such results?

Interestingly, there is a positive answer to this question, which relates to a long-standing, very difficult and open phenomenological problem. A scenario that has some common elements with our present one is that of Extended Technicolor Models (ETC) with Tumbling dynamics [183, 184]. This is a very plausible dynamical explanation for the origin of flavor physics (SM-fermion masses, mixing angles, CP violation, flavor-changing neutral-current interactions, ...), in the context of strongly coupled extensions of the Standard Model [185, 186, 187, 188, 189, 190] (see also [191] for a recent review on the subject from the gauge/gravity perspective, where references to the original works can be found). We provide here a simple summary of what this means. We also want to clarify what are the actual similarities and the substantial differences, and hence the possible intrinsic limitations into attempting to use the approach of this section in order to study tumbling ETC.

ETC addresses the following, well-known, fundamental problem, arising in the context of (strongly coupled) Dynamical ElectroWeak-Symmetry Breaking (DEWSB). DEWSB or technicolor (TC) proposes to replace the Higgs sector of the Standard Model with a new gauge theory with group G_{TC} and new (techni-fermion) fields transforming non-trivially under the action of both G_{TC} and the Standard Model gauge group. The strong dynamics associated with G_{TC} yields the formation (at the confinement scale Λ_{TC}) of non-trivial condensates

made of techni-fermions, which results in the spontaneous breaking of the SM gauge group at the ElectroWeak scale. The SM gauge interactions themselves communicate the breaking to the W and Z gauge bosons, which become massive. However, in the process of removing the Higgs field, one also loses the Yukawa couplings, and hence one needs a mechanism that couples the SM fermions to the techni-quarks, in order for the quarks and leptons to acquire a mass below the ElectroWeak scale.

ETC provides such a dynamical mechanism. The generic ETC model works in the following way. Start from some gauge theory with gauge group $G_{ETC} \times G_{SM}$ (where $G_{SM} = SU(3)_c \times SU(2)_L \times U(1)_Y$ is the familiar SM gauge group), and a given fermionic-matter content. Assume that the dynamics of G_{ETC} is such that the theory is asymptotically free, but undergoes a sequence of breaking stages

$$G_{ETC} \rightarrow G_1 \rightarrow G_2 \rightarrow G_{TC},$$

at scales $\Lambda_1 \gg \Lambda_2 \gg \Lambda_3$, respectively. At scales below Λ_3 the resulting effective field theory consists of the following.

- A gauge theory with gauge group $G_{TC} \times G_{SM}$.
- Two kinds of massless fermions: techni-quarks ψ_{TC} transforming non-trivially under $G_{TC} \times G_{SM}$, and singlets of G_{TC} that we denote by ψ_{SM} , that transform non-trivially only under G_{SM} . The latter are identified with the quarks and leptons of the Standard Model.
- Higher-order operators originating from integrating out the heavy gauge bosons of the coset G_{ETC}/G_{TC} . In particular, some of these are four-fermion operators coupling two SM fermions with two TC fermions, with the generic form

$$\frac{1}{\Lambda_i^2} \bar{\psi}_{TC} \psi_{TC} \bar{\psi}_{SM} \psi_{SM}. \quad (5.4.39)$$

We present in figure 5.12 a cartoon of the dynamics (in terms of the effective gauge coupling) of such a scenario.

Now, the resulting gauge theory is the TC theory. Ultimately, G_{TC} will confine, and produce condensates that break the gauge group down to G_{SM} . However, the presence of the four-fermion interactions means that after ElectroWeak-Symmetry Breaking the quarks and leptons will become massive. Effectively, these four-fermion operators play the same role as the Yukawa couplings in the Standard Model. Notice that, because they originate at different scales, there will be in general three families of SM fermions, and some of these operators will be suppressed as $1/\Lambda_1^2$, others as $1/\Lambda_3^2$, and so on. In general there will be a very complicated, hierarchical structure in the four-fermion couplings, which will translate after dimensional transmutation into the hierarchical structure of the masses of the SM fermions, and the mixing angles in the CKM mixing matrix.

The presence of a long (at least three-stage) sequence of breaking, and of hierarchies in the dynamical scales is absolutely necessary on phenomenological grounds, because it offers the only plausible and self-contained dynamical explanation for the pattern of phenomenological masses and mixing angles experimentally measured. On the other hand, it makes it

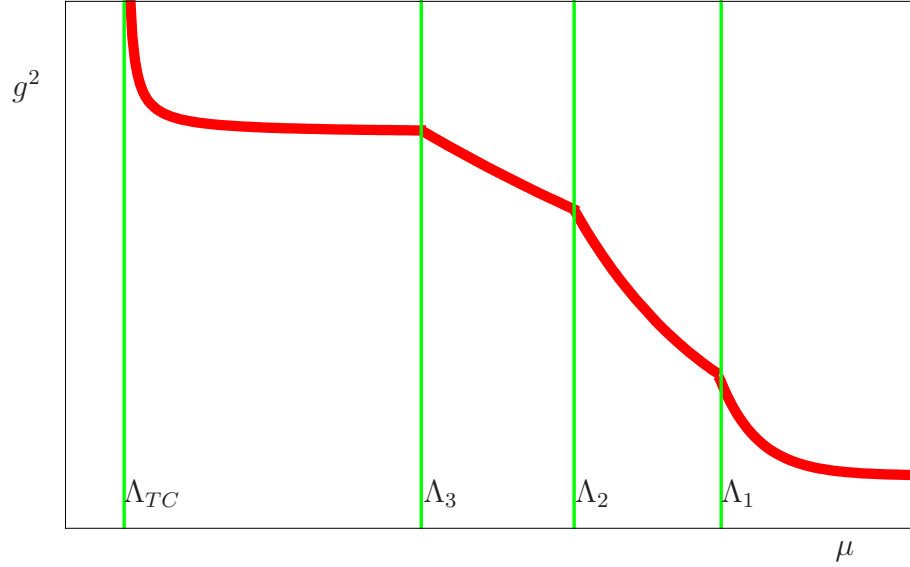


Figure 5.12: Cartoon depiction of the running of the gauge coupling g^2 in an example of multi-scale (tumbling) ETC model as a function of the renormalization scale μ . The sequential breaking at scales $\Lambda_1 > \Lambda_2 > \Lambda_3 > \Lambda_{TC}$ means that the gauge group and field content changes at each breaking scale, and so does the dynamics.

extremely difficult to study, because of the strongly coupled nature of the phenomena taking place in these field theories. Many open questions about such dynamics, and its low-energy implications, require some new tools for a quantitative (and often even qualitative) analysis to be performed. The gravity duals we are finding resemble this scenario: a sequence of Higgsing stages taking place at several scales, over a finite energy range. It is hence conceivable that some of the long-standing open problems might be addressed in this context. For example, one would also like to understand what kind of low-energy spectrum one may observe, with particular reference to the presence of possible pseudo-Goldstone bosons associated with the breaking of accidental global symmetries.

There is another long-standing problem: besides the gauge symmetries, all of the TC and ETC models also possess very large (approximate) global symmetries, which are spontaneously broken by the many condensates that form. This might yield the presence of such pseudo-Goldstones, with masses that might put them well below the current exclusion region, and hence render the models phenomenologically not viable. Computing masses and couplings of such particles requires dedicated strong-coupling calculations, and new tools are needed to perform them.

We can hence conclude that this is a first concrete example of a model which shares some of the fundamental features of *tumbling*, and that these types of models might be used to characterize in field-theory terms what are the features associated with the tumbling itself. It must also be stressed that the very nature of these models is such that a direct comparison to the real world must be done with caution: effectively we have an infinite, continuum number of Higgsing stages, rather than a few (three) distinct and hierarchical breaking stages. In other words, comparing to Figure 5.12, the Higgsing cascade differs

from the tumbling because between the scales Λ_1 and Λ_3 (which can be associated with r_S and r_Q , respectively), one has a continuum of breaking scales, rather than just a few steps. It hence remains to be understood what type of operators will replace the four-fermion operators of low-energy TC, and what type of phenomenological implications they have. This is somewhat analogous to the fact that the gravity dual of the duality cascade actually consists of an infinite continuum of Seiberg dualities, rather than a small number of such stages.

5.A A glance at the microscopic approach

Let us show here how the results obtained for the smearing form in section 5.2.2 (equation (5.2.45) in particular), using just the knowledge of one embedding of the family plus an ansatz for the functional form of Ξ (equation (5.2.9)), could be derived from a purely microscopic computation: *i.e.* by summing the contributions to the smearing form of all the embeddings in a given family.

Notice that this microscopic approach does not assume any specific ansatz for the smearing form. The computation is expected to be hard. The use of the holomorphic structure of our internal manifold developed in section 5.1.2 is instrumental to carry out this microscopic computation.

5.A.1 Holomorphic structure in the Abelian limit

For simplicity, we focus in this appendix on the UV limit ($r \rightarrow \infty$) of our backgrounds. This limit corresponds to the so-called Abelian solution (see section 3.2.2). The holomorphic structure simplifies a little bit in this limit, and one can define a new set of four complex variables ζ_i ($i = 1, \dots, 4$) that parameterize now a singular conifold:

$$\zeta_1 \zeta_2 - \zeta_3 \zeta_4 = 0. \quad (5.A.1)$$

The radial variable r is related to the ζ_i in this case as:

$$\sum_{i=1}^4 |\zeta_i|^2 = e^{2r}. \quad (5.A.2)$$

The expression of these complex variables in terms of the coordinates of the internal manifold can be read from (5.1.29). One just needs to take the $r \rightarrow \infty$ limit there, to obtain:

$$\begin{aligned} \zeta_1 &= -e^r \sin \frac{\theta}{2} \sin \frac{\tilde{\theta}}{2} e^{i \frac{\psi - \phi - \tilde{\phi}}{2}}, & \zeta_2 &= e^r \cos \frac{\theta}{2} \cos \frac{\tilde{\theta}}{2} e^{i \frac{\psi + \phi + \tilde{\phi}}{2}}, \\ \zeta_3 &= e^r \cos \frac{\theta}{2} \sin \frac{\tilde{\theta}}{2} e^{i \frac{\psi + \phi - \tilde{\phi}}{2}}, & \zeta_4 &= -e^r \sin \frac{\theta}{2} \cos \frac{\tilde{\theta}}{2} e^{i \frac{\psi - \phi + \tilde{\phi}}{2}}. \end{aligned} \quad (5.A.3)$$

This Abelian geometry inherits the $SU(2)_L \times SU(2)_R$ symmetry of the non-Abelian one (actually the isometry group is enlarged to $SU(2)_L \times SU(2)_R \times U(1)$). Again, taking carefully²¹

²¹In the Abelian limit: $a \rightarrow 0$, $\cosh(2r) \rightarrow \sinh(2r) \rightarrow \frac{e^{2r}}{2}$, and $a e^{2r} \rightarrow 1 + 4e^{2h-2g}$.

the limit $r \rightarrow \infty$ in the non-Abelian expressions (5.1.32) and (5.2.9) for the fundamental two-form J and the smearing form Ξ we get:

$$e^{-\frac{\Phi}{2}} J = \frac{e^{2k}}{2} dr \wedge (\tilde{\omega}_3 + \cos \theta d\phi) - \frac{e^{2g}}{4} \sin \tilde{\theta} d\tilde{\theta} \wedge d\tilde{\phi} - e^{2h} \sin \theta d\theta \wedge d\phi,$$

$$\frac{16\pi^2}{N_f} \Xi = \sin \theta d\theta \wedge d\phi \wedge \left(S \sin \tilde{\theta} d\tilde{\theta} \wedge d\tilde{\phi} - S' dr \wedge (d\psi + \cos \tilde{\theta} d\tilde{\phi}) \right). \quad (5.A.4)$$

Then one can define $SO(4)$ -invariant $(1,1)$ -forms η_i ($i = 1, \dots, 4$) as in (5.1.37), and express both J and Ξ in this Abelian setup as:

$$e^{-\frac{\Phi}{2}} J = 2i e^{-2r} \left[e^{2h} (\eta_1 + 2e^{-2r} \eta_2 - 2e^{-2r} \eta_3) + \frac{e^{2g}}{4} (\eta_1 + 2e^{-2r} \eta_2 + 2e^{-2r} \eta_3) - e^{2k} e^{-2r} \eta_2 \right],$$

$$\frac{16\pi^2}{N_f} \Xi = -8e^{-4r} S \eta_1 \wedge (\eta_1 + 4e^{-2r} \eta_2) + 8e^{-6r} S' \eta_2 \wedge (\eta_1 - 2e^{-2r} \eta_3), \quad (5.A.5)$$

where the η_i are the Abelian $(1,1)$ two-forms, which can be obtained from (5.1.38) by keeping the leading term when $r \rightarrow \infty$.

5.A.2 Abelian limit of the simple class of embeddings

Let us now calculate $S(r)$ for the Abelian version of the class of embeddings discussed in section 5.2.2. The first thing to notice is that the parameterization (5.2.31) is not good in the UV limit. Indeed, as $z_4 = z_1 z_2 / z_3$ when $r \rightarrow \infty$, the two equations in (5.2.31) become the same. For this reason, to study the cycle in the UV, it is better to use instead the first two equations in (5.2.32) and write the equation of the embedding as $z_1 = C z_3$ and $z_1 z_2 = \tilde{\mu}$, with C and $\tilde{\mu}$ being arbitrary complex constants. By taking the UV limit in which $z_i \rightarrow \zeta_i$, one concludes that the Abelian limit of the embedding (5.2.32) is:

$$\zeta_1 = C \zeta_3, \quad \zeta_1 \zeta_2 = \tilde{\mu}. \quad (5.A.6)$$

One nice thing of the Abelian limit is that (5.A.6) can be easily solved in terms of coordinates:

$$\theta = \theta_0, \quad \phi = \phi_0, \quad \text{and} \quad \frac{1}{2} \sin \tilde{\theta} e^{2r} e^{i\psi} = \mu \equiv \frac{1}{2} e^{2r_q} e^{i\gamma}, \quad (5.A.7)$$

where we have parameterized the constants above as $C = \tan \frac{\theta_0}{2} e^{-i\phi_0}$, $\tilde{\mu} = \mu (\sin \frac{\theta_0}{2} \cos \frac{\theta_0}{2})^{-1}$, and r_q is the minimum radial distance this embedding reaches ($e^{2r_q} = |2\mu|$). If we now rotate this embedding with the $SU(2)_L \times SU(2)_R$ isometry group (see equation (5.1.27)), we obtain the expression of a generic embedding of the family as $f_1 = 0$ and $f_2 = 0$, with:

$$f_1 = \zeta_1 - \frac{b + aC}{\bar{a} - \bar{b}C} \zeta_3, \quad (5.A.8)$$

$$f_2 = ((|k|^2 - |l|^2) \zeta_1 \zeta_2 - k \bar{l} C^{-1} \zeta_1^2 + \bar{k} l C \zeta_2^2) - (|a|^2 - |b|^2 - a \bar{b} C + \bar{a} b \bar{C})^{-1} \tilde{\mu}.$$

The smearing form should be computed as an appropriately weighted sum of the transverse volume forms of each embedding. The formula for real constraints was first written down in [111], and the generalization to complex constraints like the ones we have now is immediate²²:

$$\Xi = \frac{1}{(-2i)^2} \int_{\mathbb{C}^4} d\rho \delta^{(2)}(f_1) \delta^{(2)}(f_2) df_1 \wedge d\bar{f}_1 \wedge df_2 \wedge d\bar{f}_2, \quad (5.A.9)$$

where ρ is the (normalized to the unity) measure of $SU(2)_L \times SU(2)_R$, multiplied by N_f , and is given by:

$$d\rho = da d\bar{a} db d\bar{b} dk d\bar{k} dl d\bar{l} \delta(|a|^2 + |b|^2 - 1) \delta(|k|^2 + |l|^2 - 1) \frac{N_f}{16\pi^4}, \quad (5.A.10)$$

A shortcut for computing (5.A.9) is to notice that all the embeddings of the present family, in virtue of the first equation in (5.A.8), sit at constant values of θ and ϕ . Since it turns out that the action of $SU(2)_L$ corresponds precisely to varying these constant values over a two-sphere, the smearing form Ξ necessarily exhibits a $\frac{1}{4\pi} \sin\theta d\theta \wedge d\phi$ factor. We are not interested in getting this trivial part from (5.A.9), so we factor it out by defining an effective (complex) two-dimensional problem. We can define a new pair of effective complex variables:

$$\xi_1 = e^r \cos \frac{\tilde{\theta}}{2} e^{i\frac{\psi+\tilde{\phi}}{2}}, \quad \xi_2 = e^r \sin \frac{\tilde{\theta}}{2} e^{i\frac{\psi-\tilde{\phi}}{2}}, \quad (5.A.11)$$

and the family of embeddings over which we want to smear recasts as

$$f \equiv (|A|^2 - |B|^2) \xi_1 \xi_2 + A\bar{B} \xi_2^2 - \bar{A}B \xi_1^2 - \mu = 0, \quad |A|^2 + |B|^2 = 1. \quad (5.A.12)$$

(Recall that $\mu = \frac{1}{2} e^{2r_q} e^{i\gamma}$, see (5.A.7)). Forgetting for the moment about the correct normalization factors, the integral we want to compute is:

$$W \equiv \int_{\mathbb{C}^2} dA d\bar{A} dB d\bar{B} \delta(|A|^2 + |B|^2 - 1) \delta^{(2)}(f) df \wedge d\bar{f}. \quad (5.A.13)$$

Performing this integral requires a little bit of care with the delta functions, but other than that, it can be considered straightforward. Let us sketch how one could proceed. To simplify the calculation, we reparameterize the integration variables as follows:

$$A = \sqrt{\frac{u_1 + u_2}{2}} e^{i\alpha_1}, \quad B = \sqrt{\frac{u_1 - u_2}{2}} e^{i\alpha_2}. \quad (5.A.14)$$

Clearly, one has $|A|^2 + |B|^2 = u_1$ and $|A|^2 - |B|^2 = u_2$ and:

$$\int_{\mathbb{C}^2} dA d\bar{A} dB d\bar{B} \delta(|A|^2 + |B|^2 - 1) = \frac{1}{2} \int_{-\infty}^{\infty} du_2 \int_{|u_2|}^{\infty} du_1 \int_0^{2\pi} d\alpha_1 \int_0^{2\pi} d\alpha_2 \delta(u_1 - 1). \quad (5.A.15)$$

²²The complex Dirac delta should be understood as $\delta^{(2)}(f) = \delta(\text{Re}(f)) \delta(\text{Im}(f))$. The $\frac{1}{-2i}$ prefactor is included because $df \wedge d\bar{f} = -2i d\text{Re}(f) \wedge d\text{Im}(f)$.

The integral in u_1 is then immediate. Rewriting $e^{i\alpha_2} = x_2 + iy_2$, and using that:

$$\int_0^{2\pi} d\alpha_2 = 2 \int_{\mathbb{R}^2} dx_2 dy_2 \delta(x_2^2 + y_2^2 - 1), \quad (5.A.16)$$

we can write:

$$W = \int_0^{2\pi} d\alpha_1 \int_{-1}^1 du_2 \int_{\mathbb{R}^2} dx_2 dy_2 \delta(x_2^2 + y_2^2 - 1) \delta(R) \delta(I) df \wedge d\bar{f}, \quad (5.A.17)$$

where $R \equiv \text{Re}(f|_{u_1=1})$, $I \equiv \text{Im}(f|_{u_1=1})$. In the new variables one has:

$$f|_{u_1=1} = -\frac{1}{2}e^{i(\alpha_1-\alpha_2)}\sqrt{1-u_2^2}\xi_1^2 + u_2\xi_1\xi_2 + \frac{1}{2}e^{i(-\alpha_1+\alpha_2)}\sqrt{1-u_2^2}\xi_2^2 - \mu. \quad (5.A.18)$$

Solving $R = I = 0$ for x_2 and y_2 , the integral of the corresponding deltas produces a factor:

$$\left| \frac{dR}{dx_2} \frac{dI}{dy_2} \right|^{-1} = \frac{4}{1-u_2^2} \frac{1}{||\xi_1|^4 - |\xi_2|^4|}, \quad (5.A.19)$$

and leaves the argument of the remaining delta function as:

$$\delta(x_2^2 + y_2^2 - 1) = \delta\left(\frac{(|\xi_1|^2 + |\xi_2|^2)^2}{(1-u_2^2)(|\xi_1|^2 - |\xi_2|^2)^2}(u_2 - u_{2+})(u_2 - u_{2-})\right), \quad (5.A.20)$$

where $u_{2\pm}$ are given by:

$$u_{2\pm} = \frac{4|\mu\xi_1\xi_2|\cos(\psi - \gamma) \pm ||\xi_1|^2 - |\xi_2|^2|\sqrt{(|\xi_1|^2 + |\xi_2|^2)^2 - 4|\mu|^2}}{(|\xi_1|^2 + |\xi_2|^2)^2}. \quad (5.A.21)$$

We have at this point:

$$W = \int_0^{2\pi} d\alpha_1 \int_{-1}^1 du_2 \frac{\frac{4}{1-u_2^2}}{||\xi_1|^4 - |\xi_2|^4|} \delta\left(\frac{(|\xi_1|^2 + |\xi_2|^2)^2}{(1-u_2^2)(|\xi_1|^2 - |\xi_2|^2)^2}(u_2 - u_{2+})(u_2 - u_{2-})\right) df \wedge d\bar{f}. \quad (5.A.22)$$

In this expression, nothing depends on α_1 , so one can integrate it easily. Also, both u_{2+} and u_{2-} are between -1 and 1 , so they both contribute to the integral. Using (5.A.2), and replacing u_{2+} and u_{2-} by their values (5.A.21), we finally get:

$$\begin{aligned} W = & 4\pi \frac{1 - \cos\tilde{\theta} + 2e^{4r_q-4r}\cos\tilde{\theta}}{\sqrt{e^{4r} - e^{4r_q}}} d\xi_1 \wedge d\bar{\xi}_1 + 4\pi \frac{1 + \cos\tilde{\theta} - 2e^{4r_q-4r}\cos\tilde{\theta}}{\sqrt{e^{4r} - e^{4r_q}}} d\xi_2 \wedge d\bar{\xi}_2 - \\ & - 4\pi e^{-i\tilde{\phi}} \frac{(1 - 2e^{4r_q-4r})\sin\tilde{\theta}}{\sqrt{e^{4r} - e^{4r_q}}} (d\xi_1 \wedge d\bar{\xi}_2 + d\xi_2 \wedge d\bar{\xi}_1). \end{aligned} \quad (5.A.23)$$

Plugging the values of ξ_1 and ξ_2 of (5.A.11) in (5.A.23), and taking into account the proper normalization factors, we find exactly:

$$\frac{N_f}{4\pi i} \sin\theta d\theta \wedge d\phi \wedge W = 16\pi^2 \Xi, \quad (5.A.24)$$

where Ξ is the one written in (5.A.4) with the following function $S(r)$:

$$S(r) = \sqrt{1 - e^{4r_q-4r}} \Theta(r - r_q). \quad (5.A.25)$$

Notice that (5.A.25) is the limit of the function $S(r)$ written in (5.2.45) when r and r_q are large! This confirms our results of section 5.2.2.

5.A.3 An example of a non-compatible embedding

We have just shown how the various approaches to compute the smearing described in section 3.3.1 yield the same result. For the hybrid approach to work, we argued that the family of embeddings we choose has to satisfy some “compatibility conditions” (3.3.27)-(3.3.28). In this subsection, we explicitly show that if these conditions do not hold the hybrid approach cannot be run. To do this, we illustrate with an example the case in which the compatibility condition is not satisfied, and show with a microscopic calculation that indeed the resulting Ξ is incompatible with the initial ansatz assumed for it.

We choose to work again in the Abelian background, since it is simpler and therefore the explanation will be cleaner. Let us focus on the following embedding:

$$\zeta_1 = C \zeta_4, \quad \zeta_2 = \mu, \quad (5.A.26)$$

where the ζ_i are the complex coordinates (5.A.3) and C and μ are constants that we parameterize as $C = \tan \frac{\tilde{\theta}_0}{2} e^{-i\tilde{\phi}_0}$ and $\mu = \cos \frac{\tilde{\theta}_0}{2} e^{i\tilde{\phi}_0/2} e^{i\beta}$. We can solve the embedding equations in (5.A.26) in terms of coordinates as:

$$\tilde{\theta} = \tilde{\theta}_0, \quad \tilde{\phi} = \tilde{\phi}_0, \quad \text{and} \quad e^r \cos \frac{\theta}{2} = e^{r_q}, \quad \psi + \phi = 2\beta. \quad (5.A.27)$$

It is easy then to compute the effective radial Lagrangians of the smeared distribution and of a single brane extended along the embedding (5.A.26), with the result:

$$\begin{aligned} \mathcal{L}_{\text{WZ}}^{\text{smeared}} &= 2\pi N_f T_{\text{D5}} e^{2\Phi} \left(e^{2k} S + \frac{e^{2g}}{2} S' \right), \\ \mathcal{L}_{\text{WZ}}^{\text{single}} &= 2\pi T_{\text{D5}} e^{2\Phi} \left(e^{2k} (1 - e^{2r_q - 2r}) + 4e^{2h} e^{2r_q - 2r} \right), \end{aligned} \quad (5.A.28)$$

where we have assumed that Ξ should be as in (5.A.4). As we see, the e^{2g} term in the smeared Lagrangian is not present in $\mathcal{L}_{\text{WZ}}^{\text{single}}$ (we have instead an e^{2h} term), so the compatibility condition (3.3.27) is not satisfied (it does not make sense to wonder about (3.3.28) then).

Let us now check with a microscopic computation that, indeed, the family of embeddings generated by rotating (5.A.26) with the $SU(2)_L \times SU(2)_R$ symmetry, generates an Ξ that is not of the form of (5.A.4). After using the relation (5.A.1), the family can be characterized by $f_1 = 0$, $f_2 = 0$ with:

$$f_1 = \bar{a}\zeta_1 + \bar{b}\zeta_4, \quad f_2 = \bar{k}\zeta_2 + \bar{l}\zeta_4 + \bar{b}\mu, \quad (5.A.29)$$

with $|a|^2 + |b|^2 = 1 = |l|^2 + |k|^2$. In this case, it is easy to perform the integral (5.A.9) by making use of the following two results:

$$\int dz d\bar{z} \delta^{(2)}(w_1 z - w_2) = -\frac{2i}{|w_1|^2}, \quad (5.A.30)$$

$$\begin{aligned} &\int dx dy (x^2 + y^2 + \alpha_1 x + \beta_1 y + \gamma_1) \delta(x^2 + y^2 + \alpha_2 x + \beta_2 y + \gamma_2) = \\ &= \pi \left(\gamma_1 - \gamma_2 + \frac{\alpha_2^2 + \beta_2^2 - \alpha_1 \alpha_2 - \beta_1 \beta_2}{2} \right). \end{aligned} \quad (5.A.31)$$

The final result we get for the smearing form is:

$$\Xi = \frac{N_f}{16\pi^2} \sin \tilde{\theta} d\tilde{\theta} \wedge d\tilde{\phi} \wedge \left((1 - e^{2r_q - 2r}) \sin \theta d\theta \wedge d\phi - 2e^{2r_q - 2r} dr \wedge (d\psi + \cos \theta d\phi) \right) , \quad (5.A.32)$$

and we see that this is clearly incompatible with (5.A.4) (the roles of (θ, ϕ) and $(\tilde{\theta}, \tilde{\phi})$ are exchanged in these two expressions of Ξ).

Chapter 6

Miscellanea of more flavor physics

Contextualizing this chapter

In the previous two chapters, we have seen how holographic techniques are very powerful tools to study gauge theories, as we obtained very non-trivial non-perturbative information on the flavor physics of both three-dimensional Chern-Simons-matter theories and four-dimensional $\mathcal{N} = 1$ theories. In this chapter, we want to exemplify some other of the possible uses of the gauge/gravity correspondence to study the non-perturbative dynamics of flavor in gauge theories. The emphasis will be more on the gravity side of the correspondence, as we try to illustrate how the brainstorming goes when engineering supergravity solutions for given dual field theories.

As a first example, we discuss a possible way of realizing Kutasov duality in a holographic setup, summarizing the ideas presented in [26]. The main novelty of this work was the use of hyperbolic spaces in the supergravity construction, which provide the needed elements in the dual field theory for it to display Kutasov duality. As a second example, we focus on the use of wrapped-brane models to build gravity duals to SQCD (in the spirit of CNP) in several dimensions and with different amounts of supersymmetry. Wrapped-brane models have been used for this purpose quite extensively in the literature, but there were some cases that had been left out, with an amount of supersymmetry neither minimal nor maximal, like SQCD in two dimensions with four and two supercharges, or SQCD in three dimensions with four supercharges. These “holes in the literature” were filled in the works [28, 27], and we review the constructions briefly, bringing them altogether to display the similitudes within this class of models.

6.1 A Kutasov-like duality

In section 5.1.3, we explained how the CNP solution exhibited Seiberg duality, whose geometric realization was the swap of two two-spheres. Seiberg duality is a fully non-perturbative feature of $\mathcal{N} = 1$ field theories with fundamental matter, and the fact that the supergravity solution is capturing it is a remarkable display of the power of the gauge/gravity correspondence. But Seiberg duality is not the only acknowledged non-perturbative phenomenon of these characteristics. It is known that when one adds adjoint massless matter to $\mathcal{N} = 1$ SQCD, the theory exhibits Kutasov duality [192, 193, 194].

Kutasov duality is a generalization of Seiberg duality. It relates, in the same way as Seiberg duality does, two four-dimensional $\mathcal{N} = 1$ gauge theories. One has gauge group $SU(N_c)$, with N_f chiral multiplets in the fundamental representation, and one adjoint chiral superfield X with the following superpotential:

$$W(X) = \text{Tr} \sum_{l=1}^k g_l X^{l+1}. \quad (6.1.1)$$

where k is an integer. The second gauge theory is very similar: it has gauge group $SU(kN_f - N_c)$ with N_f fundamental chiral superfields and one adjoint one Y , and in addition it has N_f^2 mesons. Of course there is a precise prescription for what these mesons are, how the superpotential for Y is defined in terms of quantities of the first gauge theory, or how to map operators and moduli spaces between theories. The details for these subtleties can be found in the original references, but we are not interested in them. As we said, our focus is on the gravity side, and therefore we are just interested in finding a pair of type IIB supergravity backgrounds dual to the sort of theories involved in Kutasov duality, with the same IR geometry, and that can be related by:

$$N_c \rightarrow k N_f - N_c, \quad N_f \rightarrow N_f. \quad (6.1.2)$$

So then the question is: where do we even start to look for finding this sort of supergravity solutions? Since Kutasov duality can be thought of as a generalization of Seiberg duality, a good starting point is a solution that encodes the latter. This we are familiar with, as we extensively discussed the CNP solution in section 5.1. Recall that this solution could be seen as coming from a set of N_c D5-branes wrapping a two-sphere, giving rise to a $SU(N_c)$ gauge theory, plus another set of N_f smeared flavor branes, that were accounting for N_f quarks. These are two features we want to preserve, but we need an extra ingredient, which is adjoint massless matter.

A possible way to get this new adjoint matter via holography is by wrapping D5-branes on Riemann surfaces with genus $g > 1$, instead of wrapping them on a two-sphere. *We refer to such surfaces as hyperbolic cycles since we will build them as quotients of hyperbolic spaces.* The fact that the adjoint content is non-trivial is directly related to having $g > 1$. One formal way to explain this is using the index theorem like in [85], that determines the number of fermion zero-modes from the topology of the space. As shown there, having a non-trivial genus $g > 1$ implies the existence of $(g - 1)$ massless adjoint fermions. Another way to think about those adjoints is that they roughly correspond to the zero-modes of the B -field on the cycles of different homology within the Riemann surface.

6.1.1 The $\mathbb{H}_2 \times \widetilde{SL}_2$ ansatz

Our goal is then to find type IIB supergravity solutions that correspond to D5-branes wrapping Riemann surfaces of higher genus. As we know from the uniformization theorem (see section 6.1.4 for details), these admit a geometric structure modeled on the hyperbolic plane \mathbb{H}_2 , this being the reason why we will often refer to these surfaces as hyperbolic two-cycles.

As we said, in order to find this “hyperbolic” solution, we can look for inspiration in the CNP solution. Motivated by (5.1.1)-(5.1.3), we write down an ansatz for a type IIB supergravity solution representing D5-branes wrapping a hyperbolic two-cycle, plus a smeared set of N_f flavor D5-branes. The first guess would be to substitute the \mathbb{S}^2 appearing in (5.1.2) by an \mathbb{H}_2 .¹ However, we know that this \mathbb{S}^2 is not the two-cycle the D5-branes are wrapping. The latter actually involves another \mathbb{S}^2 inside the \mathbb{S}^3 as well [96]. Then it makes sense to think that we also need to substitute the \mathbb{S}^3 by some three-dimensional manifold that can accommodate the hyperbolic two-cycle inside it.

This substitution can be achieved by keeping basically the same ansatz as in the CNP case. We maintain the convention of working in units where $g_s = 1, \alpha' = 1$, but we remove² the N_c in we had in front of the internal metric in (5.1.1). Our new ansatz, in Einstein frame, is then:

$$ds^2 = e^{\frac{\Phi}{2}} \left[dx_{1,3}^2 + e^{2k} dr^2 + e^{2h} (\underline{\sigma}_1^2 + \underline{\sigma}_2^2) + \frac{e^{2g}}{4} ((\underline{\omega}_1 - A_1)^2 + (\underline{\omega}_2 - A_2)^2) + \frac{e^{2k}}{4} (\underline{\omega}_3 - A_3)^2 \right], \quad (6.1.3)$$

$$F_3 = -\frac{\hat{N}_c}{4} \bigwedge_i (\underline{\omega}_i - B_i) + \frac{\hat{N}_c}{4} \sum_i \underline{G}_i \wedge (\underline{\omega}_i - B_i) - \frac{\hat{N}_f}{4} \sigma_1 \wedge \sigma_2 \wedge (\underline{\omega}_3 - B_3), \quad (6.1.4)$$

where g, h, k are all functions of the radial/holographic coordinate r ; but now we are using a different set of left-invariant one-forms $\underline{\omega}_i$, such that they satisfy the following Maurer-Cartan relations:

$$d\underline{\omega}_1 = -\underline{\omega}_2 \wedge \underline{\omega}_3, \quad d\underline{\omega}_2 = -\underline{\omega}_3 \wedge \underline{\omega}_1, \quad d\underline{\omega}_3 = +\underline{\omega}_1 \wedge \underline{\omega}_2. \quad (6.1.5)$$

Notice the flip of the last sign with respect to (3.2.6). This choice will enforce the presence of hyperbolic cycles. We are also using a different set of one-forms $\underline{\sigma}_i$, that characterize the \mathbb{H}_2 in the same way as the σ_i characterized the \mathbb{S}^2 , and once again mimic the algebra (6.1.5) of their $\underline{\omega}_i$ counterparts: $d\underline{\sigma}_1 = -\underline{\sigma}_2 \wedge \underline{\sigma}_3$, $d\underline{\sigma}_2 = -\underline{\sigma}_3 \wedge \underline{\sigma}_1$ and $d\underline{\sigma}_3 = +\underline{\sigma}_1 \wedge \underline{\sigma}_2$. The one-forms A_i, B_i entering the fibration and the RR form stay as in the $\mathbb{S}^2 \times \mathbb{S}^3$ case:

$$A_{1,2} = a \underline{\sigma}_{1,2}, \quad A_3 = \underline{\sigma}_3 \quad ; \quad B_{1,2} = b \underline{\sigma}_{1,2}, \quad B_3 = \underline{\sigma}_3, \quad (6.1.6)$$

with $a = a(r)$, $b = b(r)$, but we have to modify slightly the definition of the gauge field-strength:

$$\underline{G}_i = dB_i + \frac{1}{2} \epsilon_{ijk} B_j \wedge B_k, \quad (i = 1, 2) \quad ; \quad \underline{G}_3 = -(dB_3 - B_1 \wedge B_2). \quad (6.1.7)$$

¹The Riemann surface can be later obtained from \mathbb{H}_2 by quotienting by a Fuchsian group Γ , and this leaves locally the same metric as that of \mathbb{H}_2 .

²With this choice, restoring units is not as immediate as substituting every-time N_c by $g_s \alpha' N_c$. But we are more interested in just seeing Kutasov duality, for which the choice is more convenient. One should keep in mind that the internal metric in (6.1.3) still has a $g_s \alpha'$ in front of it, which is not explicit because of the units we are using.

In what follows, we use this vielbein base for the metric (6.1.3):

$$\begin{aligned} e^{x^i} &= e^{\frac{\Phi}{2}} dx^i, \quad (i = 0, 1, 2, 3), & e^r &= e^{\frac{\Phi}{2}+k} dr, \\ e^1 &= e^{\frac{\Phi}{2}+h} \underline{\sigma}_1, & e^2 &= e^{\frac{\Phi}{2}+h} \underline{\sigma}_2, \\ e^3 &= \frac{e^{\frac{\Phi}{2}+g}}{2} (\underline{\omega}_1 - A_1), & e^4 &= \frac{e^{\frac{\Phi}{2}+g}}{2} (\underline{\omega}_2 - A_2), & e^5 &= \frac{e^{\frac{\Phi}{2}+k}}{2} (\underline{\omega}_3 - A_3). \end{aligned} \quad (6.1.8)$$

Let us exhibit a definite coordinate representation for the one-forms $\underline{\omega}_i$ and $\underline{\sigma}_i$ above. First, if we choose the metric of the Poincaré half-plane \mathbb{H}_2 as it is customary: $ds^2 = \frac{dz_1^2 + dy_1^2}{y_1^2}$, the following one-forms:

$$\underline{\sigma}_1 = -\frac{dy_1}{y_1}, \quad \underline{\sigma}_2 = -\frac{dz_1}{y_1}, \quad \underline{\sigma}_3 = -\frac{dz_1}{y_1}, \quad (6.1.9)$$

play the same role as the one the σ_i played for the \mathbb{S}^2 . Note that the $\underline{\sigma}_i$ are clearly not independent, as it happened with the σ_i .

Then, to specify some coordinate representation of $\underline{\omega}_i$, we should first know which three-manifold they parameterize. This will be a squashed version of the universal cover of $SL_2(\mathbb{R})$, that we will denote by \widetilde{SL}_2 , as we discuss in section 6.1.4. \widetilde{SL}_2 can be built as an \mathbb{S}^1 fiber bundle over \mathbb{H}_2 , which shows that a hyperbolic two-cycle can be accommodated inside it. Choosing z_2, y_2 for the coordinates of \mathbb{H}_2 as before, and ψ as the coordinate for the fiber, the $\underline{\omega}_i$ read:

$$\underline{\omega}_1 = \cos \psi \frac{dy_2}{y_2} - \sin \psi \frac{dz_2}{y_2}, \quad \underline{\omega}_2 = -\sin \psi \frac{dy_2}{y_2} - \cos \psi \frac{dz_2}{y_2}, \quad \underline{\omega}_3 = d\psi + \frac{dz_2}{y_2}. \quad (6.1.10)$$

The range of these coordinates $\{z_1, y_1, z_2, y_2, \psi\}$ do not bother us for the moment, since we will eventually take a quotient of both \mathbb{H}_2 and \widetilde{SL}_2 by some freely acting discrete isometry groups Γ and G respectively. These quotients need to be taken in order to generate the higher genus surface from \mathbb{H}_2 and a compact space out of \widetilde{SL}_2 . They are reflected on the fact that in the ansatz for F_3 (6.1.4), neither N_c nor N_f appear directly, but rather some related quantities \hat{N}_c, \hat{N}_f . We will see in section 6.1.3 what the relation is.

6.1.2 Supersymmetry analysis

Since the ansatz for our background (6.1.3)-(6.1.4) is very similar to the CNP one, the mathematical treatment of its preservation of supersymmetry will be very similar as well. We want our background to possess four supersymmetries. That is, one eighth of the thirty-two supercharges of type IIB supergravity should be preserved. As one can see in (6.1.3), our space is of the form $\mathcal{M}_4 \times_w X_6$ where \mathcal{M}_4 is four-dimensional Minkowski space, X_6 is a six-dimensional manifold and \times_w means a warped product. One way to dictate the preservation of only four supercharges is to impose that our six-dimensional internal manifold X_6 be endowed with an $SU(3)$ -structure. This $SU(3)$ -structure looks very much like the CNP one, and it is also parameterized by one two-form J and one three-form Ω . In the basis of (6.1.8),

one can define the $SU(3)$ -structure forms as:

$$\begin{aligned} J &= e^r \wedge e^5 + e^1 \wedge (\cos \alpha e^2 + \sin \alpha e^4) + e^3 \wedge (\sin \alpha e^2 - \cos \alpha e^4), \\ \Omega &= (e^r + i e^5) \wedge (e^1 + i(\cos \alpha e^2 + \sin \alpha e^4)) \wedge (e^3 + i(\sin \alpha e^2 - \cos \alpha e^4)), \end{aligned} \quad (6.1.11)$$

where, once again, α is a function of r only. The BPS equations are the same as for CNP (see equation (5.1.13)):

$$d(e^{2\Phi}\Omega) = 0, \quad d(e^\Phi J \wedge J) = 0, \quad d(e^{\frac{3}{2}\Phi} J) = -e^{2\Phi} *_6 F_{(3)}, \quad (6.1.12)$$

where $*_6$ indicates again the Hodge dual in the internal manifold. Solving this system will provide a solution to the type IIB equations of motion. The system of differential equations that follows from (6.1.12) can be directly obtained from the one written in the original CNP reference [108] by doing the following transformations:

$$e^g \rightarrow -i e^g, \quad e^h \rightarrow -i e^h, \quad a \rightarrow -i a, \quad b \rightarrow -i b, \quad N_c \rightarrow \hat{N}_c, \quad N_f \rightarrow \hat{N}_f. \quad (6.1.13)$$

However, it is more convenient to study it after making the following redefinitions for our functions:

$$\begin{aligned} e^{2h} &= -\frac{1}{4} \frac{P^2 - Q^2}{P \cosh \tau - Q}, & a &= \frac{P \sinh \tau}{P \cosh \tau - Q}, & \cos \alpha &= -\frac{P - Q \cosh \tau}{P \cosh \tau - Q}, \\ e^{2g} &= -P \cosh \tau + Q, & b &= \frac{\sigma}{\hat{N}_c}, & \sin \alpha &= \frac{\sinh \tau \sqrt{P^2 - Q^2}}{P \cosh \tau - Q}, \\ e^{2k} &= 4Y, & e^{2\Phi} &= \frac{D}{Y^{1/2}(P^2 - Q^2)}, \end{aligned} \quad (6.1.14)$$

where of course the new functions P, Q, Y, τ, σ, D depend only on r . Note the change of sign in the transformation of e^{2g} and e^{2h} as compared to (5.1.14). In terms of those new functions, the BPS system is exactly identical (barring the tildes in \hat{N}_c, \hat{N}_f) to the CNP one, and it can be solved in the same manner [92]:

$$\begin{aligned} \sigma &= \tanh \tau \left(Q + \frac{2\hat{N}_c - \hat{N}_f}{2} \right), \\ \sinh \tau &= \frac{1}{\sinh(2r - 2r_0)}, \\ D &= e^{2\Phi_0} \sqrt{P^2 - Q^2} \cosh(2r_0) \sinh(2r - 2r_0), \\ Y &= \frac{1}{8} (P' + \hat{N}_f), \\ Q &= \left(Q_0 + \frac{2\hat{N}_c - \hat{N}_f}{2} \right) \coth(2r - 2r_0) + \frac{2\hat{N}_c - \hat{N}_f}{2} (2r \coth(2r - 2r_0) - 1), \end{aligned} \quad (6.1.15)$$

plus a second-order differential equation for P we are already familiar with:

$$P'' + (P' + \hat{N}_f) \left(\frac{P' + Q' + 2\hat{N}_f}{P - Q} + \frac{P' - Q' + 2\hat{N}_f}{P + Q} - 4 \coth(2r - 2r_0) \right) = 0. \quad (6.1.16)$$

This is *exactly the master equation of CNP* (in the notation of (5.1.20)), and the search for solutions here also boils down to solving this master equation, which is, apart from the change $N_f \rightarrow \hat{N}_f$, identical to the master equation of the CNP case (5.1.20). However, it is important to notice that in the case at hand, in order for the transformation (6.1.14) and the solution (6.1.15) to be well-defined, we are looking for solutions such that

$$Q \geq P \coth(2r - 2r_0), \quad P^2 \geq Q^2, \quad P' + \hat{N}_f \geq 0, \quad (6.1.17)$$

which makes the solutions of this $\mathbb{H}_2 \times \widetilde{SL}_2$ case behave very differently from their CNP relatives. As we prove in section 6.1.5, these solutions only exist for a finite range of the radial coordinate $r \in [r_{\text{IR}}, r_{\text{UV}}]$.

6.1.3 Brane setup

Let us briefly discuss the brane configuration our background (6.1.3)-(6.1.4) is describing. The idea is that we have N_c D5-branes (the so-called color branes), wrapping a hyperbolic two-cycle inside a Calabi-Yau three-fold. When we take this number N_c to be very large, plus a near-horizon limit, the Calabi-Yau three-fold undergoes a geometric transition and the branes dissolve into flux [195]. The resulting internal manifold preserves the $SU(3)$ -structure,

and topologically is an interval times $\frac{\mathbb{H}_2}{\Gamma} \times \frac{\widetilde{SL}_2}{G}$, as sketched below:

$[r_{\text{IR}}, r_{\text{UV}}]$	\mathbb{H}_2/Γ	\widetilde{SL}_2/G
r	z_1, y_1	z_2, y_2, ψ

From the general geometric transition picture, one would expect to find a vanishing hyperbolic two-cycle in the IR, which by analogy with what happens in the MN solution should read³ $z_1 = z_2, y_1 = -y_2, \psi = \pi$; and a blown-up three-cycle pervaded by the three-form flux. A possible choice⁴ for this three-cycle is \widetilde{SL}_2 , and what remains from the initial N_c branes is the flux quantization condition:

$$-N_c = \frac{1}{2\kappa_{(10)}^2 T_{D5}} \int_{\widetilde{SL}_2} \iota^*(F_{(3)}) = -\frac{\hat{N}_c \text{Vol}(\widetilde{SL}_2)}{2\pi^2}, \quad (6.1.18)$$

where we are being a bit careless and denoting by \widetilde{SL}_2 the actual appropriate compact quotient \widetilde{SL}_2/G . The volume is to be understood as taking into account possible winding effects. The inclusion of this submanifold in the ten-dimensional background, used for the pullback, has been denoted by ι . Note that from here we get:

$$\hat{N}_c = \frac{2\pi^2}{\text{Vol}(\widetilde{SL}_2)} N_c. \quad (6.1.19)$$

³Actually there are two equivalent two-cycles, the other one being defined by $z_1 = -z_2, y_1 = y_2, \psi = \pi$. It can be checked that these two-cycles are indeed vanishing in the IR when we put $N_f = 0$.

⁴Recall that several choices are possible here, and this will be related with Kutasov duality. See the discussion of Seiberg duality in section 5.1.3.

As for the relation between \hat{N}_f and N_f , it can be obtained by looking at the violation of the Bianchi identity. As in the CNP solution, the \hat{N}_f in (6.1.4) is accounting for a set of N_f D5-branes extended along (r, ψ) plus Minkowski coordinates⁵ (with the transverse coordinates being constant), and homogeneously smeared over the space transverse to them. Using the definition (5.2.20) on the condition (3.2.3), it is easy to check that this configuration is supersymmetric. Thus, the violation of the Bianchi identity should read:

$$dF_3 = -2\kappa_{(10)}^2 T_{D5} \frac{N_f}{\text{Vol}(\mathbb{H}_2 \times \mathbb{H}_2)} \omega_{\text{Vol}(\mathbb{H}_2 \times \mathbb{H}_2)}, \quad (6.1.20)$$

where by ω_{Vol} we denote the volume form, and we are abusing notation once again by having \mathbb{H}_2 stand for the quotient \mathbb{H}_2/Γ . There are two \mathbb{H}_2 's in (6.1.20). Recalling the sketchy table above, one is characterized by (z_1, y_1) , and the other one, being the base space of \widetilde{SL}_2 when thought as a line bundle over \mathbb{H}_2 , is characterized by the (z_2, y_2) coordinates. As we will see later, it is possible to take simultaneously the same quotient \mathbb{H}_2/Γ in both of them.

From (6.1.4) we obtain:

$$dF_3 = -\frac{\hat{N}_f}{4} \omega_{\text{Vol}(\mathbb{H}_2 \times \mathbb{H}_2)}, \quad (6.1.21)$$

and the comparison with the previous equation (6.1.20) yields the relation we were looking for:

$$\hat{N}_f = \frac{(4\pi)^2}{\text{Vol}(\mathbb{H}_2)^2} N_f. \quad (6.1.22)$$

6.1.4 A geometrical remark

The way we substituted the \mathbb{S}^2 wrapped by the D5-branes in the CNP solution (recall this \mathbb{S}^2 was extended along both the topological two-sphere and three-sphere present in this solution) by a Riemann surface of genus $g > 1$, \mathcal{C}_g , was by replacing in (5.1.2) the metrics of the two-sphere and three-sphere by their “hyperbolic analogues”:

$$\begin{aligned} ds_{\mathbb{S}^2}^2 = \sigma_1^2 + \sigma_2^2 &\rightarrow ds_{\mathbb{H}_2}^2 = \underline{\sigma}_1^2 + \underline{\sigma}_2^2, \\ ds_{\mathbb{S}^3}^2 = \omega_1^2 + \omega_2^2 + \omega_3^2 &\rightarrow ds_{\widetilde{SL}_2}^2 = \underline{\omega}_1^2 + \underline{\omega}_2^2 + \underline{\omega}_3^2, \end{aligned} \quad (6.1.23)$$

where the one-forms σ_i , $\underline{\sigma}_i$, ω_i , $\underline{\omega}_i$ have been defined in the previous subsections. One can notice that the metrics on the right-hand side of (6.1.23) represent non-compact spaces. The way to get a hyperbolic compact space out of them is by performing a quotient by a discrete subgroup of isometries. Such a quotient will leave locally the very same metrics of (6.1.23), which will be therefore the metrics we have to use for \mathcal{C}_g and for the \mathbb{S}^1 fiber bundle over \mathcal{C}_g respectively (see section 6.1.6 for how to perform the quotient explicitly). This construction of subspaces as quotients by isometries of a bigger space is well-known in Geometry, and from it we can deduce that in our case these bigger spaces are \mathbb{H}_2 and \widetilde{SL}_2 respectively. For the sake of completeness, we comment a few words on this topic.

⁵It is easy to see that this six-cycle is κ -symmetric, for instance by looking at the calibration six-form (5.2.20), and checking that $\iota^*(\mathcal{K}) = \omega_{\text{Vol}(\iota^*(g))}$.

All closed (compact and with an empty boundary) smooth two-manifolds can be given a metric of constant curvature. The uniformization theorem for surfaces provides a way to realize this construction in terms of a so-called geometric structure. A geometric structure on a manifold M is a diffeomorphism between M and a quotient space X/Γ , where X is what one calls a model geometry, and Γ is a group of isometries, such that the projection $X \mapsto X/\Gamma$ is a covering map. In the case of two-manifolds, there are three model geometries (homogeneous and simply connected spaces with a “nice” metric): the two-sphere \mathbb{S}^2 , the Euclidean space E^2 , and the hyperbolic plane \mathbb{H}_2 . Any surface with genus $g > 1$ is obtained from the latter (see for instance [196]).

It is natural to ask whether there exists a similar classification in three dimensions. This question has only been recently, and positively!, answered by G. Perelman⁶, who has proved the Thurston geometrization conjecture [197, 198, 199]. One could naively think that the model geometries in three dimensions are in correspondence with the two-dimensional ones: \mathbb{S}^3 , E^3 and \mathbb{H}_3 . But it is easy to see that these three are not enough since all of them are isotropic, and there are three-manifolds like $\mathbb{S}^2 \times \mathbb{R}$ that are not. In 1982 W. Thurston proposed eight model geometries for the classification of three-manifolds, and proved that a large part of them admitted a geometric structure modeled on these eight geometries. The classification in three dimensions is more complicated than in two dimensions since not all three-manifolds admit a geometric structure, but it is always possible to “cut any three-manifold into pieces” such that each of them does admit a geometric structure. This is the content of the geometrization conjecture. A good account of these topics can be read in [196]; despite not being completely up-to-date, it deals with a lot of the mathematical constructions we are using.

It is clear that the construction of a geometric structure is appealing to us, since the manifold parameterized by the $\underline{\omega}_i$ ’s in (6.1.3) will be precisely realized as a quotient of a model geometry by a discrete group of isometries. In order to know which of the eight model geometries we are dealing with, we can resort to the relation between these eight geometries and the Bianchi groups: seven of the eight geometries can be realized as a simply-connected three-dimensional Lie group (which were classified by Bianchi) with a left-invariant metric. From this construction (see for instance [200] for details) it follows that the metric

$$ds^2 = (\underline{\omega}_1)^2 + (\underline{\omega}_2)^2 + (\underline{\omega}_3)^2, \quad (6.1.24)$$

corresponds to the Thurston model geometry \widetilde{SL}_2 , since the algebra of the $\underline{\omega}_i$ ’s relates to the type VIII Bianchi algebra.

6.1.5 Master equation solutions

The master equation (6.1.16) is the same as (5.1.20), and therefore we still lack analytic solutions for it. As for CNP, we can take the alternative route of finding numerical solutions, but no matter what values we use for the initial conditions, the solutions always seem to

⁶Side note: Perelman’s works have become famous because of proving the Poincaré conjecture, which says that the only simply connected three-manifold that exists is the three-sphere \mathbb{S}^3 , up to diffeomorphisms; this result however was just a corollary of the much stronger statement he proved, the Thurston geometrization conjecture, which classifies all the possible geometric structures on three-manifolds.

exist only on a finite interval $[r_0, r_{\text{UV}}]$. This issue cannot be resolved by a redefinition of the radial coordinate, since the invariant length $\int_{r_0}^{r_{\text{UV}}} dr \sqrt{g_{rr}}$ is finite for all the solutions. We identify r_0 with the deep IR, and $r \rightarrow r_{\text{UV}}$ with the UV⁷. We comment on this identification later in section 6.1.6. Now let us prove that this finite range for the solutions is not an artifact of the numerics, and that any solution of the master equation always breaks down at some finite value of r . Recall that in order for the solutions to be consistent we need the conditions (6.1.17) to hold. They are equivalent to the following ones:

$$P \leq 0, \quad |Q| \leq |P|, \quad P' + \hat{N}_f \geq 0. \quad (6.1.25)$$

Proof

Let us proceed by contradiction: Assume we have a solution extending all the way from some finite r_{IR} to ∞ . If we look at the conditions (6.1.25) for large enough r , we easily deduce that

$$-\hat{N}_f \leq \lim_{r \rightarrow \infty} P' \leq 0. \quad (6.1.26)$$

Now let us focus our attention on the $r \rightarrow \infty$ limit of the following piece of the master equation:

$$\frac{P' + Q' + 2\hat{N}_f}{P - Q} + \frac{P' - Q' + 2\hat{N}_f}{P + Q}. \quad (6.1.27)$$

We want to see that the limit of this piece is not positive. When $2\hat{N}_c = \hat{N}_f$, which implies that Q is constant, it is immediate that this limit is negative or zero in virtue of the constraints (6.1.25). In the $2\hat{N}_c \neq \hat{N}_f$ case, we can notice that these constraints imply that both denominators are always negative, and also that the $P' + \hat{N}_f$ piece is always positive. Since asymptotically we have $Q' + \hat{N}_f \sim 2\hat{N}_c$, the first summand will give a non-positive contribution. The second summand is a little bit more troublesome, since $-Q' + \hat{N}_f \sim 2(\hat{N}_f - \hat{N}_c)$ asymptotically, and this could be negative if $\hat{N}_f > \hat{N}_c$. But actually, when $\hat{N}_f > \hat{N}_c$ holds, one can see that because of the last constraint in (6.1.25), the denominator $P + Q$ goes to $-\infty$, and the contribution of this summand is null.

So we conclude that the $r \rightarrow \infty$ limit of (6.1.27) is not positive. We can then have a look at the limit of the whole master equation (6.1.16):

Assuming that P is monotonic for large r , which is a sensible physical condition to impose, one can rigorously prove that (6.1.26) implies $\lim_{r \rightarrow \infty} P'' = 0$. Then:

$$\begin{aligned} 0 = \lim_{r \rightarrow \infty} P'' &= - \lim_{r \rightarrow \infty} \left[(P' + \hat{N}_f) \left(\frac{P' + Q' + 2\hat{N}_f}{P - Q} + \frac{P' - Q' + 2\hat{N}_f}{P + Q} - 4 \coth(2r - 2r_0) \right) \right] \leq \\ &\leq -4 \left(\lim_{r \rightarrow \infty} P' + \hat{N}_f \right). \end{aligned} \quad (6.1.28)$$

The only possibility for satisfying this equation is to have $\lim_{r \rightarrow \infty} P' = -\hat{N}_f$. But actually this is ruled out by the master equation as well. This can be seen by writing $P = -\hat{N}_f r + p(r)$,

⁷Notice that r_{UV} denotes the place in the geometry where our solutions stop being valid. It is the furthest point along the RG flow we can probe in the dual field theory.

with $p(r)$ tending to zero as $r \rightarrow \infty$. The master equation could be solved asymptotically and the leading behavior for p would be $p \sim e^{4r}$: a contradiction. ■

As in CNP, we can content ourselves with getting analytic expansions both in the IR and in the UV. These expansions can be connected numerically, and a lot of physically relevant information (about the dual field theory) can be extracted from them. Since we are only interested in seeing Kutasov duality, that is seen at the level of the equations of motion, we just summarize quickly the possible expansions that can be found, to get a flavor of how the solutions look like. The details can be found in [26]. There one finds one expansion for the IR situated at $r = r_0 > -\infty$ and three different expansions for the UV situated at $r = r_{UV} < \infty$. Without loss of generality, the choice $r_{UV} = 0$ can be made, so we automatically have $r_0 < 0$.

Expansions in the IR

As we just said, there is an unique infrared expansion, around $r = r_0$. For Q not to have a pole there⁸, one needs to impose first $Q_0 = -\frac{2\hat{N}_c - \hat{N}_f}{2}(1 + 2r_0)$. Then one finds that the expansion for the function P is:

$$P = P_0 - \hat{N}_f(r - r_0) + \frac{4}{3}\tilde{c}_+^3 P_0^2(r - r_0)^3 - 2\tilde{c}_+^3 \hat{N}_f P_0(r - r_0)^4 + \frac{4}{5}\tilde{c}_+^3 \left(\hat{N}_f^2 + \frac{4}{3}P_0^2 \right) (r - r_0)^5 + \mathcal{O}((r - r_0)^6), \quad (6.1.29)$$

where P_0 and \tilde{c}_+ are free constants that need to obey $P_0 < 0$ and $\tilde{c}_+ > 0$, in order to satisfy the consistency conditions (6.1.17) imposed on the solutions of the master equation. The functions in the metric are such that the dilaton is finite, e^{2h} and e^{2k} go to 0, while e^{2g} goes to infinity. This generates a curvature singularity in the IR, very similar to the CNP one.

To analyze this singularity, we can look at the behavior of several curvature invariants around $r = r_0$:

$$R = \frac{\hat{N}_f^2 e^{-\Phi_0/2}}{2\tilde{c}_+^3 P_0^4} (r - r_0)^{-2} + \frac{7\hat{N}_f^3 e^{-\Phi_0/2}}{4\tilde{c}_+^3 P_0^5} (r - r_0)^{-1} + e^{-\Phi_0/2} \frac{189\hat{N}_f^4 - 16\hat{N}_f(8\hat{N}_c P_0^2 - 9\tilde{c}_+^3 P_0^4) + 128\hat{N}_c^2 P_0^2}{48\tilde{c}_+^3 P_0^6} + \mathcal{O}((r - r_0)),$$

$$R_{\mu\nu\rho\sigma} R^{\mu\nu\rho\sigma} = \frac{20 e^{-\Phi_0}}{\tilde{c}_+^6 P_0^4} (r - r_0)^{-8} + \frac{52\hat{N}_f e^{-\Phi_0}}{\tilde{c}_+^6 P_0^5} (r - r_0)^{-7} + \mathcal{O}((r - r_0)^{-6}). \quad (6.1.30)$$

From that, one can see that a generic solution is indeed singular in the IR, since the Ricci scalar $R \sim (r - r_0)^{-2}$. It can be seen to be a “good” singularity in the sense that the metric component $g_{x^0 x^0} = e^{\Phi/2}$ is bounded [85].

It makes sense to think that the reason for the existence of this singularity is the same as in CNP: we are dealing with backreacting massless flavors. Then an infinite number of

⁸Notice that this condition follows from the constraint on P and Q for this case: if Q has a pole, P must have a pole too, with negative residue, but this is not possible to achieve for finite r because of the $P' \geq -\hat{N}_f$ constraint.

flavor D5 branes intersect at $r = r_0$, generating a divergent density, and therefore a curvature singularity in the space. However, the singularity does not disappear in the unflavored case $\hat{N}_f = 0$, as it happens for CNP. In this unflavored case, the Ricci scalar goes to a constant in the IR, the same as $R_{\mu\nu}R^{\mu\nu}$, but the solution is still singular, as one can see by looking at $R_{\mu\nu\rho\sigma}R^{\mu\nu\rho\sigma}$.

Some speculation is needed to explain this singularity. One possibility is that the presence of higher-genus manifolds that go to zero size in the IR is troublesome, since they contain non-contractible cycles, and one should not be allowed to make them vanish. But this seems more of a topological obstruction, that should not be reflected in the quantities (6.1.30), which are local invariants. The origin of this singularity remains unclear.

Expansions in the UV

As we are looking for a solution that has a space ending in $r = r_{UV} = 0$, we have to find solutions where some function in the metric either goes to zero, or to infinity at this point. Then it is possible to find three different possibilities for the UV expansions. These can be grouped into two classes, class I and class II, looking at which are the singular functions at $r = 0$.

In class I we have e^{2h} going to 0 while e^{2k} goes to infinity, and there are two possibilities for the expansion for P depending on the sign of $2\hat{N}_c - \hat{N}_f$:

$$\begin{aligned}
 P &= Q + h_1(-r)^{1/2} + \frac{1}{6b_0}(-h_1^2 + 12b_0(b_1 + \hat{N}_f))(-r) \\
 &\quad + \frac{h_1}{72b_0^2}(5h_1^2 - 6b_0(5b_1 + 2\hat{N}_f) + 72b_0^2 \coth(2r_0))(-r)^{3/2} + \mathcal{O}((-r)^2), \quad (\hat{N}_f > 2\hat{N}_c), \\
 P &= -Q + h_1(-r)^{1/2} + \frac{1}{6b_0}(h_1^2 + 12b_0(\hat{N}_f - b_1))(-r) \\
 &\quad + \frac{h_1}{72b_0^2}(5h_1^2 - 6b_0(5b_1 - 2\hat{N}_f) + 72b_0^2 \coth(2r_0))(-r)^{3/2} + \mathcal{O}((-r)^2), \quad (\hat{N}_f < 2\hat{N}_c),
 \end{aligned} \tag{6.1.31}$$

where b_0, b_1, b_2 are the coefficients in the expansion for $Q = b_0 + b_1r + b_2r^2 + \mathcal{O}(r^3)$, namely:

$$\begin{aligned}
 b_0 &= \frac{1}{2}(2\hat{N}_c - \hat{N}_f)(2r_0 \coth(2r_0) - 1), \\
 b_1 &= \frac{1}{2}(2\hat{N}_c - \hat{N}_f) \frac{4r_0 - \sinh(4r_0)}{\sinh^2(2r_0)}, \\
 b_2 &= (4\hat{N}_c - 2\hat{N}_f) \frac{2r_0 \cosh(2r_0) - \sinh(2r_0)}{\sinh^3(2r_0)}.
 \end{aligned} \tag{6.1.32}$$

In class II, e^{2h} and e^{2k} both go to 0 while the dilaton diverges at $r = 0$. The expansion for P is

$$\begin{aligned}
 P &= -b_0 + \hat{N}_f(-r) + P_2(-r)^2 \\
 &\quad + \frac{P_2}{3b_0(\hat{N}_f - b_1)}(b_1^2 - \hat{N}_f^2 + 2b_0(b_2 - 3P_2) - 8b_0(b_1 - \hat{N}_f) \coth(2r_0))(-r)^3 + \mathcal{O}((-r)^4),
 \end{aligned} \tag{6.1.33}$$

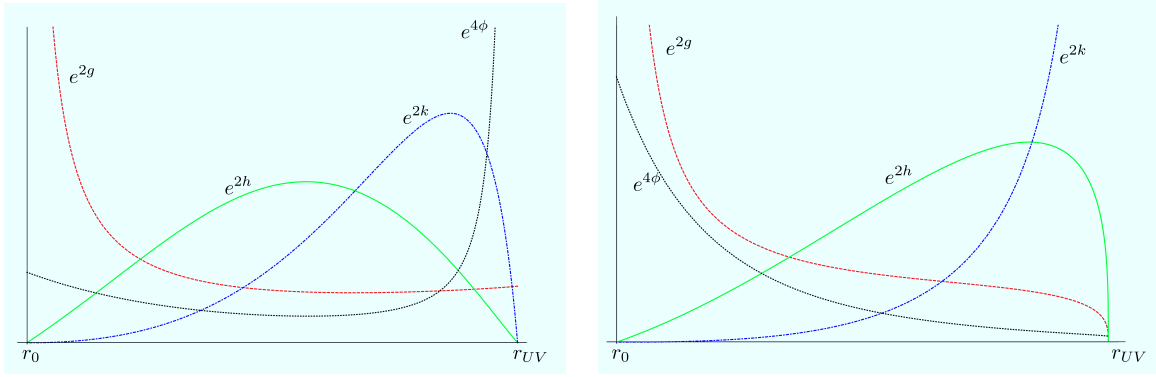


Figure 6.1: Plots of the functions e^{2g} , e^{2h} , e^{2k} and $e^{4\phi}$. On the left, the plots are of class I solutions, while on the right they are of class II.

and it is only valid for $\hat{N}_f < \hat{N}_c$.

In order to see the qualitative behavior of the metric functions for these UV's, and how they can be connected with the unique IR expansion, we show in figure 6.1 some plots coming from the numerics.

6.1.6 The Field Theory interpretation

At this point, we can claim to have found some new type IIB supergravity solutions. These solutions are describing D5-branes wrapping Riemann surfaces with genus $g > 1$. In the IR, one expects the theory on the branes to become effectively a four-dimensional gauge theory and, as explained at the beginning, to have $(g - 1)$ massless adjoint fermions. We want to argue that the dual field theory is of the SQCD-type plus adjoint matter, charged under the gauge field and self-interacting through a dangerously irrelevant polynomic superpotential. To do this, *we show how our $\mathbb{H}_2 \times \widetilde{SL}_2$ solutions encode a Kutasov-like duality*, which is typical from this kind of theories. Ideally, one would like to extract from these solutions much more information about the dual field theory. This would be especially interesting in this case, as not much is known about SQCD theories with adjoint matter. An attempt to do this was done in [26], but the interpretation of the results is not fully clear, so we just include a small discussion at the end of the subsection. Let us try to find Kutasov duality then.

As we proposed at the beginning of the section, we want to find a pair of gravity solutions, dual to theories with adjoint matter and with the same IR geometry, that can be related by the numerology of (6.1.2). Since we have been paralleling CNP the whole section, it is useful to recall the way one was able to see a geometric realization of Seiberg duality in the CNP solution: the idea was to notice that the BPS equations of the supergravity system remained the same under the change:

$$N_c \rightarrow N_f - N_c, \quad N_f \rightarrow N_f. \quad (6.1.34)$$

This implied that the same theory admitted two dual descriptions along all the RG flow, instead of just in the IR. This happened because the CNP solution is dual to $SU(N_c)$ SQCD

with a quartic superpotential, and such a theory is actually Seiberg self-dual. We expect a similar phenomenon for our $\mathbb{H}_2 \times \widetilde{SL}_2$ solutions, so that Kutasov duality also holds along all the RG flow.

Indeed, it is easy to see that in our case, the master equation (6.1.16) possesses the symmetry:

$$\hat{N}_c \rightarrow \hat{N}_f - \hat{N}_c, \quad \hat{N}_f \rightarrow \hat{N}_f. \quad (6.1.35)$$

If we take into account relations (6.1.19) and (6.1.22), we can rephrase this symmetry as:

$$N_c \rightarrow \frac{8\text{Vol}(\widetilde{SL}_2)}{\text{Vol}(\mathbb{H}_2)^2} N_f - N_c, \quad N_f \rightarrow N_f. \quad (6.1.36)$$

Calling $k = \frac{8\text{Vol}(\widetilde{SL}_2)}{\text{Vol}(\mathbb{H}_2)^2}$, we see that we get precisely the transformation needed for Kutasov duality! The geometrical interpretation of Kutasov duality is essentially the same as for Seiberg duality in CNP, where we were interchanging two two-spheres; while here the duality corresponds to the swap of the two \mathbb{H}_2 's (their quotients to be more precise) present in the geometry (6.1.3). Notice that this duality only makes sense when $\hat{N}_f > \hat{N}_c$, and exchanges $2\hat{N}_c - \hat{N}_f \rightarrow \hat{N}_f - 2\hat{N}_c$. Consequently, it is only possible to perform a Kutasov duality for the solutions with the UV asymptotics of class I.

Let us briefly discuss what are the possible quotients by discrete groups of isometries we can perform on \mathbb{H}_2 and \widetilde{SL}_2 , and what is the resulting value for the ratio

$$k = \frac{8\text{Vol}(\widetilde{SL}_2)}{\text{Vol}(\mathbb{H}_2)^2}. \quad (6.1.37)$$

Recall that in (6.1.37), the volumes stand for the finite volumes of the quotients \mathbb{H}_2/Γ and \widetilde{SL}_2/G .

The quotients of \mathbb{H}_2 are very well known. The discrete subgroups Γ of its isometry group $PSL(2, \mathbb{R})$ are the so-called Fuchsian groups, and the resulting quotients \mathbb{H}_2/Γ are Riemann surfaces of genus $g > 1$ of constant negative curvature $R = -1$. The volume of such a quotient can be straightforwardly computed from the Gauss-Bonnet theorem:

$$\text{Vol}(\mathbb{H}_2) = \int \omega_{\text{Vol}(\mathbb{H}_2)} = - \int R \omega_{\text{Vol}(\mathbb{H}_2)} = -2\pi\chi(g) = 4\pi(g-1), \quad (6.1.38)$$

where χ is the Euler characteristic of the resulting Riemann surface.

The isometry group of \widetilde{SL}_2 might be less well known, but its structure can be deduced from the exact sequence

$$0 \rightarrow \mathbb{R} \rightarrow \mathcal{I} \rightarrow PSL(2, \mathbb{R}) \rightarrow 1, \quad (6.1.39)$$

where \mathcal{I} is standing for the identity component⁹ of the isometry group of \widetilde{SL}_2 . This means that basically there are two types of isometries acting on \widetilde{SL}_2 , which can be thought as an \mathbb{S}^1 -bundle over \mathbb{H}_2 . One type comprises the isometries that rotate the \mathbb{S}^1 , i.e., that rotate

⁹The isometry group of \widetilde{SL}_2 has two connected components and the other one simply contains the isometries induced from the orientation-reversing isometries of \mathbb{H}_2 .

the fibers through a constant angle, while covering the identity map of \mathbb{H}_2 . This type is parameterized by \mathbb{R} . The other type is composed of those isometries that “rotate” the base \mathbb{H}_2 , and it is therefore parameterized by $PSL(2, \mathbb{R})$. This “rotation” on the base also induces a constant-angle rotation in each fiber \mathbb{S}^1 .

The idea to retain from the discussion of the paragraph above, is that each quotient of \widetilde{SL}_2 will be roughly a quotient of the base \mathbb{H}_2 times a quotient of \mathbb{S}^1 . The quotient we have to perform on the base \mathbb{H}_2 has to be equal to the one we performed in the other \mathbb{H}_2 of the geometry. The only freedom left is to perform an extra discrete quotient in \mathbb{S}^1 . We compute the volume of \widetilde{SL}_2 , including the effect of a winding number m of the color branes, as:

$$\text{Vol}(\widetilde{SL}_2) = m \int \omega_{\text{Vol}(\widetilde{SL}_2)} = m \int \omega_{\text{Vol}(\mathbb{H}_2)} \wedge \omega_{\text{Vol}(\mathbb{S}^1)} = m \text{Vol}(\mathbb{H}_2) \text{Vol}(\mathbb{S}^1). \quad (6.1.40)$$

We already know the volume of the base (6.1.38). The volume of the \mathbb{S}^1 , taking into account the quotienting, will be $\text{Vol}(\mathbb{S}^1) = \frac{2\pi}{n}$, where n is an integer. Then:

$$\text{Vol}(\widetilde{SL}_2) = 2\pi^2 q (g - 1), \quad (6.1.41)$$

where $q = \frac{4m}{n}$ is a rational number. And coming back to (6.1.37), the k of Kutasov duality will be, in terms of the quotient parameters:

$$k = \frac{q}{g - 1}. \quad (6.1.42)$$

In general $q \in \mathbb{Q}$, but for some particular configurations, this k becomes an integer, as required from the field theory expectation. Unfortunately, the relation between the quotienting and the generation of the $\text{Tr} X^{k+1}$ superpotential is unclear. Leaving room for some more speculation, since k is proportional to the winding number m of the color branes wrapping the hyperbolic cycle, this might be the reason why k is appearing in the superpotential for the adjoint fermions in the dual field theory: as an adjoint can be thought as a zero-mode of the B-field wrapping a particular cycle on the Riemann surface, the winding of the brane would correspond to the adjoint self-interacting $k \sim m$ times.

Additional field theory comments

Let us wrap up this section about Kutasov duality within the gauge/gravity correspondence by making some comments about the complete gauge/gravity picture of the solutions we found. We use some results of [26] (mainly section 4 of that paper) that were not discussed here.

We tried to build a type IIB supergravity solution as close as possible to a dual of SQCD plus adjoint matter. The starting point was the CNP solution, dual to SQCD plus a quartic superpotential, plus some KK dynamics that are relevant in the UV. By replacing some cycles of CNP by hyperbolic cycles, we introduce $g - 1$ adjoints in the dual theory, where $g > 1$ is the genus of the Riemann surfaces generated after quotienting the hyperbolic cycles. With this, the Seiberg duality of CNP gets replaced by something that looks like Kutasov duality. What are the differences with it (and the reasons for the “-like” in the title of the section)?

- Kutasov duality involves only one adjoint, while here we have theories with $g - 1$ adjoints. This is not a big problem, as Kutasov duality can be generalized to the case where we have multiple generations of adjoint chiral superfields [201].
- We get a value for k (that is the same for the multiple generations of adjoints) in terms of the quotients we perform, and the winding number of the color branes, that is not necessarily an integer. From the field theory, one only expects integer values. Moreover, it is not clear how the superpotential (6.1.1) is generated from these quotients. We (only) gave some qualitative reasoning on how this could happen at the end of section 6.1.6.
- Kutasov duality only relates two theories in the IR. The duality we found holds along all the RG flow. We expect that the reason is along the same lines as the one why Seiberg duality works along all the RG flow, but we lack a good field theory explanation as one has there.

Not much is known about the UV of the theories displaying Kutasov duality. The fact that in (6.1.1) $\text{Tr} X^{k+1}$ is an irrelevant operator puts these theories in need of a UV completion if they are to be well-defined. Moreover, the general expectation from the NSVZ β -function is that we might come across a Landau pole. Since

$$\frac{\partial g_{YM,4}}{\partial \log \mu} \propto g_{YM,4}^{-3} (3N_c - N_{\text{adj}}(1 - \gamma_{\text{adj}}) - N_f(1 - \gamma_f)) , \quad (6.1.43)$$

where N_{adj} is the number of chiral adjoints, and the γ 's are the anomalous dimensions; we see that the adjoints will generically push towards a Landau pole, in the same direction as the flavors. Can any of this be matched with our supergravity solutions?

The hyperbolic solutions we found are compact, in the sense that they only exist for a finite range of r , so certainly they do not provide an UV completion. Regarding the Landau pole issue, it is possible to study the gauge coupling g_{YM} from the gravity duals. The computation is basically the same as for CNP, and it yields the same result

$$\frac{1}{g_{YM,4}^2} \sim \left[e^{2h} + \frac{e^{2g}}{4}(1-a)^2 \right] = -P e^{-\tau} . \quad (6.1.44)$$

From the UV expansions, one can see that this quantity is blowing up at $r = r_{\text{UV}}$ for the UV's of Class I. Nonetheless, if one computes the holographic c -function [202], one sees that it grows from $r_{\text{IR}} = r_0$ to a point $r_* < r_{\text{UV}}$, where it blows up (for both classes of UV's). Since this function is roughly counting the number of degrees of freedom in the theory, this means that the dual field theory interpretation must stop at r_* . This behavior has also been found in other solutions with Landau pole [203].

After studying other field theory observables, it might be that the dual field theory interpretation has to stop even before r_* . There are indications that at the scale $r = r_*$, the KK dynamics are already relevant, and in consequence the interpretation via a four-dimensional field theory is no longer accurate. These indications are that some observables depend on the class of UV considered. Presumably, the two different classes of UV should

correspond, as for CNP, to different operators being turned on, and leading to different UV dynamics.

So in summary, our backgrounds seem to be describing $\mathcal{N} = 1$ field theories with adjoint matter. These theories are self-dual under a duality with the basic numerology of Kutasov duality, but the polynomial superpotential typical of Kutasov duality could not be matched rigorously from the gravity side. In addition, these theories seem to have Landau poles, which would explain the origin of the UV singularity we get in the supergravity solutions, but there is a caveat: the Landau pole scale seems to be mixed with the KK dynamics present in all wrapped-brane models, and thus it is not clear whether this Landau pole is a consequence of the four-dimensional dynamics. Clearly, a more precise and quantitative understanding of the dual field theories would be desirable.

6.2 SQCD in low dimensions

As we discussed in section 3.2.1, a way to obtain gravity duals to SYM with n supercharges in d dimensions is by wrapping Dp -branes on some k -cycle (with $p + 1 - k = d$) inside a manifold with n Killing spinors. Such a manifold has special holonomy. After taking the appropriate decoupling limit, when the number N_c of branes we wrap is large, they backreact on the geometry so that this special holonomy manifold is deformed, but a G-structure is preserved (recall the discussion in section 3.2). We are left with a supergravity solution of the form Minkowski \times (manifold with a G-structure), which is dual, in the region where the size of the k -cycle is small (in string units), to a SYM theory in d dimensions with the appropriate amount of supersymmetry.

This is the way one builds the MN solution of section 3.2.2, which is dual to $\mathcal{N} = 1$ SYM plus a UV completion, given by the dynamics of a tower of KK modes that deconstruct a two-sphere in the UV. These methods can be used for generic dimensions to find gravity duals to SYM theories plus some UV completion (whose details are irrelevant in the IR). Moreover, one can use the methods of section 3.3.1 to add flavor to these solutions, *i.e.* to build duals to SQCD-like theories. In this sense, CNP added flavor to the MN solution.

We collect in table 6.1 the efforts that have been made to study wrapped-brane models for the constructions of duals to SYM/SQCD in different dimensions and different amounts of SUSY. Notice that the maximum amount of supercharges one can obtain with these models is eight¹⁰, and we focus on dimensions $d = 4, 3, 2$. The reason for the latter is two-fold: first, for phenomenological reasons ($d = 4$ is obvious, and $d = 3, 2$ can describe systems that are confined to live on a plane or a line, as it happens for some condensed-matter systems); and second, because $d \leq 4$ is the most explored avenue theoretically (especially for $d = 2$ a lot of exact results are available: Schwinger model, 't Hooft model for mesons, etc).

All these models share some characteristics. The main one is that all the supergravity duals are valid only in the IR. Because we are using a wrapped-brane model, as we move

¹⁰When the brane is not wrapped, the amount of supercharges we preserve is sixteen. This is because the presence of a Dp -brane is only consistent with the preservation of half of the supercharges of either IIA or type IIB supergravity. Only in the very special case $p = 3$, all the thirty-two supercharges are preserved, the reason being that $\mathcal{N} = 4$ SYM is conformally invariant. It is the only maximally supersymmetric YM theory with this property.

supercharges		8	4	2	1
$d = 4$	SYM	$\mathcal{N} = 2$ [204, 205]	$\mathcal{N} = 1$ [88]	—	—
	SQCD	$\mathcal{N} = 2$ [206]	$\mathcal{N} = 1$ [108]	—	—
$d = 3$	SYM	$\mathcal{N} = 4$ [85, 207]	$\mathcal{N} = 2$ [208, 209]	$\mathcal{N} = 1$ [210]	—
	SQCD	$\mathcal{N} = 4$ [211]	$\mathcal{N} = 2$ [78, 27]	$\mathcal{N} = 1$ [212]	—
$d = 2$	SYM	$\mathcal{N} = (4, 4)$ [213]	$\mathcal{N} = (2, 2)$ [27, 28]	$\mathcal{N} = (1, 1)$ [28]	not known
	SQCD	$\mathcal{N} = (4, 4)$ [213]	$\mathcal{N} = (2, 2)$ [27, 28]	$\mathcal{N} = (1, 1)$ [28]	not known

Table 6.1: This table displays the works where duals to the type of theory indicated were first found, using the wrapped-brane approach. The theories with the dash do not exist. We focus in this section on the cases marked in red.

to the UV we start to see the dimensions of the compact cycle, and the dual field theory becomes higher-dimensional. This is inherent to the approach, and there is no way out. The way one builds the solutions is also very similar, and some geometries of different theories share some similitudes. Among all the models in table 6.1, we can distinguish two classes, the theories with minimal supersymmetry, and the others. The minimal supersymmetry depends on the dimension, and it is four supercharges in $d = 4$, two supercharges in $d = 3$, and one supercharge in $d = 2$. All the other theories have non-minimal supersymmetry.

Why make a difference between minimal and non-minimal supersymmetry? The reason is that in the latter case, a theory with a gauge boson contains also scalar particles. There will be a superpotential for these scalars, and therefore, in general, a moduli space for the vacua of the theory where the scalars take different VEV's. This moduli space has to be reflected in the geometry of the dual theory. Through, the dictionary, scalars correspond to directions transverse to the color branes. So for instance, in $\mathcal{N} = 2$ four-dimensional SYM, there is a complex scalar, equal to two real scalars. The moduli space is associated with the VEV's these two scalars can take; and this is reflected in the presence of an \mathbb{R}^2 in the geometry (see the corresponding references of table 6.1). For the cases we are going to study, the moduli space of SYM with non-minimal supersymmetry is non-compact. Then, the dual geometries must contain a non-compact space. This implies that these geometries must have, apart from the usual radial coordinate, another non-compact one. *So the dual geometries to non-minimally supersymmetric YM theories in low dimensions have two “radial coordinates”.*

Of these two non-compact coordinates, one should be the usual radial coordinate, while the other one allows to move in the moduli space. We denote them by ρ and σ respectively. However, this distinction is not so clear-cut, as the quantity that characterizes how much we move away from the color branes (what we have called the radial coordinate in all the previous chapters) is a combination of both ρ and σ . The dual field theory interpretation is not so clean in these cases, even though some nice checks can be done, especially in the cases with eight supercharges. For this reason, we focus only on the construction of the supergravity solutions in these sections. The original references can be consulted for a little bit of field theory.

As we said, all the supergravity solutions of these non-minimally supersymmetric cases are very similar. They can be built in an akin fashion. Thus, we present the basics of the geometries altogether, so that the differences and similarities are better appreciated. We always work with (smeared) flavor, *i.e.* we look for duals of SQCD, since the case without flavor is included (just put $N_f = 0$). For the construction of the supergravity solutions with flavor we use the macroscopic approach (that we described in 3.3.1). Recall that the main disadvantage of this method is that one did not know about the microscopic embeddings. In section 6.2.2, we show how some of these embeddings can be found by just looking at the terms present in the smearing form derived from the macroscopic approach.

6.2.1 A macroscopic point of view

Our goal is to build supergravity solutions dual to the theories marked in red in table 6.1. We want to use wrapped-brane models to achieve this. Then we need to choose what kind of Dp -brane we want to use, and where we want to wrap it. There are several possibilities. We choose the following ones:

- $\mathcal{N} = 2$ in $d = 3$. We wrap D4-branes on a two-sphere inside a manifold with $SU(3)$ -structure (this the only case where we use IIA supergravity). We also wrap D5-branes on a three-sphere inside another manifold with $SU(3)$ -structure.
- $\mathcal{N} = (2, 2)$ in $d = 2$. We wrap D3-branes on a two-sphere inside a manifold with $SU(3)$ -structure. We also wrap D5-branes on the product of two two-spheres inside another manifold with $SU(3)$ -structure.
- $\mathcal{N} = (1, 1)$ in $d = 2$. We wrap D5-branes on a four-sphere inside a manifold with G_2 -structure.

The flavor is always added with the same kind of branes, so that color and flavor branes are both Dp -branes for given p , but extended along different cycles. The flavor branes always wrap the non-compact direction σ . The manifold with G -structure has to be chosen in such a way that its metric is explicitly a cone over a base which is some manifold fibered over the cycle wrapped by the color branes. The fibration is determined by the twisting procedure that has to be done for wrapping a brane on a curved manifold [85]. This fibration can be found through the methods of gauged supergravity (the Ph.D. thesis [93] contains a nice account of these methods), but they happen to yield always the various conifold fibrations for manifolds with $SU(3)$ -structure, and the fibration of the Bryant-Salamon G_2 metric [214] for manifolds with a G_2 -structure. We can bypass the gauged supergravity step and assume we know the correct fibrations from the beginning. With this, an ansatz for the metric can be written. We work in string frame:

$$ds_{10}^2 = H^{-\frac{1}{2}} dx_{d-1,1}^2 + L \alpha' \left[ds_{\text{internal manifold}}^2 + H^{\frac{1}{2}} ds_{\mathbb{R}^m}^2 \right], \quad (6.2.1)$$

where $H = H(\rho, \sigma)$ is the warp factor, L is a constant proportional to some power of $g_s N_c$, and m is the dimension of the moduli space. The radial coordinate in \mathbb{R}^m is ρ , and $m = 1$ for the theories in the first and third bullet above, and $m = 2$ for the theories in the middle

bullet. The internal manifold has radial coordinate σ and is the one carrying the G-structure, and as we argued before, it has to be expressed as a cone over a given base. We can write it generally as

$$ds_{\text{internal manifold}}^2 = H^{-\frac{1}{2}} z ds_{\text{wrapped cycle}}^2 + \frac{H^{\frac{1}{2}}}{z^a} (d\sigma^2 + \sigma^2 ds_{\text{fibered directions}}^2) , \quad (6.2.2)$$

where $z = z(\rho, \sigma)$ is the “size” of the internal cycle, H is the warped factor defined above, and a is some rational number fixed by supersymmetry. This number turns out to be:

$$a = \frac{\text{dimension wrapped cycle}}{(\text{dimension internal manifold}) - (\text{dimension wrapped cycle})} . \quad (6.2.3)$$

There is also a dilaton, except for the case $p = 3$, and it is related to the warp factor H as:

$$e^\Phi = H^{\frac{3-p}{4}} . \quad (6.2.4)$$

The ansatz is completed by a RR form F_{8-p} that couples magnetically (and also electrically for $p = 3$) to the Dp -branes. In the case without flavors, this RR flux can be generated via a potential C_{7-p} , as $F_{8-p} = dC_{7-p}$. However, when we add flavors, the flux is no longer closed, and there is no RR potential anymore. The failure to be closed is measured by the smearing form Ξ , characterized by equation (3.3.10). What is the generic form of the flux?

We assume we know how to build the unflavored potential C_{7-p} (this can be found from the gauged supergravity approach, or getting inspiration in the analogy with other known cases). Then the question is how to modify the unflavored $F_{8-p} = dC_{7-p}$ to account for the presence of flavors. We write the flux as:

$$F_{8-p} = dC_{7-p} + f_{8-p} , \quad (6.2.5)$$

where f_{8-p} is a non-closed form that contains the flavor contribution to the flux¹¹. Clearly

$$(2\kappa_{10}^2 T_{Dp}) \Xi = dF_{8-p} = df_{8-p} . \quad (6.2.6)$$

We are always going to localize the flavors in the non-compact direction ρ , at some point $\rho = \rho_Q$ (and in the cases with $m = 2$, we smear them in the transverse moduli space direction). This means that $f_{8-p} \propto \Theta(\rho - \rho_Q)$. Thus, the smearing must be proportional to $\delta(\rho - \rho_Q)d\rho$. Then it must be that

$$f_{8-p} = \Theta(\rho - \rho_Q) d\Lambda \implies F_{8-p} = dC_{7-p} + \Theta(\rho - \rho_Q) d\Lambda , \quad (6.2.7)$$

where Λ is some $(7-p)$ -form. The similarity between Λ and C_{7-p} is evident. Generically, the ansatz for C_{7-p} contains some unknown functions $g_i(\rho, \sigma)$ and some forms made out the angular coordinates (the ones that are not neither radial nor Minkowski) of the metric (6.2.2). We take for Λ the same ansatz as the one for C_{7-p} , replacing

$$g_i(\rho, \sigma) \rightarrow L_i(\sigma) . \quad (6.2.8)$$

¹¹Notice that C_{7-p} will not be exactly the unflavored one, but its ansatz remains invariant.

Notice that L_i must be only a function of σ , so that Ξ is proportional to $\delta(\rho - \rho_Q)d\rho$ and closed. With this, we have a full ansatz for the supergravity solution. As we always do in this Ph.D. thesis, to solve the equations of motion we can just impose supersymmetry, since we have an ansatz satisfying the Bianchi identities for the fluxes, and solve the easier first-order BPS system. This system can be compactly written in terms of a calibration form \mathcal{K}_{p+1} for the D p -branes. It reads as in (3.2.2), where ϵ is a Killing spinor of the background, that is normalized as $H^{\frac{1}{4}}\epsilon^\dagger\epsilon = 1$. Then, in string frame, the BPS conditions read

$$*dC_{p+1} = d\left(H^{\frac{p-3}{4}}\mathcal{K}_{p+1}\right), \quad d\left(H^{\frac{p-5}{4}}*\mathcal{K}_{p+1}\right) = 0. \quad (6.2.9)$$

From (6.2.9), we derive a system of coupled system of first-order partial differential equations for the functions $H(\rho, \sigma), z(\rho, \sigma), g_i(\rho, \sigma), L_i(\sigma)$. It happens that the system can be always reduced to a second-order PDE for the function $z(\rho, \sigma)$, that can be thought of as a “master equation” for the system. Once this is solved, we can start to analyze the predictions encoded for the dual field. As a side note, when we have more than one L_i , there appears an extra differential relation between them. This relation has to be imposed independently of the master equation.

As we said, we just want to focus on the supergravity construction. So the only thing left to do here is to illustrate all the general procedure described above with the particular examples in red of table 6.1. We compile them in what follows. Later, in section 6.2.2, we care about the microscopic interpretation of the solutions we constructed macroscopically.

Building $d = 3, \mathcal{N} = 2$ from wrapped D4-branes

We wrap D4-branes on a two-sphere S^2 inside a Calabi-Yau three-fold. The resulting metric has the fibrations of the singular conifold. The flavor branes are also D4-branes, orthogonal to the color branes outside the Minkowski directions. The brane setup is summarized in the following chart:

$d = 3, \mathcal{N} = 2$	$\overbrace{\hspace{10em}}^{\text{CY}_3}$									
	$\mathbb{R}^{1,2}(x^i)$			$S^2(\theta, \phi)$		$N_4(\sigma, \bar{\theta}, \bar{\phi}, \bar{\psi})$				$\mathbb{R}(\rho)$
N_c D4	—	—	—	○	○	·	·	·	·	·
N_f D4	—	—	—	- -	- -	—	○	- -	- -	·

The notation of the box has the following interpretation: — means “extended along this non-compact direction”; ○ means “extended along this compact direction”; · means “localized in this direction”; - - means “smeared over this direction”. For the flavor D4-branes, we should understand that each brane wraps a two-dimensional “plane” within the normal space N_4 ; and that these planes are smeared in such a way that collectively they fill up the space.

According to the general discussion we have made, the relevant information is the ansatz for the metric of the internal manifold, RR potential C_2 , flavor flux deformation Λ with

constraints (if any), a calibration \mathcal{K}_5 , and the second-order “master PDE”: Recalling the forms $\bar{\omega}^1, \bar{\omega}^2, \bar{\omega}^3$ we defined in (4.1.8), the relevant information is in this case:

$$\begin{aligned} ds_{\text{internal manifold}}^2 &= H^{-\frac{1}{2}} z \left(d\theta^2 + \sin^2 \theta d\phi^2 \right) + \\ &\quad + \frac{H^{\frac{1}{2}}}{z^{\frac{1}{2}}} \left(d\sigma^2 + \sigma^2 \left((\bar{\omega}^1)^2 + (\bar{\omega}^2)^2 + (\bar{\omega}^3 + \cos \theta d\phi)^2 \right) \right), \end{aligned} \quad (6.2.10)$$

$$C_3 = g_1 \bar{\omega}^1 \wedge \bar{\omega}^2 \wedge (\bar{\omega}^3 + \cos \theta d\phi) + g_2 \sin \theta d\theta \wedge d\phi \wedge (\bar{\omega}^3 + \cos \theta d\phi), \quad (6.2.11)$$

$$\Lambda = L_1(\sigma) \bar{\omega}^1 \wedge \bar{\omega}^2 \wedge (\bar{\omega}^3 + \cos \theta d\phi) + L_2(\sigma) \sin \theta d\theta \wedge d\phi \wedge (\bar{\omega}^3 + \cos \theta d\phi), \quad (6.2.12)$$

$$\dot{L}_2 = \frac{2}{\sigma} (L_2 - L_1), \quad (6.2.13)$$

$$\mathcal{K}_5 = e^{012} \wedge (e^{34} - e^{58} - e^{67}), \quad (6.2.14)$$

$$2z\sqrt{z}(\sigma\ddot{z} + \dot{z}) = \sigma \left(z'^2 - 2zz'' \right) + \frac{16m^2 z^{3/2}}{\sigma} (L_2 - L_1) \delta(\rho - \rho_Q). \quad (6.2.15)$$

The calibration is expressed in terms of the obvious¹² vielbein for the metric (6.2.10). The prime (dot) denotes derivatives with respect to ρ (σ).

Building $d = 3, \mathcal{N} = 2$ from wrapped D5-branes

We wrap D5-branes on a three-sphere \mathbb{S}^3 inside a Calabi-Yau three-fold. The resulting metric has the fibrations of the deformed conifold. The corresponding chart is:

$\overbrace{\hspace{10em}}^{\text{CY}_3}$										
$d = 3, \mathcal{N} = 2$	$\mathbb{R}^{1,2} (x^i)$			$S^3 (\bar{\theta}, \bar{\phi}, \bar{\psi})$			$N_3 (\sigma, \theta, \phi)$			\mathbb{R}
N_c D5	—	—	—	○	○	○	·	·	·	·
N_f D5	—	—	—	○	—	—	—	—	○	·

To write the metric of the deformed conifold as a cone over an $\mathbb{S}^2 \times \mathbb{S}^3$ fibration, it is useful to define the one-forms S^i ($i = 1, 2, 3$) as:

$$\begin{aligned} S^1 &= \sin \phi \bar{\omega}^1 - \cos \phi \bar{\omega}^2, \\ S^2 &= \sin \theta \bar{\omega}^3 - \cos \theta (\cos \phi \bar{\omega}^1 + \sin \phi \bar{\omega}^2), \\ S^3 &= -\cos \theta \bar{\omega}^3 - \sin \theta (\cos \phi \bar{\omega}^1 + \sin \phi \bar{\omega}^2), \end{aligned} \quad (6.2.16)$$

where the forms $\bar{\omega}^1, \bar{\omega}^2, \bar{\omega}^3$ are the ones in (4.1.8). It is also useful to define one-forms E^1 and E^2 that cast as:

$$\begin{aligned} E^1 &= d\theta + \frac{1}{2} (\sin \phi \bar{\omega}^1 - \cos \phi \bar{\omega}^2), \\ E^2 &= \sin \theta \left(d\phi + \frac{1}{2} \bar{\omega}^3 \right) - \frac{\cos \theta}{2} (\cos \phi \bar{\omega}^1 + \sin \phi \bar{\omega}^2). \end{aligned} \quad (6.2.17)$$

¹²Notice the metric (6.2.10) is expressed a “sum of squares” already. This will happen for all the cases within this subsection. The obvious vielbein is then $e^i = H^{-1/4} dx^i$, $e^3 = H^{-1/4} \sqrt{z} d\theta$, $e^4 = H^{-1/4} \sqrt{z} \sin \theta d\phi$, $e^5 = H^{1/4} z^{-1/4} d\sigma$, $e^6 = H^{1/4} z^{-1/4} \sigma \bar{\omega}^1, \dots$

Notice that the metric of the deformed conifold can be written in terms of the one-forms S^i and E^j as follows:

$$ds_6^2 = \frac{1}{2} \mu^{\frac{4}{3}} K(\sigma) \left[\frac{1}{3K(\sigma)^3} \left((d\sigma)^2 + 4(S^3)^2 \right) + 2 \cosh^2 \left(\frac{\sigma}{2} \right) \left((S^1)^2 + (S^2)^2 \right) + 2 \sinh^2 \left(\frac{\sigma}{2} \right) \left((E^1)^2 + (E^2)^2 \right) \right], \quad (6.2.18)$$

where $0 \leq \sigma < +\infty$ is the radial coordinate, μ is the deformation parameter of the conifold and $K(\sigma)$ is the function:

$$K(\sigma) = \frac{(\sinh(2\sigma) - 2\sigma)^{\frac{1}{3}}}{2^{\frac{1}{3}} \sinh \sigma}. \quad (6.2.19)$$

The relevant information is now

$$ds_{\text{internal manifold}}^2 = H^{-\frac{1}{2}} \frac{z}{4} [(\bar{\omega}^1)^2 + (\bar{\omega}^2)^2 + (\bar{\omega}^3)^2] + \frac{H^{\frac{1}{2}}}{z} \left[d\sigma^2 + \sigma^2 \left((E^1)^2 + (E^2)^2 \right) \right], \quad (6.2.20)$$

$$C_2 = g_1 E^1 \wedge E^2 + g_2 S^1 \wedge S^2, \quad (6.2.21)$$

$$\Lambda = L_1(\sigma) E^1 \wedge E^2 + L_2(\sigma) S^1 \wedge S^2, \quad (6.2.22)$$

$$\dot{L}_2 = \frac{1}{\sigma} (L_2 - L_1), \quad (6.2.23)$$

$$\mathcal{K}_6 = -e^{012} \wedge (e^{345} + e^{367} + e^{468} - e^{578}), \quad (6.2.24)$$

$$z \left(z \ddot{z} + \frac{1}{2} \dot{z}^2 \right) = \frac{1}{2} z'^2 - z z'' + \frac{2(L_2 - L_1)}{\sigma} z^{3/2} \delta(\rho - \rho_Q). \quad (6.2.25)$$

Building $d = 2$, $\mathcal{N} = (2, 2)$ from wrapped D5-branes

We wrap D5-branes on $\mathbb{S}^2 \times \mathbb{S}^2$ inside a Calabi-Yau three-fold. The resulting metric has the fibrations of the regularized conifold. The brane setup is the simplest among all the cases of this subsection, and we can be very precise regarding where the branes are sitting. There are two stacks of flavor branes, each wrapping one \mathbb{S}^2 :

$d = 2, \mathcal{N} = (2, 2)$	$\overbrace{\hspace{10em}}^{\text{CY}_3}$									
	$\mathbb{R}^{1,1}(x^i)$		\mathbb{S}^2		\mathbb{S}^2		N_2		\mathbb{R}^2	
	x^0	x^1	θ^1	ϕ^1	θ^2	ϕ^2	σ	ψ	ρ	χ
N_c D5 (color)	—	—	○	○	○	○	·	·	·	·
N_f D5 (flavor)	—	—	○	○	--	--	—	—	·	--
N_f D5(flavor)	—	—	--	--	○	○	—	—	·	--

According to the general discussion we have made, the relevant information is the ansatz for the metric of the internal manifold, RR potential C_2 , flavor flux deformation Λ , and second-order “master PDE”:

$$\begin{aligned} ds_{\text{internal manifold}}^2 &= H^{-\frac{1}{2}} z \left(d\theta_1^2 + \sin^2 \theta_1 d\phi_1^2 + d\theta_2^2 + \sin^2 \theta_2 d\phi_2^2 \right) + \\ &\quad + \frac{H^{\frac{1}{2}}}{z^2} \left(d\sigma^2 + \sigma^2 (d\psi + \cos \theta_1 d\phi_1 + \cos \theta_2 d\phi_2)^2 \right), \end{aligned} \quad (6.2.26)$$

$$C_2 = g_1 d\chi \wedge (d\psi + \cos \theta_1 d\phi_1 + \cos \theta_2 d\phi_2), \quad (6.2.27)$$

$$\Lambda = \frac{N_f}{2} d\chi \wedge (d\psi + \cos \theta_1 d\phi_1 + \cos \theta_2 d\phi_2), \quad (6.2.28)$$

$$\mathcal{K}_6 = e^{01} \wedge (e^{2345} - e^{2367} - e^{4567}), \quad (6.2.29)$$

$$\frac{N_f}{2N_c} \sigma \delta(\rho - \rho_Q) + \rho z^2 (\dot{z} - \sigma \ddot{z}) = \sigma (2\rho z \dot{z}^2 + z' + \rho z'') . \quad (6.2.30)$$

Building $d = 2, \mathcal{N} = (2, 2)$ from wrapped D3-branes

We wrap D3-branes on a two-sphere \mathbb{S}^2 inside a Calabi-Yau three-fold. The resulting metric has the fibrations of the singular conifold. The schematic chart for the brane setup is

$\overbrace{\hspace{10em}}^{\text{CY}_3}$									
$d = 2, \mathcal{N} = (2, 2)$	$\mathbb{R}^{1,1}(x^i)$		$S^2(\theta, \phi)$		$N_4(\sigma, \bar{\theta}, \bar{\phi}, \bar{\psi})$				$\mathbb{R}^2(\rho, \chi)$
N_c D3	—	—	○	○	·	·	·	·	·
N_f D3	—	—	--	--	—	○	--	--	· --

Recalling the forms $\bar{\omega}^1, \bar{\omega}^2, \bar{\omega}^3$ we defined in (4.1.8), the relevant information is in this case:

$$\begin{aligned} ds_{\text{internal manifold}}^2 &= H^{-\frac{1}{2}} z \left(d\theta^2 + \sin^2 \theta d\phi^2 \right) + \\ &\quad + \frac{H^{\frac{1}{2}}}{z^{\frac{1}{2}}} \left(d\sigma^2 + \sigma^2 \left((\bar{\omega}^1)^2 + (\bar{\omega}^2)^2 + (\bar{\omega}^3 + \cos \theta d\phi)^2 \right) \right), \end{aligned} \quad (6.2.31)$$

$$C_4 = g_1 \bar{\omega}^1 \wedge \bar{\omega}^2 \wedge (\bar{\omega}^3 + \cos \theta d\phi) \wedge d\chi + g_2 \sin \theta d\theta \wedge d\phi \wedge (\bar{\omega}^3 + \cos \theta d\phi) \wedge d\chi, \quad (6.2.32)$$

$$\Lambda = L_1(\sigma) \bar{\omega}^1 \wedge \bar{\omega}^2 \wedge (\bar{\omega}^3 + \cos \theta d\phi) \wedge d\chi + L_2(\sigma) \sin \theta d\theta \wedge d\phi \wedge (\bar{\omega}^3 + \cos \theta d\phi) \wedge d\chi, \quad (6.2.33)$$

$$\dot{L}_2 = \frac{2}{\sigma} (L_2 - L_1), \quad (6.2.34)$$

$$\mathcal{K}_4 = e^{01} \wedge (e^{23} - e^{45} - e^{67}), \quad (6.2.35)$$

$$2\rho z \sqrt{z} (\sigma \ddot{z} + \dot{z}) = \sigma (\rho z'^2 - 2z z' - 2\rho z z'') + \frac{16(L_2 - L_1) z^{\frac{3}{2}}}{\sigma} \delta(\rho - \rho_Q). \quad (6.2.36)$$

Building $\mathcal{N} = (1, 1)$ from wrapped D5-branes

We wrap D5-branes on a four-sphere \mathbb{S}^4 inside a G_2 manifold. The resulting metric has the fibrations of the G_2 Bryant-Salamon geometry. There configuration of branes can be summarized as:

$\overbrace{\hspace{10em}}^{G_2}$										
$d = 2, \mathcal{N} = (1, 1)$	$\mathbb{R}^{1,1}(x^i)$		$S^4(\xi, \bar{\theta}, \bar{\phi}, \bar{\psi})$				$N_3(\sigma, \theta, \phi)$			$\mathbb{R}(\rho)$
D5	—	—	○	○	○	○	·	·	·	·
N_f D5	—	—	○	○	--	--	—	○	--	·

To write the metric of the G_2 Bryant-Salamon geometry as a cone over an $\mathbb{S}^2 \times \mathbb{S}^4$ fibration, it is useful to define the one-forms \mathcal{S}^ξ and \mathcal{S}^i ($i = 1, 2, 3$) as:

$$\begin{aligned}
\mathcal{S}^\xi &= \frac{2}{1 + \xi^2} d\xi, \\
\mathcal{S}^1 &= \frac{\xi}{1 + \xi^2} \left(\sin \phi \bar{\omega}^1 - \cos \phi \bar{\omega}^2 \right), \\
\mathcal{S}^2 &= \frac{\xi}{1 + \xi^2} \left(\sin \theta \bar{\omega}^3 - \cos \theta \left(\cos \phi \bar{\omega}^1 + \sin \phi \bar{\omega}^2 \right) \right), \\
\mathcal{S}^3 &= \frac{\xi}{1 + \xi^2} \left(-\cos \theta \bar{\omega}^3 - \sin \theta \left(\cos \phi \bar{\omega}^1 + \sin \phi \bar{\omega}^2 \right) \right),
\end{aligned} \tag{6.2.37}$$

where again the forms $\bar{\omega}^1, \bar{\omega}^2, \bar{\omega}^3$ are the ones in (4.1.8). It is also useful to define one-forms \mathcal{E}^1 and \mathcal{E}^2 that cast as:

$$\begin{aligned}
\mathcal{E}^1 &= d\theta + \frac{\xi^2}{1 + \xi^2} \left(\sin \phi^1 - \cos \phi \bar{\omega}^2 \right), \\
\mathcal{E}^2 &= \sin \theta \left(d\phi - \frac{\xi^2}{1 + \xi^2} \bar{\omega}^3 \right) + \frac{\xi^2}{1 + \xi^2} \cos \theta \left(\cos \phi \bar{\omega}^1 + \sin \phi \bar{\omega}^2 \right).
\end{aligned} \tag{6.2.38}$$

Then, the metric of G_2 holonomy manifold of Bryant-Salamon can be written as:

$$ds_7^2 = \frac{(d\sigma)^2}{1 - \frac{a^4}{\sigma^4}} + \frac{\sigma^2}{2} d\Omega_4^2 + \frac{\sigma^2}{4} \left(1 - \frac{a^4}{\sigma^4} \right) \left[(\mathcal{E}^1)^2 + (\mathcal{E}^2)^2 \right], \tag{6.2.39}$$

where a is a real constant and the variable σ is defined in the range $a \leq \sigma < \infty$. The geometry (6.2.39) is a resolved G_2 cone with a blown-up four-cycle at the tip of size a . Notice that the (θ, ϕ) two-sphere is fibered over the four-cycle. And the relevant info is:

$$\begin{aligned}
ds_{\text{internal manifold}}^2 &= H^{-\frac{1}{2}} z \frac{4}{(1 + \xi^2)^2} \left[d\xi^2 + \frac{\xi^2}{4} ((\bar{\omega}^1)^2 + (\bar{\omega}^2)^2 + (\bar{\omega}^3)^2) \right] + \\
&\quad + \frac{H^{\frac{1}{2}}}{z^{\frac{4}{3}}} \left[d\sigma^2 + \sigma^2 \left((\mathcal{E}^1)^2 + (\mathcal{E}^2)^2 \right) \right],
\end{aligned} \tag{6.2.40}$$

$$C_2 = g_1 \mathcal{E}^1 \wedge \mathcal{E}^2 + g_2 (\mathcal{S}^\xi \wedge \mathcal{S}^3 + \mathcal{S}^1 \wedge \mathcal{S}^2), \tag{6.2.41}$$

$$\Lambda = L_1(\sigma) \mathcal{E}^1 \wedge \mathcal{E}^2 + L_2(\sigma) (\mathcal{S}^\xi \wedge \mathcal{S}^3 + \mathcal{S}^1 \wedge \mathcal{S}^2), \tag{6.2.42}$$

$$\dot{L}_2 = \frac{1}{\sigma} (L_1 + L_2), \tag{6.2.43}$$

$$\mathcal{K}_6 = e^{01} \wedge (e^{2345} + e^{2367} + e^{3478} - e^{2468} + e^{3568} + e^{2578} + e^{4567}), \tag{6.2.44}$$

$$z^{\frac{4}{3}} \left(z\ddot{z} + \frac{2}{3} (\dot{z})^2 \right) = \frac{2}{3} (z')^2 - z z'' - \frac{3m^2(L_1(\sigma) + L_2(\sigma))}{\sigma} z^{\frac{5}{3}} \delta(\rho - \rho_Q). \tag{6.2.45}$$

6.2.2 A microscopic interpretation for the flavor branes

All of the charts above (except the one for the $d = 2, \mathcal{N} = (2, 2)$ case) are not very specific regarding how the flavor branes are placed in the geometry. The smearing form can be computed from the “relevant information” we wrote for each of the case; but this is not giving us the embeddings of the flavor branes. This illustrates the main drawback of the macroscopic approach: one cannot be sure that the $\Lambda \neq 0$ deformation is a flavor deformation (see for instance [78], where only the macroscopic approach was used to find a dual to $\mathcal{N} = 2$ SQCD in three dimensions). In this subsection, we show that this is indeed the case by finding explicit embeddings in a microscopic approach. We show how these embeddings can be inspired by the form of the smearing form, which can be obtained by the macroscopic approach.

Flavoring $d = 2, \mathcal{N} = (2, 2)$ with wrapped D5-branes

We start with the simplest case. It is very easy to check, using (3.2.3) and (6.2.29) that a brane extended along Minkowski plus the normal bundle N_2 and wrapping one of the two-spheres is supersymmetric. Such a brane is localized in the transverse directions. The smearing form that one obtains from (6.2.28), using (6.2.6) and units where $g_s = 1, \alpha' = 1$ is

$$\Xi = \frac{N_f}{4\pi^2} \delta(\rho - \rho_Q) d\rho \wedge d\chi \wedge \frac{1}{2} (\sin \theta_1 d\theta_1 \wedge d\phi_1 + \sin \theta_2 d\theta_2 \wedge d\phi_2) , \quad (6.2.46)$$

which indeed corresponds to the brane setup we have just described.

Flavoring $d = 2, \mathcal{N} = (2, 2)$ with D3-branes

We first notice a very simple solution of the constraint (6.2.34), namely:

$$L_1 = 0 , \quad L_2 = C \sigma^2 . \quad (6.2.47)$$

For this solution, the deformation introduced by (6.2.33) can be interpreted as a flavor deformation. For that, we show in what follows how to find embeddings for the flavor D3-branes generating the resulting smearing form. To characterize this family, let us next introduce the coordinates y^i ($i = 1, \dots, 4$), defined as:

$$y^2 + i y^1 = \sigma \cos \left(\frac{\bar{\theta}}{2} \right) e^{\frac{i}{2} (\bar{\psi} + \bar{\phi})} , \quad y^4 + i y^3 = \sigma \sin \left(\frac{\hat{\theta}}{2} \right) e^{\frac{i}{2} (\bar{\psi} - \bar{\phi})} , \quad (6.2.48)$$

One can verify by direct calculation that:

$$\sum_i (dy^i)^2 = d\sigma^2 + \frac{\sigma^2}{4} \sum_i (w^i)^2 , \quad (6.2.49)$$

which shows that the normal bundle N_4 has the structure of \mathbb{R}^4 fibered over the (θ, ϕ) two-sphere and that the y^i 's are just the Cartesian coordinates of this four-plane. If we write the

smearing form Ξ derived from (6.2.33) with the solution (6.2.47) in terms of the coordinates y^i , the expression is very illuminating:

$$\Xi = -\frac{2C}{\kappa_{10}^2 T_{D3}} \delta(\rho - \rho_Q) d\rho \wedge d\chi \wedge \sin \theta d\theta \wedge d\phi \wedge [dy^1 \wedge dy^2 + dy^3 \wedge dy^4]. \quad (6.2.50)$$

According to the brane array we wrote above equation (6.2.31), let us consider a D3-brane which sits at a particular point of the (θ, ϕ) two-sphere and that is localized in the \mathbb{R}^2 plane parametrized by (ρ, χ) . In addition, the D3-brane is extended along a codimension two surface of the four-dimensional plane spanned by the y^i coordinates. The pullback of the calibration for (6.2.35) for these embeddings takes the form:

$$\iota^*(\mathcal{K}_4) = \frac{1}{\sqrt{z}} dx^0 \wedge dx^1 \wedge \iota^*(dy^1 \wedge dy^2 + dy^3 \wedge dy^4). \quad (6.2.51)$$

In view of (6.2.50), and taking into account the relation (3.2.3), this looks very promising. We are then motivated to study the supersymmetry of an embedding as the one above, that in the normal bundle N_4 is described by linear relations of the type:

$$y^3 = a_1 y^1 + b_1, \quad y^4 = a_2 y^2 + b_2, \quad (6.2.52)$$

which represent a two-plane in \mathbb{R}^4 . For these linear embeddings one has:

$$\iota^*(\mathcal{K}_4) = \frac{1}{\sqrt{z}} (1 + a_1 a_2) dx^0 \wedge dx^1 \wedge dy^1 \wedge dy^2. \quad (6.2.53)$$

On the other hand, the induced metric on the D3-brane worldvolume can be written as:

$$d\hat{s}^2 = H^{-1/2} dx_{1,1}^2 + \frac{H^{1/2}}{\sqrt{z}} [(1 + a_1^2) (dy^1)^2 + (1 + a_2^2) (dy^2)^2], \quad (6.2.54)$$

and the corresponding volume form is

$$\omega_{\text{Vol(D3)}} = \frac{1}{\sqrt{z}} \sqrt{(1 + a_1^2)(1 + a_2^2)} dx^0 \wedge dx^1 \wedge dy^1 \wedge dy^2. \quad (6.2.55)$$

It is now straightforward to prove that the calibration condition (3.2.3) holds if $a_1 = a_2$. Let us parametrize:

$$a_1 = a_2 = -\cot \gamma, \quad (6.2.56)$$

where γ is a constant. Then, the embedding in the y^i hyperplane is characterized by the equations:

$$\begin{aligned} f_1 &\equiv \cos \gamma y^1 + \sin \gamma y^3 - c_1 = 0, \\ f_2 &\equiv \cos \gamma y^2 + \sin \gamma y^4 - c_2 = 0, \end{aligned} \quad (6.2.57)$$

where c_1 and c_2 are new constants. Eq. (6.2.57) defines a family of embeddings parametrized by three parameters $(\gamma, c_1 \text{ and } c_2)$.¹³ Notice that changing γ by $\gamma + \pi$ is equivalent to taking $c_i \rightarrow -c_i$ in (6.2.57). Thus, we will take γ in the interval $0 \leq \gamma < \pi$.

¹³Actually, there is a much larger family of calibrated embeddings for this background. If we complexify the y^i coordinates as $z^{1,2} = y^{2,4} + iy^{1,3}$, then any submanifold in N_4 defined by a holomorphic relation of the type $z^2 = f(z^1)$ is supersymmetric. In particular, a linear relation such as $\alpha z^1 + \beta z^2 = \text{constant}$ defines a complex line in \mathbb{C}^2 which generalizes (6.2.57). However, this more general family of planes gives rise to the same Ω as the one obtained from (6.2.57) and, thus, we will not consider any of these more general embeddings.

With this, we are ready to compute the microscopic integral (3.3.13). Since we homogeneously distribute the D3-brane embeddings over the (θ, ϕ) two-sphere χ one-sphere, while they are localized in ρ , the smearing form will look as Ξ can be written as:

$$\Xi = \delta(\rho - \rho_Q) d\rho \wedge \frac{d\chi}{2\pi} \wedge \frac{\sin \theta d\theta \wedge d\phi}{4\pi} \wedge \Gamma, \quad \Gamma = \int d\mu \delta(f_1) \delta(f_2) [df_1 \wedge df_2], \quad (6.2.58)$$

where $d\mu$ is an integration measure, and for the family of planes (6.2.57) is natural to choose is $d\mu = \pi^{-1} n_f d\gamma dc_1 dc_2$, with n_f being the density of flavor branes. The integrals over c_1 and c_2 in (6.2.58) can be immediately performed by making use of the two delta functions. Moreover, since:

$$df_1 \wedge df_2 = \cos^2 \gamma dy^1 \wedge dy^2 + \sin^2 \gamma dy^3 \wedge dy^4 + \sin \gamma \cos \gamma [dy^1 \wedge dy^4 - dy^2 \wedge dy^3], \quad (6.2.59)$$

we get:

$$\int_0^\pi d\gamma [df_1 \wedge df_2] = \frac{\pi}{2} [dy^1 \wedge dy^2 + dy^3 \wedge dy^4]. \quad (6.2.60)$$

and the resulting Ξ is, indeed, of the form (6.2.50) with the constant C related to the density n_f as:

$$C = -2\kappa_{10}^2 T_{D3} \frac{n_f}{64\pi^2}. \quad (6.2.61)$$

Flavoring $d = 3$, $\mathcal{N} = 2$ with D4-branes

The analysis of this case is exactly analogous to the previous case since, essentially, the only differences between the respective setups is the compact coordinate ρ of the previous case becoming the Minkowski direction x^2 of this case. This is reminiscent of a T-duality transformation. Since (6.2.34) and (6.2.13) are identical, the same solution (6.2.47) also works here, giving the macroscopic smearing form

$$\Xi = -\frac{2C}{\kappa_{10}^2 T_{D4}} \delta(\rho - \rho_Q) d\rho \wedge \sin \phi d\theta \wedge d\phi \wedge [dy^1 \wedge dy^2 + dy^3 \wedge dy^4]. \quad (6.2.62)$$

The non-trivial part of the smearing form is as in (6.2.50), so the microscopic computation follows the same lines as in the previous case. Now one chooses embeddings for the flavor D4-branes spanning a dimension-two surface in the normal bundle N_4 characterized by (6.2.57). These embeddings are calibrated by (6.2.14) and the microscopic computation yields for the constant C of (6.2.47) the value

$$C = -2\kappa_{10}^2 T_{D4} \frac{n_f}{32\pi}. \quad (6.2.63)$$

Flavoring $d = 3$, $\mathcal{N} = 2$ with D5-branes

The situation here is similar to the previous two cases, but the embeddings are a little more involved since as we can see in the corresponding chart, the flavor branes are extended along a two-dimensional plane in N_3 and, simultaneously, wrap an S^1 inside the three-cycle S^3 . One might expect that these two cycles are correlated. Let us show it explicitly in the case

where we are able to find a microscopic interpretation for the flavor branes. This happens just for the following particularly nice solution of (6.2.23):

$$L_1 = 0, \quad L_2 = A \sigma. \quad (6.2.64)$$

The smearing form obtained from (6.2.28) then reads

$$\Xi = \frac{A \delta(\rho - \rho_Q)}{2 \kappa_{10}^2 T_5} d\rho \wedge (d\sigma \wedge S^1 \wedge S^2 - \sigma (S^1 \wedge S^3 \wedge E^1 + S^2 \wedge S^3 \wedge E^2)). \quad (6.2.65)$$

For microscopic purposes, an alternative more inspiring form of (6.2.65) is

$$\begin{aligned} \Xi = -\frac{A \delta(\rho - \rho_Q)}{8 \kappa_{10}^2 T_5} d\rho \wedge [& d(\sigma \sin \theta \sin \phi) \wedge \bar{\omega}^2 \wedge \bar{\omega}^3 + d(\sigma \sin \theta \cos \phi) \wedge \bar{\omega}^3 \wedge \bar{\omega}^1 + \\ & + d(\sigma \cos \theta) \wedge \bar{\omega}^1 \wedge \bar{\omega}^2]. \end{aligned} \quad (6.2.66)$$

We are motivated to introduce new Cartesian coordinates for the normal bundle N_3 : Let us introduce now the following set of Cartesian coordinates for N_3 :

$$z^1 = \sigma \sin \theta \sin \phi, \quad z^2 = \sigma \sin \theta \cos \phi, \quad z^3 = \sigma \cos \theta. \quad (6.2.67)$$

The natural embeddings to consider are

$$f(\vec{z}) \equiv \vec{n} \cdot \vec{z} - z_* = 0, \quad (6.2.68)$$

where $\vec{z} = (z^1, z^2, z^3)$ are the Cartesian coordinates defined in (6.2.67), and the three-vector \vec{n} is defined as:

$$\vec{n} = (\sin \alpha \sin \beta, \sin \alpha \cos \beta, \cos \alpha), \quad (6.2.69)$$

where $0 \leq \alpha \leq \pi$ and $0 \leq \beta \leq 2\pi$. Equation (6.2.68) represents a plane having \vec{n} as its normal direction and with z_* being its minimal distance to the $\vec{z} = 0$ origin of N_3 . It is useful to next define the following two tangent vectors to the plane:

$$\begin{aligned} \vec{t}_1 &= (\cos \beta, -\sin \beta, 0), \\ \vec{t}_2 &= (\cos \alpha \sin \beta, \cos \alpha \cos \beta, -\sin \alpha). \end{aligned} \quad (6.2.70)$$

Notice that $(\vec{t}_1, \vec{t}_2, \vec{n})$ is an orthonormal basis in \mathbb{R}^3 . Let us now arrange the three $\mathfrak{su}(2)$ one-forms $\bar{\omega}^i$ in a vector, namely: $\vec{\omega} = (\bar{\omega}^1, \bar{\omega}^2, \bar{\omega}^3)$. If we define the one-forms:

$$\bar{\omega}_{t_i} \equiv \vec{t}_i \cdot \vec{\omega}, \quad \bar{\omega}_n \equiv \vec{n} \cdot \vec{\omega}, \quad (6.2.71)$$

then, the embeddings in the S^3 can be alternatively defined by the two differential conditions:

$$i^*(\bar{\omega}_{t_1}) = 0, \quad i^*(\bar{\omega}_{t_2}) = 0. \quad (6.2.72)$$

Notice that the system (6.2.72) is integrable due to the property $d\bar{\omega}_{t_1} = -\bar{\omega}_{t_2} \wedge \bar{\omega}_n$, $d\bar{\omega}_{t_2} = -\bar{\omega}_n \wedge \bar{\omega}_{t_1}$, which shows that the differential equations derived from (6.2.72) are on involution

and, according to Frobenius' theorem, they are integrable. Moreover, these embeddings are supersymmetric as one can check¹⁴ with the condition (3.2.3) imposed on (6.2.24).

To see that these embeddings generate the smearing form (6.2.66), one has to compute the integral (3.3.13), that will read as

$$\Xi = \delta(\rho - \rho_Q) d\rho \wedge \Gamma, \quad \Gamma = \int d\mu \delta(f) [df \wedge \Gamma_{S^3}], \quad (6.2.73)$$

where the natural integration measure $d\mu$ is given by $d\mu = (4\pi)^{-1} \sin \alpha d\alpha d\beta n_f dy_*$. The integral over y_* in (6.2.73) can be immediately performed using the delta function:

$$\Gamma = \frac{n_f}{4\pi} \int d\alpha d\beta \sin \alpha [df \wedge \Gamma_{S^3}]. \quad (6.2.74)$$

In order to determine Γ_{S^3} let us first consider the particular plane with $\alpha = \beta = 0$. In this case the differential equations for the embedding in the S^3 are just $\bar{\omega}^1 = \bar{\omega}^2 = 0$. After looking at the parametrization (4.1.8) of $\bar{\omega}^1$ and $\bar{\omega}^2$ in terms of the three angles $(\bar{\theta}, \bar{\phi}, \bar{\psi})$, one immediately realizes that the equation for this embedding can be integrated as:

$$f_\phi \equiv \bar{\phi} - \bar{\phi}_* = 0, \quad f_\theta \equiv \bar{\theta} - \bar{\theta}_* = 0, \quad (6.2.75)$$

where $\bar{\phi}_*$ and $\bar{\theta}_*$ are constant angles. These embeddings depend on two continuous parameters $\bar{\phi}_*$ and $\bar{\theta}_*$ which span a two-sphere. Therefore the corresponding two-form Γ_{S^3} is given by:

$$\Gamma_{S^3} = \int d\bar{\phi}_* d\bar{\theta}_* \frac{\sin \bar{\theta}_*}{4\pi} \delta(f_\phi) \delta(f_\theta) [df_\phi \wedge df_\theta] = \frac{1}{4\pi} \bar{\omega}^1 \wedge \bar{\omega}^2. \quad (6.2.76)$$

From this result it is clear that the generalization to arbitrary values of α and β is:

$$\Gamma_{S^3} = \frac{1}{4\pi} \bar{\omega}_{t_1} \wedge \bar{\omega}_{t_2} = \frac{1}{8\pi} \epsilon^{ijk} n^i \bar{\omega}^j \wedge \bar{\omega}^k, \quad (6.2.77)$$

where we have taken into account that $\vec{n} = \vec{t}_1 \times \vec{t}_2$. Finally, we have just to use

$$\int_0^\pi d\alpha \sin \alpha \int_0^{2\pi} d\beta n^i n^j = \frac{4\pi}{3} \delta^{ij} \quad (6.2.78)$$

in (6.2.74), to find that Γ can be represented as:

$$\Gamma = \frac{n_f}{32\pi^2} \left[\int_0^\pi d\alpha \sin \alpha \int_0^{2\pi} d\beta n^i n^j \right] \epsilon^{jkl} dz^i \wedge \bar{\omega}^k \wedge \bar{\omega}^l = \frac{n_f}{24\pi} \epsilon^{ijk} dz^i \wedge \bar{\omega}^j \wedge \bar{\omega}^k. \quad (6.2.79)$$

Plugging this result with (6.2.73) we conclude that the smearing form Ξ for this family of embeddings can be written as:

$$\Xi = \frac{n_f}{24\pi} \epsilon^{ijk} \delta(\rho - \rho_Q) \delta\rho \wedge dz^i \wedge \bar{\omega}^j \wedge \bar{\omega}^k. \quad (6.2.80)$$

By comparing (6.2.80) and the macroscopic expression (6.2.66), we get that both expressions coincide if the constant A is identified with:

$$A = -2\kappa_{10}^2 T_{D5} \frac{n_f}{3\pi}. \quad (6.2.81)$$

¹⁴For that it is useful to parameterize, whenever $\alpha \neq \pi/2$, $\iota^*(\bar{\omega}^1) = \sin \beta \tan \alpha \iota^*(\bar{\omega}^3)$ and $\iota^*(\bar{\omega}^2) = \cos \beta \tan \alpha \iota^*(\bar{\omega}^3)$. More details can be found in [27].

Flavoring $\mathcal{N} = (1, 1)$ with D5-branes

The microscopic analysis of flavor branes in this case has some similarities with the case just analyzed, but it is more complicated and we are not able to perform the full microscopic computation. Let us mention nonetheless some interesting partial microscopic analysis.

Again, the solution for (6.2.43) with a nice interpretation seems to be (6.2.64). For such a solution, the macroscopic Ξ computed from (6.2.42) is, expressed in the convenient frame basis of (6.2.40):

$$\Omega = -\frac{A}{2\kappa_{10}^2 T_{\text{D5}}} \frac{1}{z^{\frac{1}{3}}} \delta(\rho - \rho_Q) e^9 \wedge \left[e^7 \wedge (e^2 \wedge e^4 - e^3 \wedge e^5) + e^8 \wedge (e^2 \wedge e^3 + e^4 \wedge e^5) + e^6 \wedge (e^2 \wedge e^5 + e^3 \wedge e^4) \right]. \quad (6.2.82)$$

According to the brane array in the chart above equation (6.2.37), the flavor branes should be extended, in the internal space, along a two-cycle $\mathcal{C}_2 \subset \mathbb{S}^4$ and a one-dimensional plane in the normal bundle N_3 . One expects again that the two are correlated. Mimicking what we have done in the previous case, one would define the plane by (6.2.68), and the idea would be to find a pair of conditions like (6.2.72) defining the two-sphere inside the four-sphere. Unfortunately, we have not succeeded in finding such a characterization.

What one can see [28] is that the two spheres corresponding to the particular planes $z^i = 0$ are $\iota^*(\bar{w}^j) = \iota^*(\bar{w}^k) = 0$ with $\{i, j, k\} = \{1, 2, 3\}$, that define a two-cycle inside the \mathbb{S}^4 which is topologically an $\mathbb{S}^1 \times \mathbb{S}^1$ (for the particular case of $z^3 = 0$, this two-cycle spans the $\xi, \bar{\psi}$ coordinates). These embeddings give rise to all the components in (6.2.82) not proportional to $e^2 \propto d\xi$. Presumably, acting with the isometries of the background one could generate the whole family of embeddings, which after the smearing would generate as well the components in (6.2.82) proportional to e^2 .

Chapter 7

A final summary

In this final chapter, we regroup and give a final overview of the main ideas and achievements described in this Ph.D. thesis.

We started studying the perturbative regime of Quantum Field Theories in chapter 2. We focused on a particular observable (the most relevant for experimental purposes), scattering amplitudes, and on a particular type of theories, with massless particles at tree level. The reason for this is that in these cases there is a way to compute the amplitudes alternative to Feynman diagrams (as it is traditionally done): via on-shell recursion relations. On-shell recursion relations allow to build amplitudes from smaller amplitudes in a recursive process. The catch is that the smaller amplitudes are evaluated at complex momenta, holomorphy becoming an essential tool for their analysis. The most general on-shell recursion relation was provided by Britto, Cachazo, Feng and Witten (BCFW) in 2005. This relation is applicable to a wide range of theories, but it has a limitation: the theories must have a good complex UV behavior, which is not always the case.

We proposed a generalization of the BCFW method which works for any theory of massless particles, regardless of its complex UV behavior. We showed how to use it to build four-particle amplitudes, the first non-trivial amplitudes (its use for higher-point amplitudes remains for future clarification). In this way, one has an alternative way to compute scattering amplitudes, which does not make any reference to Lagrangians and it is closer in spirit to the S-matrix approach of the 60's. We can use this new vision to construct theories at tree level, and imposing a very simple consistency condition on this construction, we amazingly recover many extraordinary results like the need of gauge invariance to define theories of a self-interacting boson of spin 1, or the principle of equivalence for theories involving a boson of spin 2. Apart from confirming what one already knew from years of working with Lagrangians, our analysis seems to leave room for constructing theories of higher spin, even though our formalism should be tweaked to tackle this construction.

Then we moved on, for the next chapters 3-6, to the study of the non-perturbative regime of QFTs. From late 70's to late 90's, there were not that many advances in this area, although for supersymmetric theories some interesting progress was made. In the case of $\mathcal{N} = 1$ theories, this was mainly led by Seiberg works and his discovery of dualities. The appearance of *AdS/CFT* in 1997 revolutionized the field. The original idea of Maldacena that a conformal field theory could be understood in terms of a string theory living on

an AdS space was quickly extended to a duality between gauge theories and gravity: the gauge/gravity correspondence. This duality is holographic, meaning that the gravity theory lives in one more dimension than the gauge theory (this extra dimension corresponds to the energy scale of the gauge theory) and it is of the strong/weak type, which means that when the gauge theory is strongly coupled, we have a weakly coupled gravity theory (when the gauge theory is weakly coupled, the gravity theory becomes, in general, a string theory). This correspondence has inspired an immense amount of works trying to figure out the details of the duality, which remain to be completely clarified. Although the correspondence has passed so far all the tests people have come up with (especially in the AdS/CFT cases), it remains to be proven formally. Even so, it can be considered as the best tool we have nowadays to gain insight into the non-perturbative regime of QFTs.

It is therefore very interesting to explore some specific applications of the correspondence. We have presented several different examples in chapters 4 through 6. Our focus has been on the non-perturbative dynamics of gauge theories with fundamental matter (flavor), and more precisely the case of supersymmetric gauge theories. For these, more exact results are available from the field theory side. On the gravity side, supersymmetry can be compactly formulated in the language of G-structures, which is a powerful tool to have.

Our main achievement has been to find different solutions of supergravity dual to gauge theories with flavor in the Veneziano limit (large N_c , large N_f , fixed ratio N_f/N_c). Typically, the solutions without flavor were previously known. Fundamental matter is modeled on the supergravity side by flavor branes. In the Veneziano limit, we have a large number of branes, so that they backreact on the unflavored geometry. The computation of this backreaction is a very non-trivial geometrical problem. This problem is simplified if we use the so-called smearing technique that we briefly reviewed in chapter 3. Instead of placing all the flavor branes (also called sources) on top of each other, they are smeared all over the geometry. This makes the problems analytically tractable. In the case of supersymmetric sources, the formalism of the G-structures turns out to be especially adapted for this end (that is, adding smeared sources). Essentially, just by knowing the supersymmetry preserved by our manifold, G-structures determine the “macroscopic” backreaction we can have. However, one must check that this macroscopic backreaction is generated by a “microscopic” distribution of branes. These two approaches were disconnected in the literature, but in this thesis we develop a connection between them, which increases the power of the smearing method, making it applicable to a wide range of cases. Some of these cases are explored in the present work.

In chapter 4, we analyzed the introduction of flavor into the $AdS_4 \times CFT_3$ duality between the Chern-Simons-matter theory of Aharony, Bergman, Jafferis and Maldacena (ABJM) and M-theory on $AdS_4 \times S^7/\mathbb{Z}_k$ or type IIA String Theory on $AdS_4 \times \mathbb{CP}^3$. The ABJM field theory remains conformal after the addition of flavor, so one expects an AdS factor in the dual gravity solution. Such a solution with flavor was actually already known in the literature, but it has a very complicated form that renders it almost useless for practical computations. Using smeared sources (instead of localized ones), we found an extremely simple solution of the form AdS_4 times a squashed \mathbb{CP}^3 , where the squashing depends (in a simple analytical fashion) on the Veneziano ratio N_f/N_c . Since the solution is AdS , one can run all the machinery of the AdS/CFT correspondence, and compute the effect of fundamental matter

in many observables. In addition, since the solution with localized sources is known as well, this allows to compare, where possible, “smeared” and “localized” flavor. Besides, many exact results are also known for the field theory at strong coupling, derived with localization techniques. This is the cleanest setup found so far for the study of smeared flavor.

In chapter 5, we studied the more familiar four-dimensional theories (one always has QCD in the back of the mind). We concretely focused in a very well-known construction, that of Casero, Núñez and Paredes (CNP), who proposed in 2006 a gravity dual dual to an $\mathcal{N} = 1$ SQCD-like theory, which is the flavored version of the even better known theory of Maldacena-Núñez (MN). The CNP solution captures successfully many features of $\mathcal{N} = 1$ SQCD (with a quartic superpotential for the quarks), but the geometry has a singularity at the origin of the space which does not allow to fully trust its predictions. Even though many results come out correct, it would be very desirable to have a way to make this singularity disappear. This can be done by turning on a mass for the quarks on the field theory side, but this is a very challenging problem on the gravity side, that had not found an answer in the literature. We provided such an answer, using the connection we mentioned above between macroscopic and microscopic approaches. Therefore, we found a dual to a SQCD-like theory with massive quarks. The solution is completely regular and one can revisit the computation of doubtful observables of CNP. The dual theory to our solution needs a UV completion (as the CNP or the MN one) which is six-dimensional. There is a way to UV-complete the theory so that it remains four-dimensional all along the RG flow: one can apply a procedure called “rotation” to this solution to generate a new very non-trivial solution which is UV-complete. We explore this possibility in the last part of chapter 5, and analyze the resulting four-dimensional RG flow, which is very rich and resembles that of some phenomenological models of proposed Beyond-the-Standard-Model (BSM) Physics.

Finally, in chapter 6 we use the smearing technique to incorporate flavor in different setups, leading to different type of physics. In the first part, we construct a gravity solution that displays a duality with the numerology of Kutasov duality. In the second part, we construct gravity duals to SQCD-like theories in low dimensions ($d < 4$), using the models of wrapped branes. The backreaction of flavor branes is computed in various cases, illustrating how macroscopic and microscopic approaches work in practice. Unfortunately, the field theory interpretation is not clear in these cases, and it could be improved.

Chapter 8

Conclusions

This Ph.D. thesis is really divided into two independent parts, and the conclusions that can be derived from each of them are also independent.

On the one hand, we studied the perturbative regime of QFTs, where we were looking for a generalization of the BCFW recursion relation. Our main findings can be summarized in the following points.

- We were able to find a new recursion relation, very similar to the BCFW one, but which is valid in the cases the latter does not work, namely when there is a contribution “at infinity”. The new recursion relation sums over exactly the same terms that appear in the BCFW one, but it adds a sort of “weight” for each of them. These “weights” depend on some zeroes of the amplitude. In this way, the new recursion relation combines poles and zeroes of the amplitude.
- Studying the new recursion relation, we managed to characterize the complex-UV behavior of the amplitudes of any given theory (satisfying some very general assumptions). Opposite to the analysis existing in the literature, based on the knowledge of a Lagrangian, our analysis is based on the unitarity of the theory.
- These two previous findings allowed us to formulate a new point of view on theory-building, alternative to the traditional one (with Lagrangians). This new method is much more simpler, and we showed how it was possible to re-derive some spectacular results already known from the Lagrangian analysis.
- For the future, there are many lines opened by this work which are worthy of further investigation. A concrete example is to try to work out a condition for the zeroes of higher-point amplitudes analogous to the condition we derived for those of four-point amplitudes. A more ambitious long-term goal would be to keep pushing this alternative point of view on QFTs. Instead of using a Lagrangian to characterize it as usual, just focus on computing its on-shell observables by some other means. Lagrangians are cluttered with off-shell structure, which is irrelevant (and obscures the computations) for computing the on-shell quantities one finally wants, like scattering amplitudes. This off-shell structure stems from thinking in terms of local processes (emission of a photon, interactions at a point, etc), which might just not be the simplest way of

thinking. At the end what Quantum Mechanics says is that one should measure some initial state and give probabilities for measuring another final state. What happens in the middle is irrelevant. A non-local description might be more useful. Incidentally, non-locality is another issue raised by our work, seemingly hinting at the possibility of defining high-spin theories in flat spacetime (after all, String Theory is such a non-local high-spin theory). Again, a more formal and deep treatment than the one made here would be needed to clarify this point.

On the second part of the thesis, we studied the non-perturbative regime of gauge theories with string theory tools. This is possible through the gauge/gravity correspondence. More precisely, we focused on the study of theories with flavor in the Veneziano limit. For the addition of flavor to the correspondence, we used the smearing technique to place a large number of flavor branes in the gravity solution. We studied several examples of the correspondence, and we can draw the following conclusions.

- We showed how to apply the smearing technique to any example of the correspondence possessing certain symmetries. In particular, we focused on the cases with supersymmetry. In these cases, the language of G-structures and calibrations is especially useful. With the generalities we explained, one should be able to apply the smearing technique in a very general fashion. Not so much is left to be learned in this regard.
- We found an example where the solution with smeared flavor has an AdS space. This is extremely useful, since in this case the correspondence is very well understood, and we can extract a lot of non-perturbative information from the supergravity solution. It is the first time in the literature that such a simple solution with these features is found. Moreover, in this case, the solution corresponding to “localized” flavor is also known, and also localization techniques can be used on the field theory side to extract many non-perturbative exact results. It is possible then to compare “smeared-flavor” solutions with “localized-flavor” solutions. So for the future, apart from the interest of computing more flavor effects from the gravity side, it would be very interesting to use this example to learn what are the exact differences between smeared and localized flavor and why some observables are more, or less, affected by the smearing process.
- We showed how to cure the singularity of the important CNP solution, dual to $\mathcal{N} = 1$ SQCD (with some subtleties). Although the idea of how to do this was known since 2006, the realization is technically very complicated. To achieve this, we used techniques of complex geometry, and developed a framework that can serve to many other different purposes. In particular, we explored the possibility of building another supergravity solution providing a UV completion to the dual of the non-singular solution we found (the dual is $\mathcal{N} = 1$ SQCD with massive quarks). Such UV completion is attained by a solution-generating technique called “rotation”. The new solution encodes very rich non-perturbative physics of a $\mathcal{N} = 1$ theory that could model some Beyond-the-Standard-Model physics. For the future, it would be desirable to extend the framework of holomorphic techniques, and the UV-completion construction (*i.e.* the rotation) that we developed for $SU(3)$ -structures to other G-structures. Also, it is not clear what the rotation is doing microscopically: *i.e.* we do not know how to map a microscopic

interpretation in one background to the rotated background. A clarification of this point would be of obvious interest (especially because we lack this interpretation in our rotated solution).

- We also explored some other instances of the gauge/gravity correspondence, some illustrating the microscopic approach to the smearing technique, and others useful to learn about the geometry and usefulness of hyperbolic spaces. Putting altogether, as a summary of the use of gauge/gravity techniques, we can say that we have enlarged the evidence in favor of the gauge/gravity correspondence being correct. This reinforces the notion that these techniques are the best tool that we have at present to study the non-perturbative regime of gauge theories, even if the correspondence is not formally proven yet. Moreover, with them, we keep learning new things about string theory and QFTs. And the physical relevance of these techniques is only going to increase after the official announcement of the Higgs particle is made at LHC. A very likely scenario is that the Higgs mechanism is an effective theory for some BSM physics. It could very well be that this physics are strongly coupled, and the urge to understand them and quench our thirst of curiosity can only go up.

Ideally, in a near future, the two lines treated in this thesis will cease to be independent, and hopefully they could complement each other. Hints of such a thing are already starting to show up, as the tip of an iceberg, in the community of Theoretical Physics.

Chapter 9

Resumo

A descrición da Natureza depende da escala de distancias e enerxías á que a observemos. Para a vida cotiá as leis de Newton e as ecuacións de Maxwell son máis que suficientes. Ao saírmolos deste rango, teorías máis precisas son necesarias. Cando tratamos obxectos que se moven moi rápido (con moita enerxía), ou distancias moi grandes, cómpre ter en conta que a velocidade da luz é un número finito e independente do sistema de referencia, o que leva á visión relativista do espazo-tempo. Cando un observa distancias moi pequenas (da orde de 10^{-10} metros), o concepto de partículas seguindo traxectorias desaparece, e o mundo clásico debe ser substituído por un mundo cuántico.

O obxectivo da Física Teórica de altas enerxías é o de describir as interaccións entre as partículas elementais. Tanto a Relatividade (altas enerxías) como a Mecánica Cuántica (as partículas elementais son, en teoría, puntuais) son necesarias para esta descrición. As teorías que combinan ambos elementos denomínanse Teorías Cuánticas de Campos (TCCs).

As TCCs son a ferramenta máis exacta que temos a día de hoxe para modelar o xeito en que a Natureza funciona. A idea é termos diversos campos cuánticos vivindo no espazo-tempo de Minkowski, e as súas excitacións interpretámolas como partículas elementais. Cando nalgún punto do espazo tempo coinciden excitacións de varios campos, isto interp'etase como unha interacción entre as distintas partículas. As interaccións pénsanse entón como intercambios de partículas; *e.g.* a forza electromagnética repulsiva entre dous electróns pénsase como dous electróns intercambiándose fotóns, de tal xeito que un electrón emite un fotón véndose empurrado nunha dirección, e o outro electrón vese empurrado na dirección oposta ao recibir o fotón. De xeito semellante, é posíbel entender a forza forte que mantén unidos aos núcleos atómicos, a forza feble responsable da radioactividade e a forza electromagnética. É dicir, temos TCCs, en concreto teorías *gauge*, describindo estas tres interaccións. Ao modelo que engloba ás tres chamámolo Standard Model (SM)¹. Todo isto está moi ben, pero as TCCs, a pesar de seren o noso mellor aliado, non son comprendidas todo o ben que nos gustaría.

¹Á día de hoxe, o SM describe ben case todos os experimentos que podemos facer no laboratorio (nos grandes aceleradores), e é capaz de predicir certas cantidades cunha precisión de ata doce cifras significativas! Porén, non todo son flores, e sabemos xa que o SM terá que ser substituído nun futuro por outro modelo, que sexa capaz de incorporar masa para os neutrinos, explicar a asimetría bariónica, e xenericamente posuír “mellores propiedades cosmolóxicas”.

En primeiro lugar, tipicamente toda a dinámica das excitacións dos campos cuánticos está controlada por un Lagranxiano. Neste Lagranxiano temos constantes de acoplamento g caracterizando a forza das interaccións. Cando as constantes de acoplamento son pequenas $g \ll 1$, sabemos construír series de potencias en g (denominadas series perturbativas) para os observábeis da teoría. No caso en que as constantes de acoplamento son grandes $g \gg 1$, non sabemos, por regra xeral, extraer a información que contén a teoría. Neste caso falamos de información non perturbativa. Por exemplo, para a teoría da interacción forte, a cromodinámica cuántica (QCD), sabemos probar que predí a chamada liberdade asintótica, pero non sabemos calcular a masa do protón. O primeiro é un fenómeno perturbativo, mentres que o segundo é un fenómeno non perturbativo.

En segundo lugar, falta unha interacción fundamental por describir: a gravidade. A teoría clásica da gravidade é a Relatividade Xeral de Einstein, que afirma que o espazo-tempo é unha entidade dinámica que se moldea segundo a cantidade de materia e enerxía que conteña. Por outra banda, dixemos que unha TCC asume que os campos viven nun espazo-tempo fixado. Estas dúas ideas son claramente incompatíbeis. Durante moito tempo, a comunidade de físicos teóricos vén buscando un xeito de casalas. A idea máis prometedora que xurdiu ao respecto é a teoría de cordas.

Que é a teoría de cordas?

A teoría de cordas naceu nos anos 70 como unha posíbel teoría para explicar a interacción forte. Levou algún tempo en decatarse de que a teoría de cordas é, en poucas palabras, a teoría que describe unha corda oscilante, cuántica e relativista. Cando a corda tamén ten supersimetría, falamos da teoría de supercordas. Esta corda vibra en principio nun espazo-tempo D -dimensional. Resulta que a corda só quere propagarse neste espazo-tempo se D é un número moi concreto. No caso da supercorda, $D = 10$, o que significa que o espazo-tempo tería que ter dez dimensións (das cales obviamente só vemos catro)! Así como no caso das TCCs, as distintas partículas eran as excitacións dos distintos campos, na teoría de cordas as partículas correspóndense cos distintos tipos de vibración da corda. É dicir, a mesma corda vibrando de dous xeitos distintos dá lugar a distintas partículas. Aínda que os modos de vibración están cuantizados, existe un número infinito deles, e polo tanto un número infinito de partículas: unha teoría de cordas é algo bastante distinto dunha TCC. E de feito, non sabemos o que é este “algo bastante distinto”. É un gran rompecabezas do que só temos algunhas pezas, e que posibelmente levará bastante tempo resolvelo.

Unha das pezas que coñecemos é o chamado límite de baixas enerxías da teoría de supercordas. Neste caso, as únicas vibracións da corda que fan falla considerar son as que dan lugar a partículas sen masa. A teoría que resulta é a xeralización supersimétrica da teoría de Einstein: a supergravidade. Aparte de gravitóns, esta teoría contén varias outras partículas. E o que se descubriu a mediados dos anos 90 é que ademais de cordas, existen outros obxectos “estendidos” presentes na teoría: as chamadas branas. As p -branas son hipersuperficies de $p + 1$ dimensións que tamén vibran no espazo D -dimensional. Estas vibracións poden entenderse como provocadas por cordas abertas que rematan na brana e tiran dela deformándoa. O descubrimento das branas catalizou unha revolución na comunidade das supercordas, atraendo a moita xente ao campo, xa que a dinámica das teorías que as

describen garda moitas similitudes coa dinámica do SM.

A esperanza inicial era que a teoría de cordas fora a teoría de unificación que describise as catro interaccións coñecidas na Natureza, e polo tanto se convertise nunha “teoría de todo”. A realidade é que a teoría de cordas é certamente unha teoría cuántica da gravidade, capaz de describir outras interaccións tamén; máis non semella que describa o Universo no que vivimos, ao menos non de forma única. Existen distintas teorías de cordas consistentes, e de cada unha poden extraerse en principio moitos Universos distintos. Neste senso, a teoría de cordas non ten poder predictivo.

Non obstante, a teoría de cordas contén unha colección de ideas revolucionarias, que teñen servido de inspiración para descubrimentos espectaculares en moitísimos campos, dende as Matemáticas puras, ata a Física da materia condensada, pasando por teorías de campos conformes, teorías supersimétricas, amplitudes de *scattering*, etc. Esta colección de ideas aínda non está esgotada, e claramente paga a pena seguirlas investigando durante os vindeiros anos. Describimos brevemente a continuación a máis fructífera destas ideas revolucionarias motivadas pola teoría de cordas: a correspondencia AdS/CFT e as súas xeralizacións.

A correspondencia AdS/CFT

Xa a principios da década dos 90, na comunidade de Física Teórica flotaban as ideas do chamado principio holográfico, que propugnaba que unha TCC podería ser descrita mediante unha teoría que vive nunha dimensión máis e contén gravidade. Non foi ata 1997 que estas ideas se plasmaron de xeito cuantitativo. Nese ano, Maldacena propuxo [8] a chamada correspondencia AdS/CFT . Maldacena estudou un conxunto de D3-branas na teoría de supercordas de tipo IIB. En certo límite dos parámetros da teoría de cordas, este sistema pode ser estudado mediante dúas descrições independentes: unha con cordas abertas, e outra con cordas pechadas. A primeira descripción é mediante a teoría $\mathcal{N} = 4$ Super Yang-Mills (SYM), e a outra dá lugar a unha xeometría $AdS_5 \times S^5$. Isto levou a Maldacena a conxectar unha dualidade entre $\mathcal{N} = 4$ SYM e a teoría de cordas de tipo IIB vivindo en $AdS_5 \times S^5$. A conxectura é que estas teorías son completamente equivalentes a pesar de que as respectivas descrições sexan moi distintas.

As descrições son duais, e cando unha está fortemente acoplada, a outra está feblemente acoplada. Isto é extremadamente útil, pois cando a teoría de campos $\mathcal{N} = 4$ SYM está fortemente acoplada, a teoría de cordas nos prové cunha descripción alternativa. E como esta descripción está feblemente acoplada, a aproximación a baixas enerxías da teoría de cordas de tipo IIB (a supergravidade de tipo IIB), que é ben coñecida, é suficiente. Ao mesmo tempo, esta característica da dualidade de intercambiar acoplamento forte por acoplamento feble tamén fai que a conxectura de Maldacena sexa moi difícil de probar. Con todo, a cantidade de tests que se teñen realizado sobre ela, e a non trivialidade dos mesmos, fai que toda a comunidade asuma que a conxectura é certa, e que é só unha cuestión de tempo que se poida probar rigurosamente.

Dende 1997, véñse adicando unha cantidade de traballo excepcionalmente grande a entender mellor a correspondencia. O que temos aprendido é que este tipo de dualidade é algo moi xeral, e que xenericamente os graos de liberdade máis axeitados para describir unha TCC fortemente acoplada son obxectos estendidos (como unha corda) que se describen mediante

unha teoría de cordas que vive nunha dimensión máis. Esta dimensión extra está relacionada coa escala de enerxías da TCC. Unha xeralización concreta da correspondencia de Maldacena, da que nos ocuparemos nesta tese, e aquel caso no que a TCC é unha teoría *gauge* fortemente acoplada, e a descrición dual é co límite de baixas enerxías da teoría de cordas (gravidade acoplada a varios campos). Falamos entón da correspondencia gravidade/teoría *gauge*.

Contido da tese

O obxectivo desta tese é mellorar o noso entendemento das teorías cuánticas de campos usando novedosas técnicas que apareceron nos últimos anos. Os resultados presentados están baseados nas publicacións [20, 21, 22, 23, 24, 25, 26, 27, 28]. A tese está realmente dividida en dúas partes, que poden ser lidas de xeito independente.

Na primeira parte ocupámonos do réxime perturbativo das teorías cuánticas de campos. Aínda que este réxime é bastante ben comprendido, a técnica estándar, a expansión en diagramas de Feynman, deixa certas cousas que desexar cando o nivel de esixencia aumenta. Exploramos unha visión alternativa, centrándonos nas amplitudes de *scattering*, onde é posíbel facer cálculos usando novedosas relacións de recurrencia, baseadas nas propiedades holomorfas destas amplitudes no plano complexo, que aportan melloras tanto no plano práctico, coma no teórico.

Na segunda parte da tese estudamos a aplicación das ideas da correspondencia gravidade/teoría *gauge* ao estudo do réxime non perturbativo de teorías *gauge* con materia na representación fundamental no límite de Veneziano. O mundo no que vivimos ten dende logo materia deste tipo (como electróns, neutrinos, ou os quarks que forman parte dos protóns e neutróns, que forman basicamente os átomos e por tanto toda case toda a materia observábel), e é consecuentemente un ingrediente importante das TCCs con relevancia fenomenolóxica. Como xa dixemos, o réxime non perturbativo destas TCCs non é ben coñecido, e é de capital importancia ter ferramentas alternativas para a análise do mesmo. Exploramos estas ferramentas ilustrando con exemplos de aplicación da correspondencia as xeneralidades do método.

9.1 O réxime perturbativo: amplitudes de *scattering*

No capítulo 2 centrámonos no observábel de maior interese práctico dunha teoría: as amplitudes de *scattering*. O xeito que temos de comprobar se unha teoría dada describe ben a realidade ou non é por suposto facendo experimentos. En altas enerxías, os experimentos consisten en facer colisionar feixes de partículas con moita enerxía, e observando que configuración de partículas obtemos logo da colisión (isto é o que se fai nos grandes aceleradores). Pode parecer un xeito bastante groseiro de facer un experimento pero a realidade cuántica, onde a observación altera o experimento, non nos deixa outra elección. O que precisamos entón son as probabilidades de obter unha certa configuración final de partículas dada unha configuración inicial. Estas probabilidades obtéñense, *grosso modo*, tomando o módulo cadrado das chamadas amplitudes de *scattering*.

As amplitudes de *scattering* defínense a partir de elementos de matriz da chamada matriz S. Como unha antipartícula pode considerarse como unha partícula viaxando cara atrás no tempo, consideramos ás dúas partículas da configuración inicial como antipartículas na configuración final. Polo tanto, temos unha configuración de varias partículas, digamos n , cada unha con momento p_k , de tal xeito que a conservación de momento equivale a a suma de todos os momentos sexa nulo, e denotamos esquemáticamente á amplitude de *scattering* segundo

$$M_n(p_1, \dots, p_n), \quad \sum_{k=1}^n p_k = 0, \quad (9.1.1)$$

onde estamos omitindo aquí unha posíbel dependencia nos vectores de polarización, ou en posíbeis números cuánticos internos. É posíbel escribir unha expansión perturbativa para a amplitude de *scattering* tal como:

$$M_n^{\text{perturbativa}} = M_n^{\text{árbore}} + \sum_{L=1}^{\infty} M_n^L \text{ lazos}, \quad (9.1.2)$$

one cada contribución vén cunha potencia distinta na constante de acoplamento. A que vén coa menor potencia denomínase amplitude “a nivel árbore”, e o resto son contribucións de lazos.

Nesta tese estudamos $M_n^{\text{árbore}}$ (que denotaremos simplemente por M_n abusando un pouco da notación) para teorías que só conteñen partículas sen masa (como é o caso de todas as teorías “fundamentais”, ademais de ser o límite de altas enerxías de calquera teoría con partículas masivas). As amplitudes a nivel árbore son o ladrillo fundamental para reconstruír a serie perturbativa da amplitude (9.1.2).

Tradicionalmente, o cálculo de M_n faise a través de diagramas de Feynman: hai que debuxar todas as “árbores” posíbeis, e a contribución de cada unha é inmediata de calcular se temos un Lagranxiano. Isto semella bastante doado, pero á hora de facer cálculos, o método resulta ser alxebricamente moi complexo, incluso para un ordenador. A medida que n aumenta, o número de diagramas de Feynman sobre os que hai que sumar aumenta exponencialmente, e o procedemento resulta inabordable. Ademais, en moitas ocasións, existen numerosas cancelacións entre diagramas, que fan que o resultado final sexa moito máis simple ca os diagramas intermedios. Xorde entón a pregunta natural de se existe algunha outra representación alternativa.

Unha resposta afirmativa moi xeral a esta pregunta foi dada en 2005 no artigo [7], onde Britto, Cachazo, Feng e Witten (BCFW) propuxeron unhas relacións de recurrencia para calcular $M_n^{\text{árbore}}$ en teorías con partículas sen masa. A súa idea foi introducir unha deformación complexa de dous dos momentos que interveñen na amplitude de *scattering*:

$$p_i \rightarrow p_i(z) = p_i - z q, \quad p_j \rightarrow p_j(z) = p_j + z q, \quad (9.1.3)$$

onde z é unha variábel complexa, e q un momento complexo que se fixa impondo que os novos momentos deformados $p_i(z), p_j(z)$ correspondan a partículas de masa nula, *i.e.* $(p_i(z))^2 = 0 = (p_j(z))^2$. Deste xeito, é posíbel considerar formalmente a amplitude de scattering $M_n(z) = M_n^{\text{árbore}}(p_1, \dots, p_i(z), \dots, p_j(z), \dots, p_n)$. Esta amplitude é unha función meromorfa

$$M_n = \sum_{\mathcal{K}} \text{Diagram} \cdot f_{\mathcal{K}}^{(i,j)} \cdot \text{Diagram}, \quad f_{\mathcal{K}}^{(i,j)} = \begin{cases} 1 & \text{if } \nu < 0 \\ \prod_{l=1}^{\nu+1} \left(1 - \frac{P_{\mathcal{K}}^2(z_0^{(l)})}{P_{\mathcal{K}}^2}\right) & \text{if } \nu > 0 \end{cases}$$

Figure 9.1: A amplitude é obtida como unha suma de productos de subamplitudes multiplicadas por un factor axeitado. As subamplitudes son amplitudes onde os momentos $p_i(z_K), p_j(z_K)$ e $P(z_K)$ son complexos. A notación foi especificada na sección 2.2.1.

de z , que se comporta segundo $M_n(z) \sim z^\nu$ para valores grandes de z , e do estudo das súas propiedades holomorfas, é posíbel obter as relacións de recurrencia.

Estas relacións de recurrencia BCFW só son válidas no caso en que $\nu < 0$. Nesta tese describimos unha xeralización das mesmas, válidas para calquera ν . Representámolas esquematicamente na figura 9.1. No caso en que $\nu < 0$, a relación de recurrencia redúcese á de BCFW, pero cando $\nu \geq 0$, temos que incluír unha especie de “peso”, $f_{\mathcal{K}}^{(i,j)}$, que depende dun subconxunto de ceros da amplitude deformada (que dependen das partículas i, j escollidas para a deformación (9.1.3)). A nova relación comparte coa relación de recurrencia orixinal de BCFW as súas propiedades máis interesantes: por unha banda só hai que sumar un subconxunto de todas as posíbeis árbores (exactamente sobre o mesmo subconxunto que en BCFW); e pola outra temos a mesma estrutura recursiva, *i.e.* podemos aplicar sucesivamente as relacións de recurrencia nas subamplitudes xeradas, e o proceso finalizaría en xeral nas amplitudes de tres partículas (que son nulas para momentos reais, pero non para momentos complexos).

A maiores, da consistencia da construción, é posíbel determinar o expoñente ν , que baixo condicións bastante xerais resulta depender só das helicidades das partículas deformadas e do número de derivadas das interaccións da teoría. E tamén é posíbel obter condicións para saber onde se atopan os ceros da amplitude. Estas condicións poden resolverse explicitamente no caso de amplitudes de catro partículas, *i.e.* $n = 4$. A solución pode expresarse de xeito moi simple nas cantidades $P_{\mathcal{K}}^2(z_0^{(l)})$ que aparecen na definición do “peso” $f_{\mathcal{K}}^{(i,j)}$:

$$\prod_{\text{canles BCFW}} P_{\mathcal{K}}^2(z_0^{(l)}) = (-P_{ij}^2)^{\#\text{canles BCFW}}. \quad (9.1.4)$$

Con todos estes ingredientes, é posíbel formular unha visión completamente alternativa á Lagranxiana para a construción de teorías. Esta nova construción recorda ao programa da matriz S que se intentou levar a cabo nos 60, e basearíase en catro premisas fundamentais: invarianza baixo o grupo de Poincaré, existencia de estados asintóticos asociados ás partículas que van interactuar, analiticidade, e localidade.

Na sección 2.4 amosamos como partindo destas catro hipóteses, e usando a relación de recurrencia atopada anteriormente, é posíbel construír, a nivel árbore, calquera amplitude de catro partículas de calquera teoría con partículas sen masa. A idea é usar que as amplitudes de tres partículas pódense determinar exactamente usando as hipóteses anteriores, para logo construír as amplitudes de catro partículas mediante os productos axeitados que aparecen

na relación de recurrencia (para catro partículas, só temos produtos de amplitudes de tres partículas). Un punto importante é que tal construción depende en principio das partículas i, j que escollamos, así que temos que impor que outra escolla k, l nos dea o mesmo resultado:

$$M_4^{(i,j)}(0) = M_4^{(k,l)}(0) \quad (9.1.5)$$

Esta condición foi introducida en [29] e denominouse o “test de catro partículas”. Esta condición de consistencia é sorprendentemente restrictiva, e só permite definir consistentemente algunhas teorías. Isto permitiunos realizar unha análise moi xeral de que teorías son descartábeis como teorías consistentes simplemente mirando os espíns das partículas que conteñen. Restrinxímonos á análise de teorías con dous tipos de partícula (sen masa) como moito, con espín s e espín s' , e que presentan ao menos un vértice de tres partículas: dous de espín s' e unha de espín s . Cando este vértice representa unha interacción de s derivadas, chámase interacción de acoplo mínimo; e noutro caso pois interacción de acoplo non mínimo. Os nosos resultados foron:

- **Interaccións de acoplo mínimo.** Cando a teoría só contén un tipo de partícula de espín s , as únicas posibilidades son $s = 2$ (teoría da Gravidade), $s = 1$ sempre e cando se engadan números cuánticos satisfacendo unha álgebra de Lie (teoría de Yang-Mills), e $s = 0$, a teoría escalar. Engadindo unha partícula de espín s' redescubrimos todas as interaccións deste tipo coñecidas coa súa correspondente álgebra: interacción de Yukawa, teorías de Yang-Mills con fermions ou escalares, e Gravidade acoplada a escalares, fermións, fotóns ou gravitinos (obtendo nestes casos a formulación cuántica do principio de equivalencia). Ningunha outra teoría é posíbel.
- **Interaccións de acoplo non mínimo.** Non hai Lagranxianos coñecidos para este tipo de teorías. A nosa análise nestes casos non é totalmente completa, pero semella deixar entrever que sería posíbel definir certo tipo de interaccións entre as chamadas partículas de alto espín ($s > 2$). Da análise das amplitudes de catro partículas, semella que estas teorías poderían conter un número infinito de partículas de alto espín, e violar localidade.

9.2 O réxime non perturbativo

No capítulo 3, presentamos unha introdución aos conceptos básicos da correspondencia gravidade/teoría *gauge*. Centrémonos especialmente no caso en que a teoría *gauge* é supersimétrica, ten materia na representación fundamental e se atopa no límite de Veneziano. Unha teoría *gauge* supersimétrica é dual a unha solución de supergravidade, e a materia na representación fundamental, ou sabor, é dual á presenza de branas en dita solución. Estas branas teñen que ter certas características e denomínanse branas de sabor. No límite de Veneziano da teorías *gauge*, temos que introducir un número moi grande de branas de sabor, de tal xeito que deforman a xeometría na que son introducidas. Para calcular a solución de supergravidade, hai que ter en conta esta deformación, e polo tanto as ecuacións de movemento que hai que resolver derivan da acción:

$$S = S_{\text{supergravidade}} + S_{\text{fontes}} , \quad (9.2.1)$$

onde chamamos fontes ás branas de sabor. Cando estas branas están postas “unha enriba da outra” (tamén se di localizadas), as ecuacións de movemento que resultan son extremadamente difíciles de resolver. Para desfacerse desta complicación, unha posibilidade é “esparexer” homoxeneamente as branas de sabor na xeometría. Isto é o chamado proceso de “*smearing*”. As novas ecuacións de movemento son máis simples, pero aínda así o cálculo da deformación inducida polas branas segue a ser para nada trivial.

No caso en que tratamos con solucións con supersimetría, non é preciso resolver ás ecuacións de movemento, senón que basta con impor que a xeometría sexa supersimétrica. As ecuacións resultantes son de primeira orde, no canto de seren de segunda orde como as ecuacións de movemento. A maiores, a supersimetría pode ser formulada en termos xeométricos de xeito moi compacto usando a linguaxe das G-estructuras. Esta última é especialmente adaptada ao caso en que se usa a técnica de *smearing*. Na sección 3.3.1, explicamos a ideoloxía do método, de tal xeito que a súa aplicación convértese en case sistemática. Nos capítulos 4-6, ilustramos dita aplicación para diversos casos de interese, analizando como as solucións capturan, a través da correspondencia, fenómenos non perturbativos da dinámica das teorías *gauge* con sabor.

9.2.1 Sabor en teorías de Chern-Simons

En 2008, Aharony, Bergman, Jafferis e Maldacena construíron unha teoría de Chern-Simons en tres dimensións para describir a teoría vivindo no volume das M2-branas [116]. A teoría ten grupo gauge $U(N) \times U(N)$ e materia na representación fundamental, e acordouse en denominar teoría ABJM, polos nomes dos seus autores. A teoría ABJM é superconforme, e a súa descrición dual vén dada pola teoría M vivindo no espazo $AdS_4 \times S^7/\mathbb{Z}_k$, onde k é o nivel de Chern-Simons. Para un determinado rango dos parámetros da teoría, no que nós estaremos interesados, a descrición dual máis axeitada é a supergravidade de tipo IIA no espazo $AdS_4 \times \mathbb{CP}^3$.

Unha propiedade especialmente interesante da teoría ABJM é que é posíbel engadir materia (sen masa) na representación fundamental preservando a simetría conforme. Dado que a simetría conforme é dual á presenza dun espazo Anti-de-Sitter na xeometría, un agarda entón que sexa posíbel atopar unha solución de supergravidade que teña en conta a deformación producida por branas de sabor e conteña un factor AdS_4 . Espectacularmente, no caso de branas de sabor localizadas, tal solución foi atopada, pero a xeometría é extremadamente complexa, de tal xeito que non resulta demasiado útil para calcular observábeis a través da correspondencia.

No capítulo 4 retomamos o problema de atopar unha solución de supergravidade de tipo IIA que sexa dual á teoría ABJM con sabor (de masa nula), usando a técnica de *smearing*. Moi interesantemente, atopamos como solución unha xeometría extremadamente simple, onde o efecto do sabor é simplemente achatar a métrica do espazo \mathbb{CP}^3 , así como do fluxo de Ramond-Ramond F_2 , presentes na solución dual a ABJM. Estes achatamentos poden caracterizarse por un parámetro

$$\varepsilon = \frac{N_f}{k} = \frac{N}{k} \frac{N_f}{N} = \lambda \frac{N_f}{N}, \quad (9.2.2)$$

onde λ é a constante de acoplamento de 't Hooft, e o cociente N_f/N é finito e determina en

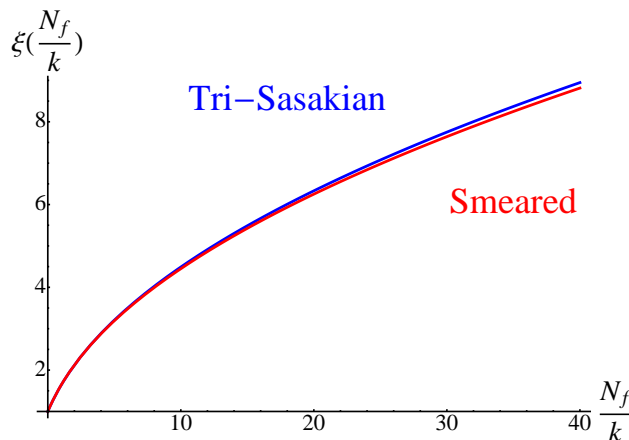


Figure 9.2: Comparativa do factor ξ obtido coa dúas solucións das que dispoñemos. As dúas curvas son practicamente iguais, e polo tanto as teorías duais teñen practicamente a mesma enerxía libre.

que punto do límite de Veneziano nos atopamos. O parámetro ε asociámolo coa deformación de sabor. No límite $\varepsilon \rightarrow 0$, recuperamos a solución de ABJM.

Como a novedosa solución que atopamos contén un factor AdS , é posíbel usar toda a potencia do dicionario para calcular observábeis na teoría dual: que ha de ser a teoría ABJM cun certo contido de sabor. Como usamos a técnica de *smearing* no dual gravitatorio, a teoría resultante non é exactamente a mesma ca' teoría de ABJM con sabor da que falamos antes, pero debería ser unha boa aproximación. Este é o primeiro exemplo na literatura no que é posíbel comparar os resultados das dúas teorías. Na teoría con sabor introducido coa técnica de *smearing* usamos a nosa solución, mentres que na teoría ABJM con sabor introducido mediante branas localizadas é posíbel usar cálculos exactos na teoría de campos (isto é posíbel grazas á técnica de localización) ou nalgúns casos concretos tamén a complicada xeometría resultante (que contén unha variedade tri-Sasakiana). Realizamos un estudo de varios observábeis, e obtivemos que efectivamente a técnica de *smearing* nos proporciona unha boa, e moito máis práctica, aproximación á complicada solución de variedades tri-Sasakianas. Obsérvese por exemplo a comparativa na figura 9.2 da enerxía libre, que conta os graos de liberdade da teoría, que é da forma $\mathbb{F} = \frac{\pi\sqrt{2}}{3} k^{1/2} N^{3/2} \xi(N_f/k)$ calculada mediante as dúas solucións. Tamén estudamos varias xeralizacións do noso modelo para teorías de Chern-Simons con sabor, como son a adición de operadores que xeran un fluxo do grupo de renormalización non trivial, ou a inclusión dun termo de masa para o sabor. Nestes casos, a teoría deixa de ser conforme, e consecuentemente o factor AdS desaparece da xeometría.

9.2.2 Sabor en teorías con supersimetría $\mathcal{N} = 1$

A configuración que estudamos no capítulo 4 é de grande interese teórico polas razóns que explicamos máis arriba. Porén, podemos estar máis interesados en usar a correspondencia gravidade/teoría *gauge* para aplicacións máis fenomenolóxicas. Máis concretamente, para estudar QCD. Desafortunadamente non é posíbel atopar unha solución de supergravidade

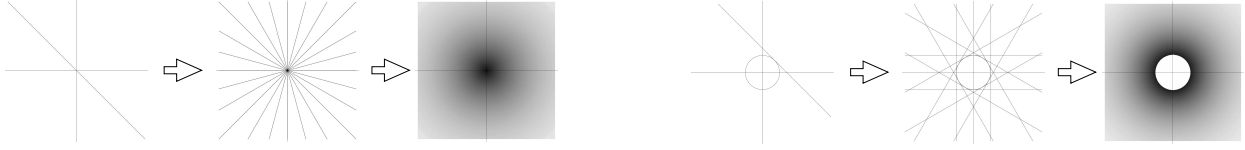


Figure 9.3: Esquerda: as branas intersécanse na orixe do espazo xerando unha densidade infinita. Dereita: cando as branas non chegan ata a orixe do espazo, non se xera unha singularidade de curvatura.

dual a QCD, xa que esta última é asintoticamente libre, o que significa que o dual gravitatorio tería que ser unha teoría de cordas (fortemente acoplada), e a día de hoxe estamos aínda lonxe de acadar tal meta. Un obxectivo con miras fenomenolóxicas algo máis modesto é o estudo de teorías cunha cantidade minimal de supersimetría, *i.e.* con supersimetría $\mathcal{N} = 1$. Para tales teorías, grazas as propiedades de holomorfía, moitos máis resultados exactos son coñecidos, e en xeral a súa dinámica non perturbativa é mellor comprendida. É un bo sitio onde pór en práctica as ideas da correspondencia gravidade/teoría *gauge*.

No capítulo 5 comezamos estudando unha solución de supergravidade de tipo IIB, que captura moitas propiedades infravermellas (IR) de Super QCD (SQCD) no límite de Veneziano. Esta solución foi atopada por Casero, Núñez e Paredes (CNP) no 2006 [108], onde a técnica de *smearing* foi usada por primeira vez co propósito de engadir sabor na correspondencia. En concreto, esta solución “engade sabor” á coñecida configuración de Maldacena-Núñez (MN), onde D5-branas enroladas nunha dous-esfera producen un dual a unha teoría que flúe a $\mathcal{N} = 1$ SYM no IR. A solución CNP incorpora un conxunto de N_f branas de sabor, estendidas ata a orixe do espazo e duais a N_f sabores de quarks non masivos, que se espaxen de xeito homoxéneo na xeometría. Obtense así unha teoría que flúe a $\mathcal{N} = 1$ SQCD cun potencial cuártico para os quarks, como se ten comprobado mediante numerosos tests.

O único problema da solución CNP é a presenza dunha singularidade de curvatura na orixe do espazo. Esta singularidade é provocada polo feito de que as N_f branas de sabor se intersecan nese punto. Como estamos no límite de Veneziano, este número é infinito, e neste punto temos unha densidade infinita que xera a singularidade. Un xeito de resolver a singularidade sería facendo que as branas non cheguen ata a orixe do espazo, senón que fiquen a unha distancia r_Q del, como amosamos na figura 9.3. Isto correspóndese na teoría dual en dar unha masa aos quarks $m_Q \sim r_Q$. Para calcular a solución de supergravidade correspondente á introdución desta escala r_Q , é preciso calcular a distribución de carga que as branas de sabor xeran na xeometría, que está caracterizada por unha función S , denominada perfil. Determinar S , así como a deformación da xeometría que produce é un problema altamente técnico que conseguimos resolver usando propiedades de holomorfía da xeometría, presentes grazas á supersimetría.

Unha vez temos caracterizada a solución de supergravidade, podemos facer o cálculo de distintos observábeis da teoría dual a través da correspondencia. Novos fenómenos como a dualidade de Seiberg en presenza de sabores masivos son capturados, e podemos calcular outros observábeis cuxo cálculo na solución CNP se vía afectado pola singularidade.

Outra característica da solución CNP da que, aínda que se entende ben, sería desexábel desfacerse, é o feito de que a teoría dual se volve seis dimensional a altas enerxías. Isto ocorre

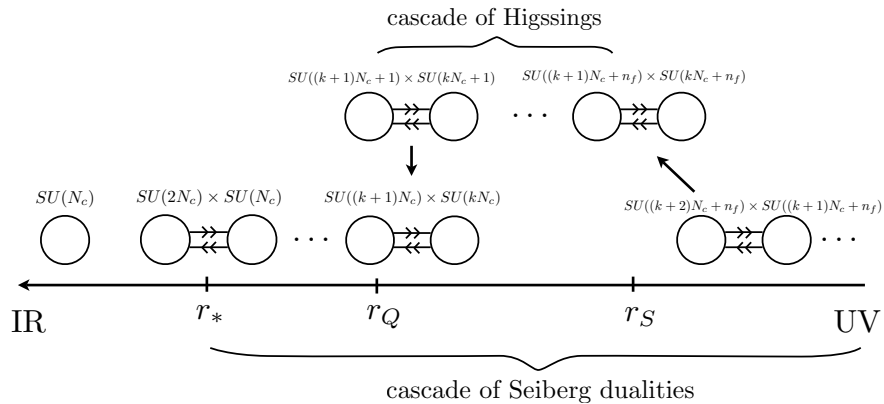


Figure 9.4: Esquema do fluxo do grupo de renormalización para a teoría UV completa

porque a teoría precisa dunha compleción ultravioleta (UV), que vén dada pola chamada “pequena teoría de cordas”, que é unha teoría en seis dimensións. Este fenómeno xa ocorría no caso da solución de MN. Nesta última solución, é posíbel realizar unha operación denominada “rotación”, que se é realizada cos parámetros axeitados, completa a teoría no UV. Esta operación pode verse como unha rotación no espazo de G-estructuras complexas, e leva a solución de MN á solución que describe a rama bariónica de Klebanov-Strassler (KS). Dende o punto de vista da teoría de campos dual, a rotación engade un novo grupo *gauge*. Isto é exactamente o xeito en que o Modelo Standard completa a teoría da interacción feble de Fermi.

Usando a técnica de rotación, é posíbel atopar unha compleción UV das recén atopadas solucións duais a SQCD con quarks masivos. O resultado que obtivemos foi que a teoría rotada é como a que se representa esquematicamente na figura 9.4. Movéndose no fluxo do grupo de renormalización dende o IR ata o UV: comezamos nun punto onde a teoría ten un só grupo *gauge* e confina. A unha certa escala r_* , aparece un novo grupo *gauge*, e estamos na rama bariónica da teoría de KS. Mais á escala r_Q , a teoría pasa da rama bariónica de KS á rama mesónica, onde se produce unha serie de cataratas de “un-Higgsing”. Ao mesmo tempo temos a catarata infinita de dualidades de Seiberg que se producen cara o UV. A catarata dos procesos de “un-Higgsing” remata na escala r_S (a función S aquí só debe ser distinta de cero nun intervalo finito $r_Q < r < r_S$). O que eran quarks na teoría sen rotar convírtense en grupos de *gauge* “Higgseados”. Ademais, a interpretación da función S na solución rotada é distinta; e de feito as funcións S fisicamente sensatas antes de rotación, deixan de sê-lo logo da rotación, e viceversa. A nova solución rotada presenta un tipo de física moi particular, con diversas escalas, que se asemella á física de certos modelos fenomenolóxicos que pretenden explicar a existencia de varias xeracións de sabor no Standard Model.

9.2.3 Outras teorías con sabor

Finalmente, no capítulo 6, exploramos outras posibilidades de uso da correspondencia para construír duais gravitatorios a teorías con sabor. Neste capítulo, centrámonos principalmente na construción das solucións en gravidade, posto que a interpretación da teoría dual non está

tan clara como nos casos anteriores.

Unha propiedade non perturbativa notábel das teorías *gauge* son as dualidades, que permiten caracterizar a física da teoría nun réxime dado mediante dúas descrições distintas, onde tipicamente unha descripción é feblemente acoplada e a outra é fortemente acoplada. Para teorías en catro dimensións, temos por exemplo a dualidade de Montonen-Olive con supersimetría $\mathcal{N} = 4$, a dualidade da teoría de Seiberg-Witten con supersimetría $\mathcal{N} = 2$, ou a dualidade de Seiberg para $\mathcal{N} = 1$ SQCD. Esta última require a presenza de sabor na teoría *gauge*. Unha propiedade non trivial da solución CNP é que captura esta dualidade. O xeito de velo é observando que as ecuacións de movemento presentan unha certa simetría baixo o intercambio:

$$N_c \rightarrow N_f - N_c, \quad N_f \rightarrow N_f, \quad (9.2.3)$$

Se engadimos materia na representación adxunta a $\mathcal{N} = 1$ SQCD, xunto cun superpotencial polinómico (de orde k) para esta materia, a teoría exhibe un novo tipo de dualidade, denominado dualidade de Kutasov, que ten unha numeroloxía parecida á da dualidade de Seiberg:

$$N_c \rightarrow N_f - k N_c, \quad N_f \rightarrow N_f. \quad (9.2.4)$$

É natural preguntarse se é posíbel atopar unha solución de supergravidade que exhiba esta dualidade. Tal solución foi presentada na sección 6.1. A idea foi construír unha solución moi parecida á de CNP, pero substituíndo as dúas dous-esferas presentes nesa xeometría por superficies de Riemann de xénero $g > 1$. Estas superficies de Riemann poden construírse como cocientes de espazos hiperbólicos, e o feito de que $g > 1$ implica a presenza de materia na representación adxunta na teoría dual, como nas teorías de Kutasov. Interesantemente, atopamos que as ecuacións de movemento da nosa configuración presentaban a simetría (9.2.4) (ao igual que en CNP tiñamos a simetría (9.2.3)). O parámetro k resulta estar relacionado co xeito en que tomamos os cocientes dos espazos hiperbólicos da nova xeometría:

$$k = \frac{q}{g-1}, \quad (9.2.5)$$

onde q é un certo número racional tamén dado en función de parámetros da xeometría.

O outro tema que investigamos neste capítulo foi a construción de duais gravitatorios a SQCD en dúas e tres dimensións e con distintas cantidades de supersimetría. Usamos o modelo de branas enroladas, de tal xeito que enrolando Dp -branas nun k -ciclo dentro dunha variedade de holonomía especial, obtemos un dual no IR a SQCD en $p+1-k$ dimensións, preservando unha certa cantidade de supersimetría. Este tipo de construcións foi bastante estudada na literatura, pero certos casos ficaban por ser analizados, especialmente no caso en que temos sabor.

Na sección 6.2 presentamos de xeito unificado todos estes casos, de tal xeito que se observe a sistemática seguida para a súa construción. A maiores, analizamos de maneira detallada como as branas de sabor estaban estendidas na xeometría, ilustrando con máis casos non triviais a técnica de “smearing”.

Chapter 10

Conclusións

A tese está realmente dividida en dúas partes, e as conclusións que se poden tirar de cada unha delas son independentes.

Por unha banda estudamos o réxime perturbativo das TCCs, onde buscabamos unha xeralización das relacións de recurrencia BCFW. Podemos resumir os nosos achados nos seguintes puntos.

- Fomos quen de atopar unha nova relación de recurrencia, moi semellante á de BCFW, pero que é válida para os casos nos que esta non funciona. Esta nova relación de recurrencia suma exactamente os mesmo termos que a de BCFW, pero engade unha especie de “peso” para cada un deles. Este “peso” depende dos ceros da amplitude. Deste xeito, a nova relación de recurrencia combina polos e ceros da amplitude.
- Estudando a nova relación de recurrencia, fomos quen de explicar o comportamento ultravioleta complexo das amplitudes dunha teoría dada. Ao contrario que as análises que xa existían na literatura, que se baseaban no coñecemento dun Lagranxiano, a nosa análise é puramente baseada na unitariedade da teoría.
- Estes dous anteriores descubrimentos permitíronnos formular un novo punto de vista á construción de teorías, alternativa ao punto de vista tradicional (con Lagranxianos). Este novo método é moito máis simple, e amosamos como era posíbel rederivar varios dos espectaculares resultados xa coñecidos da análise Lagranxiana.
- Hai moitas liñas futuras que fican abertas logo deste traballo. En primeiro lugar, habería que estudar mellor os ceros das amplitudes, e poder dar unha caracterización xeral deles (xa que nós só a demos para certos casos). Isto permitiría afondar na propugna deste novo punto de vista alternativo. Está claro que este último é máis útil dende o punto de vista experimental (permite calcular amplitudes de xeito moito máis eficiente), pero podería ser que fora tamén máis útil dende o punto de vista teórico, como argumentamos. Un bo sitio onde probar isto sería nas teorías de alto espín, moi difíciles de construír mediante Lagranxianos, pero que poderían amoldarse mellor aos nosos métodos. Máis traballo é preciso para afondar nesta liña, da que só comezamos a rascar un pequeno extremo.

Na segunda parte da tese, estudamos o réxime non perturbativo de teorías *gauge* con teoría de cordas. Isto é posíbel a través da correspondencia gravidade/teoría *gauge*. En concreto, centrámonos en estudar teorías *gauge* con sabor no límite de Veneziano. Para a introdución de sabor na correspondencia, usamos a técnica de *smearing* para espaxer branas de sabor na solución de gravidade. Estudamos distintos exemplos da correspondencia, e podemos tirar as seguintes conclusións da análise feita.

- A técnica de *smearing* é aplicábel á calquera exemplo da correspondencia que teña certas simetrías. En concreto, nós centrámonos nos casos con supersimetría. Nestes casos, a linguaxe de G-estructuras e calibracións é especialmente útil. Coas xeneralidades que explicamos, un debería ser quen de aplicar a técnica de *smearing* de xeito moi xeral. Non fica moito que aprender ao respecto.
- Atopamos un exemplo no que a solución con sabor ten un espazo *AdS*. Iso é extremadamente útil, pois neste caso a correspondencia enténdese moi ben, e podemos extraer moita información non perturbativa da solución de supergravidade. É a primeira vez na literatura que se atopa unha solución tan simple con estas características. Ademais, neste caso, tamén se coñece a solución sen usar a técnica de *smearing*, e na teoría dual pode usarse a técnica de localización para extraer moitos resultados exactos. É entón posíbel comparar a solución con sabor “esparexido” e a solución con sabor “localizado”. Isto é útil tanto dende o punto de vista de supergravidade, onde un podería tentar aprender como relacionar solucións con branas espaxeadas e solucións con branas localizadas; como dende o punto de vista da teoría dual de campos, onde é posíbel por primeira vez comparar o efecto do “smearing” nos distintos observábeis da teoría. Estas son dúas liñas que sería interesante continuar no futuro.
- Unha solución de supergravidade dual a $\mathcal{N} = 1$ SQCD (con certas sutilezas) era coñecida dende 2006. Esta solución ten unha singularidade no infravermello da que sería importante desfacerse. Aínda que se sabía que isto podería acadarse dándolle masa aos quarks, tal resolución é tecnicamente moi complicada e o problema ficou sen resolver. Nesta tese presentamos a correspondente solución. Precisamos botar man de técnicas de xeometría complexa, que poden ser aproveitadas para outras configuracións. En concreto, estudamos unha solución que se pode derivar da nosa mediante un procedemento de xeración de solucións, que dota á teoría dual da nosa solución con quarks dunha compleción ultravioleta. Esta compleción é unha teoría con supersimetría $\mathcal{N} = 1$, que posee unha dinámica non perturbativa moi rica, que podería modelar física alén do Modelo Estándar.
- Xuntando os distintos exemplos estudados, aportamos o noso gran ao crecemento e mellor entendemento da correspondencia gravidade/teoría *gauge*. Fica claro que hoxe por hoxe, é a nosa mellor baza para entender o réxime non perturbativo das teorías *gauge*. Coas novas que veñen dos grandes aceleradores, a fenomenoloxía de teorías fortemente acopladas pode ser o que nos depare o futuro, e a correspondencia, aínda que estea lonxe de ser probada nun futuro cercano, é actualmente a nosa mellor fonte de inspiración para o entendemento da dinámica destas teorías. Afondando nesta

correspondencia, vémonos forzados a aprender cousas tanto acerca da teoría de cordas e a gravidade, como acerca das TCCs.

Idealmente, nun futuro, as dúas liñas descritas nesta tese deixarán de ser independentes, e poderán complementarse. Algúns indicios disto están xa comezando a asomar na comunidade da Física Teórica.

Bibliography

- [1] S. Weinberg, *The Quantum theory of fields. Vol. 1: Foundations*. Cambridge University Press, 1995.
- [2] M. E. Peskin and D. V. Schroeder, *An Introduction to quantum field theory*. Westview Press, 1995.
- [3] A. M. Jaffe and E. Witten, “Quantum Yang-Mills theory,”. Clay Mathematics Institute Millenium Prize problem (2000).
- [4] M. Flory, R. C. Helling, and C. Sluka, “How I Learned to Stop Worrying and Love QFT,” [arXiv:1201.2714 \[math-ph\]](#).
- [5] F. Dyson, “Divergence of perturbation theory in quantum electrodynamics,” *Phys.Rev.* **85** (1952) 631–632.
- [6] E. Witten, “Perturbative gauge theory as a string theory in twistor space,” *Commun.Math.Phys.* **252** (2004) 189–258, [arXiv:hep-th/0312171 \[hep-th\]](#).
- [7] R. Britto, F. Cachazo, B. Feng, and E. Witten, “Direct proof of tree-level recursion relation in Yang-Mills theory,” *Phys.Rev.Lett.* **94** (2005) 181602, [arXiv:hep-th/0501052 \[hep-th\]](#).
- [8] J. M. Maldacena, “The Large N limit of superconformal field theories and supergravity,” *Adv.Theor.Math.Phys.* **2** (1998) 231–252, [arXiv:hep-th/9711200 \[hep-th\]](#).
- [9] G. ’t Hooft, “A Planar Diagram Theory for Strong Interactions,” *Nucl.Phys.* **B72** (1974) 461.
- [10] L. Susskind, “The World as a hologram,” *J.Math.Phys.* **36** (1995) 6377–6396, [arXiv:hep-th/9409089 \[hep-th\]](#).
- [11] N. Beisert, C. Ahn, L. F. Alday, Z. Bajnok, J. M. Drummond, *et al.*, “Review of AdS/CFT Integrability: An Overview,” [arXiv:1012.3982 \[hep-th\]](#).
- [12] V. Pestun, “Localization of gauge theory on a four-sphere and supersymmetric Wilson loops,” [arXiv:0712.2824 \[hep-th\]](#).

- [13] M. Marino, “Lectures on localization and matrix models in supersymmetric Chern-Simons-matter theories,” *J.Phys.A* **A44** (2011) 463001, [arXiv:1104.0783 \[hep-th\]](#).
- [14] M. B. Green, J. Schwarz, and E. Witten, *SUPERSTRING THEORY. VOL. 1: INTRODUCTION. VOL. 2: LOOP AMPLITUDES, ANOMALIES AND PHENOMENOLOGY*. Cambridge University Press, 1987.
- [15] J. Polchinski, *String theory. Vol. 1: An introduction to the bosonic string. Vol. 2: Superstring theory and beyond*. Cambridge University Press, 1998.
- [16] K. Becker, M. Becker, and J. Schwarz, *String theory and M-theory: A modern introduction*. Cambridge University Press, 2007.
- [17] A. Strominger and C. Vafa, “Microscopic origin of the Bekenstein-Hawking entropy,” *Phys.Lett.* **B379** (1996) 99–104, [arXiv:hep-th/9601029 \[hep-th\]](#).
- [18] J. Polchinski, “Dirichlet Branes and Ramond-Ramond charges,” *Phys.Rev.Lett.* **75** (1995) 4724–4727, [arXiv:hep-th/9510017 \[hep-th\]](#).
- [19] C. Johnson, *D-branes*. Cambridge University Press, 2003.
- [20] P. Benincasa and E. Conde, “On the Tree-Level Structure of Scattering Amplitudes of Massless Particles,” *JHEP* **1111** (2011) 074, [arXiv:1106.0166 \[hep-th\]](#).
- [21] P. Benincasa and E. Conde, “Exploring the S-Matrix of Massless Particles,” [arXiv:1108.3078 \[hep-th\]](#).
- [22] E. Conde and A. V. Ramallo, “On the gravity dual of Chern-Simons-matter theories with unquenched flavor,” *JHEP* **1107** (2011) 099, [arXiv:1105.6045 \[hep-th\]](#).
- [23] E. Conde, J. Gaillard, and A. V. Ramallo, “On the holographic dual of N=1 SQCD with massive flavors,” *JHEP* **1110** (2011) 023, [arXiv:1107.3803 \[hep-th\]](#).
- [24] E. Conde, J. Gaillard, C. Nunez, M. Piai, and A. V. Ramallo, “A Tale of Two Cascades: Higgsing and Seiberg-Duality Cascades from type IIB String Theory,” *JHEP* **1202** (2012) 145, [arXiv:1112.3350 \[hep-th\]](#).
- [25] E. Conde, J. Gaillard, C. Nunez, M. Piai, and A. V. Ramallo, “Towards the String Dual of Tumbling and Cascading Gauge Theories,” *Phys.Lett.* **B709** (2012) 385–389, [arXiv:1112.3346 \[hep-th\]](#).
- [26] E. Conde and J. Gaillard, “Kutasov-like duality from D5-branes wrapping hyperbolic cycles,” *Nucl.Phys.* **B848** (2011) 431–473, [arXiv:1011.1451 \[hep-th\]](#).
- [27] D. Arean, E. Conde, A. V. Ramallo, and D. Zoakos, “Holographic duals of SQCD models in low dimensions,” *JHEP* **1006** (2010) 095, [arXiv:1004.4212 \[hep-th\]](#).
- [28] D. Arean, E. Conde, and A. V. Ramallo, “Gravity duals of 2d supersymmetric gauge theories,” *JHEP* **0912** (2009) 006, [arXiv:0909.3106 \[hep-th\]](#).

- [29] P. Benincasa and F. Cachazo, “Consistency Conditions on the S-Matrix of Massless Particles,” [arXiv:0705.4305 \[hep-th\]](#).
- [30] T. Eguchi, P. B. Gilkey, and A. J. Hanson, “Gravitation, Gauge Theories and Differential Geometry,” *Phys.Rept.* **66** (1980) 213.
- [31] D. I. Olive, “Exploration of S-Matrix Theory,” *Phys. Rev.* **135** (1964) 745.
- [32] G. F. Chew, *The Analytic S-Matrix: A Basis for Nuclear Democracy*. W.A. Benjamin Inc., 1966.
- [33] R. J. Eden, P. V. Landshoff, D. I. Olive, and J. C. Polkinghorne, *The Analytic S-Matrix*. Cambridge University Press, 1966.
- [34] N. Arkani-Hamed, F. Cachazo, and J. Kaplan, “What is the Simplest Quantum Field Theory?,” [arXiv:0808.1446 \[hep-th\]](#).
- [35] S. Weinberg, “Photons and Gravitons in s Matrix Theory: Derivation of Charge Conservation and Equality of Gravitational and Inertial Mass,” *Phys.Rev.* **135** (1964) B1049–B1056.
- [36] C. Cheung and D. O’Connell, “Amplitudes and Spinor-Helicity in Six Dimensions,” [arXiv:0902.0981 \[hep-th\]](#).
- [37] R. Boels, “Covariant Representation Theory of the Poincaré Algebra and Some of Its Extensions,” *JHEP* **01** (2010) 010, [arXiv:0908.0738 \[hep-th\]](#).
- [38] S. Caron-Huot and D. O’Connell, “Spinor Helicity and Dual Conformal Symmetry in Ten Dimensions,” [arXiv:1010.5487 \[hep-th\]](#).
- [39] D. Gang, Y.-t. Huang, E. Koh, S. Lee, and A. E. Lipstein, “Tree-level Recursion Relation and Dual Superconformal Symmetry of the ABJM Theory,” *JHEP* **03** (2011) 116, [arXiv:1012.5032 \[hep-th\]](#).
- [40] N. Arkani-Hamed and J. Kaplan, “On Tree Amplitudes in Gauge Theory and Gravity,” *JHEP* **04** (2008) 076, [arXiv:0801.2385 \[hep-th\]](#).
- [41] F. A. Berends and W. T. Giele, “Recursive Calculations for Processes with n Gluons,” *Nucl. Phys.* **B306** (1988) 759.
- [42] M. L. Mangano, S. J. Parke, and Z. Xu, “Duality and Multi - Gluon Scattering,” *Nucl. Phys.* **B298** (1988) 653.
- [43] F. A. Berends, W. T. Giele, and H. Kuijf, “On relations between multi - gluon and multigraviton scattering,” *Phys. Lett.* **B211** (1988) 91.
- [44] M. L. Mangano and S. J. Parke, “Multi-Parton Amplitudes in Gauge Theories,” *Phys. Rept.* **200** (1991) 301–367, [arXiv:hep-th/0509223](#).

- [45] F. A. Berends, W. T. Giele, and H. Kuijf, “Exact and Approximate Expressions for Multi-Gluon Scattering,” *Nucl. Phys.* **B333** (1990) 120.
- [46] D. A. Kosower, “Light Cone Recurrence Relations for QCD Amplitudes,” *Nucl. Phys.* **B335** (1990) 23.
- [47] R. Britto, F. Cachazo, and B. Feng, “New recursion relations for tree amplitudes of gluons,” *Nucl.Phys.* **B715** (2005) 499–522, [arXiv:hep-th/0412308 \[hep-th\]](#).
- [48] S. J. Parke and T. R. Taylor, “An Amplitude for n Gluon Scattering,” *Phys. Rev. Lett.* **56** (1986) 2459.
- [49] M. Sugawara and A. Tubis, “Phase Representation of Analytic Functions,” *Phys. Rev.* **130** (1963) 2127–2131.
- [50] Y. S. Jin and A. Martin, “Connection Between the Asymptotic Behavior and the Sign of the Discontinuity in One-Dimensional Dispersion Relations,” *Phys. Rev.* **135** (1964) B1369–B1374.
- [51] Y. S. Vernov, “The Properties of the Forward Elastic Scattering Amplitude at Asymptotic and Finite Energies,” *Fiz. Elem. Chast. Atom. Yadra* **6** (1975) 601–631.
- [52] V. S. Zamiralov and A. F. Kurbatov, “On Zeros of π n Scattering Amplitude,” *Yad. Fiz.* **23** (1976) 900–903.
- [53] A. F. Kurbatov, “Zeros of Scattering Amplitude,” *Teor. Mat. Fiz.* **33** (1977) 354–363.
- [54] Y. S. Vernov and A. F. Kurbatov, “Lower Bound and Zeros of the Scattering Amplitude,” *Theor. Math. Phys.* **43** (1980) 490–494.
- [55] P. C. Schuster and N. Toro, “Constructing the Tree-Level Yang-Mills S-Matrix Using Complex Factorization,” [arXiv:0811.3207 \[hep-th\]](#).
- [56] F. Cachazo, P. Svrcek, and E. Witten, “MHV vertices and tree amplitudes in gauge theory,” *JHEP* **09** (2004) 006, [arXiv:hep-th/0403047](#).
- [57] K. Risager, “A Direct proof of the CSW rules,” *JHEP* **0512** (2005) 003, [arXiv:hep-th/0508206 \[hep-th\]](#).
- [58] Z. Bern, J. Carrasco, and H. Johansson, “New Relations for Gauge-Theory Amplitudes,” *Phys.Rev.* **D78** (2008) 085011, [arXiv:0805.3993 \[hep-ph\]](#).
- [59] N. Arkani-Hamed, F. Cachazo, C. Cheung, and J. Kaplan, “A Duality For The S Matrix,” *JHEP* **1003** (2010) 020, [arXiv:0907.5418 \[hep-th\]](#). 77 pages, 19 figures.
- [60] N. Arkani-Hamed, F. Cachazo, and C. Cheung, “The Grassmannian Origin Of Dual Superconformal Invariance,” *JHEP* **1003** (2010) 036, [arXiv:0909.0483 \[hep-th\]](#).
- [61] N. Arkani-Hamed, J. Bourjaily, F. Cachazo, and J. Trnka, “Local Spacetime Physics from the Grassmannian,” *JHEP* **1101** (2011) 108, [arXiv:0912.3249 \[hep-th\]](#).

- [62] N. Arkani-Hamed, J. Bourjaily, F. Cachazo, and J. Trnka, “Unification of Residues and Grassmannian Dualities,” *JHEP* **1101** (2011) 049, [arXiv:0912.4912 \[hep-th\]](#).
- [63] N. Arkani-Hamed, J. L. Bourjaily, F. Cachazo, S. Caron-Huot, and J. Trnka, “The All-Loop Integrand For Scattering Amplitudes in Planar N=4 SYM,” *JHEP* **1101** (2011) 041, [arXiv:1008.2958 \[hep-th\]](#).
- [64] P. Benincasa, C. Boucher-Veronneau, and F. Cachazo, “Taming tree amplitudes in general relativity,” *JHEP* **11** (2007) 057, [arXiv:hep-th/0702032](#).
- [65] C. Cheung, “On-Shell Recursion Relations for Generic Theories,” [arXiv:0808.0504 \[hep-th\]](#).
- [66] M. H. Goroff and A. Sagnotti, “The Ultraviolet Behavior of Einstein Gravity,” *Nucl. Phys.* **B266** (1986) 709.
- [67] R. M. Wald, “Spin-2 Fields and General Covariance,” *Phys. Rev.* **D33** (1986) 3613.
- [68] M. Taronna, “Higher-Spin Interactions: four-point functions and beyond,” [arXiv:1107.5843 \[hep-th\]](#).
- [69] A. Fotopoulos and M. Tsulaia, “On the Tensionless Limit of String theory, Off - Shell Higher Spin Interaction Vertices and BCFW Recursion Relations,” *JHEP* **11** (2010) 086, [arXiv:1009.0727 \[hep-th\]](#).
- [70] K. G. Wilson, “The Renormalization Group and Strong Interactions,” *Phys.Rev.* **D3** (1971) 1818.
- [71] E. Witten, “Anti-de Sitter space and holography,” *Adv.Theor.Math.Phys.* **2** (1998) 253–291, [arXiv:hep-th/9802150 \[hep-th\]](#).
- [72] S. Gubser, I. R. Klebanov, and A. M. Polyakov, “Gauge theory correlators from noncritical string theory,” *Phys.Lett.* **B428** (1998) 105–114, [arXiv:hep-th/9802109 \[hep-th\]](#).
- [73] J. M. Maldacena, “Wilson loops in large N field theories,” *Phys.Rev.Lett.* **80** (1998) 4859–4862, [arXiv:hep-th/9803002 \[hep-th\]](#).
- [74] O. Aharony, S. S. Gubser, J. M. Maldacena, H. Ooguri, and Y. Oz, “Large N field theories, string theory and gravity,” *Phys.Rept.* **323** (2000) 183–386, [arXiv:hep-th/9905111 \[hep-th\]](#).
- [75] N. Seiberg, “The Power of holomorphy: Exact results in 4-D SUSY field theories,” [arXiv:hep-th/9408013 \[hep-th\]](#).
- [76] P. Koerber, “Lectures on Generalized Complex Geometry for Physicists,” *Fortsch.Phys.* **59** (2011) 169–242, [arXiv:1006.1536 \[hep-th\]](#).

- [77] P. Koerber and D. Tsimpis, “Supersymmetric sources, integrability and generalized-structure compactifications,” *JHEP* **0708** (2007) 082, [arXiv:0706.1244 \[hep-th\]](#).
- [78] J. Gaillard and J. Schmude, “On the geometry of string duals with backreacting flavors,” *JHEP* **0901** (2009) 079, [arXiv:0811.3646 \[hep-th\]](#).
- [79] J. P. Gauntlett, “Branes, calibrations and supergravity,” [arXiv:hep-th/0305074 \[hep-th\]](#).
- [80] J. Polchinski and M. J. Strassler, “The String dual of a confining four-dimensional gauge theory,” [arXiv:hep-th/0003136 \[hep-th\]](#).
- [81] K. Pilch and N. P. Warner, “N=1 supersymmetric renormalization group flows from IIB supergravity,” *Adv.Theor.Math.Phys.* **4** (2002) 627–677, [arXiv:hep-th/0006066 \[hep-th\]](#).
- [82] I. R. Klebanov and E. Witten, “Superconformal field theory on three-branes at a Calabi-Yau singularity,” *Nucl.Phys.* **B536** (1998) 199–218, [arXiv:hep-th/9807080 \[hep-th\]](#).
- [83] I. R. Klebanov and A. A. Tseytlin, “Gravity duals of supersymmetric $SU(N) \times SU(N+M)$ gauge theories,” *Nucl.Phys.* **B578** (2000) 123–138, [arXiv:hep-th/0002159 \[hep-th\]](#).
- [84] I. R. Klebanov and M. J. Strassler, “Supergravity and a confining gauge theory: Duality cascades and chi SB resolution of naked singularities,” *JHEP* **0008** (2000) 052, [arXiv:hep-th/0007191 \[hep-th\]](#).
- [85] J. M. Maldacena and C. Nunez, “Supergravity description of field theories on curved manifolds and a no go theorem,” *Int.J.Mod.Phys.* **A16** (2001) 822–855, [arXiv:hep-th/0007018 \[hep-th\]](#).
- [86] F. Bigazzi, A. Cotrone, M. Petrini, and A. Zaffaroni, “Supergravity duals of supersymmetric four-dimensional gauge theories,” *Riv.Nuovo Cim.* **25N12** (2002) 1–70, [arXiv:hep-th/0303191 \[hep-th\]](#).
- [87] E. Witten, “Anti-de Sitter space, thermal phase transition, and confinement in gauge theories,” *Adv.Theor.Math.Phys.* **2** (1998) 505–532, [arXiv:hep-th/9803131 \[hep-th\]](#).
- [88] J. M. Maldacena and C. Nunez, “Towards the large N limit of pure N=1 superYang-Mills,” *Phys.Rev.Lett.* **86** (2001) 588–591, [arXiv:hep-th/0008001 \[hep-th\]](#).
- [89] A. H. Chamseddine and M. S. Volkov, “NonAbelian BPS monopoles in N=4 gauged supergravity,” *Phys.Rev.Lett.* **79** (1997) 3343–3346, [arXiv:hep-th/9707176 \[hep-th\]](#).

- [90] R. Andrews and N. Dorey, “Spherical deconstruction,” *Phys.Lett.* **B631** (2005) 74–82, [arXiv:hep-th/0505107](#) [hep-th].
- [91] R. Andrews and N. Dorey, “Deconstruction of the Maldacena-Nunez compactification,” *Nucl.Phys.* **B751** (2006) 304–341, [arXiv:hep-th/0601098](#) [hep-th].
- [92] C. Hoyos-Badajoz, C. Nunez, and I. Papadimitriou, “Comments on the String dual to N=1 SQCD,” *Phys.Rev.* **D78** (2008) 086005, [arXiv:0807.3039](#) [hep-th].
- [93] A. Paredes, “Supersymmetric solutions of supergravity from wrapped branes,” [arXiv:hep-th/0407013](#) [hep-th]. Ph.D. Thesis (Advisor: Alfonso V. Ramallo).
- [94] U. Gursoy and C. Nunez, “Dipole deformations of N=1 SYM and supergravity backgrounds with U(1) x U(1) global symmetry,” *Nucl.Phys.* **B725** (2005) 45–92, [arXiv:hep-th/0505100](#) [hep-th].
- [95] P. Di Vecchia, A. Lerda, and P. Merlatti, “N=1 and N=2 superYang-Mills theories from wrapped branes,” *Nucl.Phys.* **B646** (2002) 43–68, [arXiv:hep-th/0205204](#) [hep-th].
- [96] M. Bertolini and P. Merlatti, “A Note on the dual of N = 1 superYang-Mills theory,” *Phys.Lett.* **B556** (2003) 80–86, [arXiv:hep-th/0211142](#) [hep-th].
- [97] F. Benini, F. Canoura, S. Cremonesi, C. Nunez, and A. V. Ramallo, “Backreacting flavors in the Klebanov-Strassler background,” *JHEP* **0709** (2007) 109, [arXiv:0706.1238](#) [hep-th].
- [98] M. J. Strassler, “The Duality cascade,” [arXiv:hep-th/0505153](#) [hep-th].
- [99] A. Dymarsky, I. R. Klebanov, and N. Seiberg, “On the moduli space of the cascading SU(M+p) x SU(p) gauge theory,” *JHEP* **0601** (2006) 155, [arXiv:hep-th/0511254](#) [hep-th].
- [100] A. Butti, M. Grana, R. Minasian, M. Petrini, and A. Zaffaroni, “The Baryonic branch of Klebanov-Strassler solution: A supersymmetric family of SU(3) structure backgrounds,” *JHEP* **0503** (2005) 069, [arXiv:hep-th/0412187](#) [hep-th].
- [101] S. S. Gubser, C. P. Herzog, and I. R. Klebanov, “Symmetry breaking and axionic strings in the warped deformed conifold,” *JHEP* **0409** (2004) 036, [arXiv:hep-th/0405282](#) [hep-th].
- [102] A. Karch and E. Katz, “Adding flavor to AdS / CFT,” *JHEP* **0206** (2002) 043, [arXiv:hep-th/0205236](#) [hep-th].
- [103] G. Veneziano, “Some Aspects of a Unified Approach to Gauge, Dual and Gribov Theories,” *Nucl.Phys.* **B117** (1976) 519–545.

- [104] J. Erdmenger, N. Evans, I. Kirsch, and E. Threlfall, “Mesons in Gauge/Gravity Duals - A Review,” *Eur.Phys.J.* **A35** (2008) 81–133, [arXiv:0711.4467 \[hep-th\]](#).
- [105] B. R. Greene, A. D. Shapere, C. Vafa, and S.-T. Yau, “Stringy Cosmic Strings and Noncompact Calabi-Yau Manifolds,” *Nucl.Phys.* **B337** (1990) 1.
- [106] F. Benini, F. Canoura, S. Cremonesi, C. Nunez, and A. V. Ramallo, “Unquenched flavors in the Klebanov-Witten model,” *JHEP* **0702** (2007) 090, [arXiv:hep-th/0612118 \[hep-th\]](#).
- [107] F. Bigazzi, R. Casero, A. Cotrone, E. Kiritsis, and A. Paredes, “Non-critical holography and four-dimensional CFT’s with fundamentals,” *JHEP* **0510** (2005) 012, [arXiv:hep-th/0505140 \[hep-th\]](#).
- [108] R. Casero, C. Nunez, and A. Paredes, “Towards the string dual of N=1 SQCD-like theories,” *Phys.Rev.* **D73** (2006) 086005, [arXiv:hep-th/0602027 \[hep-th\]](#).
- [109] C. Nunez, A. Paredes, and A. V. Ramallo, “Unquenched Flavor in the Gauge/Gravity Correspondence,” *Adv.High Energy Phys.* **2010** (2010) 196714, [arXiv:1002.1088 \[hep-th\]](#).
- [110] F. Bigazzi, A. L. Cotrone, A. Paredes, and A. Ramallo, “Non chiral dynamical flavors and screening on the conifold,” *Fortsch.Phys.* **57** (2009) 514–520, [arXiv:0810.5220 \[hep-th\]](#).
- [111] F. Bigazzi, A. L. Cotrone, and A. Paredes, “Klebanov-Witten theory with massive dynamical flavors,” *JHEP* **0809** (2008) 048, [arXiv:0807.0298 \[hep-th\]](#).
- [112] P. Ouyang, “Holomorphic D7 branes and flavored N=1 gauge theories,” *Nucl.Phys.* **B699** (2004) 207–225, [arXiv:hep-th/0311084 \[hep-th\]](#).
- [113] S. Kuperstein, “Meson spectroscopy from holomorphic probes on the warped deformed conifold,” *JHEP* **0503** (2005) 014, [arXiv:hep-th/0411097 \[hep-th\]](#).
- [114] C. Nunez, A. Paredes, and A. V. Ramallo, “Flavoring the gravity dual of N=1 Yang-Mills with probes,” *JHEP* **0312** (2003) 024, [arXiv:hep-th/0311201 \[hep-th\]](#).
- [115] D. Arean, D. E. Crooks, and A. V. Ramallo, “Supersymmetric probes on the conifold,” *JHEP* **0411** (2004) 035, [arXiv:hep-th/0408210 \[hep-th\]](#).
- [116] O. Aharony, O. Bergman, D. L. Jafferis, and J. Maldacena, “N=6 superconformal Chern-Simons-matter theories, M2-branes and their gravity duals,” *JHEP* **0810** (2008) 091, [arXiv:0806.1218 \[hep-th\]](#).
- [117] J. H. Schwarz, “Superconformal Chern-Simons theories,” *JHEP* **0411** (2004) 078, [arXiv:hep-th/0411077 \[hep-th\]](#).
- [118] J. Bagger and N. Lambert, “Modeling Multiple M2’s,” *Phys.Rev.* **D75** (2007) 045020, [arXiv:hep-th/0611108 \[hep-th\]](#).

- [119] J. Bagger and N. Lambert, “Gauge symmetry and supersymmetry of multiple M2-branes,” *Phys.Rev.* **D77** (2008) 065008, [arXiv:0711.0955 \[hep-th\]](#).
- [120] J. Bagger and N. Lambert, “Comments on multiple M2-branes,” *JHEP* **0802** (2008) 105, [arXiv:0712.3738 \[hep-th\]](#).
- [121] A. Gustavsson, “Algebraic structures on parallel M2-branes,” *Nucl.Phys.* **B811** (2009) 66–76, [arXiv:0709.1260 \[hep-th\]](#).
- [122] I. R. Klebanov and G. Torri, “M2-branes and AdS/CFT,” *Int.J.Mod.Phys.* **A25** (2010) 332–350, [arXiv:0909.1580 \[hep-th\]](#).
- [123] N. Drukker, M. Marino, and P. Putrov, “From weak to strong coupling in ABJM theory,” *Commun.Math.Phys.* **306** (2011) 511–563, [arXiv:1007.3837 \[hep-th\]](#).
- [124] C. P. Herzog, I. R. Klebanov, S. S. Pufu, and T. Tesileanu, “Multi-Matrix Models and Tri-Sasaki Einstein Spaces,” *Phys.Rev.* **D83** (2011) 046001, [arXiv:1011.5487 \[hep-th\]](#).
- [125] O. Aharony, O. Bergman, and D. L. Jafferis, “Fractional M2-branes,” *JHEP* **0811** (2008) 043, [arXiv:0807.4924 \[hep-th\]](#).
- [126] D. Gaiotto and A. Tomasiello, “The gauge dual of Romans mass,” *JHEP* **1001** (2010) 015, [arXiv:0901.0969 \[hep-th\]](#).
- [127] D. Gaiotto and A. Tomasiello, “Perturbing gauge/gravity duals by a Romans mass,” *J.Phys.A* **A42** (2009) 465205, [arXiv:0904.3959 \[hep-th\]](#).
- [128] M. Fujita, W. Li, S. Ryu, and T. Takayanagi, “Fractional Quantum Hall Effect via Holography: Chern-Simons, Edge States, and Hierarchy,” *JHEP* **0906** (2009) 066, [arXiv:0901.0924 \[hep-th\]](#).
- [129] Y. Imamura and K. Kimura, “On the moduli space of elliptic Maxwell-Chern-Simons theories,” *Prog.Theor.Phys.* **120** (2008) 509–523, [arXiv:0806.3727 \[hep-th\]](#).
- [130] D. L. Jafferis and A. Tomasiello, “A Simple class of N=3 gauge/gravity duals,” *JHEP* **0810** (2008) 101, [arXiv:0808.0864 \[hep-th\]](#).
- [131] Y. Imamura and S. Yokoyama, “N=4 Chern-Simons theories and wrapped M-branes in their gravity duals,” *Prog.Theor.Phys.* **121** (2009) 915–940, [arXiv:0812.1331 \[hep-th\]](#).
- [132] D. Martelli and J. Sparks, “Moduli spaces of Chern-Simons quiver gauge theories and AdS(4)/CFT(3),” *Phys.Rev.* **D78** (2008) 126005, [arXiv:0808.0912 \[hep-th\]](#).
- [133] A. Hanany and A. Zaffaroni, “Tilings, Chern-Simons Theories and M2 Branes,” *JHEP* **0810** (2008) 111, [arXiv:0808.1244 \[hep-th\]](#).
- [134] A. Hanany, D. Vegh, and A. Zaffaroni, “Brane Tilings and M2 Branes,” *JHEP* **0903** (2009) 012, [arXiv:0809.1440 \[hep-th\]](#).

- [135] H. Ooguri and C.-S. Park, “Superconformal Chern-Simons Theories and the Squashed Seven Sphere,” *JHEP* **0811** (2008) 082, [arXiv:0808.0500 \[hep-th\]](#).
- [136] S. Hohenegger and I. Kirsch, “A Note on the holography of Chern-Simons matter theories with flavour,” *JHEP* **0904** (2009) 129, [arXiv:0903.1730 \[hep-th\]](#).
- [137] D. Gaiotto and D. L. Jafferis, “Notes on adding D6 branes wrapping RP^3 in $AdS(4) \times CP^3$,” [arXiv:0903.2175 \[hep-th\]](#).
- [138] M. Fujita and T.-S. Tai, “Eschenburg space as gravity dual of flavored $N=4$ Chern-Simons-matter theory,” *JHEP* **0909** (2009) 062, [arXiv:0906.0253 \[hep-th\]](#).
- [139] D. L. Jafferis, “Quantum corrections to $N=2$ Chern-Simons theories with flavor and their $AdS(4)$ duals,” [arXiv:0911.4324 \[hep-th\]](#).
- [140] F. Benini, C. Closset, and S. Cremonesi, “Chiral flavors and M2-branes at toric CY4 singularities,” *JHEP* **1002** (2010) 036, [arXiv:0911.4127 \[hep-th\]](#).
- [141] F. Benini, C. Closset, and S. Cremonesi, “Quantum moduli space of Chern-Simons quivers, wrapped D6-branes and AdS_4/CFT_3 ,” *JHEP* **1109** (2011) 005, [arXiv:1105.2299 \[hep-th\]](#).
- [142] Y. Hikida, W. Li, and T. Takayanagi, “ABJM with Flavors and FQHE,” *JHEP* **0907** (2009) 065, [arXiv:0903.2194 \[hep-th\]](#).
- [143] K. Jensen, “More Holographic Berezinskii-Kosterlitz-Thouless Transitions,” *Phys.Rev.* **D82** (2010) 046005, [arXiv:1006.3066 \[hep-th\]](#).
- [144] M. Ammon, J. Erdmenger, R. Meyer, A. O’Bannon, and T. Wrase, “Adding Flavor to $AdS(4)/CFT(3)$,” *JHEP* **0911** (2009) 125, [arXiv:0909.3845 \[hep-th\]](#).
- [145] O. Aharony, A. Hashimoto, S. Hirano, and P. Ouyang, “D-brane Charges in Gravitational Duals of 2+1 Dimensional Gauge Theories and Duality Cascades,” *JHEP* **1001** (2010) 072, [arXiv:0906.2390 \[hep-th\]](#).
- [146] J. P. Gauntlett, G. Gibbons, G. Papadopoulos, and P. Townsend, “Hyper-Kahler manifolds and multiply intersecting branes,” *Nucl.Phys.* **B500** (1997) 133–162, [arXiv:hep-th/9702202 \[hep-th\]](#).
- [147] J. Callan, Curtis G., C. Lovelace, C. Nappi, and S. Yost, “Loop Corrections to Superstring Equations of Motion,” *Nucl.Phys.* **B308** (1988) 221.
- [148] R. Emparan, C. V. Johnson, and R. C. Myers, “Surface terms as counterterms in the AdS / CFT correspondence,” *Phys.Rev.* **D60** (1999) 104001, [arXiv:hep-th/9903238 \[hep-th\]](#).
- [149] K.-M. Lee and H.-U. Yee, “New $AdS(4) \times X(7)$ Geometries with $CN=6$ in M Theory,” *JHEP* **0703** (2007) 012, [arXiv:hep-th/0605214 \[hep-th\]](#).

- [150] R. C. Santamaria, M. Marino, and P. Putrov, “Unquenched flavor and tropical geometry in strongly coupled Chern-Simons-matter theories,” *JHEP* **1110** (2011) 139, [arXiv:1011.6281 \[hep-th\]](#).
- [151] S.-J. Rey and J.-T. Yee, “Macroscopic strings as heavy quarks in large N gauge theory and anti-de Sitter supergravity,” *Eur.Phys.J.* **C22** (2001) 379–394, [arXiv:hep-th/9803001 \[hep-th\]](#).
- [152] N. Drukker, J. Plefka, and D. Young, “Wilson loops in 3-dimensional N=6 supersymmetric Chern-Simons Theory and their string theory duals,” *JHEP* **0811** (2008) 019, [arXiv:0809.2787 \[hep-th\]](#).
- [153] S. Gubser, I. Klebanov, and A. M. Polyakov, “A Semiclassical limit of the gauge / string correspondence,” *Nucl.Phys.* **B636** (2002) 99–114, [arXiv:hep-th/0204051 \[hep-th\]](#).
- [154] L. Martucci, J. Rosseel, D. Van den Bleeken, and A. Van Proeyen, “Dirac actions for D-branes on backgrounds with fluxes,” *Class.Quant.Grav.* **22** (2005) 2745–2764, [arXiv:hep-th/0504041 \[hep-th\]](#).
- [155] H. Lu, C. Pope, and P. Townsend, “Domain walls from anti-de Sitter space-time,” *Phys.Lett.* **B391** (1997) 39–46, [arXiv:hep-th/9607164 \[hep-th\]](#).
- [156] M. Grana, “Flux compactifications in string theory: A Comprehensive review,” *Phys.Rept.* **423** (2006) 91–158, [arXiv:hep-th/0509003 \[hep-th\]](#).
- [157] L. Martucci and P. Smyth, “Supersymmetric D-branes and calibrations on general N=1 backgrounds,” *JHEP* **0511** (2005) 048, [arXiv:hep-th/0507099 \[hep-th\]](#).
- [158] P. Candelas and X. C. de la Ossa, “Comments on Conifolds,” *Nucl.Phys.* **B342** (1990) 246–268.
- [159] C. P. Herzog, I. R. Klebanov, and P. Ouyang, “Remarks on the warped deformed conifold,” [arXiv:hep-th/0108101 \[hep-th\]](#).
- [160] R. Casero, C. Nunez, and A. Paredes, “Elaborations on the String Dual to N=1 SQCD,” *Phys.Rev.* **D77** (2008) 046003, [arXiv:0709.3421 \[hep-th\]](#).
- [161] N. Seiberg, “Electric - magnetic duality in supersymmetric nonAbelian gauge theories,” *Nucl.Phys.* **B435** (1995) 129–146, [arXiv:hep-th/9411149 \[hep-th\]](#).
- [162] C. Nunez, M. Piai, and A. Rago, “Wilson Loops in string duals of Walking and Flavored Systems,” *Phys.Rev.* **D81** (2010) 086001, [arXiv:0909.0748 \[hep-th\]](#).
- [163] M. J. Strassler, “An Unorthodox introduction to supersymmetric gauge theory,” [arXiv:hep-th/0309149 \[hep-th\]](#).

- [164] F. Bigazzi, A. L. Cotrone, A. Paredes, and A. V. Ramallo, “The Klebanov-Strassler model with massive dynamical flavors,” *JHEP* **0903** (2009) 153, [arXiv:0812.3399 \[hep-th\]](#).
- [165] F. Bigazzi, A. L. Cotrone, J. Mas, A. Paredes, A. V. Ramallo, *et al.*, “D3-D7 Quark-Gluon Plasmas,” *JHEP* **0911** (2009) 117, [arXiv:0909.2865 \[hep-th\]](#).
- [166] A. Barranco, E. Pallante, and J. G. Russo, “N=1 SQCD-like theories with N_f massive flavors from AdS/CFT and beta functions,” *JHEP* **1109** (2011) 086, [arXiv:1107.4002 \[hep-th\]](#).
- [167] C. Nunez, I. Papadimitriou, and M. Piai, “Walking Dynamics from String Duals,” *Int.J.Mod.Phys.* **A25** (2010) 2837–2865, [arXiv:0812.3655 \[hep-th\]](#).
- [168] D. Elander, C. Nunez, and M. Piai, “A Light scalar from walking solutions in gauge-string duality,” *Phys.Lett.* **B686** (2010) 64–67, [arXiv:0908.2808 \[hep-th\]](#).
- [169] D. Elander, J. Gaillard, C. Nunez, and M. Piai, “Towards multi-scale dynamics on the baryonic branch of Klebanov-Strassler,” *JHEP* **1107** (2011) 056, [arXiv:1104.3963 \[hep-th\]](#).
- [170] F. Bigazzi, A. L. Cotrone, C. Nunez, and A. Paredes, “Heavy quark potential with dynamical flavors: A First order transition,” *Phys.Rev.* **D78** (2008) 114012, [arXiv:0806.1741 \[hep-th\]](#).
- [171] C. P. Herzog and I. R. Klebanov, “On string tensions in supersymmetric SU(M) gauge theory,” *Phys.Lett.* **B526** (2002) 388–392, [arXiv:hep-th/0111078 \[hep-th\]](#).
- [172] C. Bachas, M. R. Douglas, and C. Schweigert, “Flux stabilization of D-branes,” *JHEP* **0005** (2000) 048, [arXiv:hep-th/0003037 \[hep-th\]](#).
- [173] J. M. Ridgway, “Confining k-string tensions with D-Branes in Super Yang-Mills theories,” *Phys.Lett.* **B648** (2007) 76–83, [arXiv:hep-th/0701079 \[hep-th\]](#).
- [174] J. Camino, A. Paredes, and A. Ramallo, “Stable wrapped branes,” *JHEP* **0105** (2001) 011, [arXiv:hep-th/0104082 \[hep-th\]](#).
- [175] J. Maldacena and D. Martelli, “The Unwarped, resolved, deformed conifold: Fivebranes and the baryonic branch of the Klebanov-Strassler theory,” *JHEP* **1001** (2010) 104, [arXiv:0906.0591 \[hep-th\]](#).
- [176] J. Gaillard, D. Martelli, C. Nunez, and I. Papadimitriou, “The warped, resolved, deformed conifold gets flavoured,” *Nucl.Phys.* **B843** (2011) 1–45, [arXiv:1004.4638 \[hep-th\]](#).
- [177] R. Minasian, M. Petrini, and A. Zaffaroni, “New families of interpolating type IIB backgrounds,” *JHEP* **1004** (2010) 080, [arXiv:0907.5147 \[hep-th\]](#).

- [178] N. Halmagyi, “Missing Mirrors: Type IIA Supergravity on the Resolved Conifold,” [arXiv:1003.2121 \[hep-th\]](#).
- [179] E. Caceres, C. Nunez, and L. A. Pando-Zayas, “Heating up the Baryonic Branch with U-duality: A Unified picture of conifold black holes,” *JHEP* **1103** (2011) 054, [arXiv:1101.4123 \[hep-th\]](#).
- [180] S. Bennett, E. Caceres, C. Nunez, D. Schofield, and S. Young, “The Non-SUSY Baryonic Branch: Soft Supersymmetry Breaking of N=1 Gauge Theories,” [arXiv:1111.1727 \[hep-th\]](#).
- [181] J. Gaillard and D. Martelli, “Fivebranes and resolved deformed G_2 manifolds,” *JHEP* **1105** (2011) 109, [arXiv:1008.0640 \[hep-th\]](#).
- [182] O. Aharony, “A Note on the holographic interpretation of string theory backgrounds with varying flux,” *JHEP* **0103** (2001) 012, [arXiv:hep-th/0101013 \[hep-th\]](#).
- [183] S. Dimopoulos and L. Susskind, “Mass Without Scalars,” *Nucl.Phys.* **B155** (1979) 237–252.
- [184] E. Eichten and K. D. Lane, “Dynamical Breaking of Weak Interaction Symmetries,” *Phys.Lett.* **B90** (1980) 125–130.
- [185] S. Weinberg, “Implications of Dynamical Symmetry Breaking,” *Phys.Rev.* **D13** (1976) 974–996.
- [186] L. Susskind, “Dynamics of Spontaneous Symmetry Breaking in the Weinberg-Salam Theory,” *Phys.Rev.* **D20** (1979) 2619–2625.
- [187] S. Weinberg, “Implications of Dynamical Symmetry Breaking: An Addendum,” *Phys.Rev.* **D19** (1979) 1277–1280.
- [188] B. Holdom, “Technicolor,” *Phys.Lett.* **B150** (1985) 301.
- [189] K. Yamawaki, M. Bando, and K.-i. Matumoto, “Scale Invariant Technicolor Model and a Technidilaton,” *Phys.Rev.Lett.* **56** (1986) 1335.
- [190] T. W. Appelquist, D. Karabali, and L. Wijewardhana, “Chiral Hierarchies and the Flavor Changing Neutral Current Problem in Technicolor,” *Phys.Rev.Lett.* **57** (1986) 957.
- [191] M. Piai, “Lectures on walking technicolor, holography and gauge/gravity dualities,” *Adv.High Energy Phys.* **2010** (2010) 464302, [arXiv:1004.0176 \[hep-ph\]](#).
- [192] D. Kutasov, “A Comment on duality in N=1 supersymmetric nonAbelian gauge theories,” *Phys.Lett.* **B351** (1995) 230–234, [arXiv:hep-th/9503086 \[hep-th\]](#).
- [193] D. Kutasov and A. Schwimmer, “On duality in supersymmetric Yang-Mills theory,” *Phys.Lett.* **B354** (1995) 315–321, [arXiv:hep-th/9505004 \[hep-th\]](#).

- [194] D. Kutasov, A. Schwimmer, and N. Seiberg, “Chiral rings, singularity theory and electric - magnetic duality,” *Nucl.Phys.* **B459** (1996) 455–496, [arXiv:hep-th/9510222](#) [hep-th].
- [195] C. Vafa, “Superstrings and topological strings at large N,” *J.Math.Phys.* **42** (2001) 2798–2817, [arXiv:hep-th/0008142](#) [hep-th].
- [196] P. Scott, “The geometries of 3-manifolds,” *Bull. London Math. Soc.* **15** (1983) 401–487.
- [197] G. Perelman, “Finite extinction time for the solutions to the Ricci flow on certain three-manifolds,” [arXiv:math/0307245](#) [math-dg].
- [198] G. Perelman, “The Entropy formula for the Ricci flow and its geometric applications,” [arXiv:math/0211159](#) [math-dg].
- [199] G. Perelman, “Ricci flow with surgery on three-manifolds,” [arXiv:math/0303109](#) [math-dg].
- [200] E. Bergshoeff, U. Gran, R. Linares, M. Nielsen, T. Ortin, *et al.*, “The Bianchi classification of maximal $D = 8$ gauged supergravities,” *Class.Quant.Grav.* **20** (2003) 3997–4014, [arXiv:hep-th/0306179](#) [hep-th].
- [201] S. Abel and J. Barnard, “Electric/Magnetic Duality with Gauge Singlets,” *JHEP* **0905** (2009) 080, [arXiv:0903.1313](#) [hep-th].
- [202] L. Girardello, M. Petrini, M. Porrati, and A. Zaffaroni, “Novel local CFT and exact results on perturbations of $N=4$ superYang Mills from AdS dynamics,” *JHEP* **9812** (1998) 022, [arXiv:hep-th/9810126](#) [hep-th].
- [203] F. Bigazzi, A. L. Cotrone, A. Paredes, and A. V. Ramallo, “Screening effects on meson masses from holography,” *JHEP* **0905** (2009) 034, [arXiv:0903.4747](#) [hep-th].
- [204] J. P. Gauntlett, N. Kim, D. Martelli, and D. Waldram, “Wrapped five-branes and $N=2$ superYang-Mills theory,” *Phys.Rev.* **D64** (2001) 106008, [arXiv:hep-th/0106117](#) [hep-th].
- [205] F. Bigazzi, A. Cotrone, and A. Zaffaroni, “ $N=2$ gauge theories from wrapped five-branes,” *Phys.Lett.* **B519** (2001) 269–276, [arXiv:hep-th/0106160](#) [hep-th].
- [206] A. Paredes, “On unquenched $N=2$ holographic flavor,” *JHEP* **0612** (2006) 032, [arXiv:hep-th/0610270](#) [hep-th].
- [207] P. Di Vecchia, H. Enger, E. Imeroni, and E. Lozano-Tellechea, “Gauge theories from wrapped and fractional branes,” *Nucl.Phys.* **B631** (2002) 95–127, [arXiv:hep-th/0112126](#) [hep-th].

- [208] J. Gomis and J. G. Russo, “ $D = 2 + 1$ $N = 2$ Yang-Mills theory from wrapped branes,” *JHEP* **0110** (2001) 028, [arXiv:hep-th/0109177](#) [[hep-th](#)].
- [209] J. P. Gauntlett, N. Kim, D. Martelli, and D. Waldram, “Five-branes wrapped on SLAG three cycles and related geometry,” *JHEP* **0111** (2001) 018, [arXiv:hep-th/0110034](#) [[hep-th](#)].
- [210] J. M. Maldacena and H. S. Nastase, “The Supergravity dual of a theory with dynamical supersymmetry breaking,” *JHEP* **0109** (2001) 024, [arXiv:hep-th/0105049](#) [[hep-th](#)].
- [211] A. V. Ramallo, J. P. Shock, and D. Zoakos, “Holographic flavor in $N=4$ gauge theories in 3d from wrapped branes,” *JHEP* **0902** (2009) 001, [arXiv:0812.1975](#) [[hep-th](#)].
- [212] F. Canoura, P. Merlatti, and A. V. Ramallo, “The Supergravity dual of 3d supersymmetric gauge theories with unquenched flavors,” *JHEP* **0805** (2008) 011, [arXiv:0803.1475](#) [[hep-th](#)].
- [213] D. Arean, P. Merlatti, C. Nunez, and A. V. Ramallo, “String duals of two-dimensional (4,4) supersymmetric gauge theories,” *JHEP* **0812** (2008) 054, [arXiv:0810.1053](#) [[hep-th](#)].
- [214] R. Bryand and S. Salamon, “On the construction of some complete metrics with exceptional holonomy,” *Duke Math.J.* **58** (1989) 829.